# Understanding the Role of Bcl-3 in Breast Cancer Metastasis

Daniel Turnham

**Thesis submitted for the award of PhD,**

**April 2017**

# Abstract

Despite recent advances in the treatment and detection of breast cancer it still remains the third most common cause of death from cancer in the UK as a result of its final metastatic stage, which is currently incurable. Numerous targets have been identified in an attempt to prevent and treat this highly aggressive form of cancer with limited success, however recent work has highlighted B-cell lymphoma 3 (Bcl-3) as a promising therapeutic target. Bcl-3 is a mediator of the well characterised NF-kB signalling pathway and both have been implicated with promoting tumour growth and progression. The role of Bcl-3 in mediating tumour proliferation and apoptosis has been extensively researched; however more recent work has also implicated Bcl-3 with an important role in regulating metastasis. Interestingly, suppression of Bcl-3 expression has been shown to inhibit breast cancer metastasis, a result which has been replicated through the use of small-molecule inhibitors designed to disrupt Bcl-3 binding to both p50 and p52. Despite this little is known, other than a reduction in cell motility, on how Bcl-3 is mediating its effects on metastasis, therefore the aims of this project were to elucidate the mechanisms through which Bcl-3 is regulating metastasis.

In this work we have shown how Bcl-3 can regulate a variety of single-cell and collective migratory phenotypes through inhibiting Rac1 and Cdc42 GTPase activity. We have also shown for the first time Bcl-3 to be upregulated during EMT, which appears to help regulate the expression of a number of EMT-inducing genes. Interestingly, we have also shown that prolonged inhibition of Bcl-3 results in a loss of cell viability through either senescence or apoptosis which appears to be dependent on cells expressing wildtype or mutant p53 respectively. Finally we have identified a novel set of small molecule Bcl-3 inhibitors that are capable of mimicking Bcl-3 suppression to regulate human breast cancer cell lines as well as both prostate and colorectal cell lines, offering a new therapeutic option for the treatment of breast and other human cancer types.

# Acknowledgments

Firstly I would like to thank my supervisor Dr. Richard Clarkson for giving me the opportunity to undertake this PhD project within his lab and for providing me with guidance and support throughout. I would also like to thank my co-supervisors Dr. Andrea Brancale and Prof. Andrew Westwell for providing their expertise and knowledge, especially towards the drug discovery components of this project.

I am also grateful to everyone who I have worked with at ECSCRI who have made my time here so enjoyable and have provided me with many memories. In particular I would like to thank all current and past members of the Clarkson lab including, Will Yang, Tim Robinson, Andreia Silva, Rhiannon French, Aleks Gruca, Cinzia Bordoni and Liv Hayward, who have all contributed with ideas and help towards my work and have kept me entertained during the slow days in the lab.

I would also like to acknowledge all of my collaborators throughput this work, especially Marta Pinto, Carla Oliveira and Joana Paredes at IPATIMUP, Porto for providing me with resources and guidance throughout my stay there. I am also grateful to the Life Sciences Research Network Wales and to Tiziana Life Sciences for funding this work and making this all possible.

Finally, I would like to thank Holly Fielding for putting up with all my weekends and long days in labs as well as my family for their constant love and support throughout my studies and for helping me to succeed in everything I do.

# Table of abbreviations

**ACTB-** Beta-actin
**Akt-** Protein kinase B
**AP-1-** Activator protein 1
**Arhgdbi-** Rho GDP-dissociation inhibitor 2
**Bcl-2-** B-cell lymphoma 2
**Bcl-3-** B-cell lymphoma 3
**Bcl-XL-** B-cell lymphoma-extra large
**BRCA-1-** Breast cancer 1
**BRCA-2-** Breast cancer 2
**BSA-** Bovine serum albumin
**C/EBPβ-** CCAAT/enhancer-binding protein beta
**CAM-** Chick-chorio allantoic membrane
**Cdc42-** Cell division control protein 42 homolog
**CDK-** Cyclin-dependent kinase
**CDK2-** Cyclin-dependent kinase 2
**CDKN1A-** Cyclin-dependent kinase inhibitor 1
**CDKN2A-** Cyclin-dependent kinase Inhibitor 2A
**CDKN2B-** Cyclin-dependent kinase 4 inhibitor B
**cDNA-** Complementary DNA
**CK5-** Cytokeratin 5
**C-MYC-** Myc
**CSC-** Cancer stem cells
**CtBP1-** C-terminal-binding protein 1
**CTC-** Circulating tumour cell
**CXCL10-** C-X-C motif chemokine 10
**CXCL12-** C-X-C motif chemokine 12
**CYLD-** Cylindromatosis
**DDR-** DNA damage response
**Dkk-1-** Dickkopf-related protein 1
**DMSO-** Dimethyl sulfoxide
**DNA-** Deoxyribonucleic acid
**dNTP-** Deoxynucleotide triphosphate
**E-cadherin-** Epithelial cadherin
**ECIS-** Electronic Cell-substrate Impedance Sensing
**ECM-** Extracellular matrix
**EDTA-** Ethylenediaminetetraacetic acid
**EGF-** Epidermal growth factor
**EGFR-** Epidermal growth factor receptor
**EMT-** Epithelial-mesenchymal transition
**Erα-** Oestrogen receptor
**EZH2-** Enhancer of zeste homolog 2
**F-actin-** Filamentous actin
**FBS-** Foetal bovine serum
**FGF-** Fibroblast growth factor

**FOXC2-** Forkhead box protein C2
**G1-** Gap phase 1
**G2-** Gap phase 2
**G-actin-** Globular actin
**gDNA-** Genomic DNA
**GDP-** Guanosine diphosphate
**GFP-** Green fluorescent protein
**GSK3-** Glycogen synthase kinase 3
**GTP-** Guanosine triphosphate
**HDAC1-** Histone deacetylase 1
**HER2-** Human epidermal growth factor receptor 2
**HER3-** Human epidermal growth factor receptor 3
**HER4-** Human epidermal growth factor receptor 4
**HGF-** Hepatocyte growth factor
**HR-** Homologous recombination
**HRP-** Horseradish Peroxidase
**Hsp90-** Heat shock protein 90
**IHC-** Immunohistochemistry
**IkB-** Inhibitor of kB
**IKK-** IkB kinase
**IL-1-** Interleukin 1
**IL-4-** Interleukin 4
**IL-6-** Interleukin 6
**IL-8-** Interleukin 8
**JAK-** Janus kinase
**M-** Mitotic phase
**Maspin-** Mammary serine protease inhibitor
**MAX-** MYC-associated factor X
**MDM2-** Mouse double minute 2
**MET-** Mesenchymal-epithelial transition
**miRNA-** Micro RNA
**MMP-** Matrix metalloproteinase
**mRNA-** Messenger RNA
**N-cadherin-** Neural cadherin
**NEMO-** NF-kappa-B essential modulator
**NF-kB-** Nuclear factor kappa-light-chain-enhancer of activated B cells
**NF-kB1-** Nuclear factor NF-kappa-B p105 subunit
**NF-kB2-** Nuclear factor NF-kappa-B p100 subunit
**NIK-** NF-κB inducing kinase
**NSAIDs-** Non-steroid anti-inflammatory drugs
**ODN-** Oligodeoxynucleotide
**OIS-** Oncogene-induced senescence
**p53-** Tumour protein 53
**PBS-** Phosphate-Buffered Saline
**PDX-** Patient derived-xenograft
**PFA-** Paraformaldehyde

**PI3K-** Phosphatidylinositide 3-kinases
**PLL-** Poly-L-lysine
**PRC2-** Polycomb Repressive Complex 2
**PRRX1-** Paired related homeobox 1
**PRα-** Progesterone receptor
**PSMB1-** Proteasome subunit beta type-1
**qPCR-** Quantitative PCR
**qRT-PCR-** Quantitive-real time-polymerase chain reaction
**Rac1-** Ras-related C3 botulinum toxin substrate 1
**Rb-** Retinoblastoma protein
**RelA-** Nuclear factor NF-kappa-B p65 subunit
**RHD-** REL Homology Domain
**RhoA-** Ras homolog gene family, member A
**RNA-** Ribonucleic acid
**RNAi-** RNA interference
**ROS-** Reactive oxygen species
**RT-** Reverse Transcriptase
**Runx1-** Runt-related transcription factor 1
**Runx2-** Runt-related transcription factor 2
**S-** Synthesis phase
**SASP-** Senescence-associated secretory phenotype
**SA-β-gal-** Senescence-associated β-galactosidase
**scRNA-** Scrambled RNA
**SEM-** Standard error of the mean
**sFRP-1-** Secreted frizzled-related protein 1
**siRNA-** Small interfering RNA
**Slug-** Zinc finger protein SNAI1
**SMAD2-** Mothers against decapentaplegic homolog 2
**SMAD3-** Mothers against decapentaplegic homolog 3
**SMAD4-** Mothers against decapentaplegic homolog 4
**Snail-** Zinc finger protein SNAI2
**SRC-1-** Steroid receptor coactivator-1
**STAT-** Signal Transducer and Activator of Transcription
**STAT3-** Signal transducer and activator of transcription 3
**TAD-** Transcriptional activation domain
**TEM-** Transendothelial migration
**TGFα-** Transforming growth factor alpha
**TGF-β-** Transforming growth factor beta
**TIS-** Therapeutic-induced senescence
**TNBC-** Triple negative breast cancer
**TNF-α-** Tumor necrosis factor alpha
**UNG-** Uracil-N glycosylase
**ZEB1-** Zinc finger E-box-binding homeobox 1
**ZEB2-** Zinc finger E-box-binding homeobox 2

# Table of Contents

## Table of Figures

## Table of tables

# Chapter 1:
# General introduction

# 1 Introduction

## 1.1 Breast Cancer

Breast cancer is the most common form of cancer in the United Kingdom with an incidence rate that has increased by 6% in females over the last 10 years and which is expected to rise by a further 2% in the next 20 years [7]. In 2014 over 50,000 new cases were reported in the UK which accounted for 15% of all cancer cases, while worldwide it was estimated that in 2012 over 1.68 million women had been diagnosed with the disease [7].

Recent advances in early detection screening as well as treatments for primary tumours have improved survival rates, with 87% of women diagnosed with breast cancer surviving for at least 5 years and 65% surviving 20 years or more [7]. Despite these improvements, breast cancer still accounts for around 7% of all deaths from cancer making it the third most common cause of death from cancer accounting for 11,400 deaths in the UK in 2014 [8]. Despite projected mortality rates set to fall by 26% between 2014 and 2035 there is still an unmet need for improved therapies for those with the most advanced stage of the disease which accounts for almost all deaths from the disease and is reflected by a 5 year survival rate of just 15% for this subset of patients [7].

Although recent advances in breast cancer research have vastly improved diagnostic and therapeutic approaches, our understanding of the disease is constantly evolving with new and old challenges requiring further exploration.

### 1.1.1 Normal mammary gland

Before trying to decipher the complicated and complex process of cancer formation in the breast it is important to first have an understanding of normal mammary morphology and how it develops. The mammary gland is a unique system of branching ducts and alveoli only found in mammals that serve a primary function of secreting milk to provide nutrition for newborns. The normal mammary gland is comprised of an epithelial compartment that can be further subdivided

into basal myoepithelial and luminal epithelial cells, as well as a surrounding stromal compartment (Figure 1.1). These structures are formed and modified in three main developmental processes, embryonic, pubertal and reproductive, all of which are regulated by a number of different growth factors and hormones.

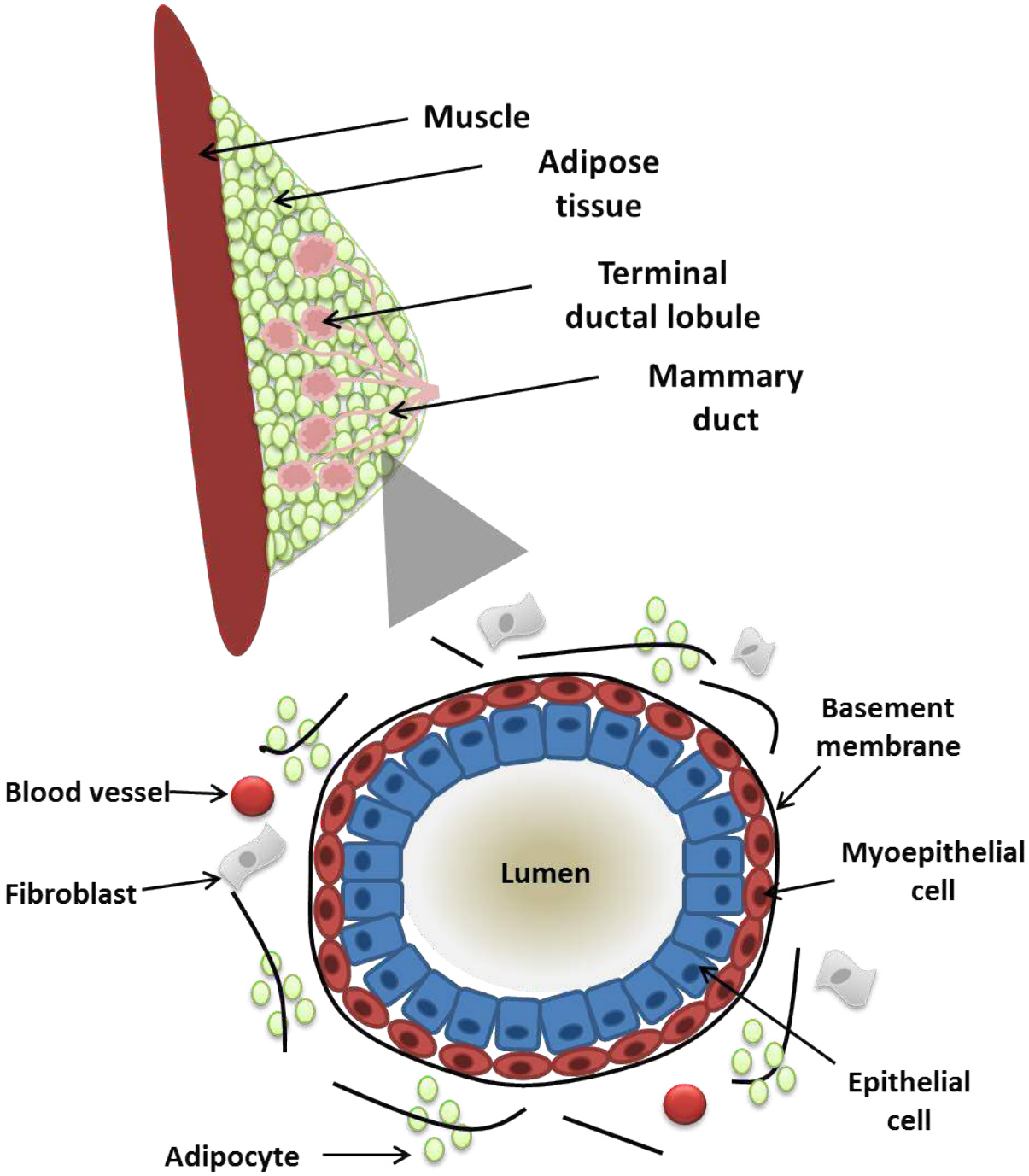


**Figure 1.1- Structure of the human mammary gland-** The human mammary gland consists of a series of branching ducts that end in terminal ductal lobules or alveoli. These ducts and alveoli are lined by epithelial luminal cells and basal-like myoepithelial cells which are surrounded by various extracellular components.

#### 1.1.1.1 Myoepithelial cells

As previously stated the mammary epithelium is comprised of two cell types, one of which is the basal layer of myoepithelial cells which when differentiated are similar in structure to smooth muscle cells giving them contractile properties that are utilised in milk ejection during lactation. Although less studied than their role in milk ejection, the myoepithelial population is thought to hold other important functions, including the regulation of luminal cell behaviour and mediating interactions between luminal and stromal compartments [9]. Furthermore, these cells have been shown to possess natural cancer suppressing properties capable of regulating tumour growth, invasion and angiogenesis [10, 11].

#### 1.1.1.2 Luminal cells

The bulk of the mammary gland is composed of the epithelial luminal cells which line the mammary ducts and the specialized cells of the alveoli formed during pregnancy. These cells are capable of both synthesising and secreting milk for lactation. Unlike myoepithelial cells, the luminal compartment is more heterogeneous as some cells express oestrogen (ERα) and/or progesterone (PRα) receptors, which help to regulate development along with a number of growth factors such as epidermal growth factor (EGF) and transforming growth factor alpha (TGFα) [12]. The development of this heterogeneity is believed to arise from two different progenitor cells, one that is $ER^+$ and another that is $ER^-$, with these cells also believed to may give rise to specific tumour types in breast cancer [13].

Despite extensive research into both luminal and myoepithelial cell types the origin and regulation of mammary cell populations is still under debate with various studies disputing the mammary cell of origin. It has been argued through transplantation and lineage tracing assays that both luminal and myoepithelial cell types arise from independent unipotent stem cells, however conflicting data has suggested that both cell types arise through a single multipotent stem cell which gives rise to committed progenitor cells for both luminal and myoepithelial cell types [14, 15].

### 1.1.2 Breast cancer classification

Formation of breast cancer almost exclusively arises from the luminal cell population with myoepithelial derived cancers very rare. Cancers derived from these mammary cells are known as adenocarcinomas as opposed to cancers that develop from the surrounding tissues such as muscle, fat, and connective tissue which are known as sarcomas [16]. Adenocarcinomas can be further classified based on their site of origin and invasive progression with histological grading and typing useful clinically for determining whether a tumour is constrained to within the epithelial wall (in situ carcinoma) or has invaded into the surrounding stroma (invasive carcinoma) as well as if the tumour site of origin is either ductal or lobular. Further histological analysis of important target proteins such as HER2 and oestrogen can also be used to make clinical decisions on both prognosis and treatment options.

Although less routinely used clinically, molecular profiling of breast cancers is also equally important and has helped to highlight the highly heterogeneous nature of the disease from both patient to patient and within individual tumours, often meaning each case will respond differently to different treatments. In order to help understand this heterogeneity, tumours can be loosely characterised into a number of different subtypes, which can then be used to help understand the weaknesses of certain tumour types for future clinical use. This classification is constantly evolving with new discoveries and better analysis techniques, however it is widely regarded that 5 distinct subtypes of breast cancer can be clearly defined based on specific genetic fingerprints. These subtypes are commonly known as luminal A, luminal B, $HER2^{+ve}$, basal and normal breast-like, however more recent studies have suggested that these may be further sub-divided to incorporate further heterogeneity within subtypes [17].

#### 1.1.2.1 Luminal A

Both luminal tumour subtypes are thought to most likely represent the luminal cells of the normal mammary gland. Luminal A breast cancers are usually $ER^+$ and/or $PR^+$ with no HER2

expression and are the most common type of tumour representing around 40-70% of all cases [18, 19]. More recent studies have suggested that this subtype may be far more heterogeneous and may be further divided into luminal A basal-positive or luminal A basal-negative based on the expression of basal markers CK5 or EGFR [20]. Despite the overall improved prognosis observed in luminal A tumours compared to other subtypes it has been shown that those expressing the basal markers mentioned have a worse prognosis than their basal-negative counterparts [20]. Low expression of the proliferative protein marker ki-67 is a hallmark of luminal A tumours which are often slow growing compared to other subtypes, while their $ER^+$ status also makes them suitable for hormone therapy.

#### 1.1.2.2 Luminal B

Similar to luminal A subtypes, luminal B tumours are usually $ER^+$ and/or $PR^+$, however they may also express HER2 as well. Luminal B tumours account for around 10-20% of breast cancer and despite the fairly high survival rates prognosis is often still worse than luminal A cancers due to poorer tumour grade, larger tumour sizes and increased lymph-node involvement [21]. The main differences of luminal B tumours compared to their luminal A counterparts is a higher expression of proliferative genes and a reduced expression of ER-related genes [22, 23]. Despite being $ER^+$ endocrine therapy is often less effective and will often result in a relapse, this is most likely due to the generally lower expression of ER than luminal A subtypes, therefore combination therapies may be required to improve patient outcome [24].

#### 1.1.2.3 HER2-positive

$HER2^+$ tumours are negative for both ER and PR but are enriched for HER2 receptors. These cancers often grow faster than both luminal subtypes and often have a poorer prognosis if left untreated; however recent advances in HER2-targeted therapies have vastly improved survival rates for patients of this subtype [25, 26]. HER2-positive tumours account for around 25% of all breast

tumours and despite improved therapeutic options a subset of these cancers will become resistant to HER2-targeted therapies which can make them difficult to treat.

#### 1.1.2.4 Triple negative

Triple negative breast cancers (TNBCs) do not express ER, PR or HER2 receptors. Around 10-20% of breast cancers are triple negative, which is often associated with a larger and more aggressive tumour, often resulting in a poorer prognosis compared to other subtypes [27, 28]. Although TNBCs and basal-like cancers are often termed the same and share many similarities, the latter possesses a distinct gene expression signature including high levels of cytokeratins 5, 6 and 17 [29]. More recent analysis has suggested that the TNBC group may be further divided into 6 subsets- basal-like 1, basal-like 2, immunomodulatory, mesenchymal, mesenchymal stem–like, luminal androgen receptor and unstable, which can help stratify clinical outcome and treatment options [30].

#### 1.1.2.5 Normal -like

The final subtype of breast tumours is known as normal-like, with these tumours exhibiting the same receptor status as luminal A tumours with ER and/or PR positivity and no expression of HER2, as well as low ki67 status. They do however differ in their gene expression pattern which resembles the profile of a normal breast. Although the prognosis of these tumours is often worse than luminal A tumours, it is thought to be intermediary as it is often better than that of basal-like tumours [31]. These tumours are not as well classified as other subtypes and are fairly rare, accounting for around 5-10% of all cases, although these figures are thought be skewed due to contaminating normal tissue in large dataset studies [32].

| Tumour subtype | ER status | PR status | HER2 status | Ki67 status | Incidence |
|---|---|---|---|---|---|
| Luminal A | + | +/- | - | Low | 30-70% |
| Luminal B | + | +/- | +/- | High | 10-20% |
| HER2-positive | - | - | + | High | 5-15% |
| Basal-like | - | - | - | High | 15-20% |
| Normal-like | + | +/- | - | Low | 5-10% |

**Table 1.1- Characterisation of breast cancer subtypes**

## 1.2 Breast cancer formation

Human cells are limited to approximately 50 cell divisions when grown in normal culture conditions *in vitro*, a phenomenon termed the 'Hayflick limit' after it's discoverer in 1961 [33]. This type of permanent proliferative arrest is due to telomere erosion during replication which builds up over repeated cell divisions and eventually leads to irreversible damage and is thus termed 'replicative senescence' [34, 35]. Cell senescence may also have an important role as a tumour suppressor providing an early defence mechanism against cancer progression, this type of senescence is known as oncogene-induced senescence (OIS) [36]. Cancer cells can often overcome this obstacle through acquiring genetic mutations that allow for immortalization and uncontrolled proliferation.

The acquisition of these mutations and ultimately the development of breast cancer can be influenced by a variety of environmental and pre-disposed genetic factors that can alter the chances of tumour formation. A number of studies have shown how environmental factors can influence this with obesity, smoking, excess alcohol, decreased exercise, early menopause and pregnancy just a few of the factors that can increase the risk of breast cancer [37-40]. These environmental factors

can increase the chance of genes being mutated which is ultimately the primary cause of cancer development.

Gene mutations are rarely inherited with only 3-10% of breast cancers caused by an underlying hereditary mutation, with the majority of these caused by BRCA-1 or BRCA-2 genes [41]. More commonly, somatic mutations arise throughout life with the majority having little or no effect on normal cell growth. However, when these mutations occur at high frequency through the acquisition of genomic instability, or in important oncogenes/ tumour suppressors, such as p53, it can lead to uncontrolled cell growth that often results in unchecked cell proliferation leading to tumour growth.

### 1.2.1 Oncogenes in breast cancer

Oncogenes can be defined as any gene that when activated can contribute to cancer development. Similarly proto-oncogenes are pre-activated genes that are required for normal cell growth but can develop into oncogenes. Mechanisms of oncogene activation include gene amplification, point mutations and chromosomal translocation, and despite the vast numbers of oncogenes evaluated in other human cancer the number of known oncogenes in breast cancer are relatively low [42].

#### 1.2.1.1 HER2

One example of a well-established oncogene in breast cancer is the previously mentioned HER2 gene that is often found amplified resulting in the overexpression of its tyrosine kinase receptor product. As previously stated the HER2 oncogene is associated with the more aggressive subtypes of breast cancer and is found overexpressed in around 20-30% of all cancers [43]. HER2 is just one of 4 tyrosine kinases which make up the HER family which also includes EGFR (HER1), HER3 (erbB3) and Her4 (erbB4). HER2 receptors can form either homodimers or heterodimers with family members that can be activated through the binding of various ligands or autonomously, which in turn activates receptor autophosphorylation [44]. This sequence of events can lead to a number of

transduction cascades which regulate a number of important pathways for tumour growth (Figure 1.2). One such pathway which is activated more commonly through HER2 heterodimerization with HER3 is the PI3K/Akt pathway which can exert a number of pro-tumorigenic processes such as proliferation, migration, metastasis and survival [45].

Targeting of the extracellular domain of the HER2 receptor has been identified as a promising therapeutic option which has led to the development of a number of therapies aimed at disrupting its binding. One such therapy is Trastuzumab (Herceptin), which has seen promising clinical responses in both early and metastatic breast cancer [46, 47]. Trastuzumab is a monoclonal antibody that binds to the extracellular domain of HER2 to exert its anti-tumour effects. Although it does not appear to reduce HER2 expression it is thought to inhibit downstream signalling which can result in a cell cycle arrest, induction of apoptosis or inhibit angiogenesis [48-50]. Other HER2-targeted therapies include lapatinib and pertuzumab which also target the extracellular domain of HER2 and are often used in combination with other therapies [46].

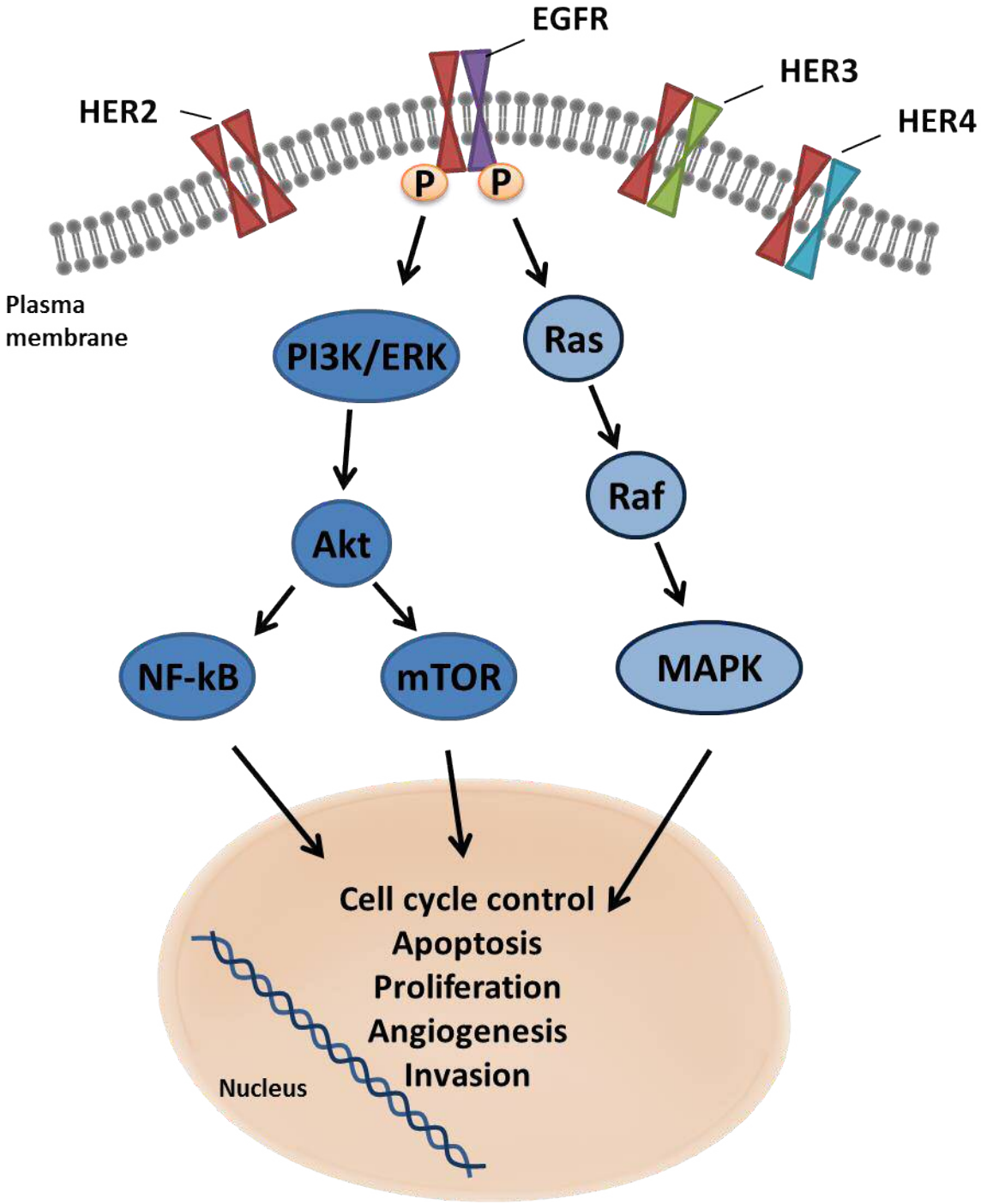


**Figure 1.2- HER2 signalling pathway-** HER2 receptor homodimerization or heterdimerization can activate downstream signalling pathways that can promote a number of important processes involved in tumour progression. PI3K/Akt signalling through NF-kB or mTOR effectors and Ras/MAPK signalling pathways are two of the most extensively studied downstream pathways that are activated through HER activation. Activation of either pathway will lead to transcriptional moderation that can influence various cellular processes.

#### 1.2.1.2 c-MYC

Another oncogene associated with breast cancer is c-MYC which is amplified and overexpressed in around 15-25% of breast tumours [51]. The c-MYC protein is a transcription factor that in conjunction with MYC-associated factor X (MAX) can activate the transcription of a number of important gene targets [52]. It is also capable of repressing gene transcription however the mechanisms behind this are less well understood. C-MYC can regulate breast cancer progression through a variety of different process, however in breast cancer it is best known for its role in mediating proliferation through promoting G1-S cell cycle transitions by activation of a variety of targets such as Cdk2 and repressing p21 activation [53, 54]. Interestingly, c-MYCs role in cell proliferation has been strongly correlated with HER2 expression with overexpression of both oncogenes appearing to result in a poorer prognosis than when either gene is amplified alone [55].

This role for c-MYC in breast cancer has led to extensive research into potential therapeutic options for managing the regulation of c-MYC, which due to its important functions in normal cell growth have to be carefully selected. Potential therapeutic approaches have looked into destabilising c-MYC at a protein level or inhibiting mRNA transcription as well as blocking the interaction between c-MYC and MAX [56]. So far the use of siRNA and antisense oligonucleotides have shown promising results *in vitro* and *in vivo,* however issues translating these towards a clinical setting have limited the progression of c-MYC-targeted therapy [57, 58].

#### 1.2.1.3 Cyclin D1 and cyclin E

Other oncogenes that have been associated with breast cancer include cyclin D1 and cyclin E which are overexpressed in around 40% and 20% of invasive and total breast cancers respectively [59, 60]. Although not commonly overexpressed together, independent overexpression results in hyperphosphorylation of the tumour suppressor pRb which results in an increase in proliferation [61]. Cyclin E is often associated with higher tumour grade because it may also induce S phase transitions independently of pRb phosphorylation and therefore increase cell cycling [59].

Therapies that target the cell cycle include flavopiridol which acts by competing with CDKs in a non-specific manner for ATP-binding resulting in an induction of apoptosis [62]. Clinical trials are ongoing and have seen mixed responses, however combination of flavopiridol with docetaxel was well tolerated in a phase 1 trial suggesting further potential [63].

### 1.2.2 Tumour suppressor genes in breast cancer

Unlike oncogenes, tumour suppressor genes promote carcinogenesis through a loss of function. Tumour suppressor genes can be 'switched off' through a number of mechanisms including inherited germline mutations as well as sporadic somatic mutations in which typically both alleles will be lost through either mutation or a deletion.

#### 1.2.2.1 p53

The first described and most widely studied tumour suppressor gene is p53 which functions to remove or inhibit the proliferation of abnormal cells. Although mutations of p53 occur in 20-30% of breast cancers it is much more frequently mutated in other solid tumours [64]. Inhibition of p53 in breast cancer can occur through a number of mechanisms including both germ-line and somatic mutations. Li-Fraumeni syndrome often occurs through a germ-line mutation of p53 and is often associated with a much higher risk of developing a number of cancer types including breast cancer [65]. Somatic mutations often occur through missense mutations which results in mutated non-functional p53 protein that accumulates in a tumour, however non-missense truncating mutations are also associated with breast cancer [66]. The accumulation of mutated p53 is thought to also harbour oncogenic effects and contribute to tumour progression independently of its loss of tumour suppressor effects [66].

Under normal growth conditions p53 protein is suppressed through interaction with the mouse double minute 2 (MDM2) ligase, however activation through cellular stresses such as DNA damage or oncogene activation results in reduced MDM2 degradation of p53 which facilitates an increase in p53 DNA binding. Transcriptional regulation of p53 controls a number of gene targets

that in turn function to regulate carcinogenesis through various processes which include inhibiting the cell cycle, inducing apoptosis or DNA repair and inhibiting metastasis (Figure 1.3).

Since p53 is mutated in over half of all human cancers there has been extensive research into strategies aimed at restoring the function of wild-type p53 or depleting its mutated form, as well as targeting downstream signalling pathways [67]. Efforts to restore the transcriptional activity lost in mutant p53 have seen the development of a number of synthetic peptides that have shown promising results by restoring the sequence-specific DNA binding activity [68, 69]. Despite promising results these compounds still appear to be a long way from being used in a clinical setting and require further optimization. Another approach has seen the development of several compounds that can specifically deplete mutant p53 without affecting the wild-type form which has been shown to reduce tumour progression [70]. One such approach is to pharmacologically inhibit the heat shock protein 90 (Hsp90) which can reactivate endogenous MDM2 leading to the degradation of mutant p53 and induction of apoptosis, an approach that is currently undergoing phase III clinical trials in lung cancer [70, 71].

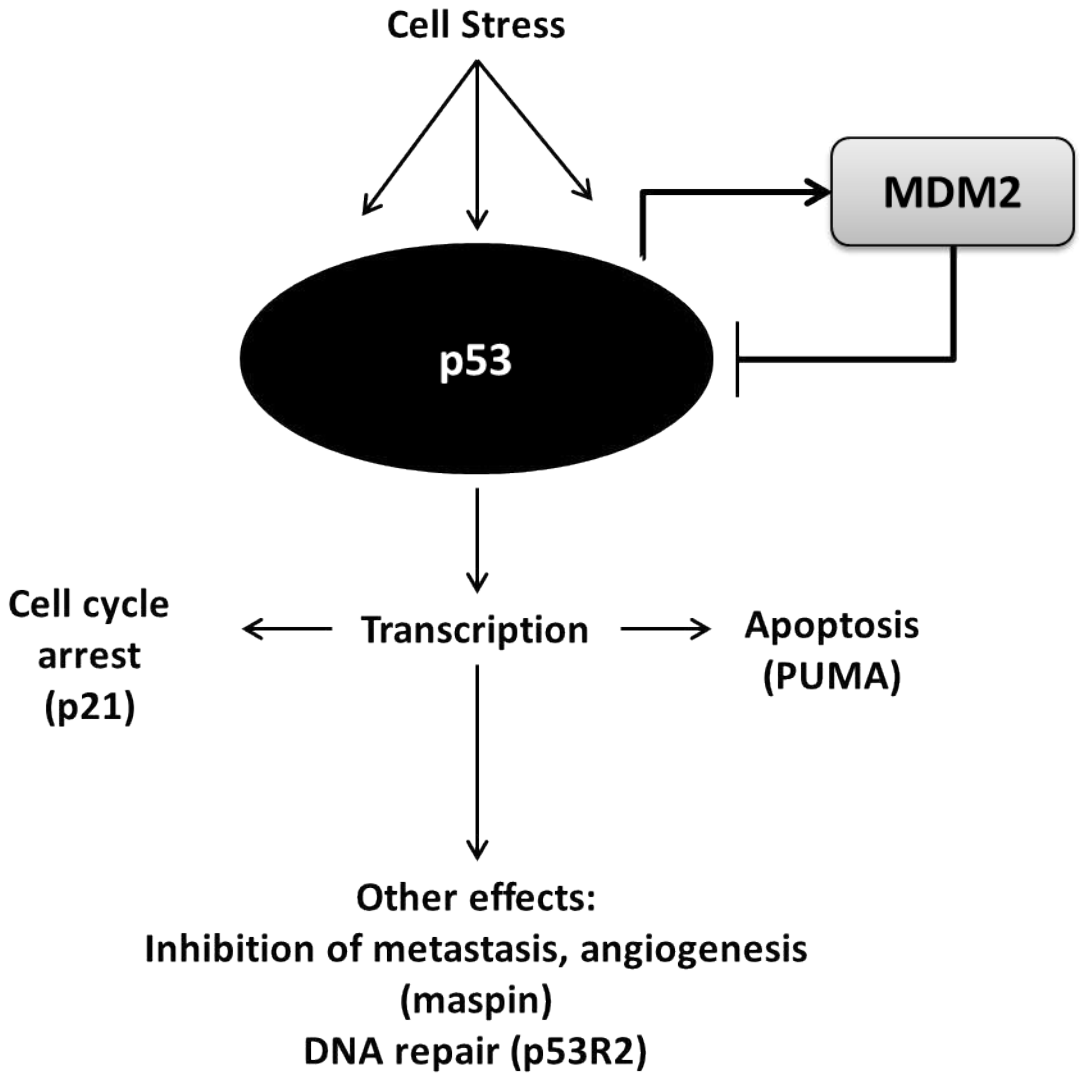


**Figure 1.3-Simplified model of p53 signalling-** Under normal physiological conditions p53 remains inactivated and is degraded by MDM2 which acts as a negative feedback regulator. Upon activation via cellular stress such as DNA damage or activation of oncogenes MDM2 mediated degradation is suppressed resulting in an increase in p53 DNA binding where it can transcriptionally regulate a number of effector genes. Differential genes are activated depending on the type or magnitude of stress and can modulate a number of different processes that mediate tumour suppressor functions such as cell cycle arrest, apoptosis and DNA repair. This model highlights some of the key modulators of this pathway but does not show the many other components that make up this pathway. (adapted from [2])

#### 1.2.2.2 BRCA1 & BRCA2

The previously stated BRCA 1 & 2 genes are also tumour suppressor genes that have been associated with both ovarian and prostate cancers and can increase the likelihood of developing breast cancer by 40-80%, making it a strong predictor of disease [72-75]. Germline mutations may occur throughout the length of the genes in the form of missense or more commonly truncating mutations [76]. Larger scale mutations such as duplications or deletions of one or more exons also form a small percentage of germline mutations accounting for up to 12% of BRCA mutations in high risk families [77].

Hundreds of different mutations have been identified for both BRCA1 and BRCA2 with a large percentage of these resulting in a truncated protein product [78]. The non-mutated BRCA1 protein has a diverse array of functions primarily in regulating the DNA damage response (DDR) through mediating signals between DNA damage sensors and DDR effectors [79]. It also forms part of a protein complex that can repair double stranded DNA breaks through homologous recombination (HR) and can also function as a cell cycle checkpoint regulator [79]. The BRCA2 protein product plays a less diverse role and it primarily acts through regulating HR in DNA repair through its binding to Rad51 [80].

The early detection of BRCA mutations can help patients make informed decisions on how best to manage their risk, however despite greatly enhancing the probability of developing breast cancer not everyone with a BRCA mutation will develop breast cancer. Precautionary lifestyle changes such as reducing caloric intake [81] and daily alcohol consumption [82] can reduce the likelihood of cancer development, however the most effective option currently for those carrying the mutation is to undergo a prophylactic bilateral mastectomy [83].

### 1.2.3 Breast cancer progression

The previously described oncogenes and tumour suppressors represent just some of the many genes that have been linked with breast cancer progression highlighting the various ways in which a cell can become malignant. The dogmatic view is that tumour formation follows on from multiple rounds of cellular mutations which will select for highly malignant clones that will go on to make up the bulk of a primary tumour [84]. In this linear model of progression individual cells may then escape and spread to distal sites, where they can form secondary tumours and begin further clonal expansion which may even eventually metastasise again [85]. Alternatively, a parallel model of tumour growth has also been suggested where by the dissemination of tumour cells occurs much earlier on, before the formation of a detectable tumour [85]. In this model disseminated cells will undergo a different set of selective pressures based on its new microenvironment, and will therefore expand to represent a different set of genetic alterations to the primary tumour which will grow alongside the secondary tumour. This second model opens up a number of different therapeutic challenges in itself but what still remains as a key area of interest is how these cells acquire the properties required to invade and metastasis irrespective of at what stage in the disease this occurs.

## 1.3 Metastasis in breast cancer

Metastasis is defined as ‘the spread of cancer from one part of the body to another’ and is often seen as the natural progression of primary tumours following a complex set of changes both within a tumour cell and its surrounding microenvironment. Almost all breast cancer-related deaths are due to metastasis, with the most common sites for metastasised secondary tumour formation being the lungs, liver, bones or the brain [86]. Although a large amount of investment has been made into the search and development of new treatments that can target metastasis at various stages it still remains an elusive and incurable aspect of the disease. Most recent estimations suggest that 20-30% of all breast cancer cases will become metastatic and coupled with a median survival length of just 3 years it is clear that further investment is needed [87].

### 1.3.1 Stages of metastasis

In order for a tumour cell to metastasise it will often undergo a precise series of events which include transformation, intravasation, migration, extravasation and re-colonization (Figure 1.4). This process requires a number of important intra and extracellular changes which have the potential to be targeted for therapeutic purposes, however in order for this to be successful, an in depth knowledge of the metastatic process is required.

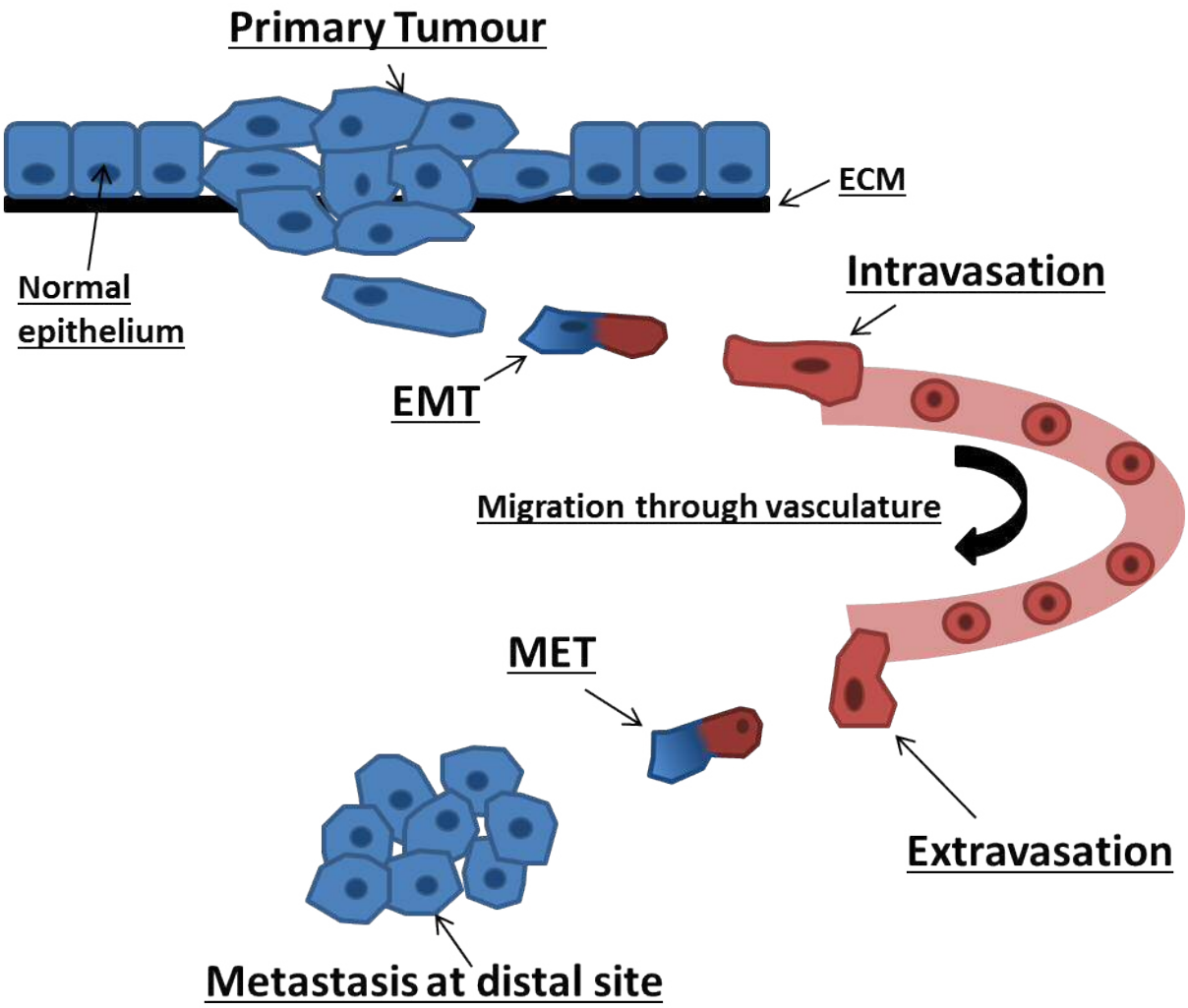


**Figure 1.4- Simplified process of metastasis-** Metastasis can be broken down into a number of different stages with each process vital for the success of an invading tumour cell. Metastasis begins with invasion away from the primary tumour which is often initiated through EMT which provides tumour cells with the properties required to break away from their site of origin. Cells will then enter the circulation through intravasation where they will migrate as circulating tumour cells (CTCs) before exciting through extravasation. Cells will then revert back to an epithelial-like cell through MET and begin colonizing at a distal site.

#### 1.3.1.1 EMT

The epithelial to mesenchymal transition (EMT) has long been recognised for its role in cell migration during embryonic development and wound healing, and is now well established as an early mediator in cancer metastasis through a similar but distinct regulatory system [88]. During cancer-associated EMT cells will transform from tightly bound, polarized layers of epithelial cells to individual, loosely bound cells with no clear apico-basal structure. This has been associated with the acquisition of key metastatic properties such as increased cell migration, invasion, apoptosis resistance and ECM production [89]. More recent evidence has suggested that these transitions between specialized epithelial and mesenchymal states may be more flexible, with a number of intermediate states now recognized in what is termed partial EMT [90]. This partial EMT phenotype has been seen to represent a hybrid of both epithelial and mesenchymal traits and has been associated with various processes including tumour budding [91]. The acquisition of these EMT-like traits is widely accredited as the initiating step in metastasis and is therefore seen as an attractive therapeutic target for inhibiting the progression of the disease.

A hallmark of EMT is the downregulation of a key cell-cell adhesion molecule, E-cadherin, and the upregulation of various mesenchymal markers such as N-cadherin and Vimentin. This EMT phenotype can be induced through a variety of signalling pathways such as TGF-ß, Wnt, Notch and TNF-α with the regulation of these signals largely attributed to various transcription factors such as Slug, Snail, Twist, ZEB1 and ZEB2 (Figure 1.5)[92]. This classical view of EMT regulation through transcriptional changes has now been expanded to include a variety of miRNA, epigenetic and post-translational modifications [90]. Many of these regulatory mediators often act on similar activators to various degrees making it difficult to define a common EMT regulatory signature, with it now widely accepted that some of these pathways may be unique to particular tumours or in certain contexts.

Interestingly, it has been reported that the induction of EMT is coupled with the acquisition of stem cell like properties, furthermore recent developments have indicated that only a small subpopulation of tumour cells, the cancer stem cells (CSC), will undergo EMT and acquire the properties necessary for metastasis [93, 94]. Once a tumour cell has acquired these properties it can begin to migrate away from the primary tumour and begin the process of metastasis at distal sites throughout the body.

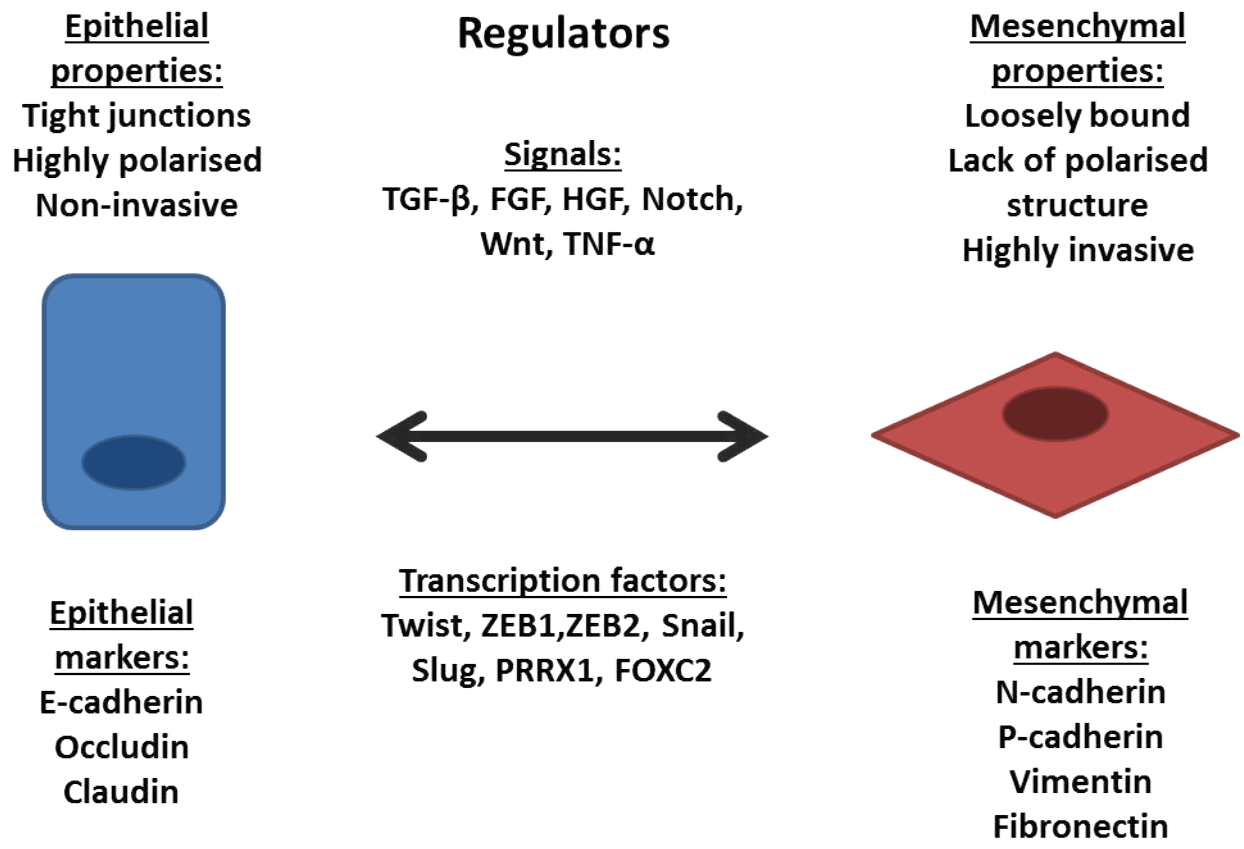


**Figure 1.5- Classical view of EMT/MET regulation-** This simplified model of EMT and MET signalling demonstrates some of the key phenotypical changes associated the changes from an epithelial to a mesenchymal-like state and represents some of the key molecules involved in its signalling and regulation. More recent studies have suggested this process is much more plastic with a number of intermediate stages now thought to exist between the fully differentiated epithelial and mesenchymal phenotypes. Micro-RNA and post-transcriptional modifications also influence the regulation of this process. (adapted from [6])

#### 1.3.1.2 Migration

Migration is a process used by various types of non-cancerous cells and plays important roles in embryonic development, wound healing and immunity. It can also be utilised by tumour cells that can use the same basic mechanisms to spread throughout the body by either collective, single cell mesenchymal or amoeboid migration [95]. These distinct migratory mechanisms share many characteristics yet exhibit plasticity, with the ability to switch between the different migratory phenotypes making it particularly difficult to inhibit cell migration if only targeting one particular migratory mechanism [96].

An integrative model for cell migration has been proposed which accounts for the shared and distinct properties of mesenchymal and the collective migration subtypes (Figure 1.6) [96]. The process begins with the extension of protrusions at a leading edge followed by the formation of focal adhesions that anchor the cell to the substrate. Space for the cell to move into is then created through focalised proteolysis before actomyosin contraction propels the cell forward which results in the detachment of the trailing edge. In collective migration this process also includes the addition of attached sheets or chains of cells that will follow the leading edge. Amoeboid-like motility is faster and less dependent on ECM contacts, instead utilising actomyosin contractions to propel and squeeze the cell through the ECM rather than relying on protease degradation to create paths to move [96].

It is widely accepted that the driving force behind cell migration in cancer is the formation of protrusions, normally in the form of lamellipodia, that attach to ECM substrates and provide the traction required for the cell to drag itself along. Numerous proteins which regulate this process have been identified to be overexpressed in breast cancer which includes LIM kinase, Cofilin, Cortactin and the Arp 2/3 complex [97-99]. Furthermore, various members of the Rho GTPase family of regulators, in particular Rac1, are also thought to play an important role in the organisation of the actin cytoskeleton during this process [100].

Cell motility can become activated by various chemokines and growth factors within the surrounding microenvironment as well as through interactions with neighbouring cells, which can trigger numerous signalling pathways that regulate the different processes required for cell movement. Host tissues that secrete chemokines to stimulate chemotaxis are thought to play an important role in migration and a number of different ligands have shown to promote cell migration in breast cancer cells [101]. Growth factors can also stimulate cell migration with EGF secreted from tumour-associated macrophages a known stimulator of motility and cell survival [102].

Once a tumour cell has escaped from its place of origin it can then migrate into the surrounding tissues utilising the various migratory modes, with the potential to switch between the different mechanisms depending on its surrounding microenvironment. This form of local invasion can then progress to spreading towards more distal sites, however this usually requires intravasation into the vasculature from where it can travel to secondary sites throughout the body.

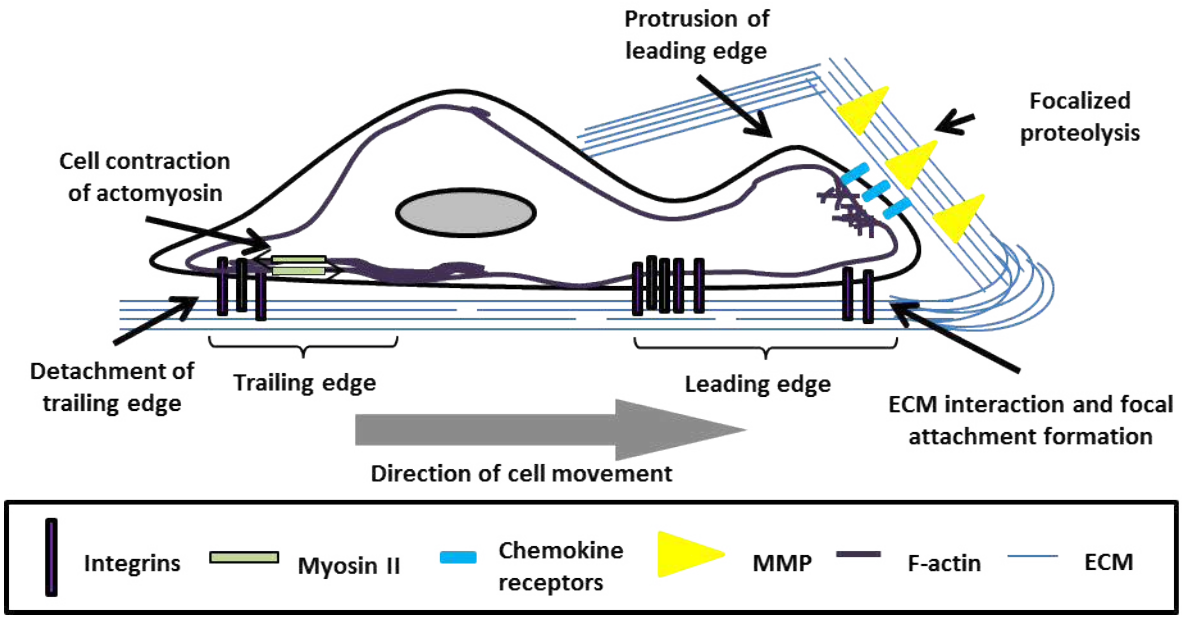


**Figure 1.6-Model of cell migration-** This model of cell migration offers a generalised view on the mechanisms involved in single cell mesenchymal-like migration as well the migration of cells at the invasion front during collective migration. Protrusion of the leading edge provides a platform for which the cell can pull itself onto through careful interactions with the ECM and contractions of the actin cytoskeleton. In addition to this model collectively migrating cells will carefully regulate cell-cell interactions which will help coordinate cellular responses and behaviour to the surrounding environment.

#### 1.3.1.3 Intravasation & Extravasation

The migration of tumour cells throughout the vasculature has long been thought of as one of the most important aspects of metastasis as it defines a critical period where cells must gain entry, survive and then leave whilst under a unique set of environmental pressures [103]. The difficulty of this process was made apparent from early research showing that only 0.01% of cancer cells injected into the circulation were capable of forming metastatic foci [104]. This lead to the assumptions that cells were either being rapidly destroyed within the circulation or struggling to make the transition back out of the vasculature. Although more recent evidence suggests that this inefficiency of metastasis may in fact be due to an inability of circulating cells to re-colonize subsequent to their extravasation at distal sites, the importance of these steps should not be overlooked [105].

Intravasation can occur either through newly formed vasculature induced by tumours via angiogenesis, through pre-existing vessels or even via lymphatic ducts [106]. The process of cell migration through the endothelium is known as transendothelial migration (TEM) and requires the disruption of endothelial junctions [103]. In general this is easier through newly formed vessels due to their weak cell-cell junctions, however in established vessels this process is permitted by disrupting the endothelial junctions and creating an opening through which cancer cells can pass through [103, 107]. This can occur through the secretion of factors such as VEGF and TGFβ1 by tumour cells which disrupt VE-cadherin-β-catenin complexes, therefore creating endothelial cell junction openings [108, 109]. Furthermore, CXCL12 and the lipid 12(S)HETE have also been shown to induce endothelial junction openings in breast cancer during TEM [110, 111]. Once inside the circulatory system these cells are termed circulating tumour cells (CTCs), with recent advances in the detection and analysis of these cells highlighting the therapeutic potential in using these cells for early diagnostics and predictive biomarkers [112].

Similarly to intravasation the process of cell extravasation from the vasculature requires a disruption of the endothelial junctions in order for the TEM to occur. Before this process can begin,

the migrating cell must first attach itself to the endothelium which typically occurs in smaller capillaries where diameters are similar in size to the cell [113]. This process begins with a weak attachment of the tumour cell to the endothelium with E-selectin and N-cadherin thought to play an important role in this initial step [114, 115]. This attachment is then strengthened through various receptors such as integrin's, CD44 and MUC1 which anchor the cell to the endothelium allowing it to begin TEM immediately or after further cell migration to an optimal position, which is influenced by chemokine secretion [103, 116-119]. Although the exact mechanisms of TEM during extravasation are not clear it is believed that cells will preferentially squeeze between the junctions of adjacent endothelial cells using paracellular TEM. This is opposed to a secondary mechanism, transcellular TEM which involves direct migration through the endothelial cell body [120, 121]. Once a cell has made it across the endothelium it can then begin the final step of metastasis, the colonization of a secondary site.

#### 1.3.1.4 Metastasis colonization

The success of a tumour cell to re-colonize once it has left the circulation is reliant on a favorable tumour-host interaction, an observation which was termed the 'seed and soil' hypothesis by Paget in 1889 [122]. As previously mentioned this process is highly inefficient and once outside the vasculature a tumour cell will either undergo cell death, remain dormant or proliferate from a micro-metastasis into a macroscopic tumour (Figure 1.7) [86]. Factors that will determine this outcome include the tumour cells interaction with components of the ECM as well as stromal cells within the target organ parenchyma [123]. Supportive niches are thought to greatly enhance the survival of metastasizing cells, for example breast cancer cells sensitized to CXCL12 through the primary tumour stroma have a much greater chance of survival in the CXCL12-rich microenvironment of the bone marrow [124]. Furthermore, colonizing tumour cells may be able to alter a favorable niche themselves, with TGF-β secreted by disseminated breast cancer cells thought to stimulate periostin production in stromal fibroblasts which in turn helps secondary colonization through the recruitment of Wnt factors [125].

The ability to adapt to this new environment will determine cell survival and another way that cells can do this is to re-transform back from a mesenchymal to an epithelial (MET) phenotype. There is a strong body of evidence suggesting that MET is a vital process for colonization and in breast metastasis distinct populations of epithelial-like cells with strong E-cadherin expression have been seen in secondary tumours [126]. This evidence is supported by a study where the metastatic foci of mesenchymal breast carcinoma cells injected into the mouse mammary fat pad were found to be E-cadherin-positive indicating some form of MET transformation [127].Furthermore, loss of EMT-inducing Twist1 and Prrx1 have both been shown to be important in the re-activation of a proliferative state in metastasizing cells and inducing the changes needed for macroscopic tumour formation [128-130].

As highlighted here, the colonization process is subject to a number of different stresses and challenges which make it a very inefficient process. This selection also ensures that those cells that are successful are highly robust and aggressive making it even harder to treat than the primary tumour. However, with progressive research uncovering key stages of this process it opens a number of exciting potential therapeutic routes which could and should be explored.

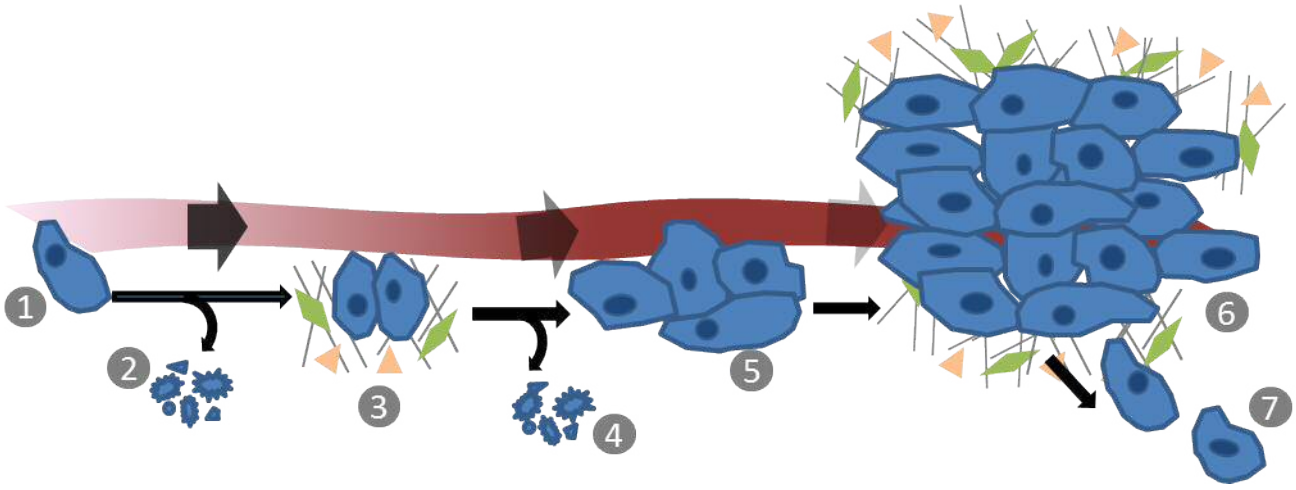


**Figure 1.7-Metastatic colonization- (1)** Tumour cell colonization begins with the extravasation of CTCs in the capillaries of distal sites, **(2)** where the majority of cells will undergo cell death or fail to escape the vasculature due to the harsh environment. **(3)** Cells that survive the host tissue defences may settle in a supportive niche for survival, **(4)** however some cells may still be susceptible to immune responses and may not survive. **(5)** A latency period will then often follow in the form of single cells or small micro-metastases which can last days or years as they acquire traits to overtake the host tissue. **(6)** If the tumour cells are able to break out of latency and reinitiate proliferation they can overtake the host tissue and form metastasise **(7)** which may eventually result in dissemination of its own tumour cells onto secondary metastasis. (adapted from [4])

### 1.3.2 Treating metastatic breast cancer

It is clear from the high mortality rates of patients suffering from metastatic disease and lack of therapeutic options that the task of treating metastasis is a difficult one. Treatment is very much based on individual disease and a number of factors dictate this, such as tumour biology, prior therapy, tumour burden and patient preference [131]. Unlike the treatment of primary tumours surgery is not usually a viable option due to systemic spread of disease throughout the body. For those with ER-positive disease the most likely form of treatment is endocrine therapy such as tamoxifen treatment, where as those with HER2 positive disease will be treated with anti-HER2 therapy using agents such as Trastuzumab [131]. Other common treatments include chemotherapy either as a single agent or as a combination therapy, and radiotherapy which is often used when metastasis has spread to the patient's bones [131]. These treatments have the ability to increase patient lifespans and improve quality of life, however ultimately metastatic breast cancer still remains incurable.

The growing wealth of knowledge on the metastatic process does however offer hope for future therapies which may be able to improve the outlook of patients diagnosed with the disease. Numerous biological targets have been identified which impact at various stages of the metastatic process all of which in theory could become a potential target for therapy. It has however been suggested that targeting the latter stages may be more plausible as it is likely that the early stages of dissemination may have already occurred at diagnosis [132]. Furthermore, the large number of metastasis-related genes and signaling pathways mean that selecting the correct targets pre-clinically is an important process that must be thoroughly evaluated first. One such pathway that has already been identified and which has shown encouraging results is the nuclear factor kB (NF-kB) signaling pathway.

## 1.4 NF-kB signaling

The NF-kB transcription factor family has been implicated in breast cancer metastasis by promoting both migration and EMT through the regulation of genes such as CXCR4 and Twist1 respectively [133, 134]. The first NF-kB transcription factor was identified over 30 years ago through the use of mobility shift assays which uncovered a new factor that could specifically bind to a 10bp sequence within the immunoglobulin κ light chain enhancer [135]. Many years on from this discovery and a whole family of transcription factors have now been identified that play important roles in regulating the expression of various genes that mediate a range of processes throughout the body, including the progression of tumour cells.

### 1.4.1 NF-kB family members

Since the discovery of the first described NF-kB factor in 1986 the family has expanded to comprise 5 members which include NF-κB1 (p50/p105), NF-κB2 (p52/p100), RelA (p65), c-Rel and RelB (Figure 1.8A&B) [136]. Each member is structurally linked by the presence of the N-terminal REL Homology Domain (RHD) that is responsible for DNA binding and dimerization [136]. Each member can be further structurally subdivided by the presence or absence of a C-terminal transcriptional activation domain (TAD). The Rel subgroup comprising of RelA, c-Rel and RelB each contain TADs meaning they are transcriptionally active upon synthesis, unlike NF-kB 1 & 2 which do not contain TADs, making them unable to bind DNA directly. The inactive NF-kB 1 & 2 are synthesized into their precursor forms of p105 and p100 respectively and are then proteolysed by the proteasome into mature forms (p50 and p52) [137]. Mature p50 and p52 can then form homodimers or heterodimers, as can each NF-kB member other than RelB which cannot form homodimers [138]. Various dimer complexes are then held inactivated through interactions with the IkB family of proteins [136].

### 1.4.2 Regulation of NF-kB

Members of the NF-kB family are tightly regulated by a group of proteins known as the inhibitors of NF-kB (IkBs) which predominantly work by sequestering NF-kB dimers within the cytoplasm. The family, which consists of IκBα, IκBβ, IκBε, IkBγ and the atypical Bcl-3 are structurally related through a set of ankyrin repeats at their C-terminal motif (Figure 1.8C) [139]. These ankyrin repeats are important for mediating the binding of NF-kB subunits which help sequester them in the cytoplasm through masking the nuclear localization domain found within the RHD [136, 140].

NF-kB stimulation results in phosphorylation of IkB proteins by an IkB kinase (IKK) complex through either the canonical or non-canonical pathways (Figure 1.9). This in turn results in proteasome-mediated degradation of IkBs allowing NF-kB proteins to translocate into the nucleus and become transcriptionally active [139]. The canonical signalling pathway mediates phosphorylation of IkB through a NEMO-dependent activation of the IKK complex which relies heavily on IKKβ-mediated activation and can be stimulated through most physiological NF-kB stimuli [141]. In contrast, the non-canonical pathway is activated through TNF family cytokines and relies on IKKα, and not IKKβ or NEMO to mediate IKK activation and phosphorylation of p100 associated with RelB [141]. IKKα mediated activation also requires NIK which acts as an IKKα-activating kinase as well as a scaffold linking IKKα with p100 [142]. Termination of NF-kB signalling is mediated through newly synthesized IkB proteins which can enter the nucleus and disassociate DNA binding of NF-kB's. Bound NF-kB can then be exported back into the cytoplasm and maintained in their inactivated state [143].

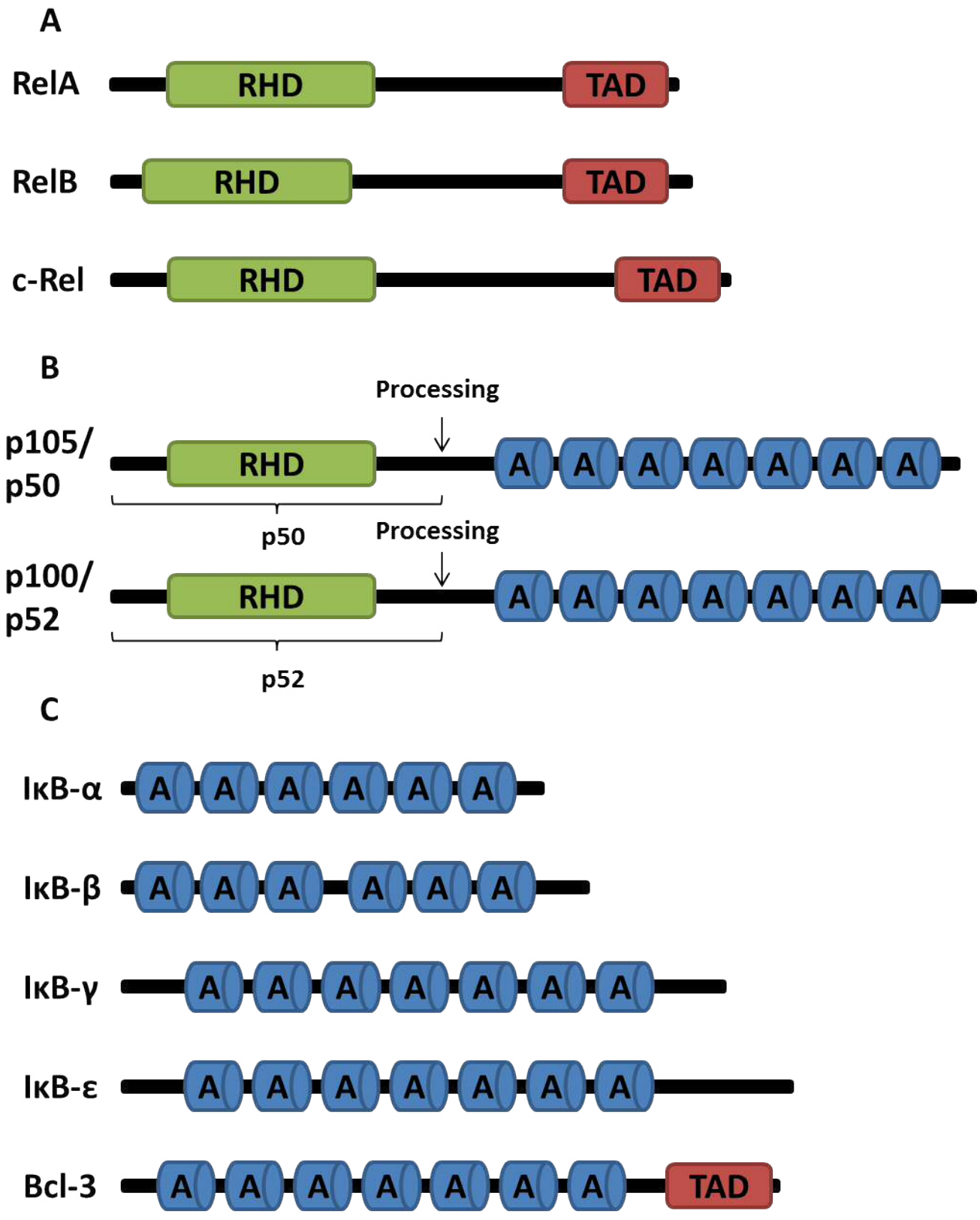


**Figure 1.8- NF-kB family members-** Despite the NF-kB family of transcription factors all sharing a conserved Rel homology domain (RHD) they can be further subdivided two subtypes. **(A)** RelA, RelB and c-Rel all contain a transactivation domain (TAD) however **(B)** p50 and p52 do not and are produced through processing of their precursor forms p105 and p100 respectively. **(C)** The IkB family of regulators each contain a set of several ankyrin repeats (A) with the atypical member Bcl-3 also containing a transactivation domain.

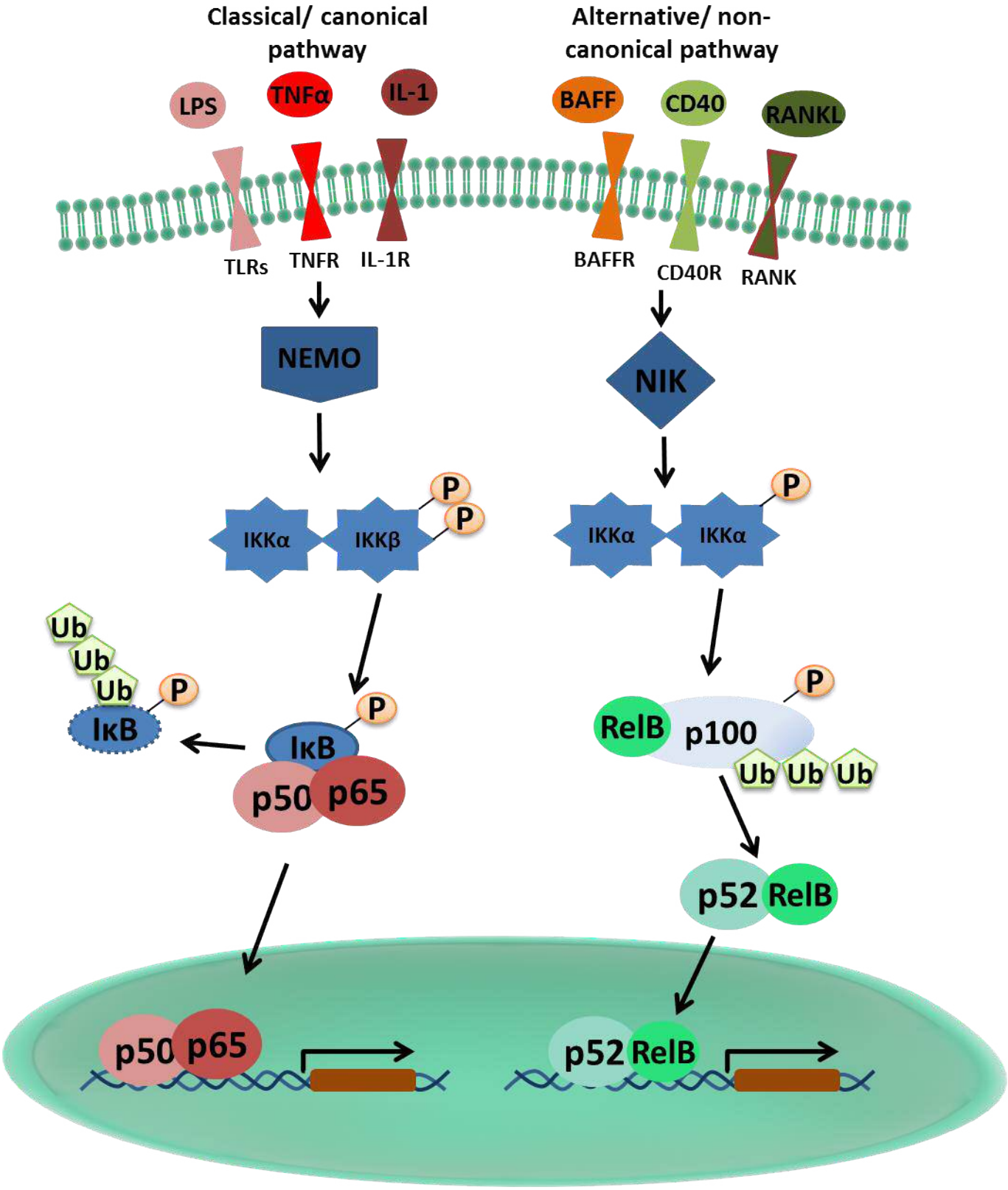


**Figure 1.9- NF-kB signalling pathways-** Activation of NF-kB signalling can be propagated through either the canonical or non-canonical signalling pathways. Activation of the canonical pathway results in the formation of the IKK complex mediated through NEMO that will result in the phosphorylation of IkB complexes that will in turn be removed through proteasome degradation. Loss of IkB binding to NF-kB enables the translocation of NF-kB dimers into the nucleus where they can regulate gene expression. Stimulation of the non-canonical pathway results in a similar IKK complex mediated through NIK that will activate the processing of precursor NF-kB molecules which are then capable of nuclear translocation and proceeding to regulate transcription. (Adapted from [5])

### 1.4.3 NF-kB in cancer development

Aberrant expression of NF-kB has been associated with the development and progression of multiple types of cancers, including breast cancer [144]. The association was first explored through the relationship between inflammation and carcinogenesis, where substantial evidence has shown correlations between NF-kB and inflammation, and a predisposition to cancer [145]. The common view is that increased NF-kB signalling in both premalignant cells as well as cells of the microenvironment, work synergistically to induce the expression of a number pro-tumorigenic genes, such as anti-apoptotic genes, that are required to potentiate cancer development [137]. Inflammation-induced NF-kB activation in tumour microenvironment cells mediates the generation of a number of cytokines such as TNF-α, which in turn stimulates NF-kB in pre-malignant cells inducing gene expression that favors tumour cell development [146, 147]. In addition DNA damage to premalignant cells caused by reactive oxygen species (ROS) produced by NF-kB activated microenvironment cells may further increase NF-kB activity [148].

### 1.4.4 NF-kB and breast cancer progression

In the normal mammary gland, NF-kB signalling has been shown to play an important role in mediating epithelial proliferation, architecture, and branching during post-natal development [149]. It was therefore not surprising when the aberrant expression of NF-kB was discovered in a range of breast cancer cell lines [150]. Both the canonical and non-canonical pathways have been implicated in the progression of breast cancers through the regulation of various processes. The canonical pathway has been implicated in regulating tumour progression by inhibiting apoptosis and initiating proliferation and EMT [144, 151]. Similarly, overexpression of p100/p52 in a transgenic mouse model was shown to induce small areas of hyperplastic growth and was associated with tumour development [152]. Furthermore, both pathways are thought to be required for the self-renewal and the induction of EMT in tumour-initiating cells, with p52 recently implicated with an important regulatory role in cancer stem cells (CSC) in HER2 enriched tumours [153]. The important roles of NF-

kB signalling in cancer progression highlighted here have made it an attractive therapeutic target for the treatment of both primary tumours and metastatic disease.

### 1.4.5 Inhibiting NF-kB signalling in cancer

The use of NF-kB inhibitors to treat cancer progression has seen added importance since the association of NF-kB activation and resistance to chemotherapy, with studies in various cancer types showing NF-kB inhibition to improve the efficacy of these drugs *in vivo* [154-156]. The use of NF-kB inhibitors is therefore an attractive option for use as a stand-alone treatment as well as in combination with other recognized anti-cancer agents. Over 700 inhibitors of NF-kB have been identified ranging from synthetic molecules to viral proteins that can act through general inhibition of NF-kB to more specific inactivation of certain molecules [157].

#### 1.4.5.1 Inhibiting IkB degradation

One well established strategy is to stop proteasome-mediated degradation of IkB proteins and therefore maintain NF-kB proteins inactivated within the cytoplasm. This can be achieved by either inhibiting the activation of the IKK complex or its binding to NF-kB molecules, as well as blocking the 26S proteasome from degrading IkB proteins.

The anti-inflammatory compound BAY 11-7082 is an example of a widely used NF-kB inhibitor which exerts its anti-NF-kB effects through inhibiting the activity of IKK, resulting in reduced degradation of IkB proteins that maintain NF-kB in its inactive form [158]. Inhibition of IKK activation has also been shown to specifically inhibit NF-kB gene expression through loss of IkB degradation [159]. Blocking of proteasome-mediated degradation of IkB results in a similar outcome in maintaining NF-kB within the cytoplasm and compounds such as Bortezomid have shown promising results in treating breast cancer progression, however fears still remain over its non-specificity for NF-kB pathways [160]. Other mechanisms of inhibiting IkB degradation include inhibiting the functions of IKK complex mediator NEMO as well as targeting inducing structural changes to both IKKα and IKKβ [161].

#### 1.4.5.2 Inhibiting NF-kB mediated gene transcription

Other methods of suppressing NF-kB activity include inhibiting phosphorylation, translocation, or DNA binding of NF-kB heterodimers which directly inhibits their ability to activate gene transcription [162]. Blocking of the nuclear translocation of NF-kB dimers has been achieved through the use of the synthetic peptide SN50 which competes within the nucleus for the machinery utilized by p50 for nuclear translocation [163]. This has shown promising anti-tumour responses in different cancer models, however it has also been shown to block the translocation of various other transcription factors [164, 165].

Modulating the nuclear acetylation of activated p65 has seen increased interest as a novel way of inhibiting NF-kB in recent years. Specific acetylation at lysine residues $K^{122}$ and $K^{123}$ has been shown to reduce p65 DNA binding affinity as $K^{221}$ and $K^{310}$ are associated with increased NF-kB target gene transcription, highlighting the various points in which NF-kB may be targeted [166]. Various compounds that mediate p65 acetylation such as gallic acid and Daxx have been identified, however the direct inhibition of DNA binding, which offers the most direct strategy for blocking NF-kB activation, appears to be a more appealing therapeutic approach [161]. One method that can be used to accomplish this is through the use of decoy oligodeoxynucleotides (ODNs) which compete with NF-kB factors for the binding of NF-kB sites on genomic promoters [167]. Despite issues with effective delivery *in vivo,* the use of ODNs in prostate cell lines has shown promising anti-proliferative responses *in vitro*, however its effect on inhibiting NF-kB activity was inconclusive and it has also been shown to inhibit off-target gene expression [168].

#### 1.4.5.3 Other mechanisms of NF-kB inhibition

Various other mechanisms of NF-kB inhibition have been suggested and tested which include the transfer of genes that can suppress NF-kB activation, antioxidants, viral protein inhibition, anti-inflammatories and p53 induction [169-171]. Of these, non-steroid anti-inflammatory drugs (NSAIDs) are thought to be held in high regard as a therapeutic option for breast cancer and

may reduce risk by 20%, however issues regarding the optimal type, dose, and duration of treatment have limited the use of these clinically [172].

Despite the array of compounds that have been identified to target NF-kB signalling, many of these lack specific inhibition to NF-kB, resulting in off-target toxicity through changes to non-NF-kB pathways [157, 173]. Furthermore, global inhibition of NF-kB pathways, which lack selectivity to specific components, can lead to on-target toxicity due to the ubiquitous requirement for NF-kB signalling in multiple tissue types [174]. These issues are highlighted by the fact that despite hundreds of known inhibitors, no NF-kB specific blockers have been approved for human use. It is therefore not surprising that specific modulation rather than complete inhibition of the pathway has emerged as an interesting and promising route for new therapeutics. One target which has shown early promise is B-Cell Lymphoma 3 (Bcl-3), which has the potential to specifically regulate important tumorigenic processes that are reliant on NF-kB activity.

## 1.5 Bcl-3

Bcl-3 is a proto-oncogene that was originally identified as a translocation in the immunoglobulin alpha-locus within a sub-set of B-cell lymphomas [175]. It is an atypical member of the IkB family of NF-kB regulators, as although it shares structural homology with other members it differs in function and predominantly localizes within the nucleus compared to the cytoplasm [176]. Bcl-3 primarily interacts with p50 and p52 homodimers providing the transactivation domain that these complexes lack, and through which it can act indirectly as either a transcriptional activator or repressor [176, 177].

### 1.5.1 Transcriptional regulation via Bcl-3

As previously stated, Bcl-3 mediates NF-kB signalling primarily through the binding of p50 and p52 within the cell nucleus unlike other IkB proteins which sequester NF-kB targets within the cytoplasm. When unphosphorylated Bcl-3 may in fact compete with other IkB proteins and can actively remove p50 from the nucleus; this removal of repressor p50 homodimers from target gene

promoters is thought to allow p65-mediated activator dimer complexes to bind [178]. In a similar manner to p50, Bcl-3 can also inhibit p52 homodimers from DNA binding within the nucleus making it capable of regulating both canonical and non-canonical NF-kB pathways [179].

Bcl-3 phosphorylation facilitates the formation of heterocomplexes with both p50 and p52 through binding within its 7 ankyrin repeats which promotes nuclear stabilization and activates transcriptional co-regulation [180]. Bcl-3-mediated regulation of canonical p50 signalling has been implicated with the regulation of cell proliferation, inflammation and EMT through genes such as iNOS, IL-10 and N-cadherin (figure 1.10) [181-183]. Alternatively Bcl-3/p52 complexes have been shown regulate apoptosis, proliferation and cell adhesion through mediating transcription of Bcl-2, Cyclin D1 and P-selectin respectively (figure 1.11) [184-186]. Interestingly, Bcl-3 has also been shown regulate transcription independently of NF-kB via a proline/serine rich region at its C-terminal [177]. Transcriptional activation can be induced via interactions with c-Jun, c-Fos, CREB-binding protein/p300 and the steroid receptor coactivator-1 (SRC-1) which has been linked with tumorigenesis [187]. Furthermore, Bcl-3 has recently been shown to regulate transcription of the TGF-β signalling pathway through the direct stabilization of SMAD3 in breast cancer [188].

### 1.5.2 Regulation of Bcl-3

Expression of Bcl-3 has been shown to be regulated through various stimuli transcriptionally as well as through a number of post-transcriptional modulators. Multiple regulation pathways help Bcl-3 mediate its various transcriptional functions and can invoke varied responses to Bcl-3 activation.

At a transcriptional level Bcl-3 has been shown to be upregulated by various cytokines such as TNF-α, IL-1, IL-4, IL-6 and IL-10 [189-192]. Furthermore, IL-4 and IL-6-mediated activation of Bcl-3 expression has been shown to be regulated by the direct binding of AP-1 and STAT3 transcription factors respectively to the Bcl-3 promoter [191, 193]. The tumour suppressor p53 has also been shown to negatively regulate Bcl-3 expression and induces a switch from p52/Bcl-3 activator

complexes to p52/HDAC-1 repressor complexes resulting in a repression of cyclin D1 transcription [194]. Interestingly, Bcl-3 has also been found to form an autoregulatory loop to mediate its own expression which can also be induced via NF-kB1 [193, 195].

Post-transcriptionally Bcl-3 can also be regulated by modifications during translation via both integrin signalling and through biomechanical stimulation [196, 197]. Phosphorylation of two C-terminal residues via the protein kinase GSK3 is thought to play an important role in regulating Bcl-3 turnover by targeting PSMB1-mediated proteasome degradation [198, 199]. Furthermore, accumulation of Bcl-3 in the nucleus can also be inhibited through CYLD-mediated deubiquitination resulting in a reduction in both p50 and p52-dependent signalling [200]. Finally, recent evidence has suggested microRNA-mediated regulation of Bcl-3, with miR-125b capable of suppressing Bcl-3 translation in ovarian cancer cells [201].

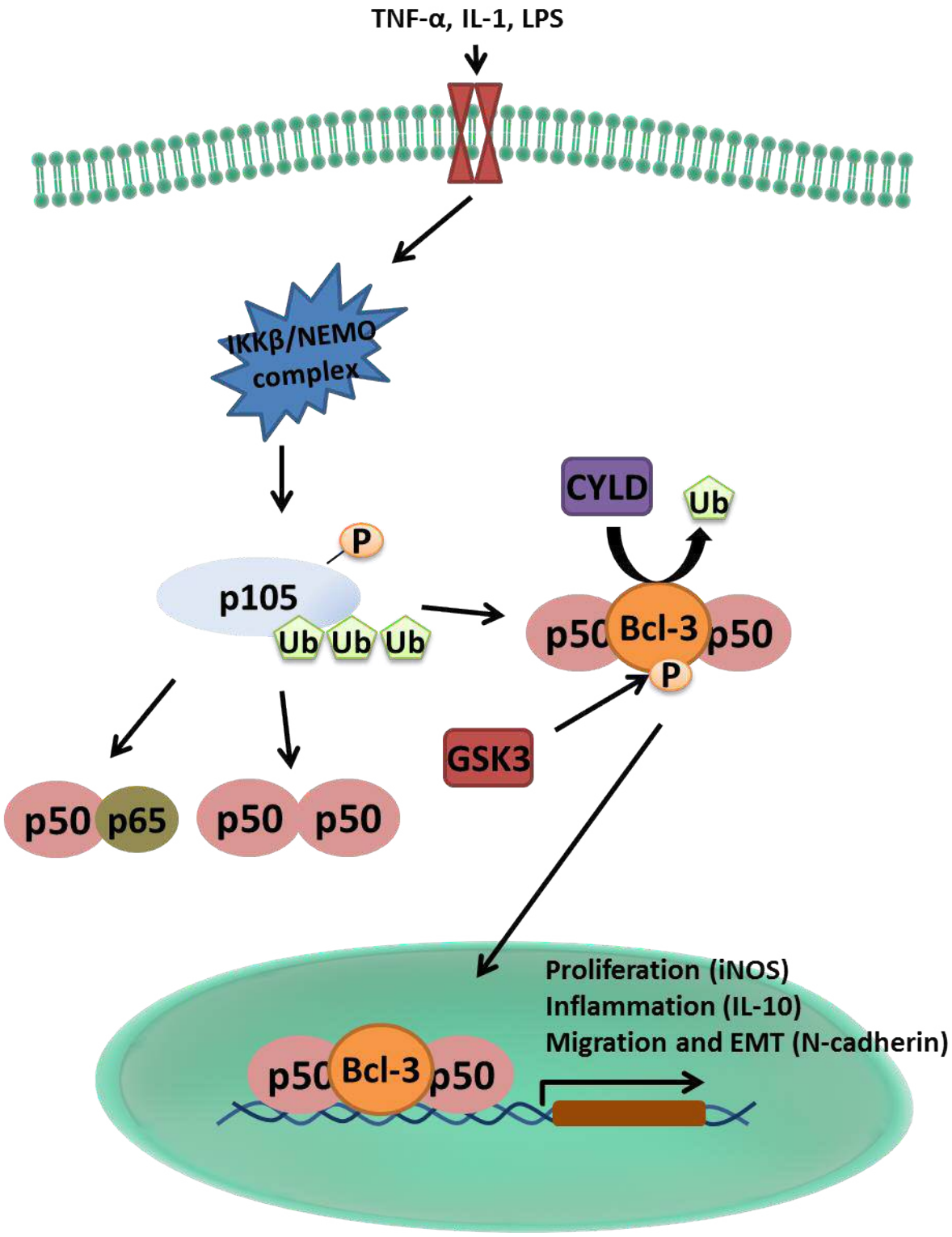


**Figure 1.10- Role of Bcl-3 in canonical signalling**- Stimulation of the canonical signalling pathway results in activation of the IKK complex mediated by IKKβ and NEMO which in turn processes the precursor p105 to p50. This can then form either heterodimers with other NF-kB molecules or homodimers with other p50 molecules. Repressor complexes formed by p50 homodimers are transcriptionally inactive; however the binding of phospho-Bcl-3 provides a transactivation domain and allows them to regulate a diverse array of genes. Bcl-3 itself is also regulated through phosphorylation by GSK3 and ubiquitination by CYLD which can delay proteosomal degradation and nuclear translocation respectively. (Adapted from [3])

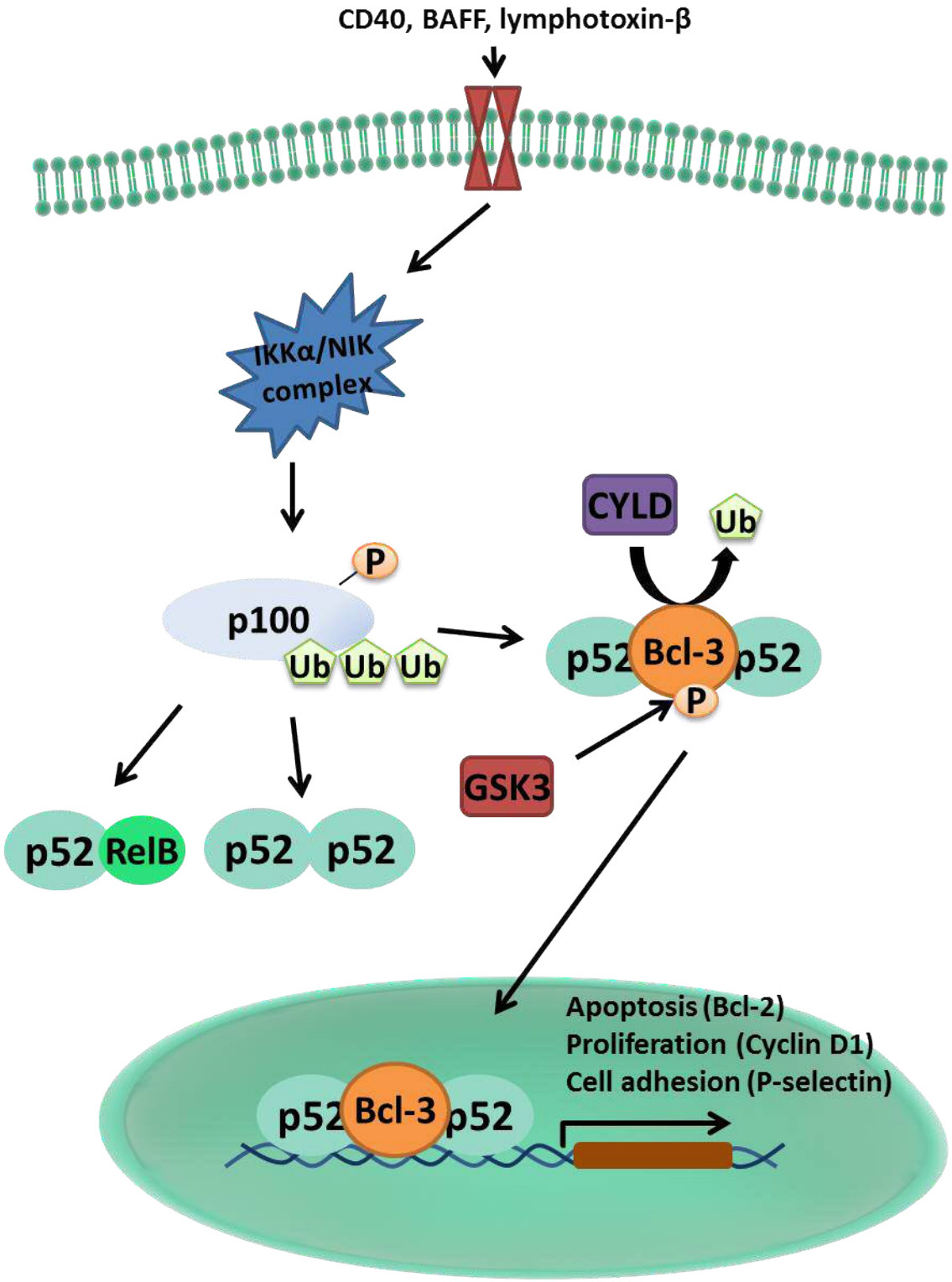


**Figure 1.11- Role of Bcl-3 in non-canonical signalling-** Stimulation of the non-canonical signalling pathway results in activation of the IKK complex mediated by IKKα and NIK which in turn processes the precursor p100 to p52. This can then form either heterodimers with other NF-kB molecules or homodimers with other p52 molecules. Repressor complexes formed by p52 homodimers are transcriptionally inactive; however the binding of phospho-Bcl-3 provides a transactivation domain and allows them to regulate a diverse array of genes. Bcl-3 itself is also regulated through phosphorylation by GSK3 and ubiquitination by CYLD which can delay proteosomal degradation and nuclear translocation respectively.(Adapted from [3])

### 1.5.3 The role of Bcl-3 in cancer

As well as its known association with hematological malignancies, overexpression of Bcl-3 has also been implicated in a number of solid tumours such as nasopharangyeal, ovarian, colorectal and breast cancers [188, 202-204]. Interestingly, the first solid cancer to be associated with Bcl-3 deregulation was breast cancer when Bcl-3 mRNA and protein was shown to be overexpressed in both cell lines and tumours [205]. Furthermore, p52 and Bcl-3 were significantly upregulated within the nucleus of some breast cancers compared to adjacent non-tumorigenic tissues, suggesting they are functionally active [205].

Since the discovery of aberrant Bcl-3 expression in solid tumours, a number of studies have highlighted its importance in regulating cell death and proliferation. The first indication of this came from hematopoietic malignancies in Bcl-3-overexpressing transgenic mice, whereby overexpression was correlated with B-cell expansion and splenomegaly [206]. Inhibition of apoptosis was then attributed to Bcl-3-mediated survival of T cells through blocking of the apoptosis initiator and Bcl-2 family member Bim [207]. This work has since been expanded to show that in breast cancer Bcl-3 can activate Bcl-2 expression through transactivation of p50 and p52 homodimers [186].

Interestingly, Bcl-3 has been shown to be upregulated during DNA damage in MCF-7 breast cancer cells, which through an MDM2 mediated inhibition of p53 activation, can regulate apoptosis [208]. In contrast, during normal physiological conditions Bcl-3 can regulate basal apoptosis in a range of cancer cells through a JNK1-induced regulatory loop that has no role in non-cancerous cells [209]. Furthermore, this resistance to apoptosis in breast cancer cells may be mediated by the Bcl-3-dependent stabilization of the C-terminal-binding protein 1 (CtBP1) through inhibiting its ubiquitination [210].

It was previously stated that Bcl-3 expression can be regulated via STAT3, however it has also been shown that STAT3 can be regulated via Bcl-3 in cervical cancer, with Bcl-3 suppression resulting in a decrease in STAT3 expression [211]. Overexpression of Bcl-3 in this model resulted in

increased proliferation through cell cycle progression [211]. Furthermore, inhibition of Bcl-3 has been shown to inhibit proliferation, induce a G2/M cell cycle arrest, and present a DNA damage response [212]. Proliferation in breast cancer has also been associated with Bcl-3, however in this model co-activation with p52 dimers resulted in increased G1/S cell cycle phase through an increase in cyclin D1 [213]. This can also be linked to p53, which as previously mentioned, can decrease Bcl-3 binding to the cyclin D1 promoter thereby inhibiting its expression [194].

### 1.5.4 Role of Bcl-3 in metastasis

As well as the previously identified roles of Bcl-3 in regulating cell proliferation and cell death it may also have a wider role in mediating metastasis, with nuclear Bcl-3 being associated with metastatic colorectal cancer, thus making it an interesting prognostic marker [202]. Furthermore, recent findings have associated high Bcl-3 expression with a reduced metastasis-free survival which also correlated with increased Bcl-3 levels in cell lines with higher metastatic potential [188].

The association between Bcl-3 and metastatic breast cancer was previously highlighted in a HER2-positive mouse tumour model which suggested a role for Bcl-3 in promoting metastasis but not primary tumour growth [214]. The role of Bcl-3 in promoting metastasis has been independently associated with an increase in cell motility and has recently been attributed to the regulation of TGF-β signalling through the stabilization of SMAD3 [188, 214]. This ability to mediate TGF-β signalling has also raised the question of whether Bcl-3 may also play a role in promoting EMT, however this is yet to be explored in detail.

Together these data have suggested that not only is Bcl-3 important for balancing cell proliferation and death but it can also promote cell migration and metastasis. This suggests that Bcl-3 could potentially play a key role in mediating tumour progression through the regulation of various processes, making it an interesting therapeutic target.

### 1.5.5 Bcl-3 as a therapeutic target for breast cancer

Previous work has shown the role of Bcl-3 in regulating cell death, proliferation, migration and metastasis in breast cancer, however little work has addressed how targeting Bcl-3 may have therapeutic benefits. Suppression of Bcl-3 in ErbB2-positive tumour models resulted in significant reductions in pulmonary metastasis without any disruption to normal cell homeostasis, highlighting the potential for Bcl-3 inhibition as a clinical therapy [214]. These results have since been replicated in a triple-negative tumour model which also showed significant reductions in metastatic burden without affecting primary tumour growth following Bcl-3 suppression [188]. These results demonstrate a potential for targeting Bcl-3 to treat metastatic cancer in one of the most aggressive breast cancer subtypes.

The reduction in metastasis through Bcl-3 inhibition has so far been attributed to a reduction in cell migration which has been replicated *in vitro,* in a number of cell lines, independent of tumour subtype or endogenous levels of Bcl-3 [215]. Interestingly, this phenotype was replicated through inactivating Bcl-3 binding to p50 and p52 dimers through overexpression of a Bcl-3 binding mutant, leading to the hypothesis that small molecule inhibitors could be used to mimic this disruption and may have potential therapeutic benefits [215].

Extensive molecular modelling has uncovered a unique binding pocket on the Bcl-3 protein between ankyrin repeats 6 and 7 which, through virtual screening, has led to the discovery of a novel small-molecule inhibitor with the potential to bind to this pocket and disrupt the binding of Bcl-3 to p50 and p52 subunits [215]. This compound can mimic Bcl-3 RNAi suppression by inhibiting cell migration and NF-kB activity as well as disrupting the binding of Bcl-3 to p50 and p52, which has been analyzed through ELISA assays [215]. This translated *in vivo* to a significant reduction in metastatic tumour burden and showed no signs of adverse toxic effects making it a promising therapeutic option [215].

Despite these promising results little is known about the mechanisms that underlie Bcl-3-mediated metastasis other than a general reduction in cell motility. Therefore, in order to progress the use of small-molecule inhibition of Bcl-3 towards a clinical setting it is important to further elucidate the mechanisms by which Bcl-3 may promote metastasis. A better understanding of how Bcl-3 is regulating metastasis is vital in order to improve our ability to target this process in a therapeutic setting and may also determine whether it can be utilized for treatment of other cancer types.

## 1.6 Project aims and objectives

As previously described, inhibition of Bcl-3 can reduce breast cancer metastasis without affecting primary tumour growth in both HER2 and triple-negative tumour models. Despite this, little is known about how Bcl-3 is regulating metastasis other than a general reduction in cell motility that has not been explored in detail. Therefore, the first aim of this project was to:

- Undertake a detailed evaluation of the migratory phenotype that Bcl-3 is regulating and to understand how this is being altered through Bcl-3 inhibition.

Bcl-3-mediated metastasis has been attributed to a role for Bcl-3 in regulating TGF-β signalling through SMAD3 stabilization which is a known regulator of a key initiating step in metastasis, EMT. As the role of Bcl-3 in regulating EMT in breast cancer is yet to be explored the second aim of this project was to:

- Establish a cell based model of EMT and MET so that the role of Bcl-3 in this system could be characterised, as well as determining the effects of Bcl-3 inhibition on this process.

As previously mentioned the use of small-molecule inhibitors has the potential to be used as a therapeutic option for the treatment of metastatic breast cancer. Therefore, the final aim of this project was to:

- Characterise a new class of novel Bcl-3 inhibitor analogues and compare how their function compares with siRNA inhibition of Bcl-3 in the regulation of metastasis, as well as testing the efficacy of using these compounds in different cancer types.

# Chapter 2:
# Materials and methods

# 2 Materials and methods

## 2.1 Cell culture

### 2.1.1 Cell Lines

The human breast cancer cell lines MDA-MB-231 & MCF-7 were a gift from Dr. Julia Gee (Department of Pharmacy, Cardiff University); and the mutant MDA-MB-231 cell line overexpressing Bcl-3 was generated by William Yang using a construct gifted to the lab by Dr Alain Chariot, (Interdisciplinary Cluster for Applied Genoproteomics, Liege). The human breast cancer cell lines MDA-MB-436 and HCC1954 were purchased from ATCC, UK and the mouse mammary cell line EpH4 were provided by Dr Carla Oliveira (Ipatimup, Porto University). Finally, human breast cancer line BT-549, prostate cancer cell line PC-3 and colorectal cell line RKO, were all used in collaboration with the Life Sciences Research Network Wales cancer metastasis modelling platform headed by Professor Wen G. Jiang (Cardiff University). All cell lines were maintained in RPMI including GlutaMAX (Invitrogen) supplemented with 10% foetal bovine serum (Invitrogen) and incubated at 37°C and 5% $CO_2$. Cells were grown in 5 mL for T25 or 10 mL for T80 tissue culture flasks (Nunc, Leics, UK) with growth media changed every 2-3 days and cells passaged regularly when confluent.

### 2.1.2 Passaging cells

When cells became 80-90% confluent they were split at a ratio between 1:6-1:10 depending on the cell line (Table 2.1). To remove cells, all media was aspirated and cells were washed with PBS (Invitrogen) to remove any remaining media. Either 1 mL for a T25 or 2 mL for a T80 flask of 0.25% trypsin/EDTA (Invitrogen) was added to the flask and left to incubate at 37°C for 5-10 min until cells had become detached. Cell detachment was confirmed using microscopic observation, before adding 4 mL for a T25 or 6 mL for a T75 of normal growth media to inactivate trypsin activity. Cells were then split at an appropriate ratio, with remaining cells carefully discarded, re-plated for cell based assays, or harvested for analysis.

| Cell line | Tumour type | Molecular subtype | p53 status | Passaging ratio |
|---|---|---|---|---|
| **MDA-MB-231** | Human breast | TNBC | Mutant | 1:10 |
| **MDA-MB-436** | Human breast | TNBC | Mutant | 1:6 |
| **MCF-7** | Human breast | ER positive | WT | 1:10 |
| **HCC1954** | Human breast | Her2 positive | Mutant | 1:6 |
| **BT-549** | Human breast | TNBC | Mutant | 1:8 |
| **EpH4** | Normal mouse breast | NA | WT | 1:8 |
| **PC-3** | Human prostate | NA | Mutant | 1:8 |
| **RKO** | Human colorectal | NA | WT | 1:8 |

**Table 2.1- List of cell lines used in this project**

### 2.1.3 Long term storage

Low passage number cell lines were frozen and cryo-stored in liquid nitrogen. Cells were detached from culture flasks as previously described, however following trypsin inactivation cells were centrifuged at 1200 rpm for 5 min at room temperature. The supernatant was removed and resuspended in complete growth medium containing 10% dimethyl sulfoxide (DMSO; Sigma, UK) and aliquoted into 1 mL cryo-tubes (Nunc). Cells were then slowly frozen at -80°C in a cryo-freezing vessel containing isopropanol (Fischer Scientific) for 24h before being transferred to liquid nitrogen storage.

### 2.1.4 Raising cells from storage

Cells stored in liquid nitrogen were transferred into dry ice before being thawed in a water bath at 37$^{o}$C until 90% defrosted. Cells were then transferred to a 15 mL falcon (Nunc) containing 3 mL of complete growth medium and centrifuged at 1200 rpm for 5 min. The supernatant was then removed, with the pelleted cells resuspended in normal growth medium before being plated into a T25 culture flask.

### 2.1.5 Cell Seeding

Following cell detachment using trypsin, non-passaged cells were collected in a 15 mL falcon tube and pelleted at 1200 rpm for 5 min before being resuspended in 500 µL of growth medium. To ensure correct cell seeding densities, cells were counted using a Luna automated cell counter (Logos Biosystems). Single cells were then counted automatically by adding 10 µL of cell suspension to the Luna cells counting slides (Logos Biosystems) and inserting slides into the Luna cell counter. Cells were then diluted accordingly with culture medium and seeded into appropriate culture plates depending on the assay being performed (Table 2.2). Although seeding densities varied between assays, in general 1 x $10^5$ cells/mL were seeded for 3 day experiments while for longer 7 day experiments 1 x $10^4$ cells/mL were seeded.

| Plate | Relative Surface Area | Volume (µL) |
|---|---|---|
| **96-well (Costar)** | 0.2 | 100 |
| **24-well (Costar)** | 1 | 500 |
| **12-well (Costar)** | 2.5 | 1000 |
| **6-well (Costar)** | 5 | 2000 |
| **T25 (Nunc)** | 12.5 | 5000 |

**Table 2.2- List of plate formats and normal culture media volumes**

## 2.2 Transfection and compound treatment of cell lines

### 2.2.1 Single RNA transfection

In order to knockdown Bcl-3 in respective cell lines, a mixture of 4 small interfering RNAs (siRNA) each designed to target Bcl-3 were transfected into selected cells (ON-Target plus SMART pool, Dharmacon). A pool of control RNAs (scRNA) designed to have minimal effect on human gene expression was used to control for transfection (ON-Target plus SMART pool, Dharmacon). Each

siRNA pool was resuspended according to the manufacturer protocol in 250 µL of RNA-free water to obtain a 20 µM stock concentration.

Transfection was performed on 70% confluent adherent cells using lipofectamine 3000 (Invitrogen) and serum-free Opti-MEM (Invitrogen). The different volumes of each reagent were determined based on the culture medium volume of different culture plates shown in Table 2.3.The appropriate volume of siRNA was diluted in Opti-MEM in a 1.5 mL eppendorf (VWR) before the appropriate volume of lipofectamine 3000 was added. The siRNA mixture was then vortexed for 15 sec and left to incubate for 5 min at room temperature. Lipofectamine-siRNA complexes were then added to adherent cells in appropriate growth medium to give a final siRNA concentration of 20 nM and cultured for 48h before being harvested.

### 2.2.2 Double RNA transfection

In order to knockdown Bcl-3 in conjunction with p53, p15 or C/EBPβ, selected cells were transfected with SMART pool siRNAs targeting a specific gene of interest (Table 2.4). Adherent cells at 40-50% confluency were transfected with either Bcl-3 targeting siRNA or scRNA as previously described for 24 h. Growth medium was then removed and a second ON-Target pool of siRNA's, designed to knockdown the appropriate secondary target, was added following the same protocol. Cells were then left for 5 days before being harvested.

| Tissue culture plate | Culture medium | Opti-MEM medium | Final siRNA concentration | Volume of 20 µM siRNA | Lipofectamine 3000 |
|---|---|---|---|---|---|
| **12-well** | 1.125 mL | 125 µL | 20 nM | 1.25 µL | 2.5 µL |
| **6-well** | 2.25 mL | 250 µL | 20 nM | 2.5 µL | 5 µL |
| **T25 plate** | 4.5 mL | 500 µL | 20 nM | 5 µL | 10 µL |

**Table 2.3- Transfection concentrations for siRNA**

| siRNA | Target sequence (5'-3') | Catalogue number |
|---|---|---|
| Human control ON-Target plus SMART pool | UGGUUUACAUGUCGACUAA | Dharmacon D-001810-10 |
| | UGGUUUACAUGUUGUGUGA | |
| | UGGUUUACAUGUUUUCUGA | |
| | UGGUUUACAUGUUUUCCUA | |
| Human Bcl-3 ON-Target plus SMART pool | AGACACGCCUCUCCAUAUU | Dharmacon L-003874-00-0005 |
| | GGCCGGAGGCGCUUUACUA | |
| | GCGCAAAUGUACUCCGGCA | |
| | GCCGGGAGCUCGACAUCUA | |
| Human p53 ON-Target plus SMART pool | GAAAUUUGCGUGUGGAGUA | Dharmacon L-003329-00-0005 |
| | GUGCAGCUGUGGGUUGAUU | |
| | GGAGAAUAUUUCACCCUUC | |
| | GCAGUCAGAUCCUAGCGUC | |
| Human p15 ON-Target plus SMART pool | GCACUUAUGCAGUAAAUUA | Dharmacon L-003245-00-0005 |
| | CUUAAGCACUCAAUCAUUA | |
| | ACUAGUGGCUCUCAGUUAA | |
| | GCACUGCUUUGGGAUUUAA | |
| Human C/EBPβ ON-Target plus SMART pool | CCUCGCAGGUCAAGAGCAA | Dharmacon L-006423-00-0005 |
| | CUGCUUGGCUGCUGCGUAC | |
| | GCGCUUACCUCGGCUACCA | |
| | GCACCCUGCGGAACUUGUU | |

**Table 2.4- Sequences of siRNA used in this project**

### 2.2.3 Transfection of reporter plasmids

For NF-kB luciferase assays (see section 2.3.5), 1 x $10^4$ cells were seeded into 12-well plates (Costar) in normal growth media and left to adhere overnight. After siRNA inhibition each well was transfected with 900 ng of 3x κB luciferase plasmid and 100 ng pcDNA 3.1-LacZ plasmid using appropriate amounts of lipofectamine 3000, p3000 reagent and Opti-MEM (Table 2.5). After 24h of incubation cells were harvested for analysis.

| Transfection Reagent | Volume per well |
|---|---|
| **DNA** | 1000 ng |
| **Lipofectamine 3000** | 2 μL |
| **p3000 reagent** | 4 μL |
| **Opti-MEM** | 100 μL |

**Table 2.5- Luciferase reporter transfection volumes**

### 2.2.4 Compound treatments

A number of novel small-molecule inhibiters designed to block the interaction of Bcl-3 to p50 and p52 homodimers were synthesised by Cinzia Bordoni, Cardiff University, and supplied in powder form at room temperature. Each compound was diluted in an appropriate amount of fresh DMSO (Sigma) to a stock concentration of 10 mM (Table 2.6). Compounds were then aliquoted and frozen at -20$^{o}$C until used, with compounds disposed of after being freeze thawed 2 times. For cell treatments each compound was diluted in the appropriate volume of normal growth media to the required concentration, with fresh DMSO also diluted at the same ratio for vehicle treated controls.

| Compound | Molecular Weight | DMSO volume per mg | Final concentration |
|---|---|---|---|
| **CB-1** | 401.43 | 249.11 µL | 10 mM |
| **CB-14** | 401.43 | 249.11 µL | 10 mM |
| **CB-18** | 387.86 | 257.82 µL | 10 mM |
| **CB-23** | 419.42 | 238.42 µL | 10 mM |
| **CB-30** | 389.36 | 256.83 µL | 10 mM |
| **CB-35** | 389.40 | 256.80 µL | 10 mM |
| **CB-36** | 384.43 | 260.13 µL | 10 mM |
| **CB-42** | 403.47 | 247.85 µL | 10 mM |
| **CB-43** | 403.48 | 247.84 µL | 10 mM |
| **CB-44** | 385.20 | 259.61 µL | 10 mM |
| **CB-45** | 414.47 | 241.27 µL | 10 mM |
| **CB-46** | 384.45 | 260.11 µL | 10 mM |
| **SD-2** | 367.20 | 272.33 µL | 10 mM |
| **SD-5** | 384.20 | 260.28 µL | 10 mM |
| **SD-9** | 378.85 | 263.96 µL | 10 mM |

**Table 2.6- List of novel Bcl-3 inhibitors**

### 2.2.5 EMT stimulation

To assess the role of Bcl-3 in EMT, epithelial MCF-7 cells were stimulated into EMT using StemXVivo media supplement (R&D systems), which contains a mixture of recombinant proteins and neutralising antibodies (Table 2.7). Cells were seeded in either 6-well plates or T25 dishes at a concentration of 1 x $10^4$ cells/mL in 2 or 4 mL of growth media respectively. Attached cells were then treated with 20 µl or 40 µL of 100X StemXVivo to make a final 1X concentration with cells left to culture for 2 days before media was replaced with fresh EMT inducing supplement. After a further 3 days cells of culture cells were harvested for endpoint assays.

| **StemXVivo media supplement contents** |
|---|
| **Recombinant human Wnt-5a protein** |
| **Recombinant human TGF-beta1 protein** |
| **Anti-Human E-cadherin antibody** |
| **Anti-Human sFRP-1 antibody** |
| **Anti-Human Dkk-1 antibody** |

**Table 2.7- StemXVivo supplement components**

## 2.3 Cell based assays

### 2.3.1 Migration assays

#### 2.3.1.1 Fluoroblok migration assay

For assessing the amoeboid-like migratory capacity of human cancer cell lines and for high throughput screening of small molecule inhibitors, Fluoroblok migration assays (Corning) were used. After appropriate experimental pre-treatment of cells as defined by individual experiments, cells were harvested and suspended in phenol red free growth medium (Invitrogen) without FBS. After diluting cells to a concentration of 1 x $10^5$ cells/mL, 50 µL per well was seeded into the top chambers of a 96-well Fluoroblok culture plate (Corning). To stimulate chemotaxis migration across the membrane, 200 µL of phenol red free growth medium with 10% FBS was added to the bottom chambers. After 24h of incubation the top and bottom chambers were detached and the growth medium removed from the bottom wells by shaking into a waste container. The top chamber was then carefully reassembled onto the bottom chamber and 200 µL of 1 µM Calcein AM (eBioscience) in PBS was added to the bottom wells and incubated for 1h at 37$^o$C. After incubation the fluorescence intensity of each well was read at 500 nm from the bottom of the plate using a Clariostar plate reader (BMG Labtech).

#### 2.3.1.2 Wound-healing assay

For assessing the collective migratory potential of human cancer cell lines after Bcl-3 inhibition, wound-healing assays were performed. Cells were seeded at 1 x $10^5$ cells/well in 12-well plates and left to adhere overnight. When cells reached 70-80% confluency they were treated with selected compounds or transfected with siRNA and incubated for 48h. Three separate wounds were created on confluent cell monolayers using P10 pipette tips (Anachem) before media was gently removed and cells washed with PBS. Fresh media, supplemented with compounds if required, was added to appropriate wells before 4 random marks per well were made on the bottom of the plate, using a permanent marker to define the areas to be monitored. Pictures were then taken on an

inverted microscope (Leica) at each of the 4 different fields of view before cells were left to incubate for the appropriate length of time (8h for MDA-MB-231 and 24h for MCF-7 cells). Final pictures were then taken at the same positions as previously marked before images were analysed using ImageJ to measure changes in the total area covered by cells.

#### 2.3.1.3 Single cell migration assays

To assess the ability of individual cancer cells to migrate in a single cell, mesenchymal-like manner, real-time single cell migration assays were performed. Cells were seeded into 6-well plates at a density of 1 x $10^5$ cells/mL and left to adhere overnight before being treated with selected compounds or transfected with siRNA for 48h. Cells were then removed, counted and re-seeded in Leibovitz's L-15 growth medium (Invitrogen), supplemented with compounds if needed, at a low density of 5 x $10^4$ cells/well into 12-well plates. Once cells had adhered overnight, they were placed into a time-lapse incubation chamber (Leica) pre-warmed to 37$^o$C with 5% $CO^2$ and left to equilibrate for 1h. Each well was then marked at 4 different locations selected at random using the mark and find software on the time-lapse (Leica) before cells were monitored over an 18h period with photos taken automatically every 10 min until stopped.

The first 50 images, equivalent to an 8h timecourse, were selected and exported as Tiff images which were then converted into an 8-bit grayscale image sequences using imageJ. Image sequences were then uploaded into CellTracker image processing software and analysed semi-automatically. For analysis, a minimum of 10 cells per image sequence were selected at random and monitored throughout the sequence, with any dividing cells removed from the data set, and any tracks not-matching cell movement manually adjusted. Once every tracked cell had been checked statistics were exported and analysed by taking the average of each cell movement for individual image sequences.

#### 2.3.1.4 ECIS migration assay

To compare the migratory potentials of cancer cell lines from different tumour types Electronic Cell-substrate Impedance Sensing (ECIS) assays were performed, which electronically measures cellular changes from wound-healing assays in a fully automated system. In this system cells are grown across small gold electrodes that transmit a weak AC signal which is altered through cellular changes. Before cells were detached and counted, 200 µL of normal growth media was added to each well of 96-well ECIS plates (Ibidi) and added onto the ECIS system (Ibidi) to stabilise. Cells were then removed and counted before being diluted to a concentration of 1.2 x $10^6$ cells/mL in normal growth media. Once the plate had stabilized, media was removed and 100 µL of cell suspension was added to individual wells before a further 100 µL of growth media, containing 2X the required concentration of selected compounds, was added to appropriate wells. ECIS plates were then placed back into the ECIS system inside a 37$^o$C incubator with 5% $CO^2$. Wounds were set to be automatically created after 8 and 18h of incubation using 20V of electricity to remove cells growing on top of the electrodes. Each plate was monitored at multiple frequencies every 20 min, over a 24 h period, to track the movement of cells back across the electrodes. Data was analysed by monitoring changes in resistance (ohm) for 5 h post wound creation.

### 2.3.2 Cell adhesion assays

#### 2.3.2.1 Cell-substrate adhesion assay

To assess the effect of Bcl-3 inhibition on cell-substrate adhesion the ECM-screening kit (Merck Millipore) was used, which includes five 96-well plates coated with either fibronectin, vitronectin, laminin, collagen I, or collagen IV. Wells pre-coated with a specific ECM substrate were rehydrated with 200 µL of PBS for 15 min at room temperature. During this time pre-treated cells based on individual experiments were removed gently using PBS/EDTA (Lonza) and counted before being diluted to 1 x $10^6$ cells/mL in normal growth medium. Once substrates had been rehydrated PBS was removed and 100 µL of cell suspension was added to each well for 1h at 37$^o$C in 5% $CO^2$ to

allow cells to adhere. After incubation wells were very carefully washed with 200 µL of PBS twice to remove unattached cells, before remained wells were fixed and stained with 100 µL of crystal violet/ethanol solution (Sigma) for 15 min at room temperature. Crystal violet was then removed and wells were washed with water three times, before 50 µL of 10% glacial acetic acid (Sigma) was added for 5 min at room temperature under gentle agitation. Fluorescence intensity was then measured at 570 nm using a Clariostar plate reader.

#### 2.3.2.2 Slow aggregation assay

In order to test the effect of Bcl-3 inhibition on cell-cell adhesion the slow aggregation assay was used. On the day of the assay 96-well plates were coated with Bacto-agar (BD Biosciences) solution, which was made by dissolved 100 mg of agar in 15 mL sterile Ringer's salt solution (Fisher) in a glass flask and boiling several times in the microwave. Once the solution had cooled to 40-50$^{o}$C, 50 µL of agar solution was added to each well and incubated at 4$^{o}$C on a flat surface for 1h. Whilst the agar was setting pre-treated cells were detached, counted and prepared as a single cell suspension of 1 x $10^5$ cells/mL in normal growth medium. Once agar plates had set, 200 µL of cell suspension was added to agar coated wells and if necessary selected compounds added. Plates were incubated at 37$^{o}$C with 5% $CO_2$ for 48h to allow cell-cell adherence, with cell aggregates evaluated under an inverted microscope. Results were quantified by automated measurements taken using a GelCount plate reader and software (Oxford Optronix).

### 2.3.3 Colony formation assay

To assess the ability of individual cells to survive, proliferate, and expand into small colonies the colony formation assay was performed. Cells were seeded at low density of 125 cells per/mL in 6-well plate format, in normal growth medium, and left for 8 days. To quantify colonies, media was removed and cells gently washed with PBS before being stained with crystal violet/ethanol solution for 15 min at room temperature. The crystal violet solution was then removed before cells were washed twice with PBS and if necessary under running water to remove any excess solution.

Colonies were then either counted manually or automatically using a GelCount plate reader and software set to count colonies of sizes between 100-1000 μm.

### 2.3.4 Cell titre blue assay

To determine cell viability after Bcl-3 inhibition the Cell Titre Blue assay (Promega) was used, which measures the ability of viable cells to convert resazurin into resorufin, a fluorescent product that can then be quantified. Cells to be analysed were plated into 12-well plates and on the day of analysis, 20 μL of Cell Titre Blue reagent (Promega) was added for every 100 μL of growth medium in each well. After 1h of incubation at $37^{O}C$ in 5% $CO^{2}$ fluorescence intensity was measured at 560/590 nm using a ClarioStar plate reader.

### 2.3.5 NF-kB reporter assays

NF-kB reporter assays were performed to analyse the NF-kB activity of cells previously transfected with luciferase-NF-kB reporter after Bcl-3 inhibition (see 2.2.3). On the day of analysis cells grown in 12-well plate format were lysed with 350 μL/well of Glo-lysis buffer (Promega) and incubated on a rocker for 10 min to facilitate complete lysis. To measure LacZ activity as a transfection efficiency control, 50 μL of lysate from each well was removed, transferred to a white bottomed 96-well plate with 50 μL of Beta-Glo substrate (Promega), and incubated for at least 20 min at room temperature. Subsequently, another 50 μL of lysate was added to a different white walled plate with 50 μL of Bright-Glo luciferase substrate (Promega), which was assessed immediately for luminescent activity. Each plate was read using the Clariostar plate reader (BMG labtech) before luciferase activity was normalized against LacZ activity.

### 2.3.6 SA-β -gal assay

To determine cellular senescence the activity of senescence-associate β-galactosidase (SA-β-gal), which is a hallmark of senescent cells, was determined using a cell senescence assay (Merck Millipore). On the day of analysis cells grown in 12-well plate format were washed with 1 mL of PBS before being fixed with 500 μL of 1X fixation solution at room temperature for 15 min. Fixation

solution was then removed and cells washed 2X with 1 mL of PBS, before 1 mL of freshly prepared SA-β-gal detection solution containing: 100 µL of solution A, 100 µL of solution B, 25 µL of X-Gal and 775 µL of PBS was added. Cells were then incubated at 37$^{o}$C protected from light overnight before detection solution was removed and cells washed 2X with 1 mL of PBS. SA-β-gal activity was then analysed by counting the number of positively stained cells using bright field microscopy (Leica).

### 2.3.7 Flow cytometry

#### 2.3.7.1 DAPI cell cycle

For analysis of cell cycle progression flow cytometry was performed using the nuclear marker DAPI to determine the DNA content of individual cells which was used to determine the cell cycle stage of cells. On the day of analysis cells were harvested, counted and diluted in PBS to equal cell numbers up to 1 x $10^{6}$ cells/mL. Cells were then pelleted again by centrifugation for 5 min at 1200 rpm before being resuspended in DAPI solution containing 5 µg/mL DAPI (ThermoFisher scientific) in 0.01% IGEPAL CA-630 (Sigma) in PBS and incubated for 5 min at room temperature. Cells were then placed on ice and covered from light until analysed.

To analyse DAPI stained cells, each sample was filtered through a 40 µm cell strainer (BD Biosciences) into a flow cytometry collection tube (BD Biosciences) to form a single cell suspension. Flow cytometry was performed on a BD LSRFortessa flow cytometer (BD Biosciences) and analysed using FlowJo analysis software. Cells were gated by FSC-area/SSC-area and by FSC-area/FSC-height to obtain a single cell population and to remove artefacts and doublets. Single cells were then analysed by histogram plots using DAPI-area to determine the DNA content of cells.

#### 2.3.7.2 Annexin V apoptosis assay

To analyse the levels of early and late apoptotic cells in differentially treated cell lines the annexin V apoptosis assay (ThermoFisher scientific) was used to detect levels of external phosphatidylserine on apoptotic cells. On the day of analysis cells were harvested, pelleted and

washed in cold PBS before being recentrifuged. Washed cells were resuspended in 100 µL of 1X annexin-binding buffer and counted. Cells were then diluted in 1X annexin-binding buffer to 1 x $10^6$ cells/mL, with 100 µL of diluted cell suspension used per assay. To 100 µL of cells, 5 µL of FITC annexin V was added and left to incubate for 15 min at room temperature. After the incubation period a further 400 µl of 1X annexin-binding buffer was added along with 5 µL of 5 µg/mL DAPI in PBS, with cells mixed and kept on ice for a minimum of 5 min before analysis. Cells were then analysed by flow cytometry using a BD LSRFortessa flow cytometer and analysed using FlowJo analysis software. Cells were gated by FSC-area/SSC-area and by FSC-area/FSC-height to obtain a single cell population and to remove artefacts and doublets. Single cells were then gated based on the expression of green-FITC conjugated to annexin V and DAPI expression to determine cells that were either alive, dead, early apoptotic or late apoptotic.

## 2.4 Protein analysis

### 2.4.1 Immunofluorescence

For analysis of protein expression and localisation immunofluorescence staining was performed on fixed cells. Cells were grown on glass coverslips in 6-well plates that had been sterilized with 100% ethanol and left to air-dry under ultraviolet light. On the day of analysis cells were washed with PBS to remove dead cells and fixed in 4% paraformaldehyde (PFA) (ThermoFisher scientific) for 20 min. Following fixation, PFA was removed with cells subject to 3 x 5 min PBS washes. Individual coverslips were then moved into 24-well plates in PBS before being permeabilized with 0.2% triton-x-100 (Sigma)in PBS for 5 min and then blocked for 30 min with 1% BSA (Sigma) in PBS/T (10 PBS tablets in 1 L water and 1 mL of tween 20). Cells were then incubated with primary antibody diluted in 1% BSA/PBST solution overnight at 4$^{o}$C before being removed and washed 3X with PBS. A fluorescence-conjugated secondary antibody (Abcam) was then added to cells alongside phalloidin conjugated with atto-565 (Sigma) in 1% BSA/PBST for 1 h at room temperature covered from light. Secondary antibody was then removed and cells washed 3X with PBS before being

incubated with 5 µg/mL DAPI nuclear stain for 10 min. After 2 washes with PBS coverslips were dipped into dd$H_2O$ and mounted using Mowiol solution (Sigma).

| Antibody | Dilution | Species | Origin |
|---|---|---|---|
| **E-cadherin (610182)** | 1:200 | Mouse | BD Biosciences |
| **Twist (ab50887)** | 1:500 | Mouse | Abcam |
| **p21 (F-5)** | 1:200 | Mouse | Santa Cruz |
| **p15 (ab94688)** | 1:200 | Rabbit | Abcam |
| **Anti-mouse 488** | 1:200 | Goat | Abcam |
| **Anti-rabbit 488** | 1:200 | Goat | Abcam |

**Table 2.8- List of antibodies used for immunofluorescence**

### 2.4.2 G-LISA assays

#### 2.4.2.1 Lysate preparation

To determine changes in Rho-GTPase activity after Bcl-3 inhibition, G-LISA GTPase activation assays (Cytoskeleton) were performed. Lysates from pre-treated cells grown on 6 cm dishes (Nunc) were harvested on ice by removing growth medium and washing cells with 4 mL of ice cold PBS. After remaining PBS was aspirated, 250 µL of lysis buffer including protease inhibitor (Cytoskeleton) was added before cells were removed using cell scrapers (ThermoFisher Scientific). For protein quantification, 10 µL of cell lysate was added to 290 µL of precision red protein detection reagent (Cytoskeleton) in a clear 96-well plate (Nunc). The remaining lysates were moved into 1.5 mL eppendorfs and snap frozen in liquid nitrogen before being stored at -80$^{o}$C until used. For protein quantification, samples were incubated for 1 min at room temperature before absorbance was read

at 600 nm using a ClarioStar plate reader. Protein concentration was determined by multiplying absorbance by 3.75 to give a concentration in mg/mL. Each GTPase assay was performed separately using fresh lysates in triplicate using optimized reagents provided in each kit.

On the day of analysis 100 µL of ice cold water was added to the appropriate number of wells required, in sets of 8-well strips placed into a strip holder on ice, with the remaining strips stored at 4$^{o}$C for future experiments. Snap frozen lysates were then thawed in a water bath at room temperature and immediately placed on ice before protein concentrations were equalized in ice-cold lysis buffer. Water was then removed from each well by vigorously flicking the solution out into a waste container followed by 7 vigorous pats onto paper towels before placing strips back onto ice. Equalized protein lysates were then immediately added to each well, with 50 µL added per well, along with 50 µL of lysis buffer as a blank and 50 µL of Rac1 positive control (Cytoskeleton). Strip plates were then immediately shaken on an orbital microplate shaker (Eppendorf) for 30 min at 400 rpm and 4$^{o}$C.

#### 2.4.2.2 Antigen retrieval and antibody incubation

After 30 min the solution was removed from each well and washed 2X with 200 µL of wash buffer at room temperature using a multichannel pipette (Eppendorf). Liquid was removed by vigorously flicking and patting onto paper towel before immediately adding 200 µL of antigen presenting buffer (Cytoskeleton) into each well and incubating at room temperature for exactly 2 min. Buffer was flicked out and wells washed 3X with 200 µL of wash buffer. After the final wash the appropriate primary antibody was diluted in antibody dilution buffer (Table 2.9), with 50 µL added per well and left to incubate in an orbital microplate shaker at 400 rpm for 45 min at room temperature. Following this, primary antibody was removed and wells washed 3X with 200 µL of wash buffer before a secondary HRP-conjugated antibody was diluted appropriately (Table 2.9), with 50 µL added to each well and placed in an orbital microplate shaker at 400 rpm for 45 min at room temperature.

#### 2.4.2.3 HRP Detection

Immediately prior to the end of secondary antibody incubation the detection solution was made up by adding equal volumes of HRP detection reagents A and B (Cytoskeleton). Secondary antibody was then removed and wells washed with 3X 200 µL of wash buffer before 50 µL of the mixed HRP detection reagents was added per well and incubated at room temperature for 20 min. To stop the detection reagents 50 µL of HRP stop buffer was added to each well before the absorbance of each well was measured at 490 nm using a Clariostar plate reader.

| GTPase | Primary antibody dilution | Secondary antibody dilution |
|---|---|---|
| **RhoA** | 1:250 | 1:62.5 |
| **Rac1** | 1:50 | 1:100 |
| **Cdc42** | 1:20 | 1:62.5 |

**Table 2.9- Antibody dilution ratios (Cytoskeleton)**

## 2.5 RNA analysis

Prior to working with RNA all equipment and work surfaces were cleaned using RNAseZAP (Ambion) to prevent contamination from RNAses.

### 2.5.1 RNA extraction

Cultured cells were pelleted via centrifuge at 1200 rpm for 5 min before being resuspended in 350 µL RLT buffer (Qiagen) and placed on ice for immediate extraction or frozen at -80$^{o}$C for future extraction. RNA extraction was performed using the Qiagen RNEasy kit following the manufacturer's instructions. The concentration and quality of RNA was analysed using a nanodrop 3000 spectrophotometer (Thermo Scientific).

### 2.5.2 cDNA synthesis

Previously isolated RNA was synthesized into cDNA using the QuantiTect Reverse Transcription kit (Qiagen). Frozen template RNA was thawed on ice along with gDNA Wipeout buffer, Quantiscript Reverse Transcriptase, Quantiscript RT buffer and RT Primer mix. 1 µg of RNA was diluted in 2 µL of gDNA Wipeout buffer and RNase-free water to a total volume of 14 µL and incubated for 2 min at 42 $^{o}$C before being placed immediately on ice. A master mix (Table 2.10) was then added to each reaction and incubated for 30 min at 42$^{o}$C followed by 3 min at 95$^{o}$C to inactivate the reverse transcriptase. The cDNA product was then either used immediately or stored at -20$^{o}$C for future use.

| Component | Volume per 1 µg reaction |
|---|---|
| **Quantiscript Reverse Transcriptase** | 1 µL |
| **Quantiscript RT Buffer, 5x** | 4 µL |
| **RT Primer Mix** | 1 µL |

**Table 2.10- cDNA synthesis reagents**

### 2.5.3 Quantitive-real time-polymerase chain reaction (qRT-PCR)

#### 2.5.3.1 Primer selection

All primers were selected and bought from ThermoFischer Scientific using their inventoried TaqMan gene expression assay search tool and were selected to target human sequences (Table 2.11). Each primer was designed to carry a FAM-reporter dye with the exception of ACTB controls which were designed to carry a VIC-reporter dye so multiplex PCR reactions could be performed.

| EMT targets | | Senescence/apoptosis targets | |
|---|---|---|---|
| **Target name** | **Assay ID** | **Target name** | **Assay ID** |
| **CDH1 (E-cadherin)** | Hs01023894_m1 | **TP53 (p53)** | Hs01034249_m1 |
| **CDH2 (N-cadherin)** | Hs00983056_m1 | **EZH2** | Hs00544830_m1 |
| **SNAI1 (Snail)** | Hs00195591_m1 | **MDM2** | Hs00540450_s1 |
| **SNAI2 (Slug)** | Hs00161904_m1 | **CDKN1A (p21)** | Hs00355782_m1 |
| **Vimentin** | Hs00958111_m1 | **CDKN2B (p15)** | Hs00793225_m1 |
| **TWIST1 (Twist)** | Hs01675818_s1 | **CDKN2A (p16)** | Hs00923894_m1 |
| **Axl** | Hs01064444_m1 | **IL-6** | Hs00985639_m1 |
| **FOXC2** | Hs00270951_s1 | **IL-8** | Hs00174103_m1 |
| **Runx1** | Hs00231079_m1 | **CXCL10** | Hs01124251_g1 |
| **Runx2** | Hs01047973_m1 | **C/EBPβ** | Hs00270923_s1 |
| **GATA3** | Hs00231122_m1 | **BCL2** | Hs00608023_m1 |
| **ZEB1** | Hs00232783_m1 | **BCL2L1(BCL-XL)** | Hs00236329_m1 |
| **mir-221** | Hs04231481_s1 | **BBC3 (PUMA)** | Hs00248075_m1 |
| **Target name** | | **Assay ID** | |
| **Bcl-3** | | Hs00180403_m1 | |
| **ACTB** | | Hs99999903_m1 | |

**Table 2.11-Taq man probes used for gene expression analysis**

#### 2.5.3.2 qRT-PCR reaction

All qRT-PCR experiments were designed to include both target gene probes as well as an ACTB control probe, which was selected as expression levels should remain constant across cell lines and therefore can be used to normalize target amplification to the amount of cDNA present in each sample. No template controls were also run alongside where cDNA was replaced with $dH_2O$ to control for the presence of contaminating DNA.

For each experiment TaqMan Universal Master Mix II, with UNG (ThermoFischer Scientific) was used, which includes: AmpliTaq gold DNA polymerase, dNTPs (with dUTP), ROX passive reference dye, Uracil-N glycosylase (UNG) and optimized buffer components. TaqMan master mix was added to target and ACTB control probes as well as RNase free $H_2O$ to make individual target master mixes containing all reaction components, with the exception of cDNA, which was then added to either 96-well or 384-well qPCR plates (Applied Biosystems) (Table 2.12). Either 18 µL or 8 µL of master mix was added to 96 or 384-well plates respectively before the appropriate amount of cDNA was added to each well.

| qRT-PCR component | Volume added per well for 96-well plate | Volume added per well for 384-well plate |
|---|---|---|
| **Target primer/FAM-probe (20x)** | 1 µl | 0.5 µl |
| **ACTB primer/VIC-probe (20x)** | 1 µl | 0.5 µl |
| **TaqMan master mix (2x)** | 10 µl | 5 µl |
| **RNase free-$H_2O$** | 6 µl | 3 µl |
| **cDNA** | 2 µl | 1 µl |
| **Total volume** | 20 µl | 10 µl |

**Table 2.12- qRT-PCR master mix components**

Once each component had been added plates were sealed with Micro AMP optical adhesive films (Applied Biosystems) before being shaken for 30 sec and centrifuged for 1 min at 1200 rpm at 4$^{o}$C. Plates were then run on a QuantStudio 7 Real-Time PCR machine (Applied Biosystems) set to the following protocol: initial denaturation at 95$^{o}$C for 10 min, followed by 40 cycles of 95$^{o}$C for 15 sec (denaturation), and 60$^{o}$C for 1 min (annealing/elongation).

#### 2.5.3.3 qRT-PCR data analysis

Data was analysed in the automated Thermo cloud software (ThermoScientific) using relative quantification whereby samples are quantified to a reference sample. First, target Ct values were subtracted from ACTB control Ct values for individual wells to create a ΔCt value, which was then averaged from triplicated wells for each sample. A relative value for the difference in transcript levels between samples was then calculated as a difference of ΔCt between samples and a reference sample resulting in the ΔΔCt value. This value was then calculated as $2^{-\Delta\Delta Ct}$ to give the relative fold change which was then transformed on a log10 scale. Statistical analysis was then performed by assessing the overlap between 95% confidence intervals as described in [1].

## 2.6 Chick-chorio allantoic membrane experiments

### 2.6.1 Tumour growth assay

Chick-chorio allantoic membrane (CAM) experiments were performed at Ipatimup, Porto to test and optimise a new high throughput *in vivo* assay for screening novel Bcl-3 inhibitors. For tumour growth assays, chicken eggs (Ipatimub, Porto) were incubated on E0 at 37$^{o}$C and left until E3 when windows were cut into the shell to expose the growing embryo, before being taped over and left to incubate until reaching E10. On the day of inoculation, E10, cells that had been pre-treated with 10 µM CB-1 or DMSO for 24h prior were detached as previously described and counted. Cells were aliquoted into eppendorfs containing 2 x $10^{6}$ cells in 10 µL PBS, mixed with matrigel (BD Biosciences) plus CB-1 or DMSO and kept on ice until inoculation. At the site of inoculation a small plastic ring was placed in the centre of the CAM, near a blood vessel where possible, with cells

added inside the ring and onto the CAM. For 5 days post inoculation 10 µL of compound or DMSO at 10 µM in PBS was added to the site of inoculation daily. Embryos were incubated for an additional 2 days without treatment before being harvested, measured and either stored for either DNA extraction or fixed in formalin for IHC analysis.

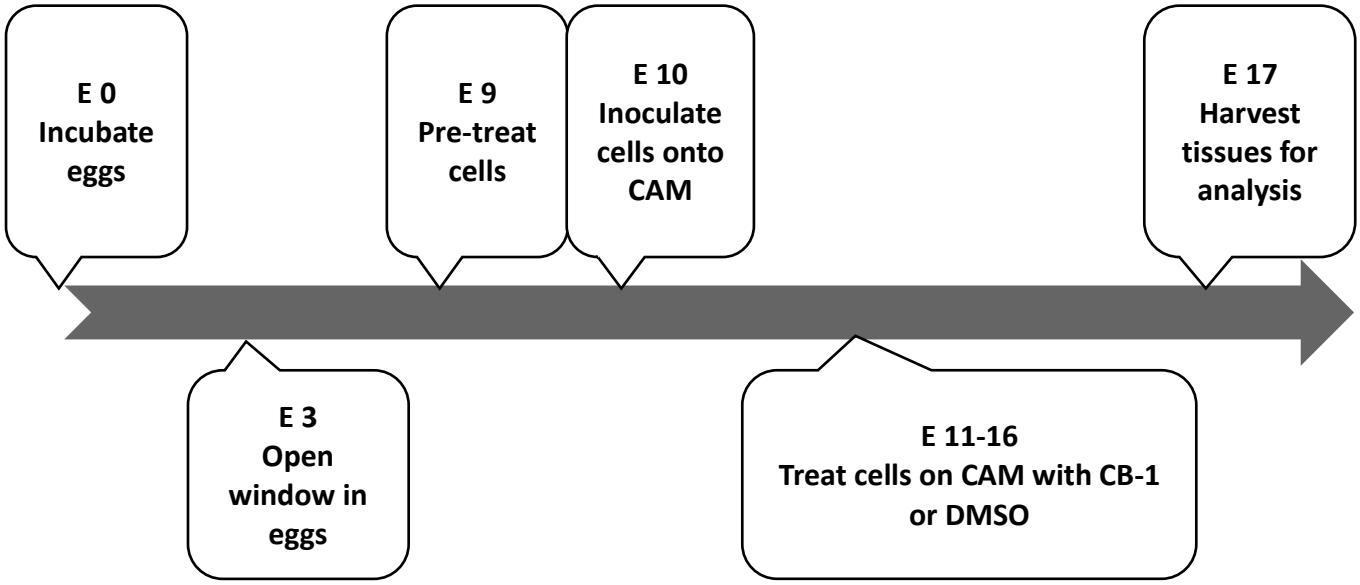


**Figure 2.1- CAM experiment timeline**

### 2.6.2 Immunohistochemistry

#### 2.6.2.1 Tissue processing

For assessing the local invasion of tumours grown on the CAM, immunohistochemistry (IHC) was used. Previously described tumours grown on the CAM were harvested along with their surrounding normal tissue so that the level of local invasion into the CAM could be compared. Cells were fixed in 4% formalin overnight before being embedded into paraffin wax (Ipatimub, Porto) and cut at a thickness of 5 µm on a microtome cutter (Leica). Sections were then placed on poly-L-lysine (PLL) coated slides (ThermoFisher) and heated at 58°C for 24 h before being used for IHC staining.

#### 2.6.2.2 De-waxing and rehydration

Tumour sections were de-waxed by soaking slides in xylene (2X 5 min washes), before being rehydrated through decreasingly concentrated washes in ethanol (2X 2 min washes in 100% ethanol, a 2 min wash in 95% ethanol and a 2 min wash in 70% ethanol) before being transferred to $dH_2O$.

#### 2.6.2.3 Antigen retrieval and blocking endogenous peroxidase activity

Antigen retrieval was performed by immersing tumour sections in citrate buffer (2.94g sodium citrate (Sigma) in 900 mL $dH_20$ and pH adjusted to 6.0) and microwaving for 3X 5 min before being rinsed in $dH_2O$ to ensure easy binding of the primary antibody to the sample. Tumour sections were then blocked for endogenous peroxidase activity using DAKO real peroxidase blocking solution (DAKO). A few drops of the peroxidase block were pipetted onto each section and incubated at room temperature for 20 min. After incubation the slides were washed 2X for 5 min in $dH_2O$ and the once with PBS/T. Non-specific binding of antibodies was then blocked by incubating sections for 20 min at room temperature, in 20% normal rabbit serum in PBS/T. After incubation the slides were washed 2X for 5 min in $dH_2O$ and then once in PBS/T.

#### 2.6.2.4 Incubation of primary and secondary antibodies

Sections were incubated in 1:500 mouse-anti-GFP (b2, Santa Cruz) in 20% normal rabbit serum in PBS/T overnight at 4°C. Before addition of the secondary antibody, slides were washed 2X for 5 min in PBS/T. Sections were then incubated in 1:200 Biotin-conjugated rabbit anti-mouse secondary antibody (DAKO) in 20% normal rabbit serum, in PBS/T for 30 min at room temperature. Following incubation slides were washed 2X for 5 min in PBS/T.

#### 2.6.2.5 Signal amplification and detection

Signal amplification was achieved by the formation of an Avidin-Biotin Complex (ABC) using the Vectastain ABC kit (Vector Labs). The ABC reagents were prepared at least 15 min prior to use through the addition of reagent A (1 drop) and reagent B (1 drop) in 5 mL of PBS/T before mixing well. After secondary antibody had been removed and slides washed, 200 µL of ABC reagent was

added to each slide, ensuring full coverage of tissue sections and left to incubate at room temperature for 30 min. Slides were then washed 3X for 5 min with PBS/T before DAB detection reagents were made up. DAB chromagen detection solution (DAKO) was prepared by adding 1 drop of chromagen to 1 mL of substrate buffer. Freshly made detection solution was then added to each slide and incubated for 5-10 min or until slides turned brown. Slides were then washed for 5 min in PBS/T followed by 2 washes in $dH_2O$.

#### 2.6.2.6 Counterstain, dehydration and visualisation

Slides were counterstained with Mayer's haematoxylin (R.A. Lamb) for 30 sec and run under cold water until the water became clear. Slides were then dehydrated through soaking in increasing concentrations of ethanol (30 sec washes in 70% ethanol and 95% ethanol before 2X 30 sec washes in 100% ethanol) followed by 2X 2 min washes in xylene before being mounted immediately using DPX mounting solution (Sigma).

### 2.6.3 Quantitative PCR

#### 2.6.3.1 DNA Extraction

Quantitative PCR (qPCR) was performed on tissue samples taken from the lungs of chick embryos from previously described CAM tumour growth studies for the determination of distant metastasis. Samples were immediately harvested at experiment endpoints, snap frozen in liquid nitrogen and stored at -80$^{o}$C. Genomic DNA (gDNA) was extracted using a QIAamp DNA mini kit (Qiagen) using manufacturer's instructions before concentration and quality was quantified using a nanodrop 3000, with each sample then diluted in RNase free water to a concentration of 500 ng/µL. The gDNA of 1.5 x $10^6$ MDA-MB-231 cells was also extracted and serially diluted in RNase free water to produce gDNA concentrations equivalent to 5 x $10^5$, 1 x $10^5$, 1 x $10^4$, 1 x $10^3$ and 1 x $10^2$ cells to be used as a standard curve for quantifying the number of metastasising cells in each sample.

#### 2.6.3.2 PCR reaction

To quantify the number human cancer cells that had metastasised to the lungs of embryos from tumours grown on the CAM, qPCR was performed. Primers and probes as described in [216] were used, with primers for human Alu: Forward- YB8-ALU-S68 5'-GTCAGGAGATCGAGACCATCCT-3', reverse-YB8-ALU-AS244 5'-AGTGGCGCAATCTCGGC-3' and TaqMan probe YB8-ALU-167 5'-6-FAM-AGCTACTCGGGAGGCTGAGGCAGGA-TAMRA-3' (ThermoFisher scientific).

A master mix was prepared containing 5 µL of 2X TaqMan Universal master mix II (ThermoFisher scientific), 0.5 µL of human Alu primers, 3.5 µL of RNase free water and added to individual wells of a 384-well plate along with 1 µL of gDNA. Adhesive film was placed over the top of the multi-well plate and centrifuged for 1 min at 1200 rpm before being run on a QuantStudio 7 Real-Time PCR machine. Each sample was run in triplicate and was subjected to initial denaturation of 95°C for 10 min, followed by 40 amplification cycles of denaturation at 95°C for 15 sec and annealing/elongation at 60°C for 1 min.

#### 2.6.3.3 qPCR data analysis

To quantify the number of human cells present in each sample a standard curve was produced using the previously described MDA-MB-231 cells that had been serially diluted to represent the gDNA content of various cell numbers. A line of linear regression was automatically formulated based on the Ct values of different cell numbers run alongside tumour samples, which was then used to calculate then number of cells in each sample.

## 2.7 Statistical analysis

Error bars on all graphs represent standard error values with the exception of gene expression data which are represented by 95% confidence intervals. An unpaired student's T-test was used to determine statistical differences between normally distributed data sets and between data sets with sample sizes of n=3 unless stated, which was performed using Graphpad prism.

# Chapter 3:
# Establishing the role of Bcl-3 in breast cancer migration

# 3 Establishing the role of Bcl-3 in breast cancer migration

## 3.1 Introduction

Metastasis is the most aggressive and difficult stage of cancer to treat making it responsible for almost all deaths from breast cancer and highlighting it as a key risk area requiring improved research and therapeutic intervention. One potential regulator of metastasis is the proto-oncogene Bcl-3, which has been shown to drive metastasis in both triple negative and ERBB2-driven tumours [188, 214]. Inhibition of Bcl-3 in these models resulted in a significantly reduced metastatic tumour burden which was attributed to a suppression of cell migration. This reduction in metastasis was also shown to be independent of primary tumour growth or normal mammary development making Bcl-3 an interesting candidate for targeting metastatic disease [214].

Further research has now shown that overexpression of mutant Bcl-3 with impaired ability to bind to p50 and p52 can also reduce Bcl-3-mediated migration [215]. This has led to the development of a number of small molecule inhibitors designed to disrupt the function of Bcl-3 by blocking a small binding pocket within its protein structure and has shown promising results *in vitro* and *in vivo* [215]. This work has identified a potential anti-metastatic target which could lead to therapeutic benefits, however little research has followed this to investigate the biological role of Bcl-3 in human breast cancer. The effects observed with Bcl-3 inhibition have so far been solely attributed to a reduction in the migratory ability of tumour cells, however other than this very little is known about the biological effects of Bcl-3 in human tumour cells.

Cell migration during metastasis is a highly plastic event with tumour cells capable of utilising both mesenchymal and amoeboid-like single cell migration as well as various forms of collective migration in response to changing microenvironments, making it particularly difficult to target [217, 218]. In order to progress the development of Bcl-3 inhibitors towards a more clinical setting it is first important to have a detailed understanding of how Bcl-3 is acting upon tumour cells to regulate its metastasis/migration phenotype.

Based on previous work and published observations we hypothesise that Bcl-3 may be capable of regulating different modes of migration in breast cancer cells of various types to promote metastasis. Therefore, the aim of this chapter was to further elucidate the mechanisms by which Bcl-3 may regulate tumour progression and metastasis using siRNA to deplete Bcl-3 in breast cancer cell lines, and a new class of Bcl-3 inhibitor designed to disrupt Bcl-3 from performing its normal function.

## 3.2 Effect of Bcl-3 suppression on cell motility

It has been previously shown that suppressed Bcl-3 potentiates its anti-metastatic effects by reducing the migratory capacity of tumour cells [188, 214]. This has been observed in a number of human cell lines independent of their tumour type or endogenous Bcl-3 expression suggesting a conserved method of regulation [215]. All previous data on migration however has been observed in amoeboid-like motility using classic Boyden chamber assays, which, although are informative of a basic migratory capacity, does not take into account the various other mechanisms of cell migration. It is therefore important to identify whether Bcl-3 is acting globally on cell motility or more specifically towards a certain aspect of this process which may help target its use towards certain tumour types and/or different *in vivo* contexts.

### 3.2.1 Selection of cell lines

To analyse the contrasting mechanisms of motility that have been reported within the literature it was important to choose cell lines that represented distinct migratory characteristics. The epithelial MCF-7 cell line and the mesenchymal MDA-MB-436 cell line were selected based on their morphological characteristics, with the luminal-like MCF-7 cells thought to migrate collectively compared to the mesenchymal-like single cell-like motility observed in MDA-MB-436 cells. The mesenchymal-like MDA-MB-231 cells which offer an intermediate phenotype between the two were also selected as a comparison (Figure 3.1A). Bcl-3 expression in each cell line was previously

evaluated within the lab (data not shown) with MDA-MB-436 cells expressing highest levels, followed by MDA-MD-231 cells, with MCF-7 expressing the lowest levels of Bcl-3.

#### 3.2.1.1 Bcl-3 siRNA inhibited Boyden chamber migration in MDA-MB- 436 and MDA-M-231 cells

As all previous data concerning Bcl-3-related migration had been performed using Boyden chamber assays each cell line was assessed for the response to Bcl-3 inhibition in an adapted version of this assay. The Fluoroblok migration assay from Corning replicates the standard Boyden chamber assay but is easily quantifiable by using a fluorescent stain to detect migrating cells instead of manually counting them. In this assay cells are stimulated to migrate through chemotaxis and must migrate through 8 µm pores mimicking an amoeboid-like cell migration.

Each cell line was first compared for their ability to migrate in this system. MDA-MB-231, MDA-MB-436 and MCF-7 cells were seeded into UV-impermeable transwell plates in serum-free media and incubated for 24h, before the migrated cells on the underside of the transwell membrane were stained with the cell viability dye calcein AM and measured for fluorescence intensity. In this assay the MDA-MB-231 cell line was capable of migrating more efficiently than both MDA-MB-436 and MCF-7 cells, with the latter showing barely any migration above background signal (Figure 3.1B).

Each cell line was then tested for their response to 48h of Bcl-3 siRNA treatment to confirm that Bcl-3 expression could be efficiently inhibited, with a minimum of an 80% reduction in Bcl-3 expression observed in each line compared to scRNA controls (Figure 3.1C). For all further experiments performed results were only used when Bcl-3 expression was less than 80% unless stated. To confirm Bcl-3 suppression could inhibit amoeboid-like cell migration in both MDA-MB-231 and MDA-MB-436 cells the same Fluoroblok assay was repeated, however cells were treated for 48h with either Bcl-3 siRNA or scrambled RNA control (scRNA) before seeding. Both cell lines showed significantly reduced migration after siRNA treatment compared to scRNA controls with no concomitant loss in cell viability determined in parallel wells by cell titre blue (Figure 3.1D&E).

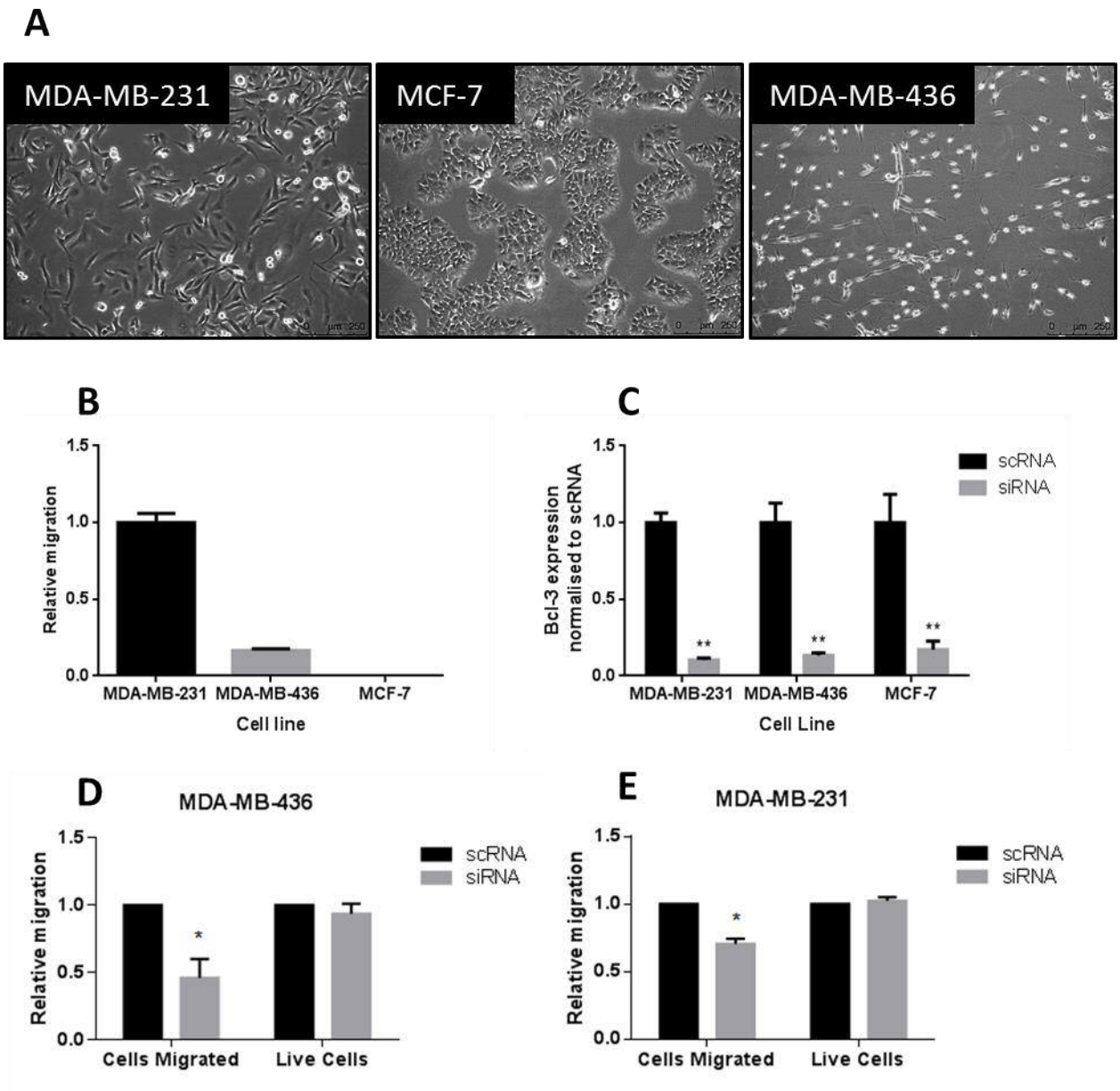


**Figure 3.1- Bcl-3 suppression inhibited amoeboid-like cell migration- (A)** Representative images of the three cell lines selected to evaluate the role of Bcl-3 in cell migration (scale bar=250 µM). **(B)** Boyden chamber assays were performed to determine the amoeboid-like migration capabilities between the three cell lines (N=2). **(C)** Representative figure indicating Bcl-3 expression in each cell line after 48h Bcl-3 siRNA or scRNA treatment, quantified using qRT-PCR. The two cell lines capable of amoeboid-like migration **(D)** MDA-MB-436 and **(E)** MDA-MB-231, were tested for their ability to migrate after Bcl-3 inhibition with siRNA 48h prior to seeding (N=3)(T-test, *=p<0.05 as compared to scRNA control).

#### 3.2.1.2 Small molecule Bcl-3 inhibitor CB-1 suppressed amoeboid migration in MDA-MB-436 cells

One of the subsidiary aims of this project was to aid in progressing small molecule Bcl-3 inhibitors towards pre-clinical development of a clinical anti-metastatic agent. In doing so it was hoped that one or more hit compounds would be used alongside siRNA inhibition of Bcl-3 to compare how these two different mechanisms of Bcl-3 inhibition affected the tumour cell phenotype. A number of novel small molecule inhibitors were formulated for testing by collaborators Cinzia Bordoni, Andrew Westwell and Andrea Brancale in the School of Pharmacy, Cardiff University, based around a previously identified hit molecule, JS6, that had been shown to disrupt Bcl-3 binding to p50 and p52 [215]. From this panel of inhibitors, the lead compound CB-1 had been identified based on its potent anti-metastatic effects *in vivo* (Clarkson, unpublished data). CB-1 had also been shown to act *in vitro* at 10 µM, which is equivalent to its plasma concentrations *in vivo* metastasis models (data not shown), by inhibiting amoeboid-like cell migration and was used as bench mark for new analogues (Figure 3.2A).

Given the established effect of Bcl-3 inhibition of Boyden chamber-like migration and the easily quantifiable endpoint of the adapted FluoroBlok assay, it was selected as a medium throughput platform to screen new compound analogues. In order to identify compounds with similar or greater potency to CB-1, the panel of CB-1 related compounds was screened for their ability to inhibit the migratory capacity of the MDA-MB-436 cell line (Figure 3.1A). From the 15 compounds tested, 7 showed a significant inhibition in migration compared to vehicle (DMSO) controls when treated at 10 µM, with one compound having the opposite effect of enhancing cell migration. Interestingly, compounds CB-30 & CB-43 showed significantly greater efficacy at 10 µM than the lead compound CB-1 (Figure 3.2A). The top 6 compounds based on inhibition of migration (excluding analogues such as SD-5 that failed *in vitro* stability/toxicology studies) were also tested at 1 µM. However, no compounds showed any significant reductions in migration (Figure 3.2B).

#### 3.2.1.3 Lead compound CB-1 had no effect on cell viability at up to 100 µM

The best performing compounds were also tested for their effects on cell viability in MDA-MB-436 cells after 48h treatments at 10 and 1 µM. Treatment with compound SD-2 at 10 µM resulted in a significant increase in viability, while at 1 µM CB-23, CB-30 and SD-2 all showed a small but significant reduction in viability, which may have been due to improved solubility at lower concentrations, however this was not investigated (Figure 3.2C). Lead compound CB-1 and the best performing analogue CB-43 were further tested for their effect on cell viability at a range of concentrations with CB-1 having no effect on cell viability at any concentration. CB-43 however reduced significantly the number of viable cells at 100 µM and appeared to have some effect at 50 µM (Figure 3.2D). On the basis of this data, and additional unpublished solubility, stability and *in vitro* toxicity data, CB-1 remained the lead compound in parallel drug development assays.

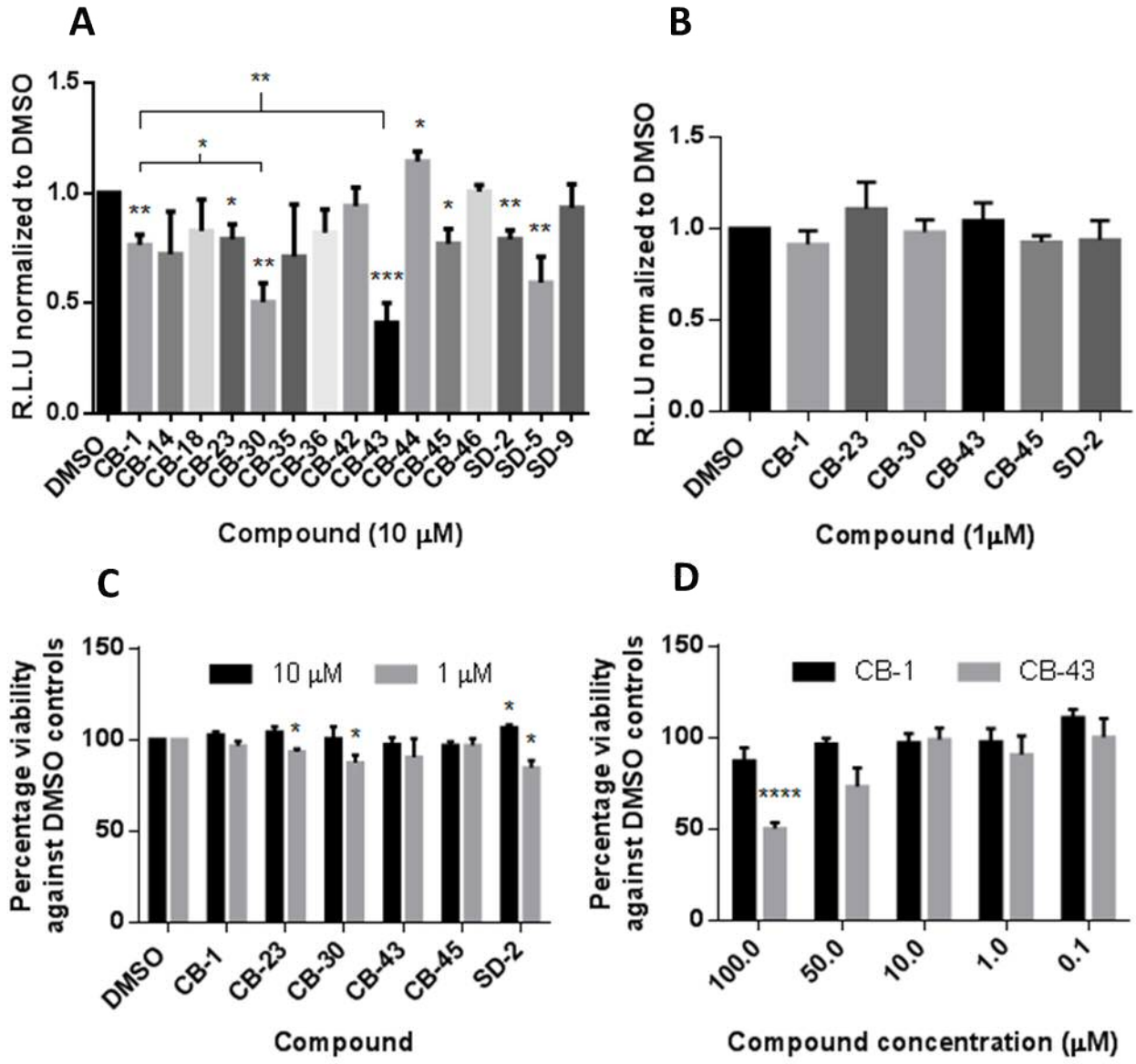


**Figure 3.2- Compound screening-** Screening was performed using MDA-MB-436 cells cultured with the chemically identified top 15 compounds at 10 μM or DMSO control for 24h before being seeded onto 96-well Fluoroblok migration plates and left for a further 24h **(A)**. The top 6 compounds were also tested for their effect on Fluoroblok migration at 1 μM **(B)**. The migration activity of cells was quantified as relative light units using a calcein stain and normalized to DMSO controls. The top 6 performing compounds were also screened for toxicity by Cinzia Bordoni at both 10 μM and 1 μM using cell titre blue **(C)**. Two lead compounds CB-1 and CB-43 were further screened for toxicity at range of concentrations using cell titre blue **(D)**. Error bars represent ± SEM of 3 independent experiments. (T-test, *=p<0.05, **=p<0.01, ***=p<0.005).

### 3.2.2 Bcl-3-mediated single cell motility in mesenchymal MDA-MB-436 cells

The effect of Bcl-3 inhibition on Boyden chamber, amoeboid-like migration has been clearly characterised in a number of human breast cancer cell lines, however this assay only gives a limited overview of the potential role Bcl-3 may be playing in cell migration. Tumour cells have the capacity to use alternative migratory methods such as mesenchymal-like or by moving collectively to metastasize. Therefore, to gain a better insight into whether Bcl-3 had a role in these other distinct forms of cell migration, time-lapse technology was initially used to track individual cells in real time to assess whether Bcl-3 could regulate mesenchymal-like single cell migration. MDA-MB-436 and MDA-MB-231 cells were treated with either Bcl-3 siRNA or small molecule inhibitors for 48h before being placed into a time-lapse incubator and photographed every 10 minutes for 8h. A minimum of 40 cells were then tracked and analysed using CellTracker software and the averages of 3 independent experiments combined. MCF-7 cells were also tested, however these cells lack the ability to migrate individually and therefore no data could be taken from them in this assay.

#### 3.2.2.1 RNAi of Bcl-3 inhibited single cell migration in MDA-MB-436 cells

Firstly, the effect of Bcl-3 siRNA inhibition on single MDA-MB-436 and MDA-MB-231 cell motility was analysed. The average distance each cell had travelled from its origin was assessed over an 8h time period, with siRNA treated cells showing a significantly reduced average distance travelled compared to controls in MDA-MB-436 cells (Figure 3.3A). Furthermore, the total distance that each cell travelled irrespective of how far away from their origin was significantly reduced in Bcl-3-inhibited cells, as was the average speed that each cell moved at throughout the time course (Figure 3.3B&C). These differences in motility are highlighted by the representative images in figure 3.4 and in supplementary videos 1&2. In MDA-MB-231 cells the average distance of migration from the origin of each cell appeared to be reduced slightly after Bcl-3 siRNA treatment, however this change was not significant (Figure 3.3D). Similar trends were also observed in the total distance travelled and the average cell speed, however again no significant changes were observed (Figures 3.3E&F) which is highlighted in figure 3.5 and supplementary videos 3&4.

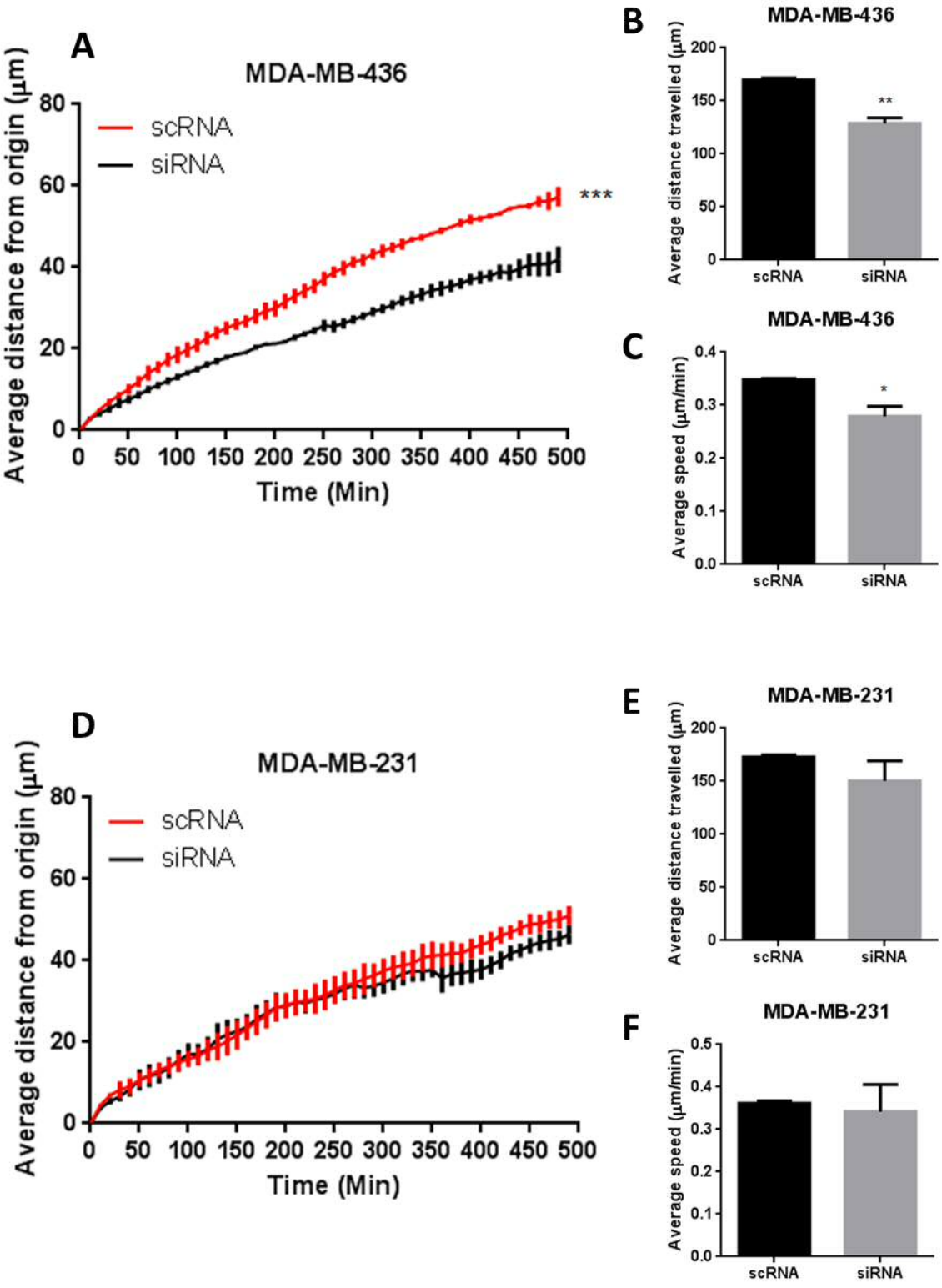


**Figure 3.3- Bcl-3 suppression reduced single cell mesenchymal-like migration-** Analysis of mesenchymal-like cell motility was performed in **(A,B,C)** MDA-MB-436 and **(D,E,F)** MDA-MB-231 cell lines. Cells were incubated with Bcl-3 siRNA or scRNA for 48h before beginning time-lapse. Cells were then photographed every 10 min for 8 h and analysed using CellTracker software. **(A&D)** Cells were tracked over time to show their average distance from starting point (2-way ANOVA= ***=p<0.005). **(B&E)** Average total distance travelled over 8h time period was measured, **(C&F)** with the average speed at which each cell moved throughout also measured. Error bars represent ± SEM of 3 independent experiments. (T-test, *=p<0.05, **=p<0.01).

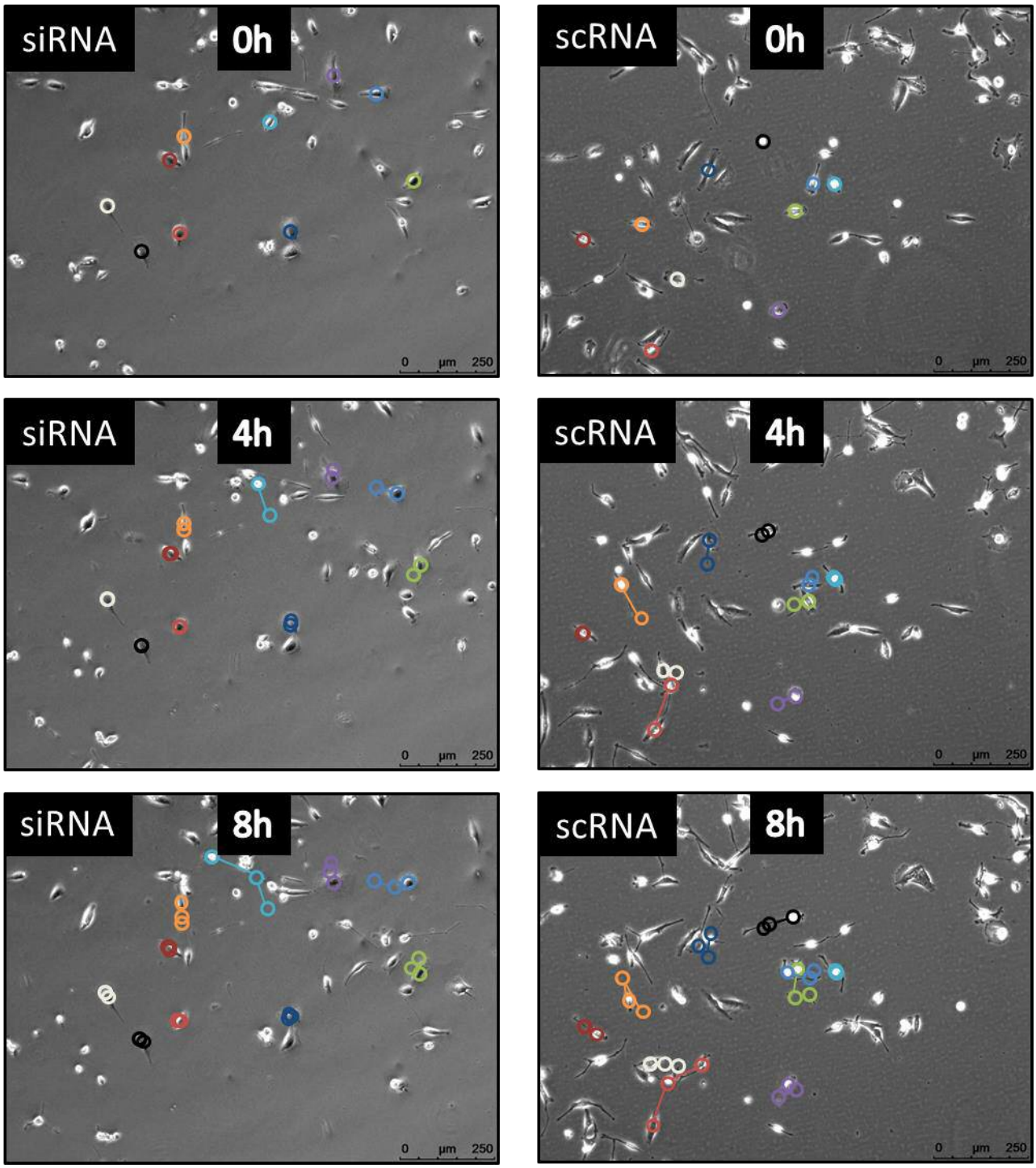


**Figure 3.4- MDA-MB-436 single cell migration assay-** Representative images of mesenchymal-like cell motility in MDA-MB-436 cells. Cells were incubated with Bcl-3 siRNA or scRNA for 48h before beginning time-lapse. Cells were then photographed every 10 min for 8 h and analysed using CellTracker software. Figure shows representative images of cell motility at 0h as well as 4 and 8 h after time-lapse start point with either Bcl-3 siRNA or scRNA control (Scale bar= 250µm).

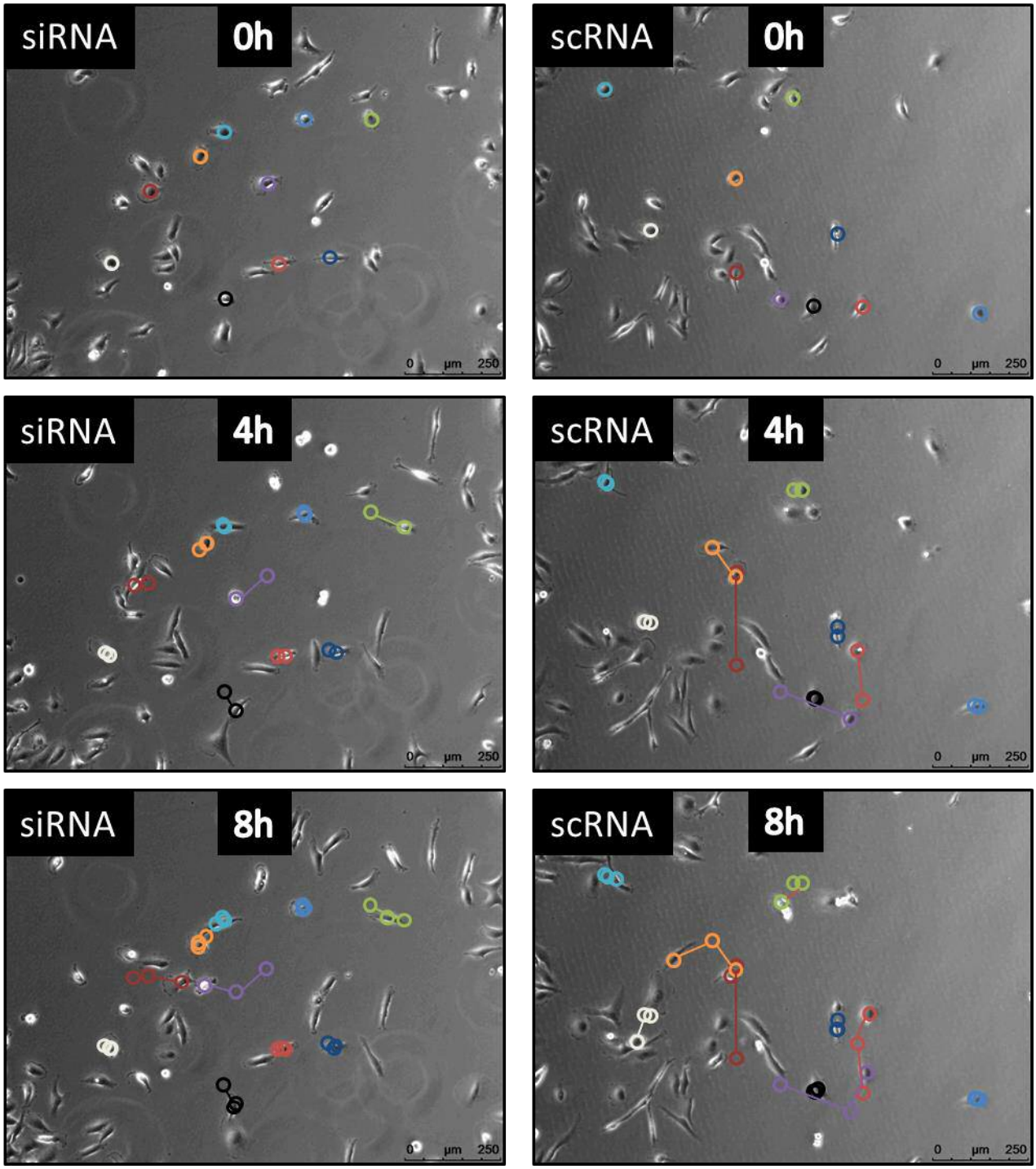


**Figure 3.5- MDA-MB-231 single cell migration assay-** Representative images of mesenchymal-like cell motility in MDA-MB-231 cells. Cells were incubated with Bcl-3 siRNA or scRNA for 48h before beginning time-lapse. Cells were then photographed every 10 min for 8 h and analysed using CellTracker software. Figure shows representative images of cell motility at 0h as well as 4 and 8 h after time-lapse start point with either Bcl-3 siRNA or scRNA control (Scale bar= 250µm).

#### 3.2.2.2 CB-1 had a small effect on single cell migration in MDA-MB-436 cells

The effect of CB-1 on single cell motility was also assessed by time-lapse microscopy in both MDA-MB-436 and MDA-MB-231 cell lines. After 48h treatment with either 10 μM CB-1 or 0.1% DMSO MDA-MB-436 cells were assessed, with those treated with CB-1 showing a non-significant trend towards reduced migratory ability (Figure 3.6A). On average these cells tended to migrate less from their starting point compared to DMSO-treated cells as well as having a reduced total migration distance and average speed of migration (Figure 3.6B&C). In MDA-MB-231 cells no differences were observed between CB-1 and DMSO treated cells (Figure 3.6D, E&F).

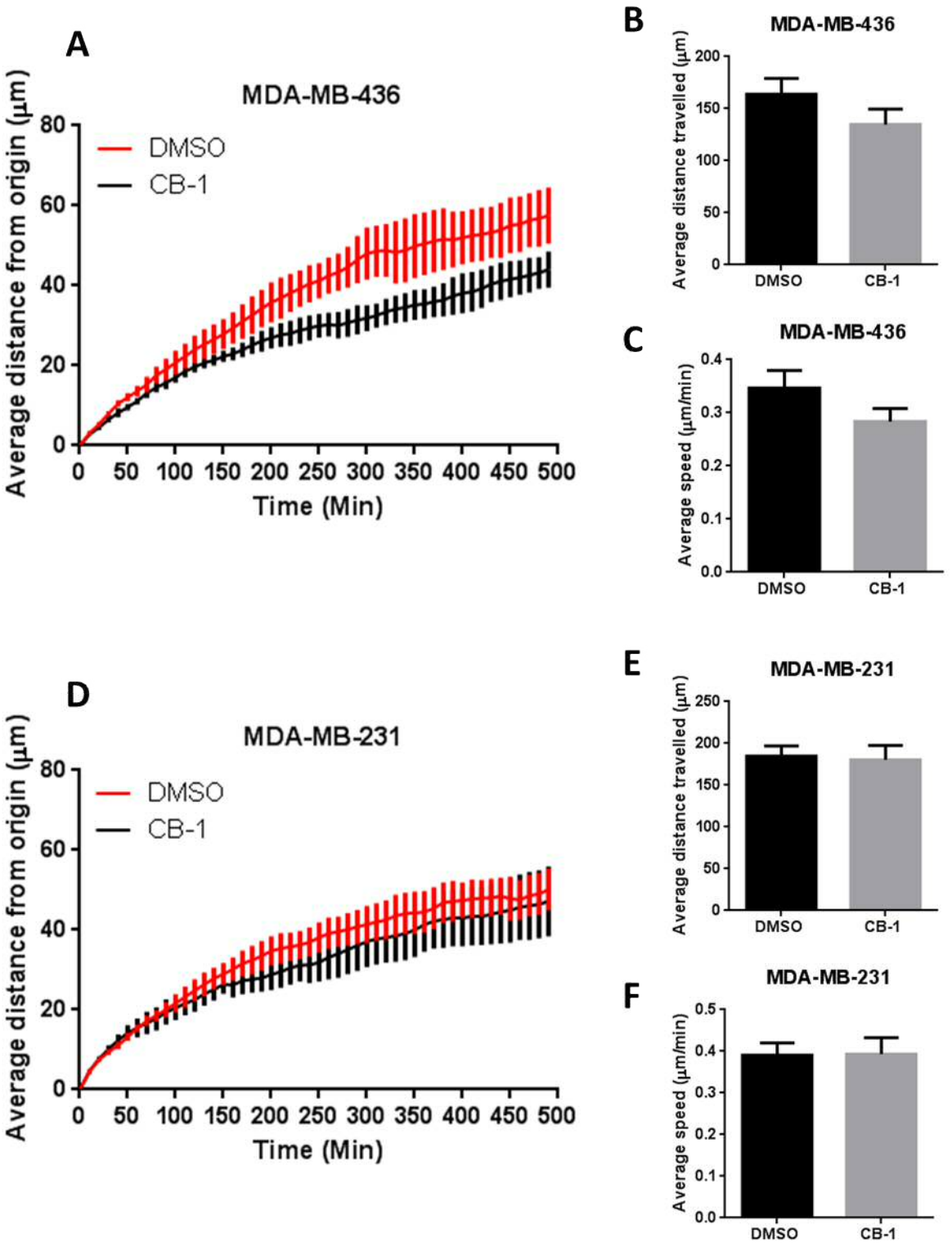


**Figure 3.6- CB-1 reduced single cell mesenchymal-like migration-** Analysis of mesenchymal-like cell motility in (**A,B,C**) MDA-MB-436 and (**D,E,F**) MDA-MB-231 cell lines. Cells were incubated with 10 µM CB-1 or 0.1% DMSO for 48h before beginning time-lapse. Cells were then photographed every 10 min for 8 h and analysed using CellTracker software. **(A&D)** Cells were tracked over time to show their average distance from starting point (2-way ANOVA= *=p<0.05). **(B&E)** Average total distance travelled over 8h time period was measured, **(C&F)** with the average speed at which each cell moved throughout also measured. Error bars represent ± SEM of 3 independent experiments. (T-test, *=p<0.05).

### 3.2.3 Bcl-3-regulated collective cell migration

Collective migration represents a very different type of cell movement compared to the single cell motility previously assessed. It incorporates the ability of cells to co-operate together moving as a sheet in a directional movement, unlike the motility of a single cell via either mesenchymal or amoeboid-like migration. To assess whether Bcl-3 inhibition could also affect this form of migration, MCF-7 cells, which lack the ability to migrate individually, were observed using wound-healing assays after Bcl-3 RNAi and CB-1 treatment. MDA-MB-231 cells were also analysed by measuring their collective invasion front rather than individual cells that migrated away from the bulk cell population. As previous data, not shown here, had shown Bcl-3 to have little effect on cell proliferation in these cell lines, it was concluded that any effects on their migratory potential were not due to changes in cell division. This assay could not be performed in MDA-MB-436 cells as they do not form a cohesive migration front and therefore cannot be analysed for collective migration.

#### 3.2.3.1 RNAi of Bcl-3 inhibited collective migration in MDA-MB-231 & MCF-7 cells

After a 48h transfection of Bcl-3 siRNA or scRNA control in MDA-MB-231 or MCF-7 cells, wounds were created using a 10 µm pipette tip and immediately photographed. MDA-MB-231 and MCF-7 cells were left for 8h and 24h respectively to migrate before final photographs were taken. Both cell lines treated with Bcl-3 siRNA showed a significant reduction in migration compared to scRNA treated cells, represented by a reduced percentage area of wound closure (Figure 3.7 & 3.8).

#### 3.2.3.2 CB-1 inhibited collective migration in MDA-MB-231 cells

To confirm whether CB-1 could mimic the reduction in collective migration observed after siRNA knockdown of Bcl-3, cells were treated for 48h with 10 µM CB-1 or equivalent percentage of DMSO for 48h before performing wound-healing assays. MDA-MB-231 cells showed a significant reduction in collective migration after CB-1 treatment compared to DMSO controls (Figure 3.9). MCF-7 cells replicated this trend where CB-1 appeared to reduce migratory capacity, however this change was not significant (Figure 3.10).

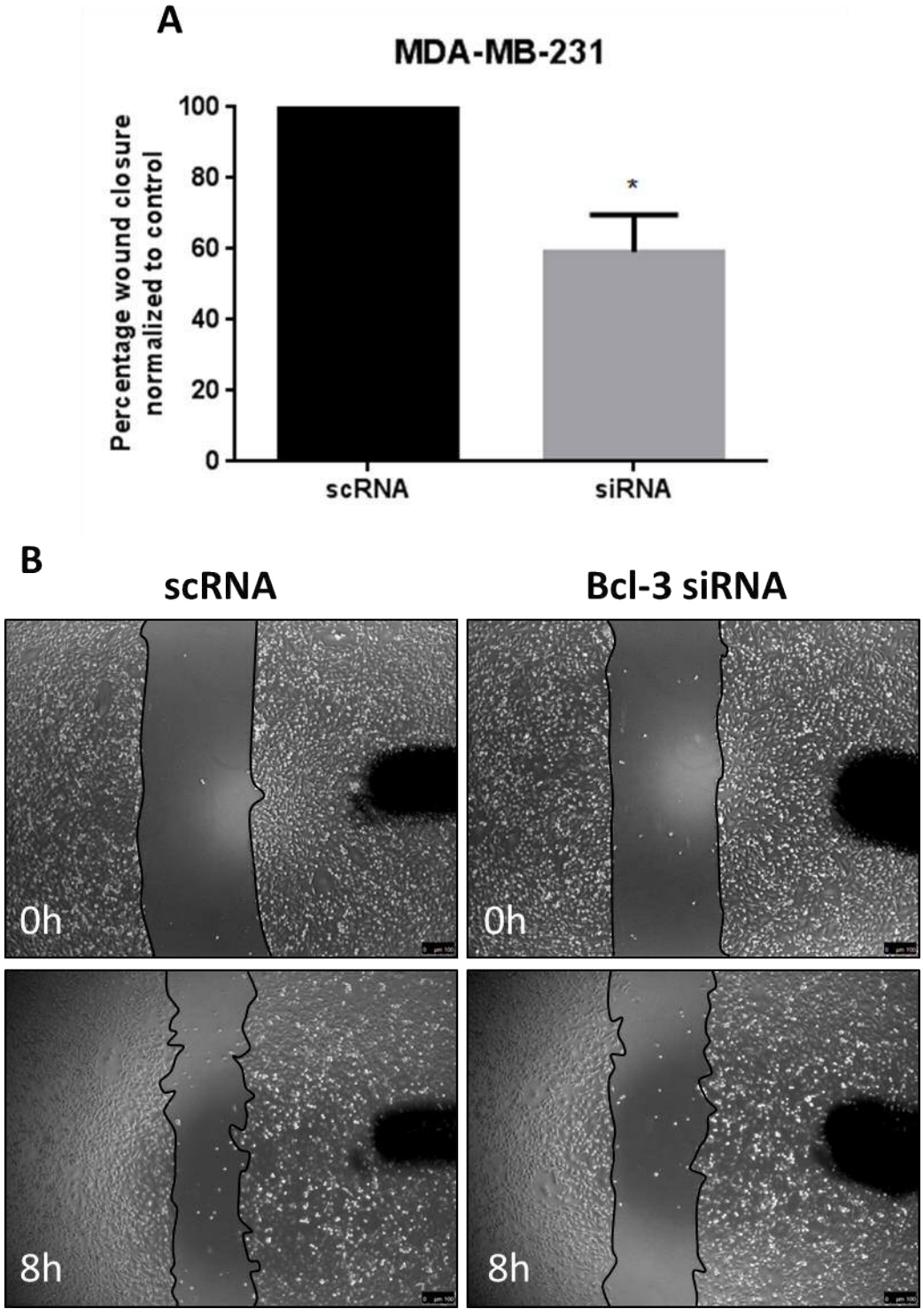


**Figure 3.7- Bcl-3 RNAi reduced MDA-MB-231 collective migration-** Wound healing assays of collective cell migration were performed in MDA-MB-231 cells. Cells were incubated with Bcl-3 siRNA or scRNA for 48h prior to wound formation using P10 pipette tip before being photographed. Wounds were then photographed again after 8h before total migration was measured by percentage of wound closure **(A)**. Error bars represent ± SEM of 3 independent experiments. (T-test, *=$p<0.05$ siRNA compared to scRNA control). **(B)** Representative images of siRNA and scRNA treated cells at 0h and 8h after wound creation (Scale bar= 100μm).

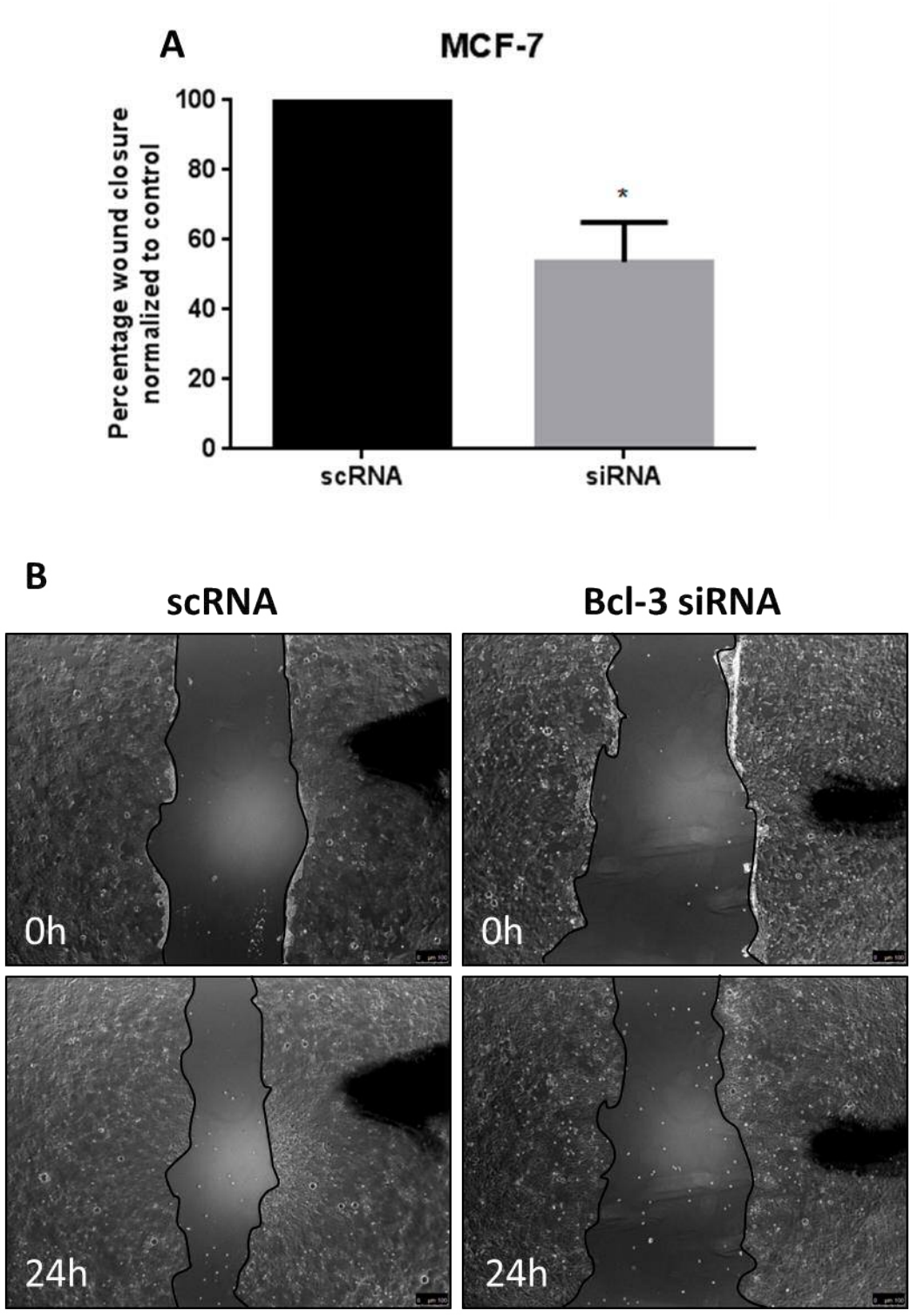


**Figure 3.8- Bcl-3 RNAi reduced MCF-7 collective migration-** Wound healing assays of collective cell migration were performed in MCF-7 cells. Cells were incubated with Bcl-3 siRNA or scRNA for 48h prior to wound formation using P10 pipette tip before being photographed. Wounds were then photographed again after 24h before total migration was measured by percentage of wound closure **(A)**. Error bars represent ± SEM of 3 independent experiments. (T-test, *=$p<0.05$ siRNA compared to scRNA control). **(B)** Representative images of siRNA and scRNA treated cells at 0h and 24h after wound creation (Scale bar= 100µm).

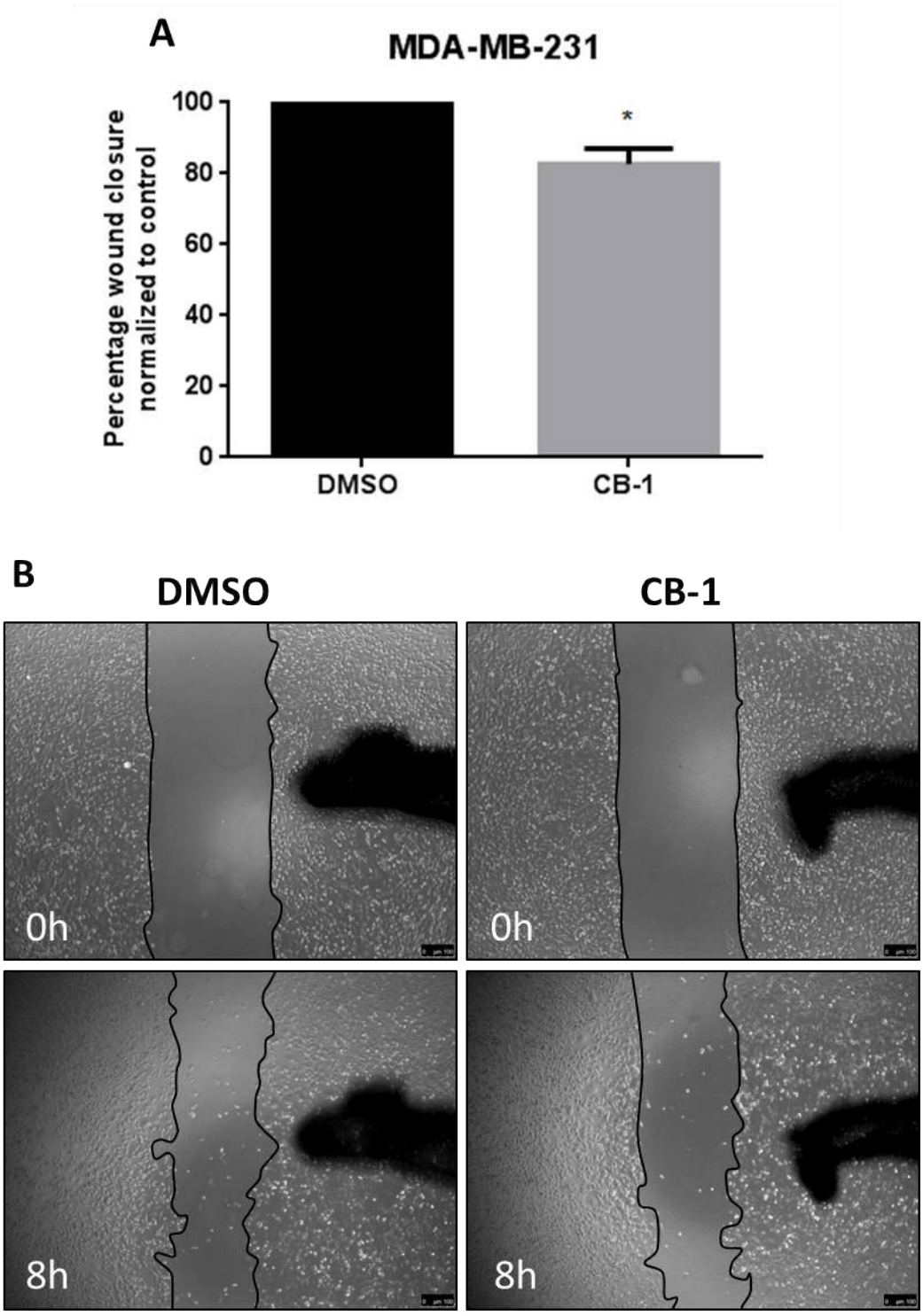


**Figure 3.9- CB-1 reduced MDA-MB-231 collective migration-** Wound healing assays of collective cell migration performed in MDA-MB-231 cells. Cells were incubated with 10 µM CB-1 or DMSO for 48h prior to wound formation using P10 pipette tip before being photographed. Wounds were then photographed again after 8h before total migration was measured by percentage of wound closure **(A)**. Error bars represent ± SEM of 3 independent experiments. (T-test, *=$p<0.05$ CB-1 compared to DMSO control). **(B)** Representative images of CB-1 and DMSO treated cells at 0h and 8h after wound creation (Scale bar= 100µm).

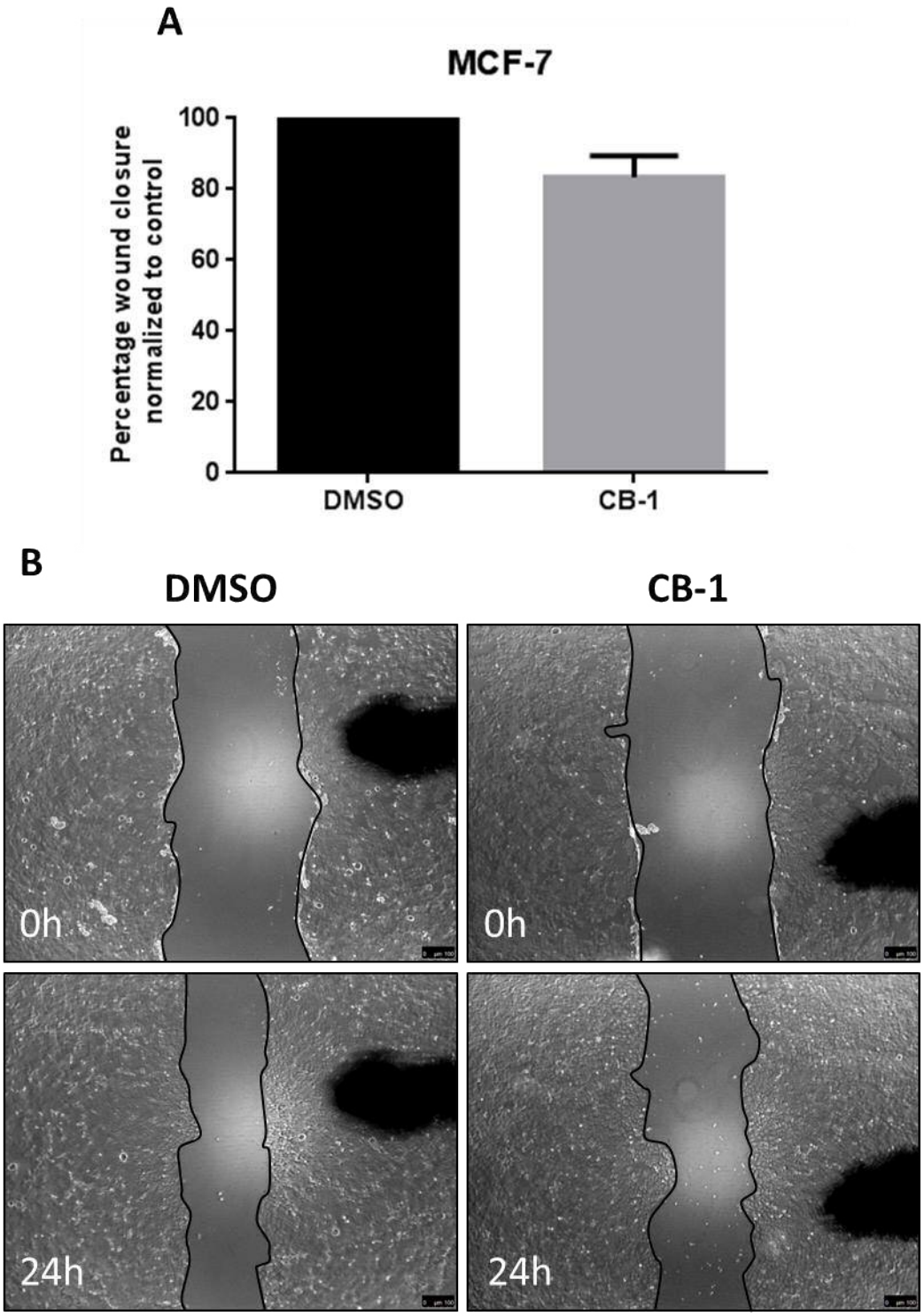


**Figure 3.10- CB-1 reduced MCF-7 collective migration-** Wound healing assays of collective cell migration performed in MCF-7 cells. Cells were incubated with 10 µM CB-1 or DMSO for 48h prior to wound formation using P10 pipette tip before being photographed. Wounds were then photographed again after 24h before total migration was measured by percentage of wound closure **(A)**. Error bars represent ± SEM of 3 independent experiments. (T-test, *=p<0.05 CB-1 compared to DMSO control). **(B)** Representative images of CB-1 and DMSO treated cells at 0h and 24h after wound creation (Scale bar= 100µm).

### 3.2.4 RNAi of Bcl-3 reduced Rac1 and Cdc42 activity in MDA-MB-436 cells

The Rho GTPase family of signalling G proteins regulate a number of cellular processes including the formation of lamellipodia, filopodia and membrane ruffling during cell migration predominantly through the regulation of filamentous actin. This family of regulators is known to be involved in the regulation of NF-kB-dependent transcription, however Bcl-3 has never been implicated within this regulation [219]. Interestingly, the Rho GDP dissociation inhibitor Arhgdbi has been shown to be significantly upregulated after Bcl-3 RNAi in mouse cells. Furthermore, the migration phenotype seen with Bcl-3 inhibition can be rescued with simultaneous knockdown of Arhgdbi suggesting GTPase regulation may play a key role in Bcl-3-mediated migration in tumour cells [214].

To test whether Bcl-3-mediated migration may be regulated through the Rho GTPase family, G-LISA assays were performed against key family members RhoA, Rac1 and Cdc42. After 24h of Bcl-3 inhibition using siRNA the relative quantities of activated GTPases in MDA-MB-436 cells was analysed against scRNA controls. Both Rac1 and Cdc42 were significantly downregulated compared to controls, however no significant change was observed in the levels of activated RhoA (Figure 3.11A, B&C). Rac1 activation was also examined after 1 and 24h of CB-1 treatment, however no difference was observed compared to DMSO controls (Figure 3.11D).

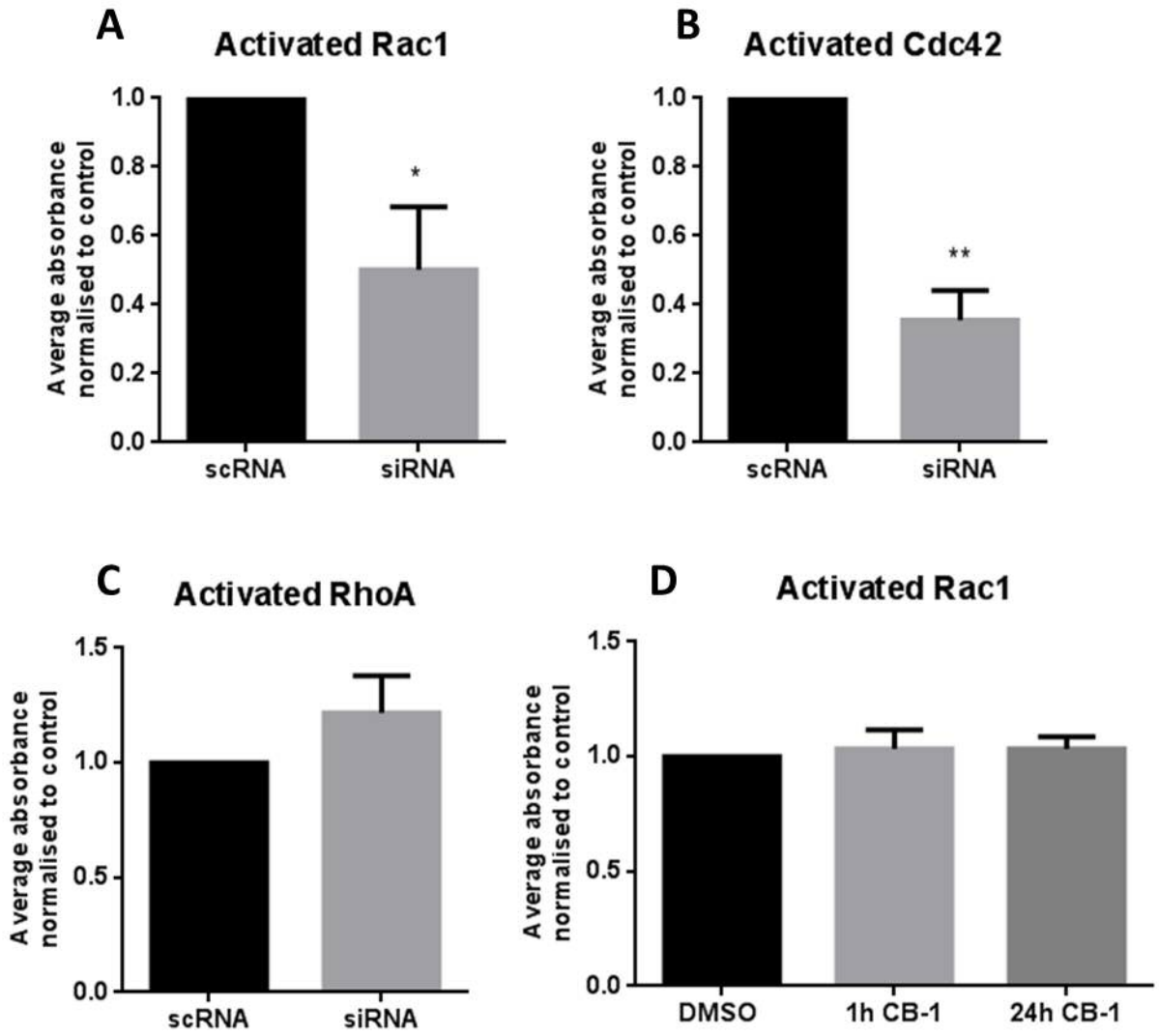


**Figure 3.11- Bcl-3 RNAi reduced Rac1 and Cdc42 activity in MDA-MB-436 cells-** G-LISA activation assays were performed in MDA-MB-436 cells were grown in 60mm dishes and treated with either Bcl-3 siRNA or scRNA control **(A,B,C)** for 24h before protein lysates were harvested on ice. Compound treated cells **(D)** were treated for either 1h or 24h with 50 μM CB-1 or DMSO control before being harvested. After protein equalization samples were immediately quantified for activated Rac1 **(A&D)** Cdc42 **(B)** and RhoA **(C)** using cytoskeletons G-LISA assay. Error bars represent ± SEM of 3 independent experiments. (T-test, *=$p<0.05$, **=$p<0.01$ as compared to control).

## 3.3 Bcl-3 inhibition did not affect breast cancer cell adhesion

Regulation of cell adhesion is an important aspect of tumour progression with adhesion to neighbouring tumour cells, the surrounding extracellular matrix (ECM) and non-cancerous cells all contributing to metastasis. The maintenance of these interactions is highly plastic and context-dependent with both the loss and acquisition of adhesion beneficial in certain settings. Many regulators of cell adhesion such as the cadherin family are anchored within the cyto-skeleton and can therefore be regulated through the Rho GTPase family with both Rac1 and Cdc42 known to be important mediators in the maintenance of both cell-cell and cell-substrate adhesion [220, 221]. The role of Bcl-3 in regulating cell adhesion has never been tested, however, given previous data suggesting a link between Bcl-3 and Rac1/Cdc42 signalling, it may have some role to play in this complex process. To test this hypothesis, the ability of cells to adhere to various matrix components as well as other tumour cells was tested.

### 3.3.1 Bcl-3 inhibition did not affect cell-substrate adhesion in MDA-MB-436 cells

To test the ability of tumour cells to attach to various substrates after Bcl-3 inhibition, MDA-MB-436 cells were treated with Bcl-3 siRNA or CB-1 and tested for their ability to attach to Laminin, Vitronectin, Fibronectin, Collagen I and Collagen IV. After suppression of Bcl-3 with siRNA a trend of increased cell-substrate adhesion in 3 out of 5 substrates was seen, however only adhesion to Vitronectin resulted in a significant increase (Figure 3.12A). When cells were treated with CB-1, similar trends were not observed and no significant changes could be detected at either 10 or 50 μM of compound concentration (Figure 3.12B).

### 3.3.2 Bcl-3 inhibition did not affect cell-cell adhesion in MCF-7 cells

Along with cell-substrate adhesion, the ability of cells to adhere to each other is another indicator of the metastatic potential of a cancer. Cells that are less adherent are more likely to detach and therefore move away from the tumour, potentially forming metastases. Slow aggregation assays were performed using the highly adhesive MCF-7 cells to determine whether Bcl-3 inhibition could affect the ability of these cells to collectively adhere to each other and form aggregates after Bcl-3 knockdown or after treatment with CB-1. No significant changes were observed with either Bcl-3 siRNA or CB-1 treated cells (Figure 3.12C&D).

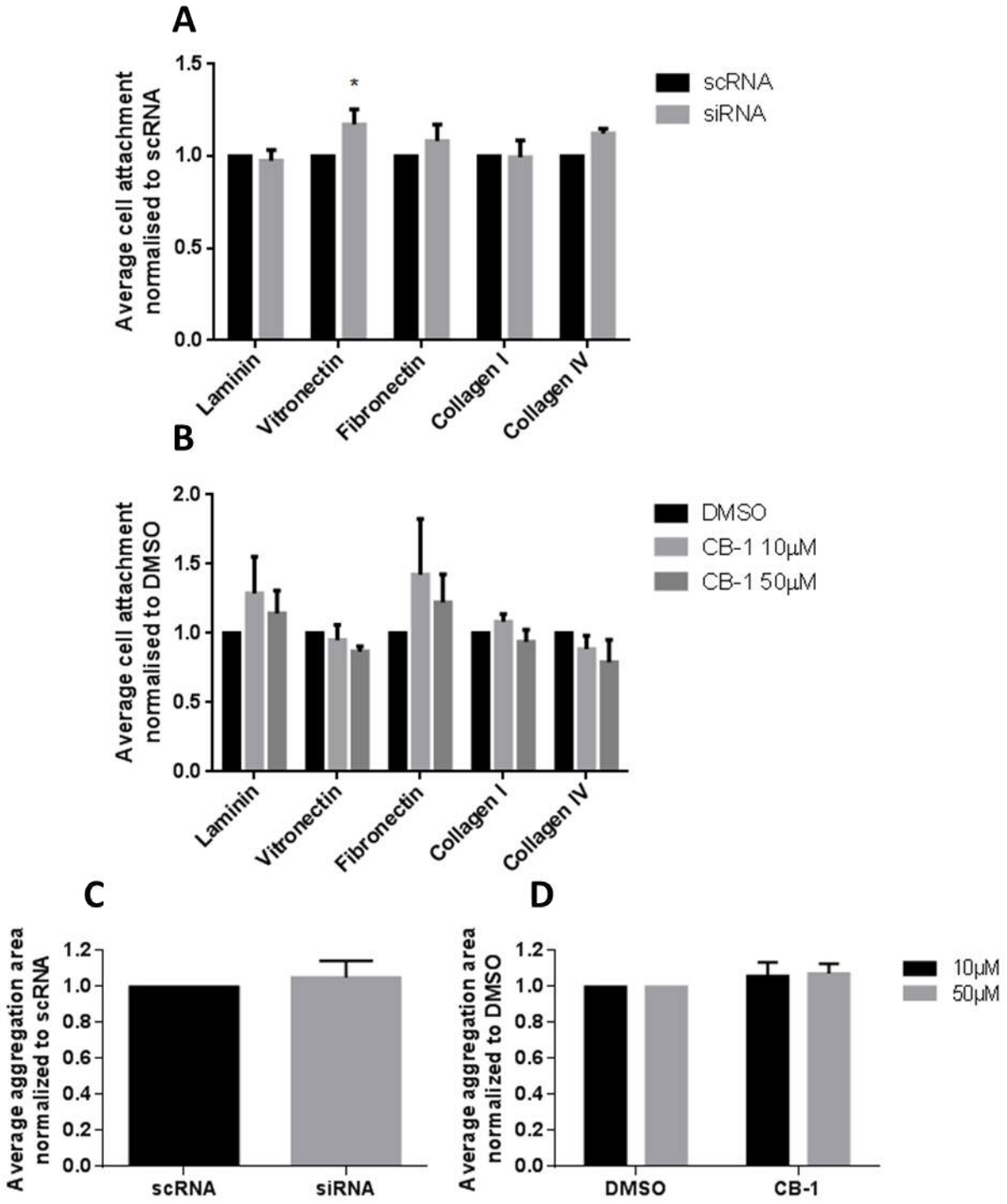


**Figure 3.12- Bcl-3 inhibition had little effect on cell adhesions-** Cell-substrate adhesion assays **(A&B)** were performed in MDA-MB-436 cells. Cells were seeded in 6-well plates and pre-treated with **(A)** siRNA or **(B)** CB-1 along with appropriate controls. After a 48h incubation cells were removed, counted and seeded into 96-well plates coated with various substrates. After 1h incubation un-attached cells were gently washed off with remaining cells stained and counted. Cell-cell adhesion assays **(C&D)** were performed in MCF-7 cells. Cells were seeded into agar coated wells of a 96-well plate with either **(C)** Bcl-3 siRNA or **(D)** CB-1 along with appropriate controls. After 48h incubation aggregate size was measured and analysed. Error bars represent ± SEM of 3 independent experiments. (T-test, *=$p<0.05$ as compared to control).

## 3.4 Effect of Bcl-3 inhibition on invasion and metastatic seeding

Inhibition of the NF-kB signalling pathway has often been seen as an attractive therapeutic approach for cancer treatment, however current approaches have seen limited success due to lack of specificity and issues with significant patient toxicity [222]. More specific inhibition of this pathway has therefore been suggested to reduce side effects and specifically target tumour cells. Previous work in the lab has shown that specific inhibition of Bcl-3, a key regulator of the NF-kB pathway, using small-molecule inhibitors can dramatically reduce metastatic tumour burden *in vivo* [215]. Screening of a panel of novel small molecule inhibitors had identified CB-1 as a lead compound which had been shown to inhibit various forms of cell migration previously in this chapter. Therefore, to further progress its use towards a clinical setting, the effects of CB-1 inhibition on primary tumour growth and metastasis were investigated using the chick chorio-allantoic membrane (CAM) model. Furthermore, as Bcl-3 has been implicated in a variety of other cancer types the effect of Bcl-3 inhibition on prostate and colorectal cancer cell line migration was also tested to determine whether it may have potential therapeutic benefits for different cancer types.

### 3.4.1 Using the chick chorio-allantoic membrane as a model for tumour progression

Testing potential therapeutic drugs *in vivo* can be time consuming and expensive when using standard mouse models, the CAM assay however offers a cheap and relatively simple alternative. It can be utilised to model a variety of different processes involved in tumour progression such as primary tumour growth, metastasis and angiogenesis in a system that usually takes just 14 days to complete. Therefore this model was utilised using the expertise of Marta Pinto (IPATIMUP, Porto) to test the efficacy of CB-1 *in vivo* using GFP-labelled MDA-MB-231 cells which were known to respond to CB-1 *in vitro*. Furthermore, a Bcl-3 overexpressing version of these cells made within the lab by William Yang was also used as a further parameter to test whether increased Bcl-3 expression could drive tumour growth and metastasis.

#### 3.4.1.1 CB-1 did not affect MDA-MB-231 tumour growth in chick-chorioallantoic model

The effects of CB-1 on primary tumour growth were tested by treating cells with 10 µM of CB-1 or DMSO equivalent for 24h before being transplanted onto the CAM and grown for 7 days. Inoculated cells were treated daily with CB-1 or DMSO for the first 5 days after transplantation before being harvested and measured on the 7$^{th}$ day. CB-1 had no significant effect on tumour size in either parental MDA-MB-231 or Bcl-3 overexpressing MDA-MB-231 cells (Figure 3.13A) which was consistent with previous data in mice showing only partial effects of the agents on tumour growth [223]. Furthermore, Bcl-3 overexpressing cells showed no difference in tumour growth when compared to parental control cells.

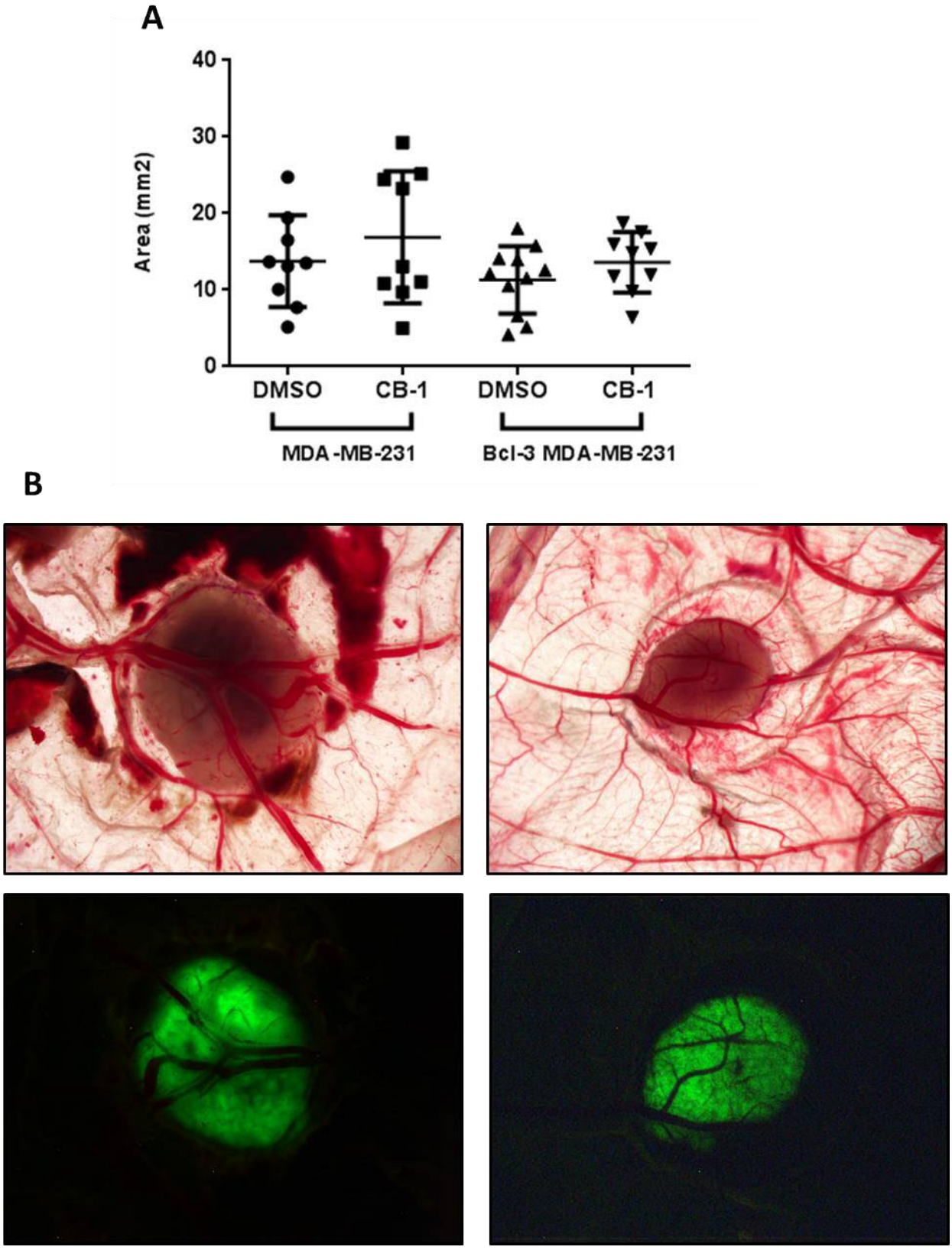


**Figure 3.13- CB-1 had no effect on tumours grown on the CAM- (A)** MDA-MB-231, or Bcl-3 overexpressing MDA-MB-231 cells were inoculated onto the CAM after 24h pre-treatment with either 10 µM CB-1 or DMSO control. Tumours were treated for 5 days post inoculation and left a further 2 days before being harvested and measured. Plots represent individual tumour size of embryos that survived to experiment endpoint at E17 with error bars representing ± SEM of with mean tumour size also shown. (T-test, *=p<0.05 of CB-1 vs DMSO control)**(B)** Representative images of tumours grown on the CAM before being harvested. Top images are brightfield pictures showing growing tumours surrounded by chick CAM and vasculature with fluorescent images shown below highlighting GFP-labelled tumour cells against the non-GFP chick CAM.

#### 3.4.1.2 CB-1 inhibited local invasion of MDA-MB-231 cells on the CAM

The ability of CB-1 to inhibit a variety of different modes of migration has been shown previously in this chapter; however its effect on cell invasion has not been tested. Cell invasion not only requires migration but also cell-adhesion and proteolysis of the extracellular-matrix and can be replicated closely in the CAM.

Immunohistochemistry was performed with help from Stephanie Windsor, Cardiff University, on paraffin embedded sections of CB-1 or DMSO-treated tumours and their surrounding CAM tissue to determine the extent of local invasion away from the primary tumour. Tumour cells were visualized by using a GFP-targeting antibody making it easy to distinguish MDA-MB-231 cells from normal chick tissue (Figure 3.14A&B). Each tumour section was scored for its level of invasion into the CAM by 3 independent scorers (Figure 3.15A). The level of invasion was given a score of 1, 2 or 3 based on the parameters outlined in Table 3.1 with 1 being the least invasive and 3 being the most. In both parental MDA-MB-231 and Bcl-3-overexpressing MDA-MB-231 cells, CB-1 treated tumours showed similar trends of reduced local invasion (Figure 3.15B). Furthermore, DMSO-treated Bcl-3-overexpressing cells appeared to have an increased invasion potential compared to DMSO-treated parental tumours, further indicating the important role of Bcl-3 in tumour invasion and metastasis.

| Invasion score | |
|---|---|
| 1 | Tumour cells in the tumour are tight together forming a compact mass. The invasion front (area where tumour cells touch the CAM mesenchyme) is a clearly defined (encapsulated -like structure) |
| 2 | Tumour cells in the tumour are looser, and in some cases matrigel can be detected. Cells are oriented towards the invasion front. |
| 3 | Tumour cells are oriented towards the invasion front and it is possible to observe single cells or small clusters of cells after the invasive front |

**Table 3.1 - Local invasion scoring system**- Scoring was performed blindly by 3 independent scorers**.**

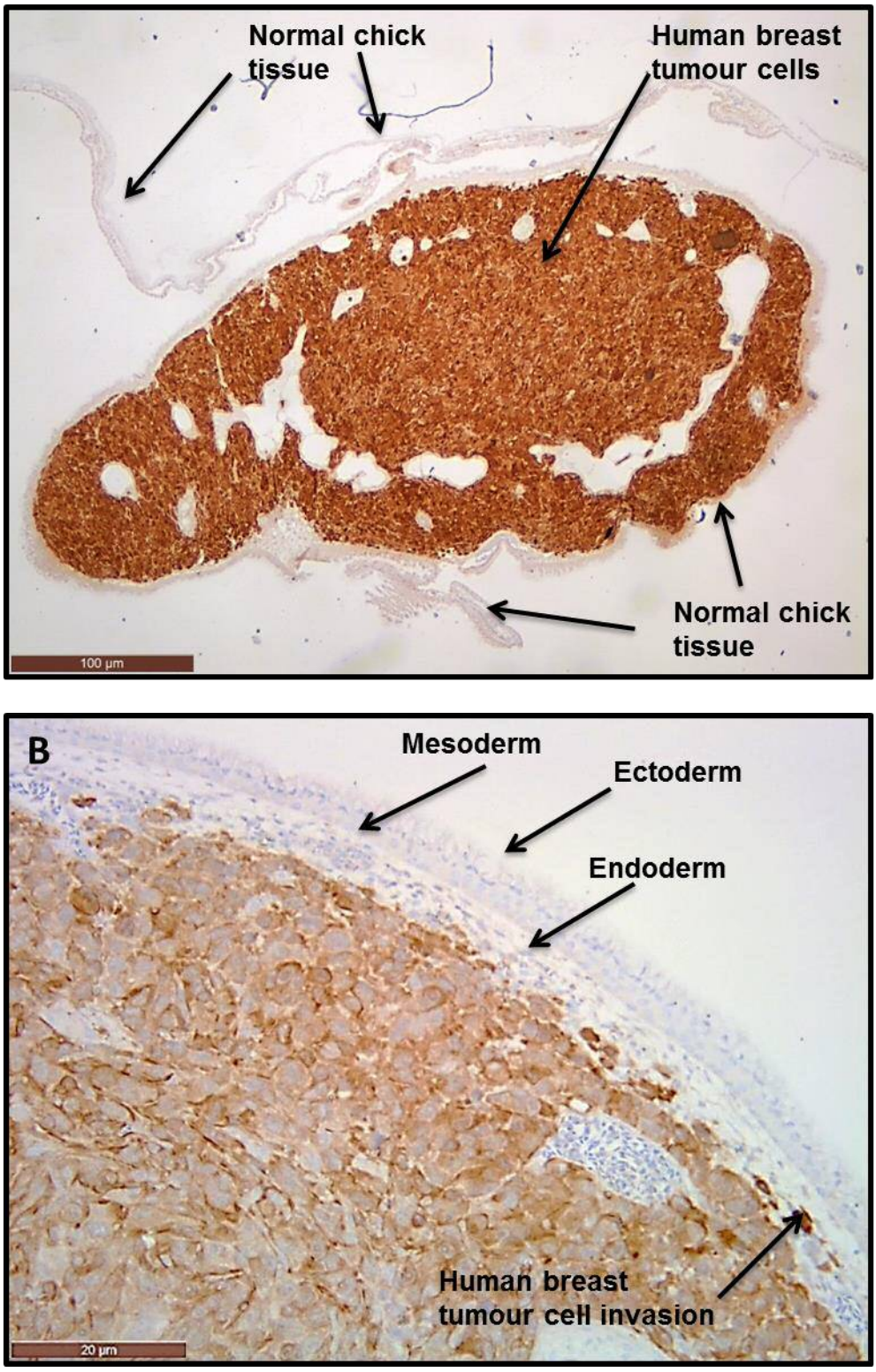


**Figure 3.14-Example of IHC staining used for scoring local tumour invasion- (A)** Gross structure of a tumour grown on the CAM, distinguishing between the GFP expressing breast cancer cells surrounded by normal chick tissue (scale bar = 100 µm). **(B)** Representative image of the CAM/tumour border. The CAM comprises of 3 layers: ectoderm, endoderm and mesoderm. Here tumour cells are shown to be invading through the CAM endoderm towards the mesoderm (scale bar = 20 µm).

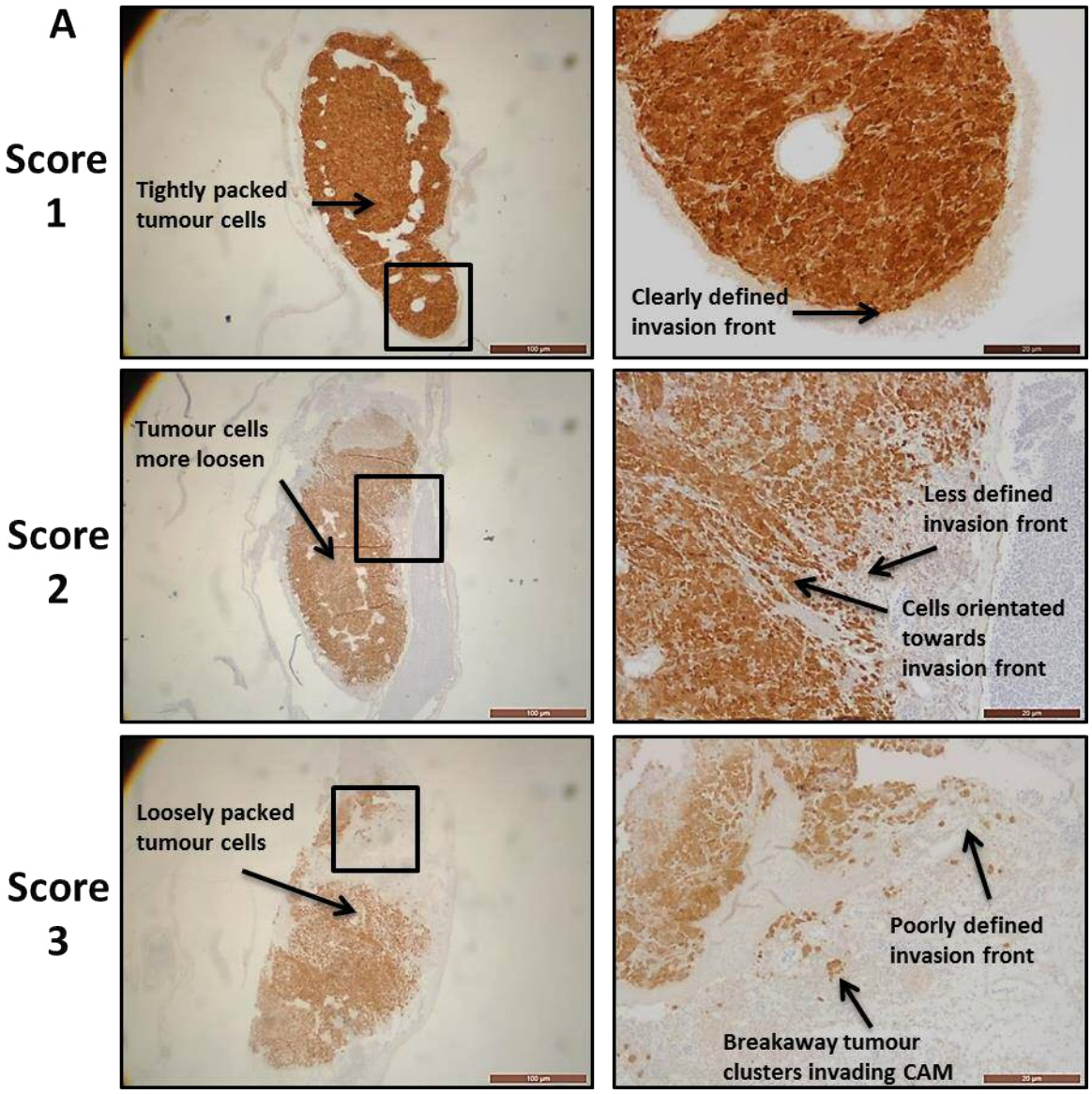


**Figure 3.15- Local tumour invasion scoring using the CAM model**- **(A)** Representative images of the local invasion scores given to MDA-MB-231 or Bcl-3 MDA-MB-231 tumours grown on the CAM. Tumour cells were stained against GFP to distinguish invading cells from normal chick tissue. **(B)** Local invasion scores were given to each tumour type that was treated with either 10 µM CB-1 or DMSO. Scores were assessed blindly by 3 independent researchers (Daniel Turnham, Marta Pinto & Stephanie Windsor with total agreement (3/3 scores) observed in 57% of tumours and majority agreement (2/3 scores) in 43% of tumours) with each condition represented by a minimum of 3 different tumours per condition. (Chi-squared test, *=p<0.05)

#### 3.4.1.3 CB-1 treatment reduced distal metastasis to the chick lungs

Current treatments of final stage metastatic breast cancer are ineffective and in desperate need of improvement. Small molecule inhibition of Bcl-3 using novel compound CB-1 has shown to reduce cell migration and invasion (Figures 3.2 and 3.15), and has been shown to inhibit experimental metastasis of circulating tumour cells in a mouse xenograft model (Clarkson, unpublished data), however its effect on spontaneous metastasis arising from a proximal tumour mass, is unknown. The CAM model has been utilised previously to measure metastatic tumour burden through the use of a Taq-man based quantification system using a human Alu sequence to detect invading human tumour cells at distal sites within the chick embryo [216]. This model was therefore adopted to determine whether treatment of CB-1 could reduce spontaneous metastatic tumour burden in MDA-MB-231 and Bcl-3 MDA-MB-231 tumours grown on the CAM.

Lungs harvested from tumours treated with either 10 µM CB-1 or 0.1% DMSO were extracted for gDNA before qPCR was performed for human Alu. The number of human tumour cells was then determined using a standard curve of serially diluted MDA-MB-231 cells of known quantity. In treated MDA-MB-231 tumours the average number of tumour cells was significantly lower in CB-1-treated samples compared to DMSO controls, however in Bcl-3-overexpressing tumours no difference was observed between CB-1 and DMSO treatment (Figure 3.16).

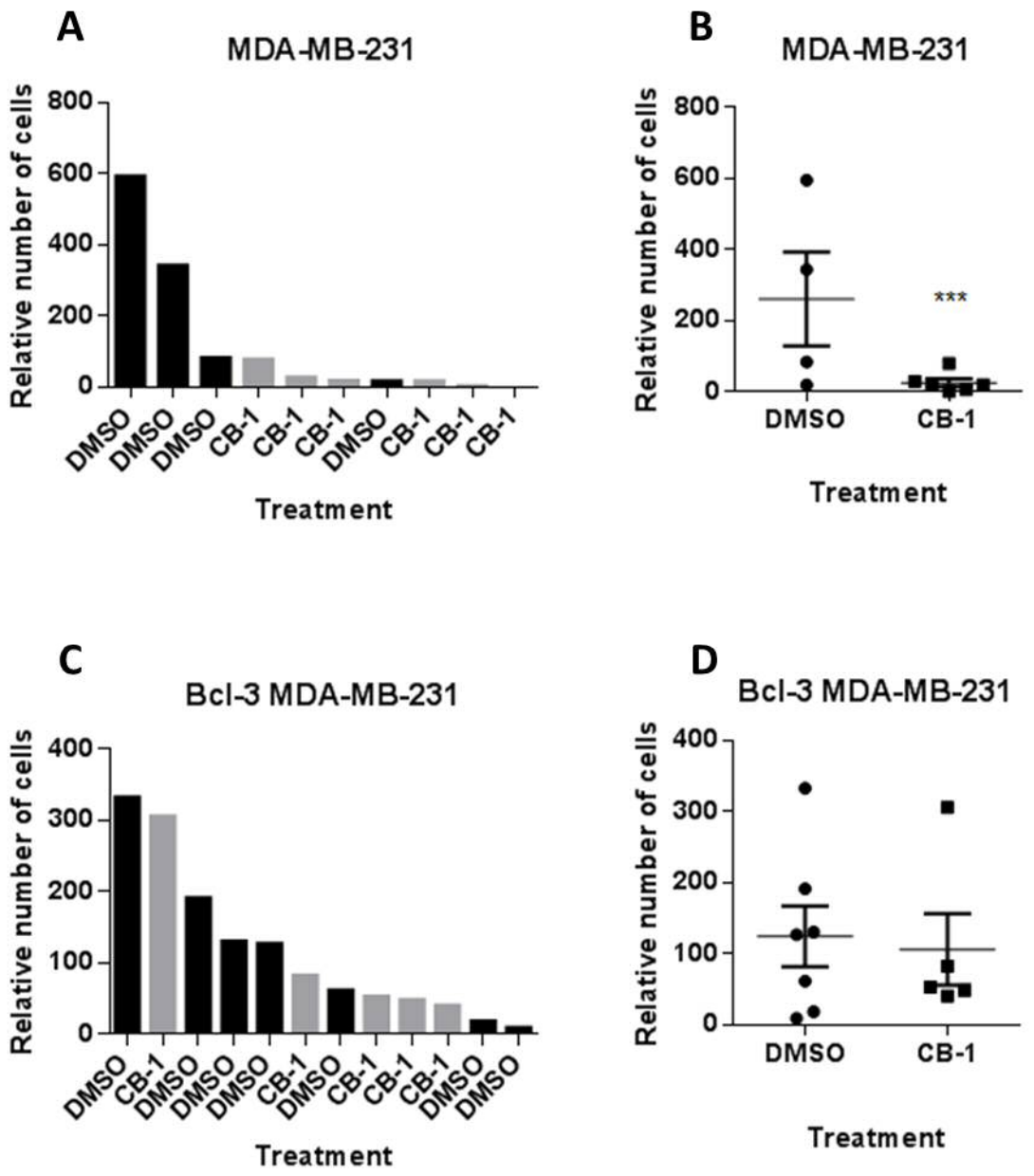


**Figure 3.16- CB-1 reduced MDA-MB-231 pulmonary metastasis in CAM metastasis model-** The lungs of chick embryos were harvested 7 days after the inoculation of MDA-MB-231 or Bcl-3 MDA-MB-231 cells treated with either 10 µM CB-1 or 0.1% DMSO. After gDNA was extracted from the lungs the total number of cells was determined by qPCR against human Alu and quantified using a standard curve of known numbers of MDA-MB-231 cells. The number of cells in individual tumours is displayed as a waterfall plots for both MDA-MB-231 **(A)** and Bcl-3 MDA-MB-231 tumours **(C)** or as scatter plots **(B&D respectively)** to show the number of cells for individual tumours. Error bars represent ± SEM of all tumours shown. (T-test, ***=p<0.005 as compared to DMSO).

### 3.4.2 CB-1 treatment inhibited cell migration in different cancer types

Since the discovery of the involvement of Bcl-3 in breast cancer, it has been found to be upregulated in a number of other solid tumour types such as nasopharyngeal, cervical and prostate [204, 224, 225]. Furthermore, the expression of nuclear Bcl-3 in colorectal cancer has been associated with an increased chance of death and has been highlighted as a potential therapeutic target **[226]**. Although the effects of Bcl-3 inhibition using siRNA have been studied to various degrees within these cancers the use of small molecule inhibitors to specifically block Bcl-3 function has not. Therefore, the effect of lead compound CB-1 was tested against various types of cancer cell lines to test its potential therapeutic benefits on different cancer types. This was performed using the Electric Cell-substrate Impedance Sensing (ECIS) assay through collaboration with the Life Sciences Research Network Wales cancer metastasis modelling platform headed by Professor Wen G. Jiang.

To first test the ECIS platform two breast cancer cell lines, HCC1954 and BT-549, which have previously been optimised by our collaborators were tested for their response to CB-1 treatment. Cells were seeded onto the ECIS platform with either 10 μM CB-1 or 0.1% DMSO and monitored for 48h. Wounds were created automatically after 18h and changes in electrical impedance caused by the cells migrating back over the wounds were monitored continuously. The changes in impedance over 5h post-wound creation were analysed and normalised to DMSO controls with cells treated with CB-1 showing a significantly reduced migratory capacity in both HCC1954 and BT-549 cell lines (Figure 3.17).

To test the effects of CB-1 treatment on the migratory ability of different cancer types the prostate cell line PC-3 and the colorectal cell line RKO were tested following the same protocol as previously used for the breast cancer cell lines. Both cell types showed a significant reduction in migratory capacity after CB-1 treatment compared to DMSO over a 5h post-wound period (Figure 3.18).

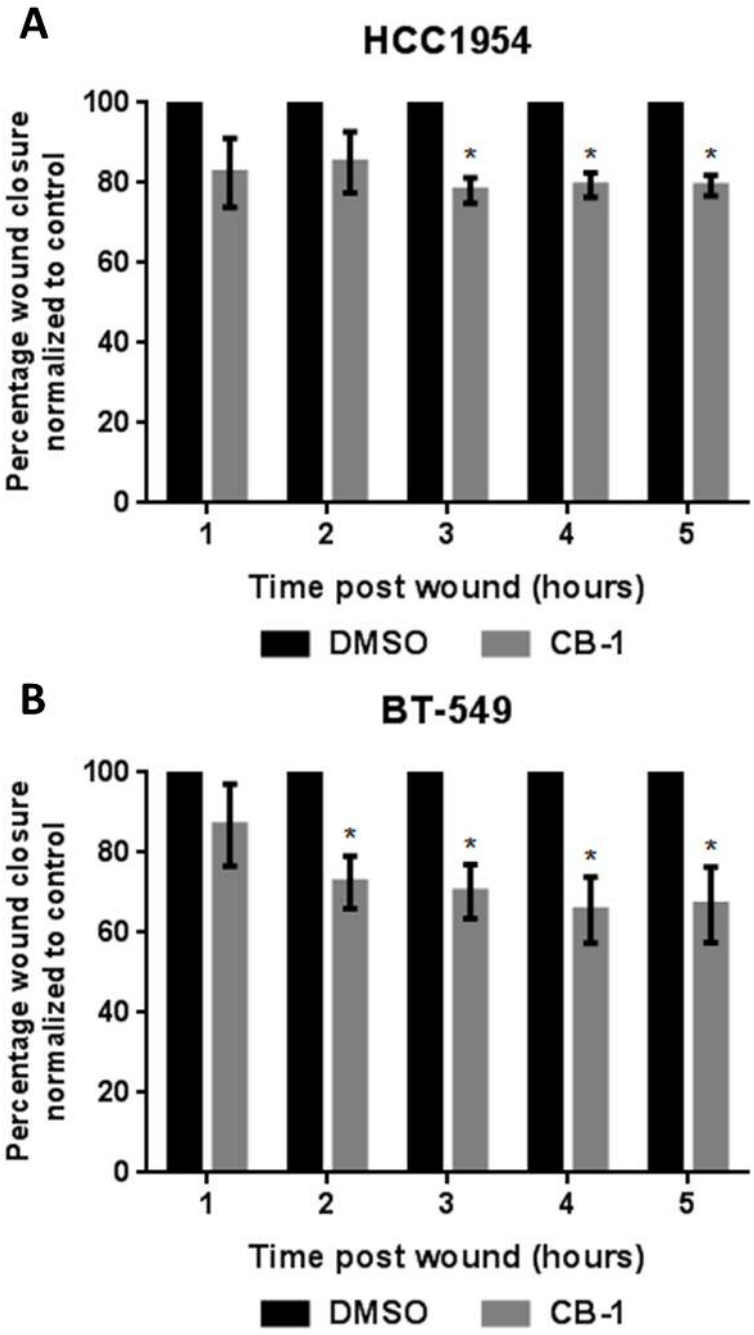


**Figure 3.17- CB-1 inhibited breast cancer cell line migration in ECIS motility assays**- ECIS migration assays were performed using breast cancer cell lines HCC1954 **(A)** and BT-549 **(B)**. Equal numbers of cells were seeded onto ECIS plates with either 10 µM CB-1 or 0.1% DMSO and left to adhere before wounds were created automatically after 18h. Cells were monitored for their ability to migrate back over the wounds and analysed by measuring changes in impedance for the first 5h post wound formation before being normalized to DMSO controls. Error bars represent ± SEM of 3 independent experiments. (T-test= *=$p<0.05$).

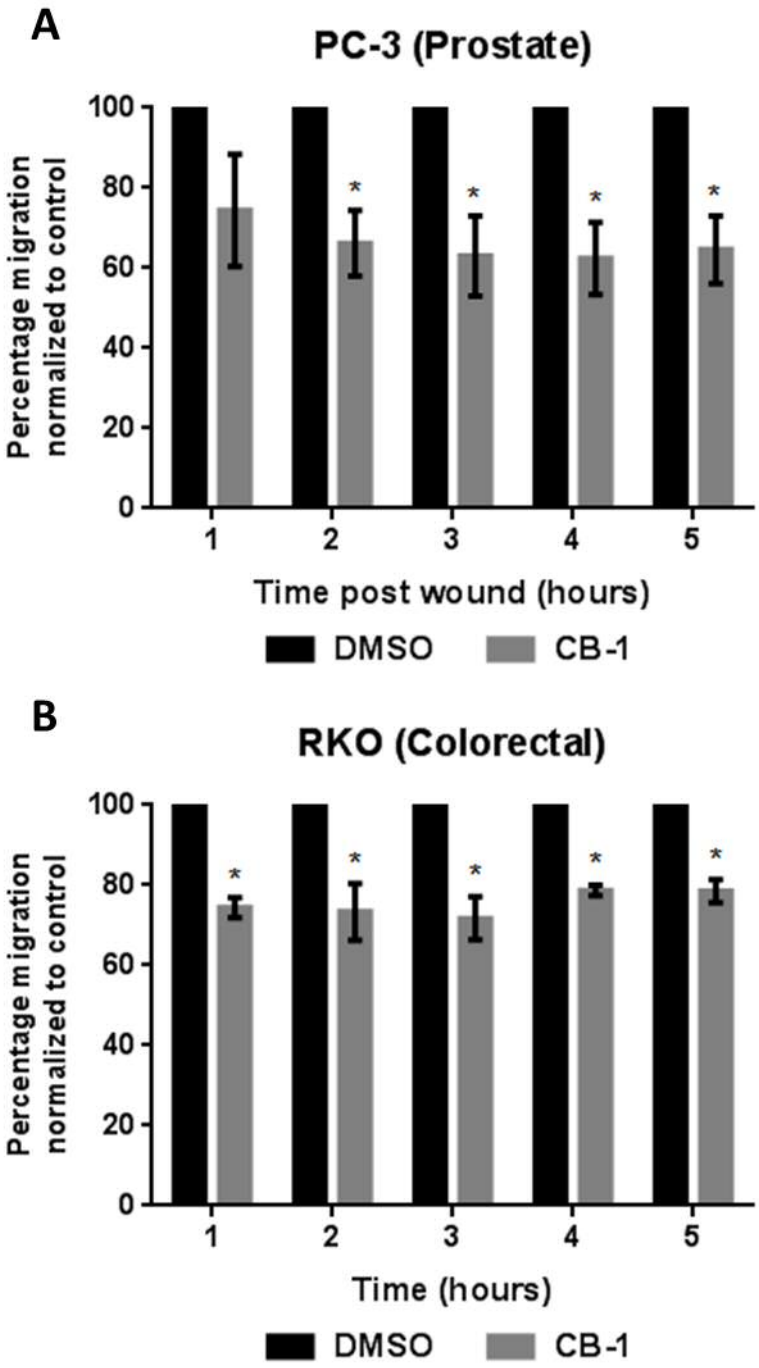


**Figure 3.18- CB-1 inhibited prostate and colorectal cancer cell line migration**- ECIS assays were performed using prostate PC-3 **(A)** and colorectal RKO **(B)** cancer cell lines. Equal numbers of cells were seeded onto ECIS plates with either 10 µM CB-1 or 0.1% DMSO and left to adhere before wounds were created automatically after 18h. Cells were monitored for their ability to migrate back over the wounds and analysed by measuring changes in impedance for the first 5 h post wound formation before being normalized to DMSO controls. Error bars represent ± SEM of 3 independent experiments. (T-test= *=$p<0.05$).

## 3.5 Discussion

Previous work has shown that inhibition of Bcl-3 can reduce cell migration as well as metastatic tumour burden in models of human breast cancer [188, 214]. This suppression of migration and metastasis can be replicated by blocking Bcl-3 function using a small-molecule inhibitor designed to block Bcl-3 from binding to p50 and p52 [215]. The effect of Bcl-3 inhibition has been widely tested using only Boyden chamber-like assays, however a deeper evaluation of the different types and mechanisms of migration in which Bcl-3 may regulate in metastasising cells has never been tested. Therefore, the aim of this chapter was to investigate whether Bcl-3 inhibition by either siRNA or a new class of novel Bcl-3 inhibitors could impair different types of cell migration in varying types of breast cancer cells.

In this chapter we characterise the migratory capabilities of three distinct breast cancer cell lines MDA-MB-231, MDA-MB-436 and MCF-7s which each have distinct morphological traits which we postulated would affect their migratory capabilities. Indeed the highly mesenchymal MDA-MB-436 cells showed both amoeboid and mesenchymal-like single cell migration capabilities but were unable to migrate collectively due to their inability to form cell-cell contacts. Contrary to this, the epithelial cell line MCF-7 was only capable of collective migration with no single cell migration ability observed, most likely due to the need for strong cell-cell contacts. In another mesenchymal-like cell line, MDA-MB-231, both mesenchymal and collective migration was observed, with these cells also showing an improved amoeboid-like migration potential compared to MDA-MB-436 cells. This data along with their profound morphology suggests that both MDA-MB-436 and MCF-7 cells are more differentiated towards their mesenchymal and epithelial phenotypes respectively whereas the MDA-MB-231 cell line is less specialised and capable of switching between the different migratory mechanisms depending on their environment. This may offer a substantial advantage during metastasis and could explain the relatively low metastatic potential of both MCF-7 and MDA-MB-436 cells in mouse xenograft models [227, 228].

The 'plasticity' observed in MDA-MB-231 cell migration further highlights the difficulty in targeting metastasis and the importance of synthesising anti-metastasis therapeutics capable of ubiquitously inhibiting cell motility. This ability of tumour cells to switch between migratory types in response to changing microenvironments and drug treatments make targeting more primitive and conserved pathways utilised in various mechanisms of migration a more likely source of success. We have shown in this chapter that Bcl-3 may have this potential with its suppression using siRNA capable of reducing at least 3 different migratory phenotypes, amoeboid, mesenchymal and collective migration (Figures 3.1, 3.3 and 3.7). Furthermore, we have demonstrated that in MDA-MB-436 cells this may be through a reduction in Rac1 and Cdc42 GTPase activity (Figure 3.11), two key regulators of cytoskeletal organization that drive cell migration through the formation of cell protrusions such as lamellipodia and filopodia [229, 230]. This builds upon previous data showing that Arhgdib, a GDP exchange inhibitor, which preferentially binds to both Rac1 and Cdc42 to regulate cell migration, is upregulated after Bcl-3 inhibition [214, 231, 232]. Interestingly, inhibition of Rac has also been shown to inhibit the Bcl-3 regulating transcription factor STAT3, however recent work has also shown STAT3 to be downregulated by Bcl-3 inhibition, suggesting a potential pathway that could be further explored [211, 233]. Taken together this data suggests a role for Bcl-3 in the regulation of cytoskeletal organization through GTPase activity, which could explain how Bcl-3 is able to regulate a variety of migratory mechanisms. Further experiments are required to determine GTPase activity in other invasive and non-tumorigenic cell lines after Bcl-3 inhibition, and whether a reduction in Rac1/Cdc42 activity results in downstream changes in the ratio of G and F actin as well as invasive protrusion formation.

Two processes that are known to be regulated through GTPase-mediated cytoskeletal changes are cell-cell and cell-ECM adhesions, which also play important roles in metastasis and cell migration [234, 235]. Cell-ECM assays were performed in MDA-MB-436 cells as they had previously been shown to be more sensitive to Bcl-3 inhibition compared to MDA-MB-231 cells. Despite a slight trend for Bcl-3 inhibition to increase cell-ECM adhesions, the only significant change was a small

increase in vitronectin adhesion (Figure 3.12). Rac1 and Cdc42 have been shown to mediate integrin-dependent cell spreading during cell-ECM adhesions suggesting that Bcl-3 inhibition may reduce the ability of these cells to adhere to different substrates [236]. The general increase observed after Bcl-3 inhibition contradicts this research and suggests that Bcl-3-mediated GTPase activity may be specific to cell migration. Cell-ECM adhesions were not tested in MDA-MB-231 and MCF-7 cells, however if similar trends were observed in future experiments it could help support this hypothesis. MCF-7 cells were tested in a cell-cell aggregation assay as they were the only cell line to form tightly bound quantifiable aggregates, with Bcl-3 inhibition having no noticeable effect on aggregate formation (Figure 3.12). It should be noted that although crudely informative, this assay is not the most sensitive assay to quantify cell-cell adhesions and a more in depth analysis of cell-cell adhesion molecules through immunofluorescence may be more informative.

Throughout this chapter Bcl-3 inhibition was performed by siRNA as well as CB-1; a novel Bcl-3 inhibitor that has been specifically synthesised to block Bcl-3 from binding to p50 and p52 therefore impairing its function. Although CB-1 was outperformed by two analogues in the Fluoroblok migration assay (Figure 3.2) it exhibited no signs of toxicity at higher concentrations, showed good aqueous and microsomal solubility as well as reduced plasma protein binding and hERG cardiotoxicity compared to the better performing analogues (Clarkson, unpublished), confirming it as our lead compound. Our data suggests that CB-1 is capable of mimicking siRNA by inhibiting the various migration phenotypes although this effect was not as profound as siRNA, and potentially not acting through a reduction in GTPase activity. This suggests that CB-1 inhibition of Bcl-3 is either not as efficient as siRNA knockdown or is acting through a different mechanism, potentially off-target. The first scenario is more likely as knockdown of Bcl-3 with siRNA is a highly efficient process with a minimum of 85% reduction in Bcl-3 expression observed in most assays, whereas CB-1 has no effect on the expression of Bcl-3 and only acts through blocking Bcl-3 binding to p50 and p52. Furthermore, the half-life of CB-1 is not fully characterised and it is possible that CB-1 may be acting transiently and may not be as long-lasting as siRNA inhibition. The second scenario is

also plausible however, as pharmacological inhibition of Bcl-3:p50 or Bcl-3:p52 binding likely represents only a fraction of Bcl-3 functions, and it remains to be fully established the full extent of CB-1's molecular intervention on downstream Bcl-3 activities outside of NF-kB activity. Moreover, further experiments examining the efficiency of CB-1 in blocking Bcl-3 binding to both p50 and p52 are ongoing through both ELISA and immunoprecipitation assays in order to confirm CB-1 is acting on-target throughout the timecourse of *in vitro* treatments, as formally this too could be responsible for diminished effects of Bcl-3 pharmacological inhibition compared to siRNA. Increasing the concentration of CB-1 and replenishing compound treatments more regularly as well as making small adjustments to its chemical formula which is also currently ongoing may improve its effects *in vitro* and *in vivo.*

The main aim of testing CB-1 alongside Bcl-3 siRNA was to develop its use towards a clinical setting. This was furthered by *in vivo* CAM assays which were used to model CB-1 effect on tumour growth, local invasion and metastatic burden. This experimental model is less frequently used than mouse models; however it was used here to test its efficacy as an alternative model for future compound screening due to its relatively low cost and short experimental time frame. Both parental 231 and a Bcl-3 overexpressing 231 cell line (confirmed by Will Yang) was used for CAM assays, however no changes in primary tumour growth were observed after CB-1 treatment or Bcl-3 overexpression (Figure 3.13). This was not surprising given previous data suggesting Bcl-3 may regulate metastasis independently of primary tumour growth [214]. CB-1 treatment did however reduce the extent of local tumour invasion (Figure 3.15) which correlates with its effect on migration *in vitro,* however further replicates are required to confidently confirm this. Overexpression of Bcl-3 in this model did appear to increase invasion, however again more replicates would be required to confirm this observation (Figure 3.15). Metastatic tumour burden was determined by qRT-PCR targeting the human Alu gene in chick lungs harvested after CB-1 or DMSO treatment, with CB-1 significantly reducing the number of tumour cells metastasising to the lungs compared to DMSO controls in normal MDA-MB-231 cells (Figure 3.16). Bcl-3-overexpressing MDA-MB-231 cells showed

no change in metastatic tumour burden after CB-1 treatment (Figure 3.16) and may require higher or more frequent CB-1 treatments to compensate for a higher turnover of Bcl-3 protein compared to parental 231 cells. Together this data correlates with previous work that suggests blocking of Bcl-3 can mimic siRNA inhibition of Bcl-3 and inhibit cell migration and metastatic burden, making this a promising therapeutic target for the treatment of metastasis in breast cancer [215]. Further experiments looking into the long term effects of CB-1 treatment still need evaluating using a longer lasting tumour model other than the CAM which is limited to only 14 days, as well as models of different cancer types as only the triple-negative MDA-MB-231 cells were tested here.

Although primarily our focus here was to understand the effects of Bcl-3 in breast cancer, a number of other human cancers have shown correlations with Bcl-3 and poor prognosis making it an interesting therapeutic target [224, 226, 237]. Therefore, the effect of CB-1 was tested on different tumour types using the ECIS assay to test the efficacy of Bcl-3 inhibitors in prostate and colorectal cancer cell lines. Two breast cancer cell lines were used to test the system with CB-1 significantly reducing cell migration in both lines (Figure 3.17), an observation that was replicated in both prostate and colorectal cells (Figure 3.18). Although only preliminary, this does support previous data in this chapter suggesting Bcl-3-mediated migration is not cell-specific and may be a relevant target for a variety of tumour types, further enhancing its appeal for development towards a more clinical setting.

In conclusion, our data suggests that Bcl-3 is capable of regulating both single cell and collective types of cell motility which may not be limited to breast cancer. This may be due to a reduction in GTPase activity, more specifically Rac1 and Cdc42, however further research is required to fully understand how Bcl-3 is regulating this. Reduced cell migration can at least partially be mimicked by small molecule inhibition of Bcl-3, with lead compound CB-1 capable of reducing invasion potential and metastatic tumour burden *in vivo* making it an interesting candidate for further pre-clinical evaluation.

# Chapter 4:
# Identifying the role of Bcl-3 in EMT

# 4 Identifying the role of Bcl-3 in EMT

## 4.1 Introduction

Previous work has suggested the importance of Bcl-3 in promoting metastasis, however very little research has tried to understand its role in what is regarded as the initiating step of this process, epithelial to mesenchymal transition (EMT). During EMT epithelial cells differentiate into an invasive mesenchymal-like phenotype, a process that is tightly regulated by a number of factors that facilitate a change in morphology and invasive potential.

NF-kB signalling has been shown to regulate various EMT-associated transcription factors such as Twist, Slug, ZEB1 and ZEB2, indicating its importance in EMT induction and maintenance; whether Bcl-3 plays a part in this regulation is unknown [151, 238, 239]. Previous research using a murine breast cancer model has suggested that the EMT markers E-cadherin, N-cadherin, and Snail are not regulated through Bcl-3. However, in human melanoma, Bcl-3 has been shown to regulate Slug expression independently of Snail indicating the potential for Bcl-3 to partially regulate certain mediators of EMT [214, 240]. Further evidence of a potential role for Bcl-3 in EMT has been seen from microarray analysis where Bcl-3 was shown to be upregulated in EpH4 cells stimulated into EMT using TGF-β [241]. Interestingly, a recent publication has shown an important role for Bcl-3 in regulating TGF-β signalling through the stabilization of the transcriptional modulator SMAD3 [188]. This paper also suggests that disruption of this stabilization through Bcl-3 inhibition in the mesenchymal MDA-MB-231 cell line can stimulate a reversion through an MET-like process, further eluding to the importance of Bcl-3 in EMT and potentially MET in breast cancer [188]. Although these studies have suggested a potential role for Bcl-3 in mediating EMT and MET it has yet to be explored in detail and therefore requires a more detailed analysis in a model that truly represents this process.

The main aims of this chapter therefore were to determine the role of Bcl-3 in EMT of human breast cancer cells, as well as investigating its role during the reversion back to an MET-like

state. To investigate this it was important to first develop a model of EMT in which epithelial cells could be stimulated into an EMT-like state as well allowing them to revert back to their original condition. This model could then be used to assess the role of Bcl-3 during both EMT and MET. From the previously mentioned studies we hypothesised that Bcl-3 may, at least in part, regulate this process through mediating the expression of important transcription factors that mediate EMT.

## 4.2 Pilot study of EMT in normal mouse mammary EpH4 cells using CB-1

The induction of epithelial cells into an EMT-like state has been demonstrated previously through the use of TGF-β stimulation as well as various methods of genetic modification [242, 243]. As an initial pilot study to test the effect of Bcl-3 inhibition during EMT, we utilised the expertise of our collaborators Dr Carla Oliveira and Dr Patricia Oliveira (Ipatimup, Porto) who have developed an EMT model in the normal mouse mammary EpH4 cell line. In this fully-characterised model TGF-β is used to stimulate epithelial EpH4 cells into EMT, which can then be removed allowing EMT-like cells to revert back through MET making this a useful model for the study of both processes.

Due to constraints limiting the time available to utilise this model it was decided that instead of trying to optimise the addition of Bcl-3 siRNA into the model it would be more efficient to use small molecule inhibitors of Bcl-3 as they could be incorporated easily into the established system. To maximise any effects seen in this model, lead compound CB-1 was selected as well as the best performing analogue CB-43. Migration assays and immunofluorescence were used to determine any effects of Bcl-3 inhibition on EMT or MET.

### 4.2.1 Effect of Bcl-3 inhibition on EMT & MET migration

Firstly, EpH4 cells were tested with Bcl-3 inhibitors CB-1 and CB-43 for their ability to inhibit migration in parental, EMT-stimulated, and MET-reverting cells. EpH4 cells were stimulated with TGF-β to induce EMT before being treated with 10 μM DMSO, CB-1 or CB-43 for 48h before wound healing assays were performed. Cells stimulated into EMT were also left to revert back in the absence of TGF-β but in the presence of DMSO, CB-1, or CB-43, for a further 48h to determine the effects of Bcl-3 inhibition on MET-like cells.

Unstimulated EpH4 cells showed a significant reduction in cell migration after treatment with both compounds compared to DMSO, with CB-43 outperforming CB-1 similar to what was observed previously during compound screening (Figure 4.1A). In both EMT EpH4 and MET EpH4 cells, a significant reduction in cell migration was observed after CB-43 treatment; however no changes were seen after CB-1 treatment (Figure 4.1B&C). This correlates with previous data showing that Bcl-3 inhibition can inhibit cell migration independent of cell type or mode of migration. Interestingly, although not quantified, CB-43 treated cells did appear to be less sensitive to EMT stimulation with a higher proportion of cells maintaining a normal epithelial-like morphology with fewer mesenchymal-like cells appearing suggesting that fewer cells had been stimulated into EMT.

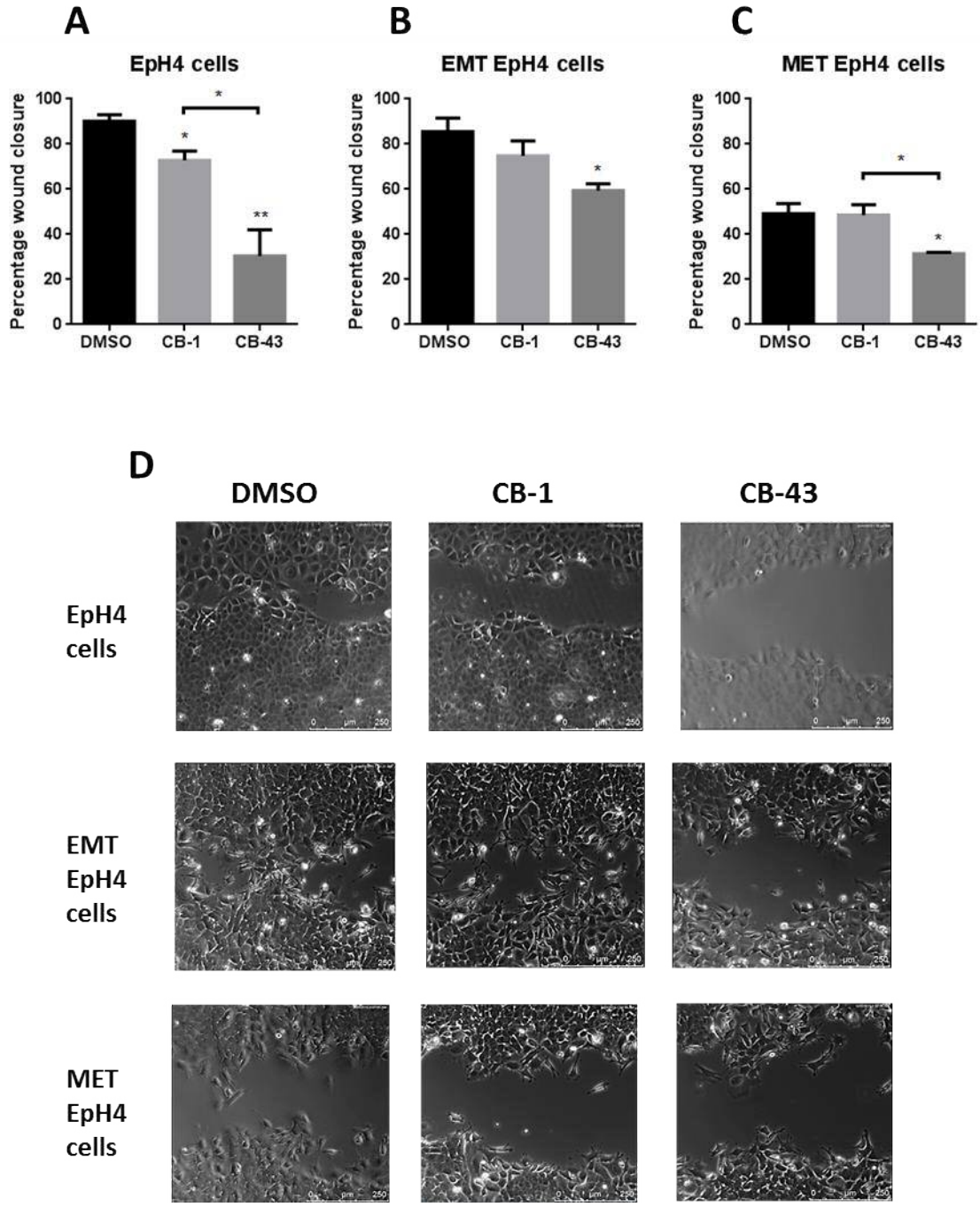


**Figure 4.1-Bcl-3 inhibition inhibited EMT induced EpH4 cell migration-** Wound healing assays for cell migration were performed in the normal mouse mammary epithelium cell line EpH4. **(A)** Parental EpH4 cells were incubated with 10µM of CB-1, CB-43 or equivalent DMSO for 48h prior to wound formation where they were maintained in the presence of compound for a further 12h before assessment of migration (measured by percentage of wound closure). **(B)** Cells were induced for 7 days with TGF-ß to create EMT EpH4 cells with compound added 48h prior to wound formation. **(C)** Cells were induced for 7 days with TGF-ß before being allowed to revert back into MET EpH4 cells for 48 hours whilst being incubated with 10µM of compound prior to wound formation. Error bars represent ± SEM of 3 independent experiments (T-test, *=p<0.05 and **=p<0.01). **(D)** Representative images of EpH4, EMT EpH4 and MET EpH4 cells after treatment with DMSO, CB-1 or CB-43 12h post wound formation. Scale bar= 250 µm.

### 4.2.2 CB-43 treatment disrupted E-cadherin localisation

To determine whether Bcl-3 inhibitors affected the ability of EpH4 cells to undergo EMT or MET cells were analysed by immunofluorescence in parallel with the migration assays. This however was only performed in parental and MET EpH4 cells due to a lack of EMT EpH4 cells caused by a reduced proliferative capacity and a need to utilise these to create MET EpH4 cell populations. Cells were stained for the epithelial marker E-cadherin and the mesenchymal marker fibronectin, with both EpH4 and MET EpH4 showing a clear redistribution (and possible loss of overall levels, although this has not been quantified) of E-cadherin after CB-43 treatment (Figure 4.2). In parental EpH4 cells after CB-43 treatment, E-cadherin appeared to become redistributed from the plasma-membrane to the cytosol suggesting a disruption of the cell-cell junctions, which is usually associated with an induction of EMT; however this was not coupled with an increase in fibronectin staining. A small subset of cells also exhibited a similar redistribution of E-cadherin following CB-1 treatment, however this was not as uniform or as clearly defined. Similarly in MET EpH4 cells, CB-43 reduced the expression of E-cadherin homogeneously across the cell population, while CB-1 had a more localised effect resulting in small patches (or colonies) of E-cadherin staining compared to untreated controls that exhibited larger inter-linked areas of cells with E-cadherin staining.

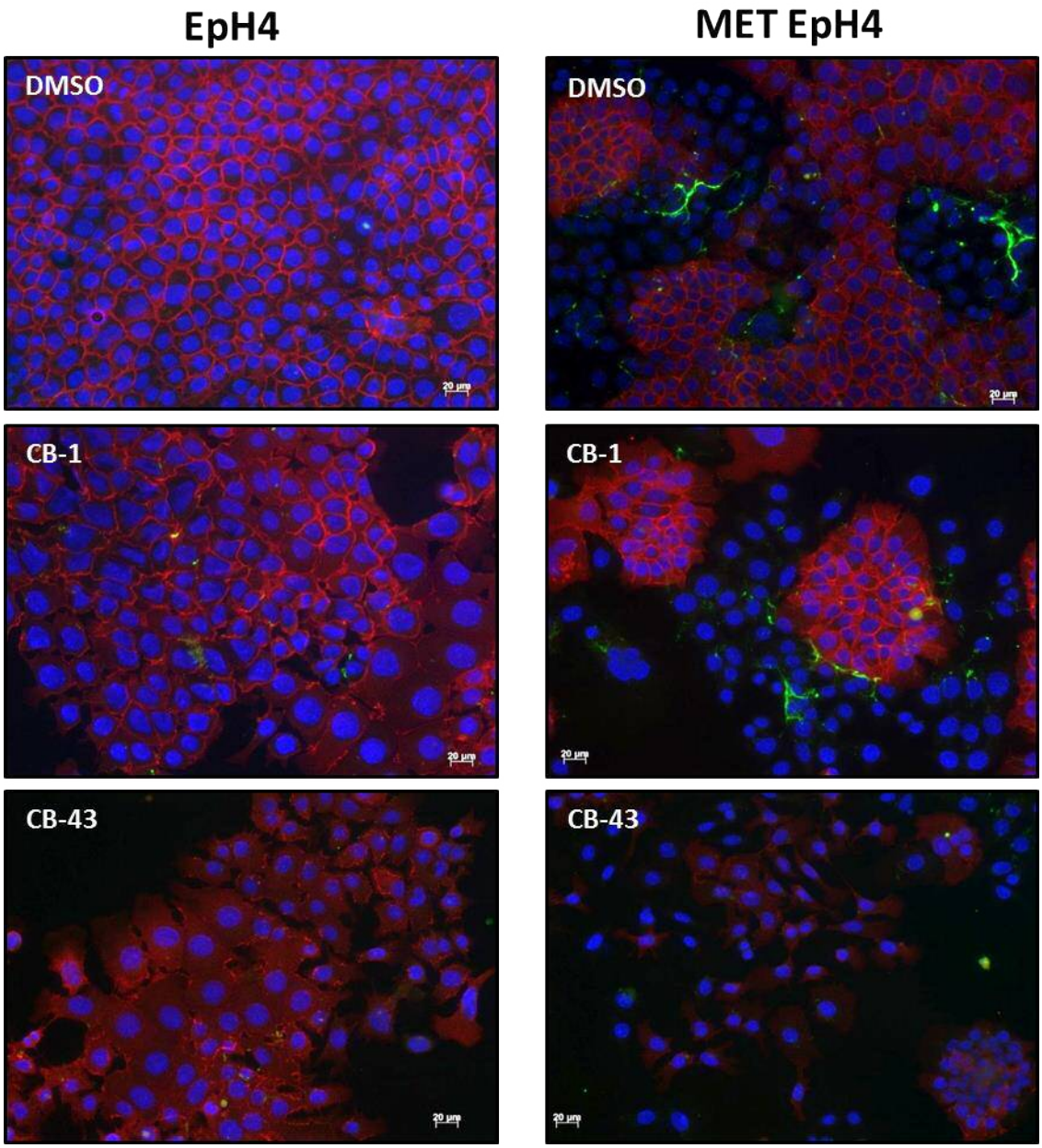


**Figure 4.2- Bcl-3 inhibition disrupted E-cadherin localization in EpH4 cells-** Representative images of immunofluorescence performed in EpH4 cells treated with 10µM of CB-1, CB-43 or equivalent DMSO for 48h and MET EpH4 cells induced into EMT for 7 days with TGF-ß before being allowed to revert back for 48h in the presence of inhibitor or DMSO. After treatment cells were fixed in methanol and stained for epithelial and mesenchymal markers E-Cadherin (red) and fibronectin (green) respectively as well as the nuclear stain DAPI (blue). Scale bar= 20 µm.

## 4.3 Optimisation of Epithelial to Mesenchymal transition in MCF-7 cells

Despite a limited data set the pilot study previously described suggested a potential role for Bcl-3 in EMT; however this was not substantiated and needed to be further explored. Furthermore, this data was taken from a non-tumorigenic mouse mammary cell line and although informative, required repeating in a human breast cancer model. For this reason the epithelial MCF-7 cell line was selected as it has previously been shown to be capable of undergoing EMT and had previously responded to Bcl-3 inhibition (see chapter 3) [242]. Although some studies have shown that TGF-β stimulation induces EMT in MCF-7 cells, this has been disputed by other studies suggesting they are unresponsive [242, 244]. Therefore, we employed a new method of EMT-induction that has recently been made commercially available (R&D systems). This approach uses a combination of Wnt and TGF-β signalling as well as blocking of E-cadherin-based adhesion and has been shown to induce EMT in a range of cell types that are unresponsive to TGF- β-stimulation alone [245]. As this media supplement is relatively new and untested in the literature it was fully characterised for its ability to induce EMT in MCF-7 cells by looking at changes in cell morphology, motility and gene expression.

### 4.3.1 EMT stimulated MCF-7 cells showed mesenchymal like morphology and enhanced cell motility

MCF-7 cells were stimulated for 5 days in EMT-inducing media before analysing cell morphology and motility. After EMT stimulation a large proportion of cells appeared less polarised gaining spindle like protrusions similar to those seen in mesenchymal cells, thus indicating some degree of EMT induction (Figure 4.3). When these cells were analysed by time-lapse microscopy in a wound-healing assay, the ability of EMT-stimulated cells to migrate collectively was clearly disrupted, with a number of cells moving away from the invasion front as individual cells, which was not observed in unstimulated controls (Figure 4.4 & supplementary videos 5&6). It should be noted that although a large proportion of these cells did appear to become more mesenchymal, this was not a universal change with some cells remaining in epithelial-like colonies.

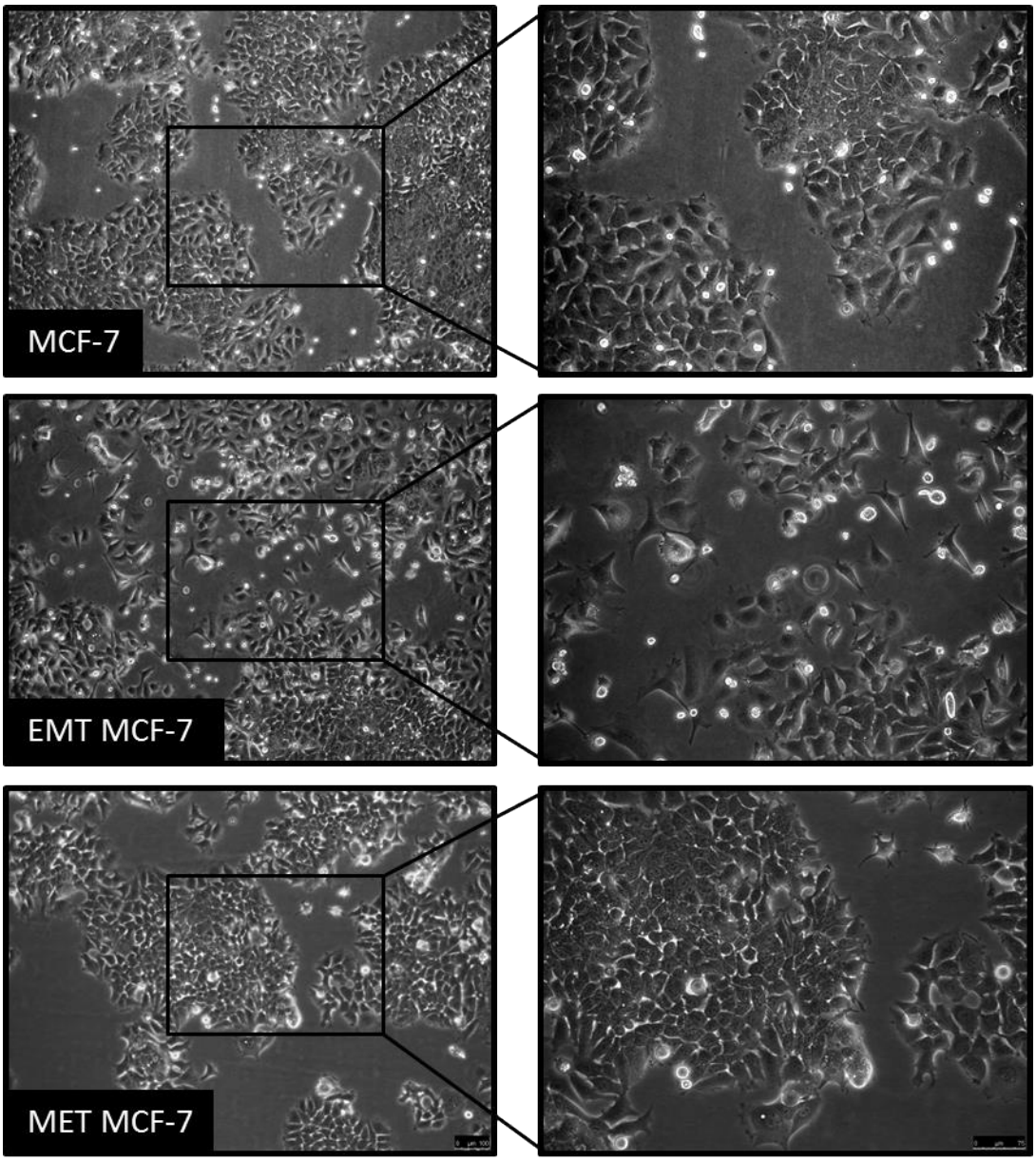


**Figure 4.3- Morphological changes after EMT stimulation in MCF-7 cells-** Representative images of unstimulated (MCF-7) cells, EMT stimulated cells (EMT MCF-7) and reverting (MET MCF-7) cells. EMT MCF-7 cells were stimulated with StemXVivo media supplement for 5 days with MET MCF-7 cells pictured 5 days after the removal of EMT media supplements. Scale bar= 100 µm and 75 µm for low and high magnification respectively.

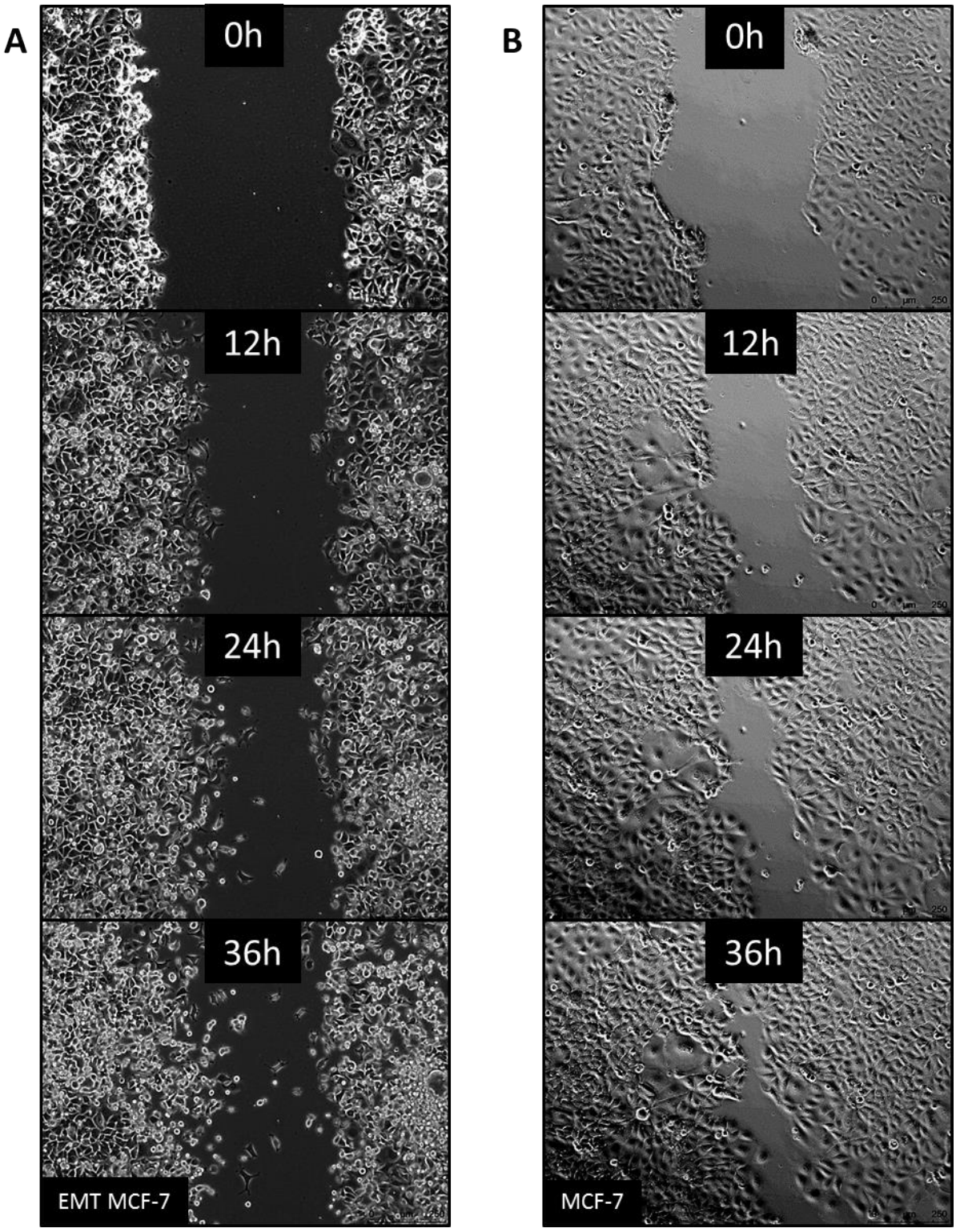


**Figure 4.4- Changes in migration after EMT stimulation in MCF-7 cells- (A)** MCF-7 cells were plated in normal adherent growth conditions with the addition of StemXVivo EMT inducing media supplement for 5 days to create EMT MCF-7 cells. **(B)** Parental MCF-7 cells grown in normal conditions were run alongside as a control. Wounds were then created using a 10 µm pipette tip before cells were placed into a time-lapse chamber at 37 $^{o}$C with $CO^{2}$ and imaged automatically every 10 minutes until stopped. Images are representative of 2 independent experiments and show changes in migration over 36h with images shown at 12h intervals. Scale bar= 250 µm.

### 4.3.2 EMT induction induced Twist expression and reduced cell-cell contacts

To confirm the effects of EMT stimulation in MCF-7 cells, immunofluorescence was performed on unstimulated, 5 day EMT-stimulated, and reverting MET-like MCF-7 cells. Reverting MET-like cells had been stimulated into EMT and allowed to revert back for a further 5 days in the absence of EMT supplements (MET MCF-7). Twist and E-cadherin were used as mesenchymal and epithelial markers respectively and visualised for changes in expression and localisation. EMT MCF-7 cells showed a clear upregulation of Twist which was not expressed in either unstimulated MCF-7 or MET MCF-7 cells (Figure 4.5). Furthermore, E-Cadherin staining showed a clear disruption of the cell-to-cell contacts in EMT MCF-7 cells, an observation that was confirmed by the F-actin stain phalloidin. These cell-to-cell contacts were re-established in MET MCF-7 cells suggesting these cells had undergone an MET reversion back to their original state.

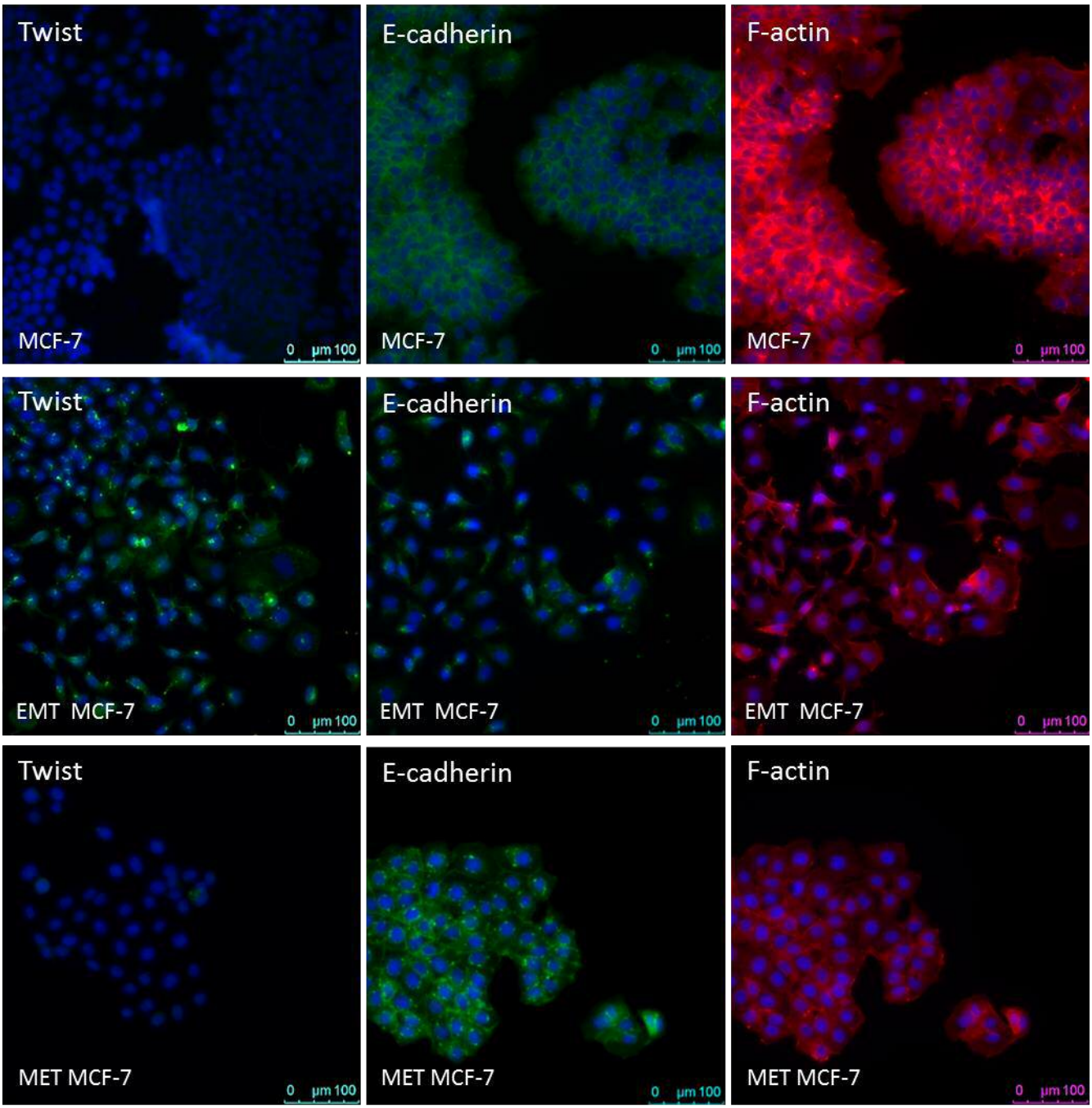


**Figure 4.5-Immunofluorescence staining of MCF-7, EMT MCF-7 and MET MCF-7 cells –** Representative images of immunofluorescence performed on MCF-7, EMT MCF-7 and MET MCF-7 cells. Cells were grown on coverslips and fixed at assay endpoints with 4% PFA before being stained for mesenchymal marker Twist, epithelial marker E-cadherin, cytoskeletal marker phalloidin (F-actin) and the nuclear marker DAPI (Blue). Images are representative of 2 independent experiments. Scale bar=100 µm.

### 4.3.3 Bcl-3 expression was increased during EMT in MCF-7 cells

To further characterise the effect of EMT stimulation, qRT-PCR was used to determine changes in gene expression between MCF-7, EMT MCF-7, and MET MCF-7 cells. A gene panel was selected based on known regulators of EMT from the literature as well as some less well established targets that have more recently been reported to regulate EMT. When the gene expression profiles of MCF-7 and EMT MCF-7 cells were compared, nine EMT-associated markers, including N-cadherin, Vimentin, Slug and ZEB1 were upregulated in the EMT-stimulated cells suggesting a transcriptional EMT response (Figure 4.6A). In MET MCF-7 cells the expression of these genes was similar to basal unstimulated MCF-7 levels suggesting a reversion back to their original epithelial state. Interestingly, Bcl-3 was also significantly upregulated in EMT MCF-7s and significantly downregulated in MET MCF-7 cells compared to parental MCF-7s further indicating its potential role during EMT and MET. No significant changes were observed in Snail or Runx1 expression; however GATA-3 or mir-221 expression was significantly downregulated in MET MCF-7 cells compared to both parental and EMT MCF-7 cells. Interestingly, E-cadherin was non-significantly increased after EMT stimulation and downregulated in MET MCF-7 cells compared to EMT MCF-7 cells. ZEB2, PRRX1 and mir-222 were also tested, however no amplification was observed in any of the cell types. Together this data suggested a partial transcriptional response after EMT stimulation that could be rescued after 5 days of reversion through MET, a profile that was mirrored by Bcl-3 expression.

### 4.3.4 NF-kB activity was upregulated during EMT in MCF-7 cells

The NF-kB pathway has been associated with the induction and maintenance of EMT in cancer, therefore NF-kB activity was analysed by NF-kB luciferase assays in MCF-7, EMT MCF-7 and MET MCF-7 cells. A significant increase in NF-kB activity was observed in EMT MCF-7 cells that had been stimulated with EMT-inducing media compared to controls. This was restored back to basal levels in MET MCF-7 cells after 5 days of MET reversion (Figure 4.6B). Furthermore, when the NF-KB activity of unstimulated MCF-7 cells was compared against the mesenchymal MDA-MB-436 cell line a significantly higher level of activity was observed in the mesenchymal line (Figure 4.6C).

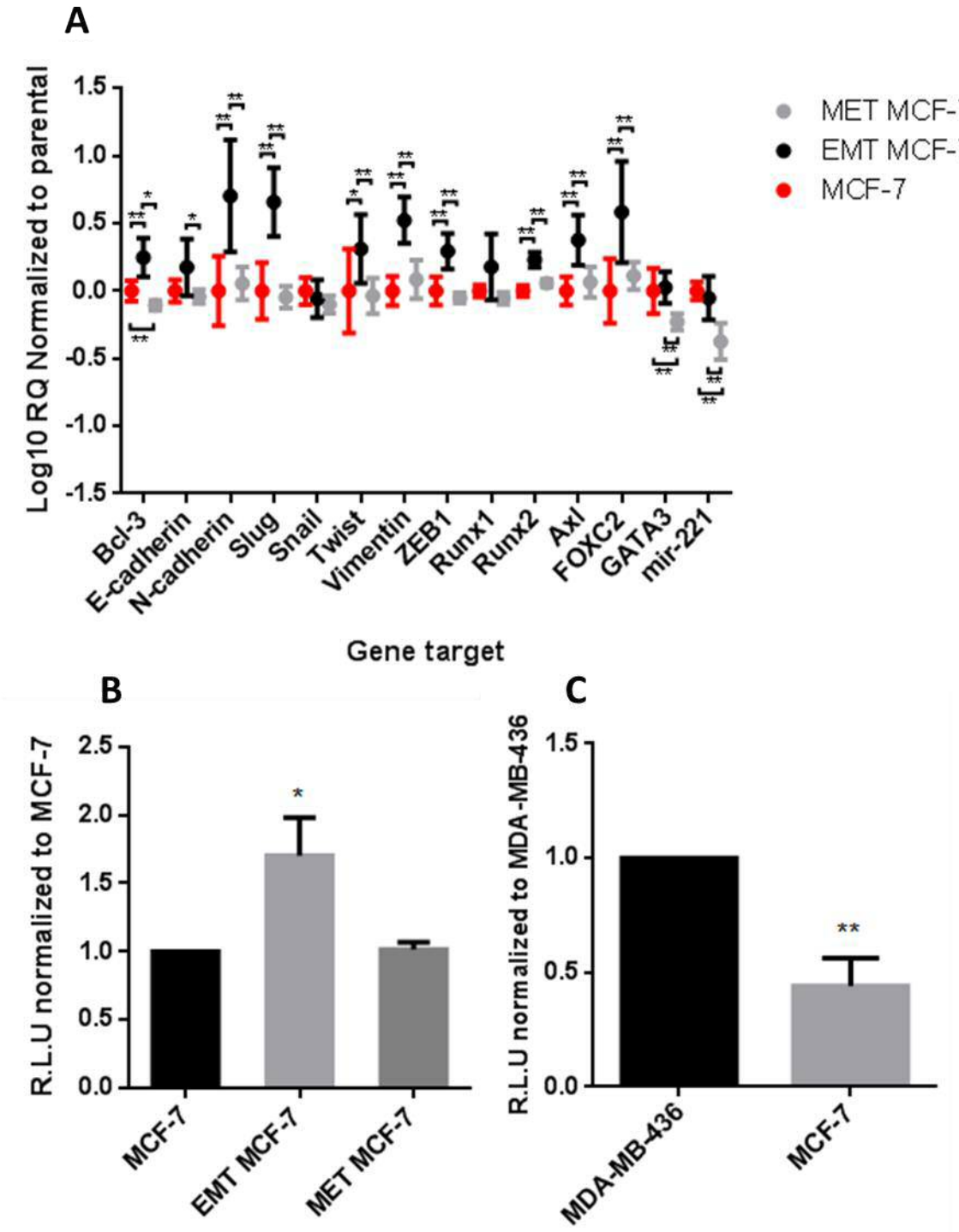


**Figure 4.6- Gene expression and NF-kB activity after EMT stimulation in MCF-7 cells- (A)** Gene expression analysis was performed by qRT-PCR to compare a panel of EMT responsive genes in MCF-7, EMT MCF-7 and MET MCF-7 cells. RNA was harvested from cells after stimulation with EMT inducing media supplement for 5 days to create EMT MCF-7 cells. EMT induced cells were also left for a further 5 days without EMT supplements to revert back into MET MCF-7 cells before RNA was harvested. Parental MCF-7 cells grown in normal conditions were run alongside as a control and harvested for RNA after 5 days of growth. Gene expression was normalised to ACTB housekeeping control to ensure equal loading. Error bars represent 95% confidence intervals of 3 independent experiments. Significance was determined using the 95% confidence interval overlap rule described in [1]**(B)** NF-kB luciferase assays were used to compare NF-kB activity in MCF-7, EMT MCF-7 and MET MCF-7 cells and were performed after 5 days of growth with or without EMT supplemented media. **(C)** MDA-MB-436 and MCF-7 cells grown in normal growth conditions were also compared for NF-kB activity using the same luciferase reporter. Error bars represent ± SEM of 3 independent experiments (N=2 for MET MCF-7 NF-kB experiment). (T-test, *=p<0.05 and **=p<0.01).

## 4.4 The outcome of Bcl-3 suppression during EMT

After establishing a robust model of EMT in MCF-7 cells, in order to determine whether Bcl-3 suppression impaired the ability of cells to undergo EMT, MCF-7 cells were transfected with either Bcl-3 siRNA or scRNA control for 24h before being induced into EMT for 5 days (Figure 4.7A). To determine the role of Bcl-3 during MET, MCF-7 cells were transfected with Bcl-3 siRNA after being stimulated into EMT and allowed to revert back for a further 5 days (Figure 4.7B). Each set of cells were then tested for changes in morphology, migration, gene expression, and NF-kB activity. This was also performed using un-induced MCF-7 and MDA-MB-436 cells to compare these effects to a stable epithelial and mesenchymal-like cell.

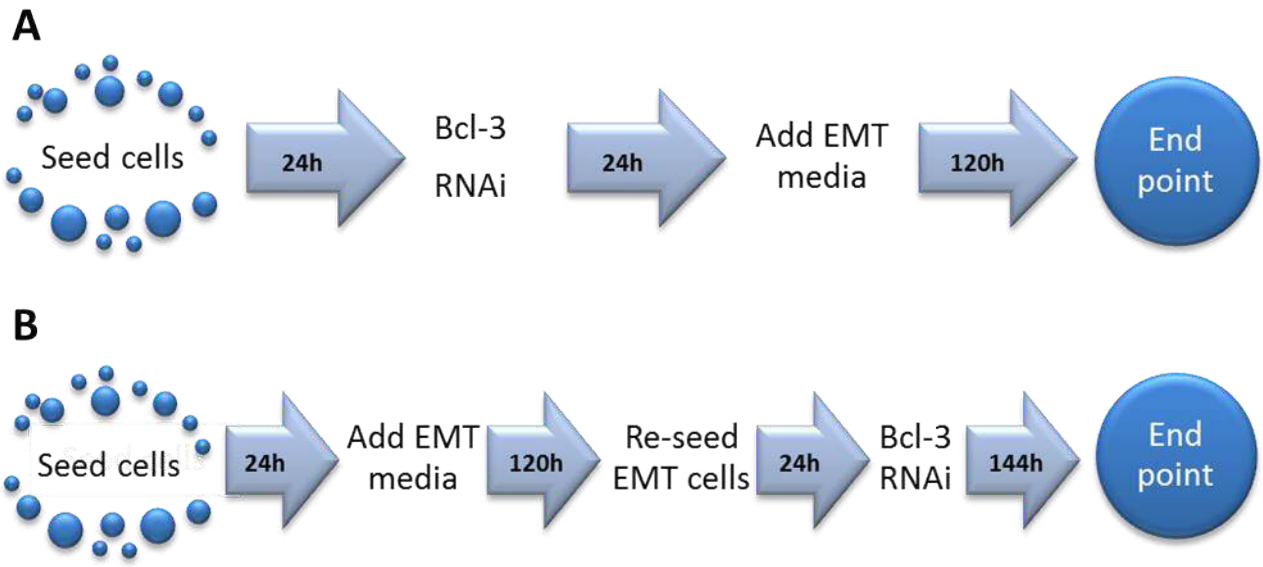


**Figure 4.7- Experimental model for EMT and MET MCF-7 cell assays- (A)** MCF-7 cells were treated with Bcl-3 siRNA for 24h before EMT inducing media supplements were added and cells left for a further 120h before performing end point assays. **(B)** To create MET MCF-7 cells, EMT stimulated cells were reseeded and treated with Bcl-3 siRNA before being left to revert back for 144h.

### 4.4.1 Prolonged Bcl-3 inhibition changed the morphology of MCF-7 cells

After Bcl-3 inhibition MCF-7, EMT MCF-7 and MET MCF-7 cells were analysed for changes in cell morphology to determine whether loss of Bcl-3 expression could inhibit the morphological switch from an epithelial to mesenchymal-like state. After 6 days of Bcl-3 inhibition, EMT MCF-7 cells contained a mixture of normal mesenchymal-like cells and a population of large, flattened cells similar to that of a senescent cell (Figure 4.8A). This change in morphology was exaggerated in both MET MCF-7 and unstimulated MCF-7 cells, suggesting this change were due to a prolonged exposure to Bcl-3 siRNA rather than a change induced through undergoing EMT (Figure 4.8A). This change in morphology was not observed in MDA-MB-436 cells after 6 days of Bcl-3 RNAi (not shown).

### 4.4.2 Prolonged inhibition of Bcl-3 reduced cell viability

The previously described change in morphology implied a change in the viability of MCF-7 cells after prolonged Bcl-3 inhibition, to confirm this cell titre blue assays were performed on Bcl-3 modified MCF-7, EMT MCF-7 and MET MCF-7 cells. When Bcl-3 was inhibited for 48h there was no effect on viability in MCF-7 cells, however when these cells were inhibited for 6 days there was a significant reduction in cell viability (Figure 4.8B). This effect was increased when the cells were stimulated into an EMT-like state and further still once the cells had been through EMT and beginning to revert back to a more MET-like phenotype (Figure 4.8B). This effect of prolonged Bcl-3 inhibition was also replicated in the mesenchymal MDA-MB-436 cells, with no effect seen after 48h but a significant reduction in viability after 6 days of RNAi, despite no clear morphological changes (Figure 4.8C).

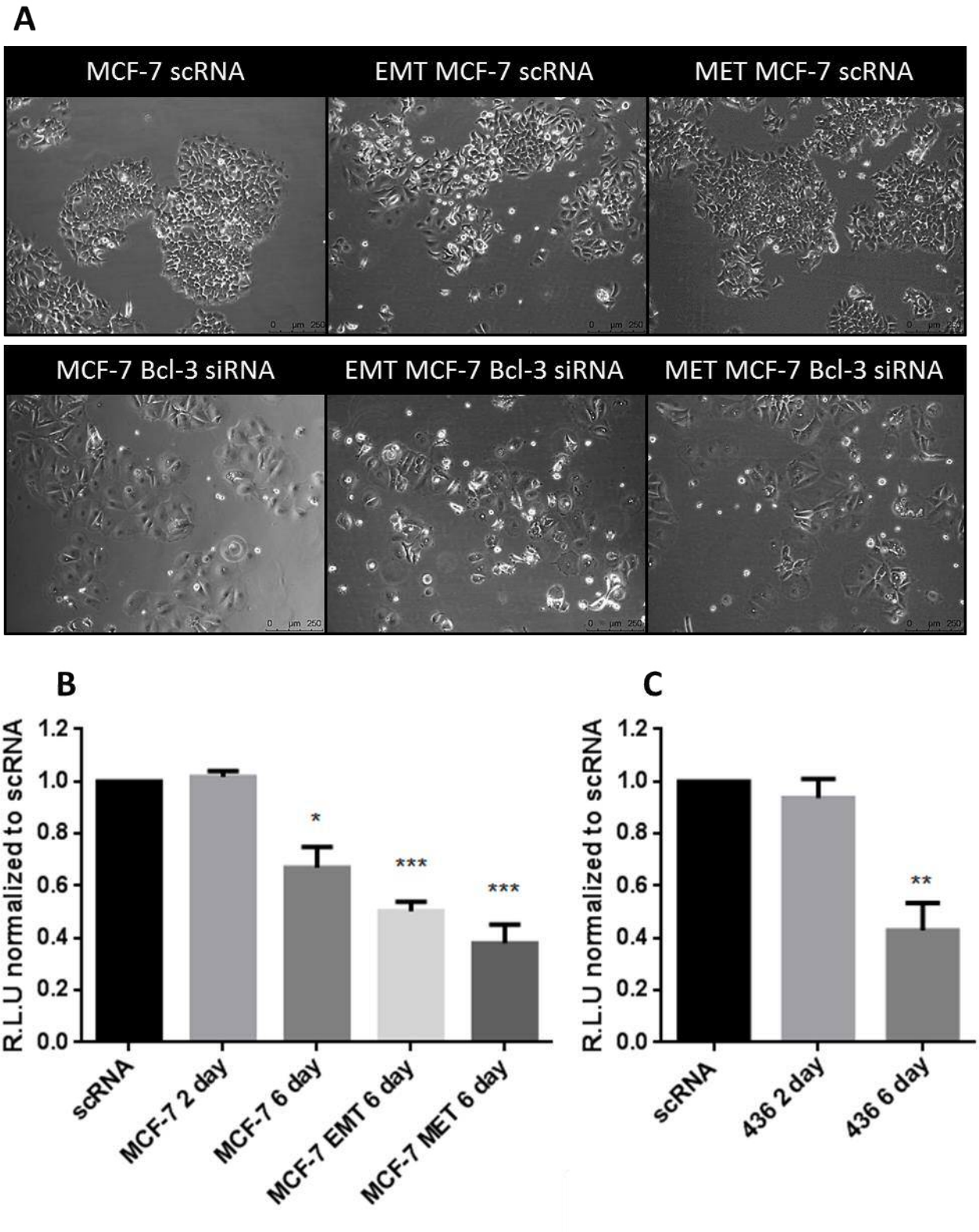


**Figure 4.8- Bcl-3 inhibition in MCF-7, EMT MCF-7 and MET MCF-7 resulted in morphological changes and reduced viability- (A)** Representative images of unstimulated (MCF-7) cells, EMT stimulated cells (EMT MCF-7) and reverting (MET MCF-7) cells after treatment of Bcl-3 siRNA or scRNA control. Scale bar= 250 µm. **(B)** MCF-7, EMT MCF-7, MET MCF-7 and **(C)** MDA-MB-436 cells were analysed with cell titre blue after 2 or 6 days of treatment with Bcl-3 siRNA or scRNA control. Error bars represent ± SEM of 3 independent experiments. T-test, *=p<0.05, **=p<0.01, ***=p<0.005 compared to scRNA.

### 4.4.3 Bcl-3 RNAi can reduce EMT-like cell migration

One of the hallmarks of EMT is increased invasiveness which facilitates the migration of cells away from the site of primary tumours. The ability of Bcl-3 to regulate cell migration has been shown in a number of human breast cancer cell lines including MCF-7 and MDA-MB-436 cells (chapter 3), however it has not been tested in a cancer cell line undergoing EMT. To test whether RNAi of Bcl-3 could also inhibit the added migratory potential of an EMT-like cell, scratch assays were performed on EMT MCF-7 cells that had been treated with Bcl-3 siRNA or scRNA control for 48h prior to creating wounds. The length of Bcl-3 inhibition was reduced to 48h to analyse the effects on EMT cell migration without changing the viability of the cells. Inhibition of Bcl-3 resulted in a significant reduction in wound closure compared to controls (Figure 4.9A) and appeared to inhibit the ability of EMT-like single cells to migrate away from the invasive front. The effect of Bcl-3 RNAi on single cell migration was quantified using the Fluoroblok migration assay where pre-treated EMT MCF-7 cells were harvested and seeded into Fluoroblok plates for a further 48h before being analysed. Again, Bcl-3-inhibited EMT MCF-7 cells showed a significant reduction in migration compared to controls (Figure 4.9B).

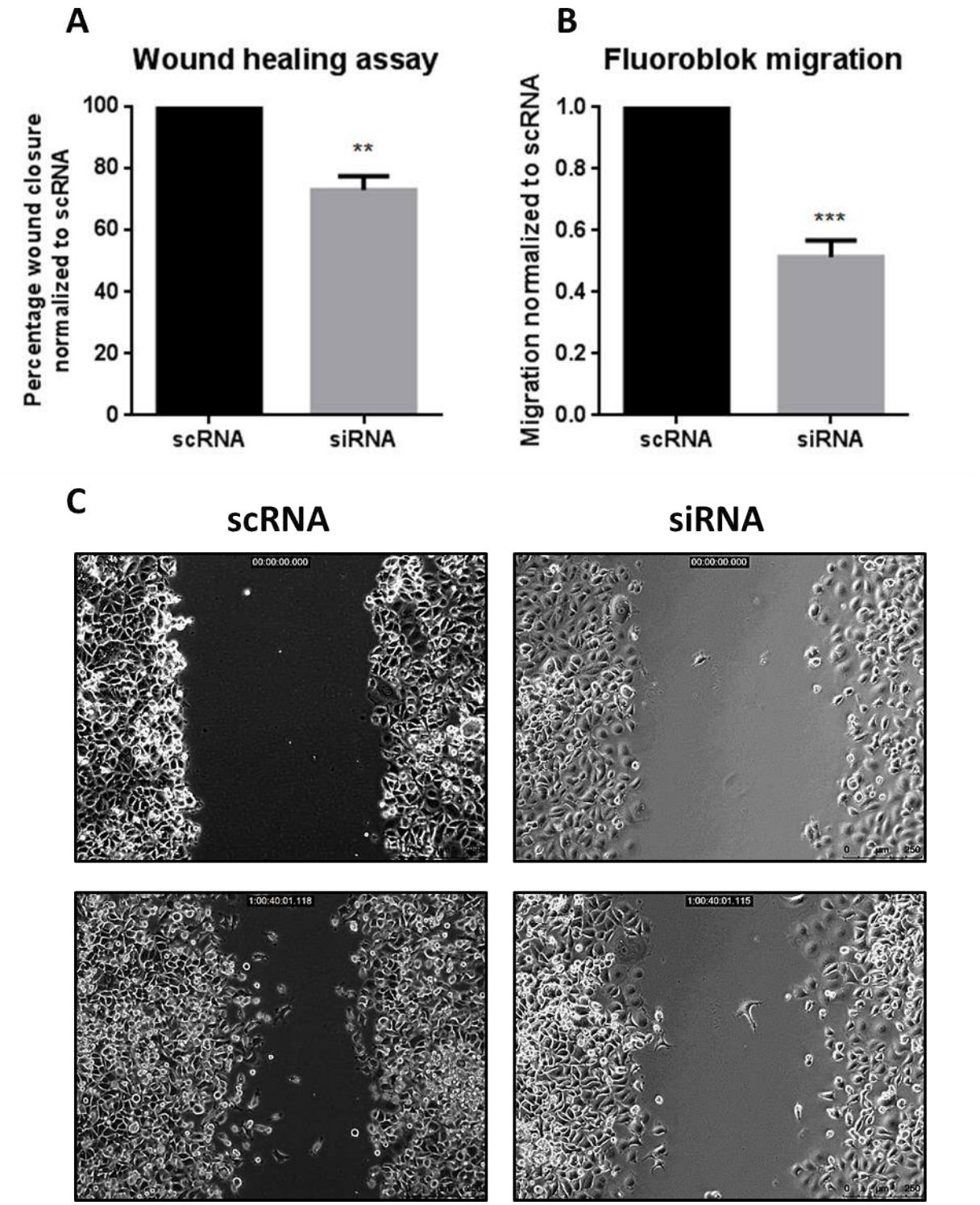


**Figure 4.9- EMT MCF-7 migration was reduced after Bcl-3 knockdown- (A)** MCF-7 cells were stimulated for 3 days into EMT before being transfected with Bcl-3 siRNA or scRNA control and stimulated for a further 2 days after which wounds were created. Once wounds had been created cells were imaged a 0h and then again 24h later with wound closure at the leading edge of the wounds measured as a percentage of area closure before normalizing to scRNA controls. **(B)** Cells created in wound healing assays were harvested at point of wound creation and seeded into Fluoroblok migration assays for a further 48h before being stained with calcein AM and analysed. Error bars represent ± SEM of 3 independent experiments. (T-test, *=$p<0.05$ as compared to DMSO control and **=$p<0.01$ as compared to scRNA) **(C)** Representative images of migrating EMT MCF-7 cells treated with either Bcl-3 siRNA or scRNA control. Scale bars represent 250 μm.

### 4.4.4 Bcl-3 inhibition reduced NF-kB activity

Increased NF-kB activation has been associated with EMT induction, an observation that is supported in our model of EMT in MCF-7 cells. Therefore, the levels of NF-kB activity were assessed after Bcl-3 inhibition to determine whether this effect could be abrogated. MCF-7 cells were induced into EMT after 24h of treatment of siRNA and left for a further 5 days to test the effect of prolonged Bcl-3 inhibition on NF-kB activity. Short term effects were also tested by treating with siRNA for 48h after 3 days of EMT stimulation in MCF-7 cells. Parental MCF-7 and MDA-MB-436 cells were also tested alongside EMT-stimulated cells tested. No changes in NF-kB activity were observed in parental MCF-7 or EMT MCF-7 cells despite over an 80% reduction in Bcl-3 expression (data not shown), however after 2 and 6 days of Bcl-3 inhibition in MDA-MB-436 cells a significant reduction was seen (Figure 4.10A, B&C). It is possible that Bcl-3 may still be regulating NF-kB signalling in our MCF-7 EMT model through regulating a different kB site as has been previously described, however a different reporter was not tested here [246].

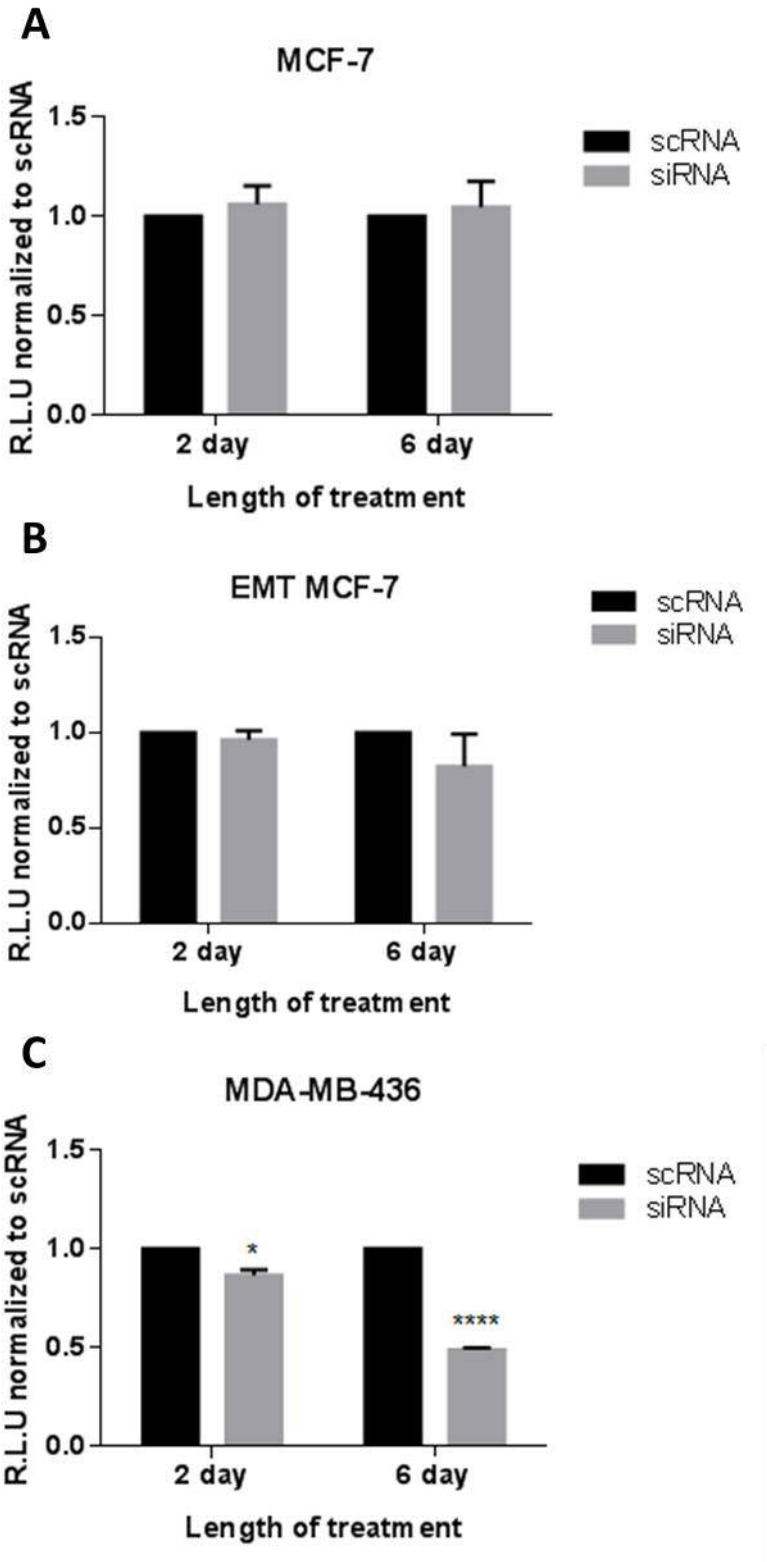


**Figure 4.10- NF-kB activity was reduced after Bcl-3 knockdown in MDA-MB-436 cells- (A)** MCF-7 **(B)** EMT MCF-7 **(C)** MDA-MB-436 cells were transfected with Bcl-3 siRNA or control siRNA for either 6 or 2 days before the assay endpoint. NF-kB and LacZ reporters were transfected 24h before the assay endpoint after which NF-kB activity was measured and normalized to LacZ activity before being normalized to control siRNA activity. Error bars represent ± SEM of 3 independent experiments. (T-test, *=p<0.05 as compared to DMSO control and ****=p<0.0001 as compared to scRNA).

### 4.4.5 Effect of Bcl-3 inhibition on EMT gene expression

As shown previously, stimulation of MCF-7 cells with an EMT-inducing media supplement was able to significantly alter the pattern of gene expression from a normal epithelial-like cell to a more EMT-like profile (Figure 4.6A). As Bcl-3 was shown to be significantly upregulated in this system the effect of Bcl-3 inhibition on this gene expression profile was tested in parental MCF-7, EMT MCF-7 and MET MCF-7 cells. Parental MDA-MB-436 cells were also tested as a representation of a fully differentiated mesenchymal cell type.

#### 4.4.5.1 Prolonged Bcl-3 inhibition induced profound transcriptional changes in MCF-7 and 436 cells

Before looking at the role of Bcl-3 during the EMT process the effect of Bcl-3 inhibition on the transcription of unstimulated epithelial and mesenchymal cells was tested using MCF-7 and MDA-MB-436 cells respectively. Bcl-3 was suppressed using siRNA for 2 days and 6 days to compare the short and long term effects of Bcl-3 inhibition. After a 2 day inhibition of Bcl-3 both MCF-7 and MDA-MB-436 cells showed a significant increase in Runx1 expression (Figure 4.11A&B). The only other transcriptional change in MCF-7 cells was an increase in mir-221 expression (Figure 4.11A) where as in MDA-MB-436 cells Twist, Slug, FOXC2 and GATA3 expression were all upregulated (Figure 4.11B). When Bcl-3 suppression was prolonged for 6 days in MCF-7 cells a much more profound transcriptional change was observed, with 9 different targets showing significant changes in gene expression (Figure 4.11C). Of these E-cadherin, N-cadherin, Slug, Runx2, FOXC2, mir-221 and Runx1 expression were significantly upregulated, with Vimentin and GATA3 downregulated after Bcl-3 inhibition compared the scRNA control. In the MDA-MB-436 cells after 6 days of Bcl-3 inhibition Slug, Runx1, FOXC2 and GATA3 were upregulated similar to what was observed after 2 days of inhibition (Figure 4.11D). In addition, Vimentin and mir-221 were also upregulated with E-cadherin, N-cadherin, Snail and Runx2 all significantly downregulated in Bcl-3-inhibited cells. These data suggest Bcl-3 may differentially regulate the transcription of EMT-associated genes depending on cell state; however similarities in Slug, Runx1, FOXC2 and mir-221 expression after Bcl-3 inhibition do suggest at least in part some shared pathways in this regulation.

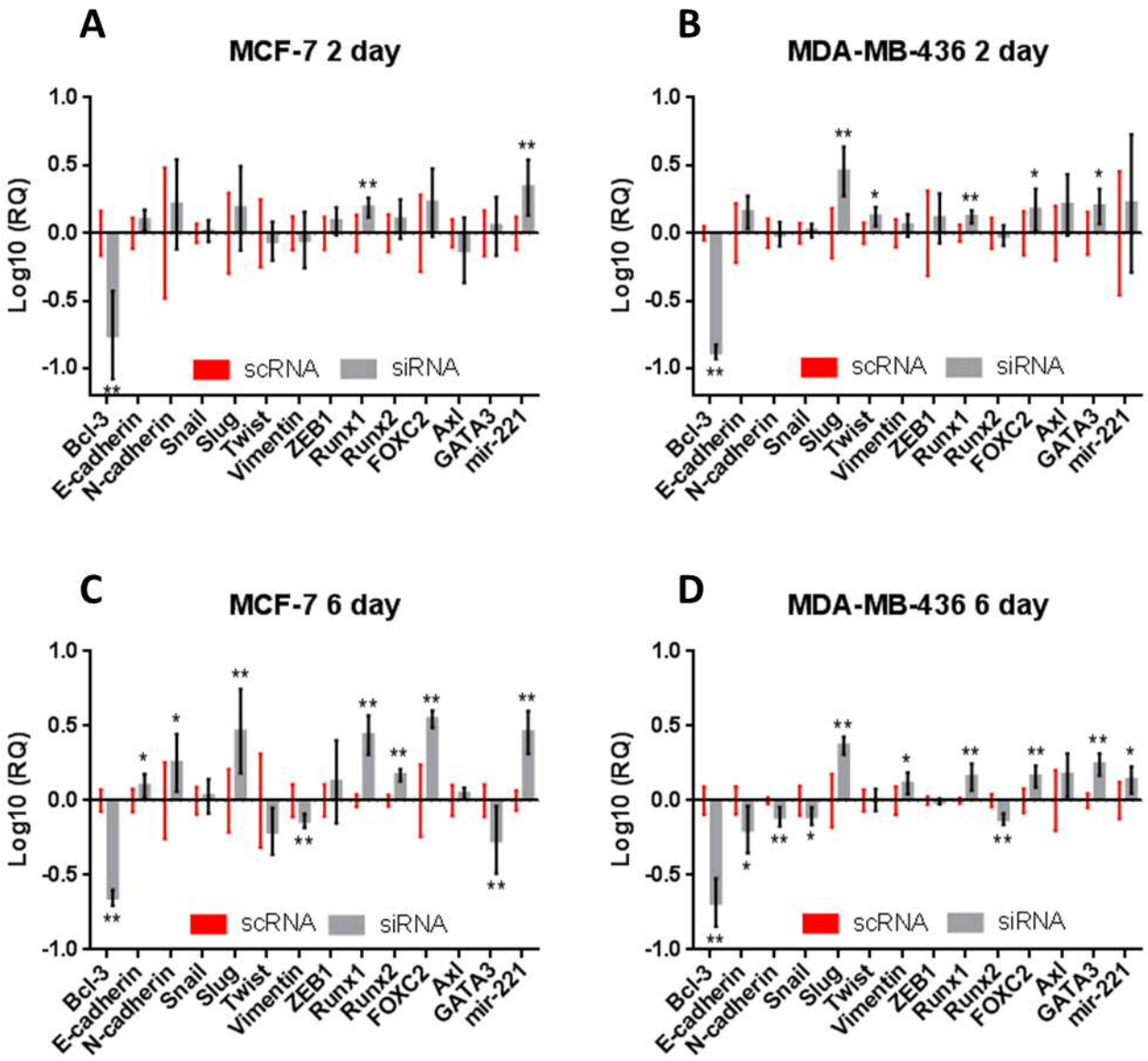


**Figure 4.11- Gene expression of MCF-7 and MDA-MB-436 cells after short and long term Bcl-3 inhibition-** MCF-7 **(A&C)** and MDA-MB-436 **(B&D)** cells were treated with Bcl-3 siRNA or scRNA control for 2 **(A&B)** or 6 days **(C&D)** before RNA was harvested to compare the effects of Bcl-3 inhibition on gene expression. Gene expression was normalised to ACTB housekeeping control to ensure equal loading. Error bars represent 95% confidence intervals of 3 independent experiments. Significance was determined using the 95% confidence interval overlap rule described in [1].

#### 4.4.5.2 Bcl-3 inhibition altered the EMT gene expression profile

Bcl-3 suppression was able to significantly alter the expression of certain EMT-related factors in both epithelial and mesenchymal cell lines (Figure 4.11). To test whether Bcl-3 is important in mediating the transition between these cell types at the transcriptional level, Bcl-3 was inhibited with siRNA in MCF-7 cells for 24h followed by the addition of EMT stimulating supplement for a further 5 days before being harvested for RNA. Analysis by qRT-PCR showed a significant reduction in N-cadherin, Twist and Vimentin expression after Bcl-3 inhibition suggesting some reduction in EMT-like transcription (Figure 4.12A). Similar to parental MCF-7 cells, mir-221 and Runx2 were both upregulated as was Snail which was previously shown to be unchanged in MCF- 7 cells, and was downregulated in MDA-MB-436 cells after 6 days of Bcl-3 inhibition.

To test whether these effects could be mimicked with inhibition of Bcl-3 using small molecule inhibitors, cells were treated with 50 μM CB-1. However, this was not the case, with only Bcl-3, Vimentin and GATA3 showing a small increase in expression (Figure 4.12C).

#### 4.4.5.3 Bcl-3 inhibition in MET reverting cells altered gene expression similarly to EMT cells

The effect of Bcl-3 inhibition on the gene expression profile of reverting MET-like cells was also analysed. After suppressing Bcl-3 using siRNA, both Twist and Vimentin were significantly downregulated compared to controls in a similar manner to EMT MCF-7 cells, however unlike in EMT MCF-7 cells, no change was observed in the expression of N-cadherin with further targets Snail, Axl and GATA3 also downregulated (Figure 4.12B). Similar to what was observed after 6 day siRNA inhibition in parental MCF-7 cells Slug, Runx1, FOXC2 and mir-221 were all upregulated. When Bcl-3 was inhibited with small molecule inhibitor CB-1, a different expression profile was observed with Bcl-3, Slug and ZEB1 all significantly downregulated and Runx2 upregulated (Figure 4.12D).

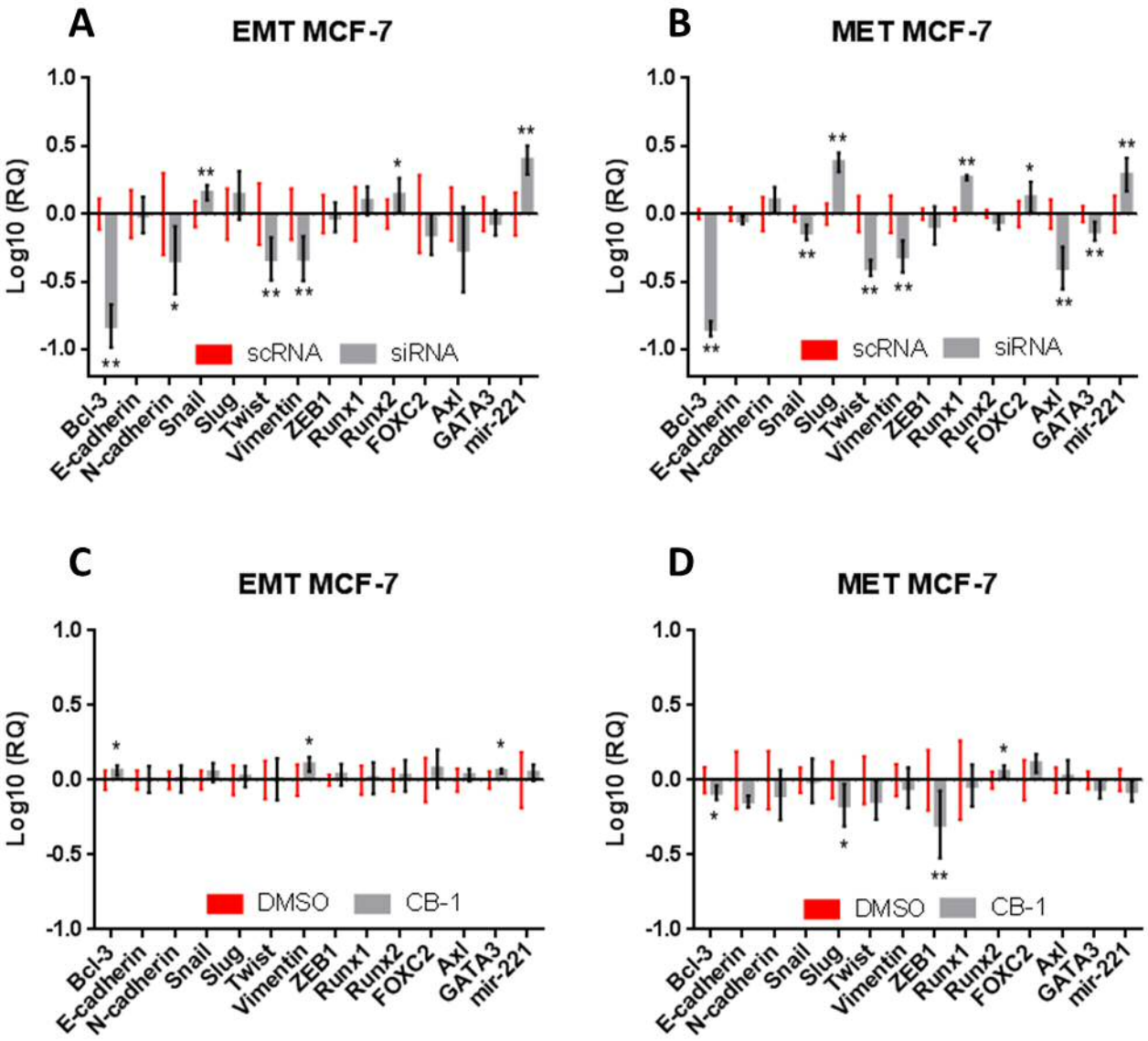


**Figure 4.12- Gene expression of EMT MCF-7 and MET MCF-7 cells after Bcl-3 inhibition with either siRNA or CB-1-** EMT MCF-7 **(A&C)** and MET MCF-7 **(B&D)** cells were inhibited for Bcl-3 using siRNA **(A&B)** or CB-1 **(C&D)** to determine the effects of Bcl-3 inhibition on gene expression during the processes of EMT and MET. Gene expression was normalised to ACTB housekeeping control to ensure equal loading. Error bars represent 95% confidence intervals of 3 independent experiments. Significance was determined using the 95% confidence interval overlap rule described in [1].

#### 4.4.5.4 Overall gene expression profile

The previously described gene expression profiles offered an insight into how Bcl-3 may regulate a number of different targets during the process of EMT and the reversion back through MET in MCF-7 cells. To further summarise the changes in expression of each target due to Bcl-3 suppression the profiles of MCF-7, EMT MCF-7 and MET MCF-7 cells inhibited with Bcl-3 siRNA were normalized to MCF-7 scRNA treated cells and each target individually mapped.

A similar pattern was observed in a number of different genes whereby an increase in expression in EMT MCF-7 scRNA treated cells was abrogated in those treated with Bcl-3 siRNA. This was observed in N-cadherin, Twist, Vimentin, FOXC2 and Axl expression with each remaining at basal expression levels following Bcl-3 inhibition, suggesting that Bcl-3 may be mediating the upregulation of these genes. This was not a universal effect however with E-cadherin, ZEB1 and GATA3 all showing no significant differences between the cell states. Furthermore, both Slug and mir-221 showed an increase in expression levels following Bcl-3 knockdown independent of cell state suggesting this effect was not driven by induction of EMT. Runx1 showed a similar gene expression pattern, however the upregulation mediated by Bcl-3 siRNA was abrogated in EMT MCF-7 cells. Finally, both Runx2 and Snail were upregulated after Bcl-3 inhibition in EMT MCF-7 cells; however Runx2 was also upregulated in parental MCF-7 cells but not in MET MCF-7 cells. On the other hand Snail expression was unchanged in parental MCF-7 cells but was slightly downregulated in MET MCF-7 cells. Taken together this data suggests Bcl-3 may function during EMT to help mediate the expression of a number of key EMT-regulating genes. It is also capable of regulating various other targets such as Slug and mir-221, however this is probably irrespective of either EMT or MET.

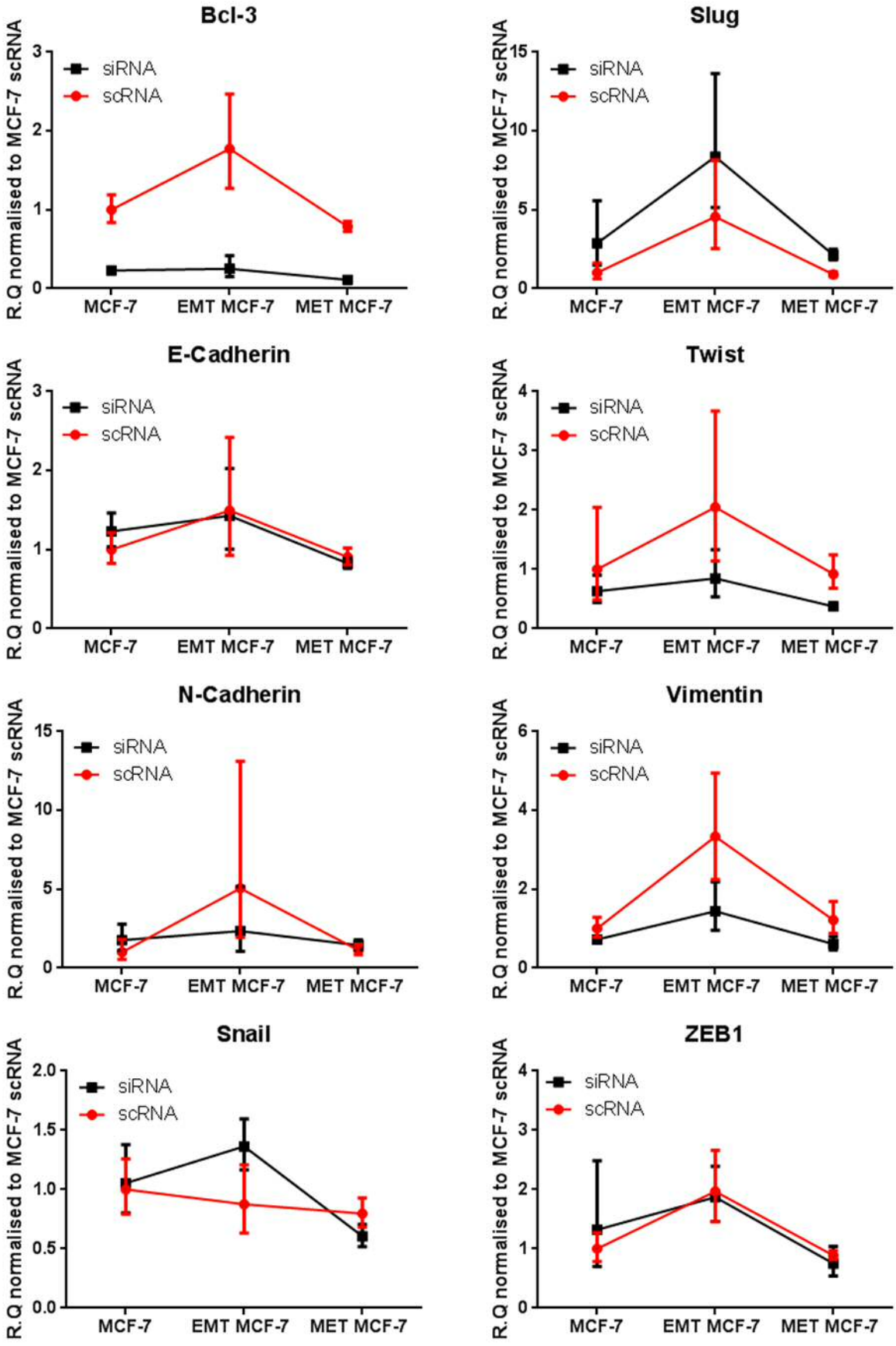


**Figure 4.13- Gene expression profiles of EMT MCF-7 and MET MCF-7 cells after Bcl-3 RNA inhibition-** MCF-7, EMT MCF-7 and MET MCF-7 cells were all treated with either Bcl-3 siRNA or scRNA for 6 days prior to RNA being harvested. Each gene target was then normalized to the expression of MCF-7 scRNA treated cells to create a profile map of how each gene changed in expression with and without Bcl-3 inhibition. Error bars represent 95% confidence intervals of 3 independent experiments.

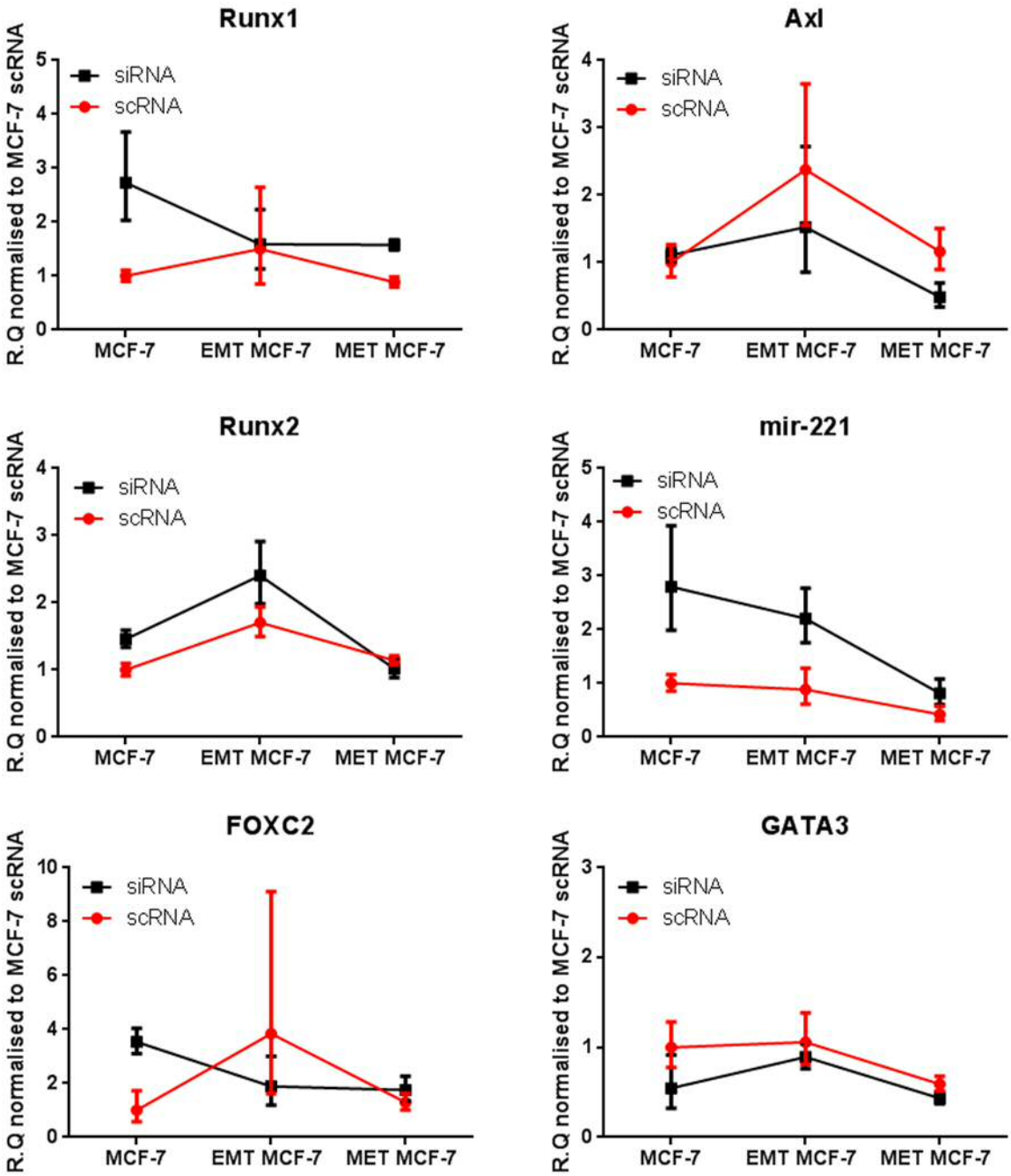


**Figure 4.14- Gene expression profiles of EMT MCF-7 and MET MCF-7 cells after Bcl-3 RNA inhibition-** MCF-7, EMT MCF-7 and MET MCF-7 cells were all treated with either Bcl-3 siRNA or scRNA for 6 days prior to RNA being harvested. Each gene target was then normalized to the expression of MCF-7 scRNA treated cells to create a profile map of how each gene changed in expression with and without Bcl-3 inhibition. Error bars represent 95% confidence intervals of 3 independent experiments.

### 4.4.6 Bcl-3 RNAi did not affect E-cadherin localisation in MCF-7 cells

The previously described gene expression profiles of EMT and MET-like MCF-7 cells suggested the potential of Bcl-3 to partially mediate EMT and MET through the regulation of certain gene targets, however no change was observed in the expression of what many believe as a key mediator of EMT, E-cadherin. As preliminary data in Eph4 cells had suggested a disruption in E-cadherin protein localisation after Bcl-3 inhibition, immunofluorescence was used to determine whether Bcl-3 inhibition could replicate this in EMT and MET MCF-7 cells (Figure 4.15). Phalloidin was also used to visualise filamentous actin and to highlight the changes in cell morphology (Figure 4.16).

After Bcl-3 inhibition in EMT MCF-7 cells, E-cadherin appeared to be more abundant in the cytosol and membranes of these cells compared to controls, however this may be due to the increased size of these cells making it easier to visualize. MET MCF-7 cells that had been treated with Bcl-3 siRNA appeared to have reduced E-cadherin expression at cell-cell junctions, however this was not clear due to the lack of cells and requires further analysis to confirm. F-actin staining of the cells confirmed the clear change in cell morphology of these cells further highlighting the increase in size and shape after prolonged Bcl-3 inhibition. Despite these observations further analysis by western blotting or flow cytometry may be required to produce a more concise idea of the protein levels in these cells.

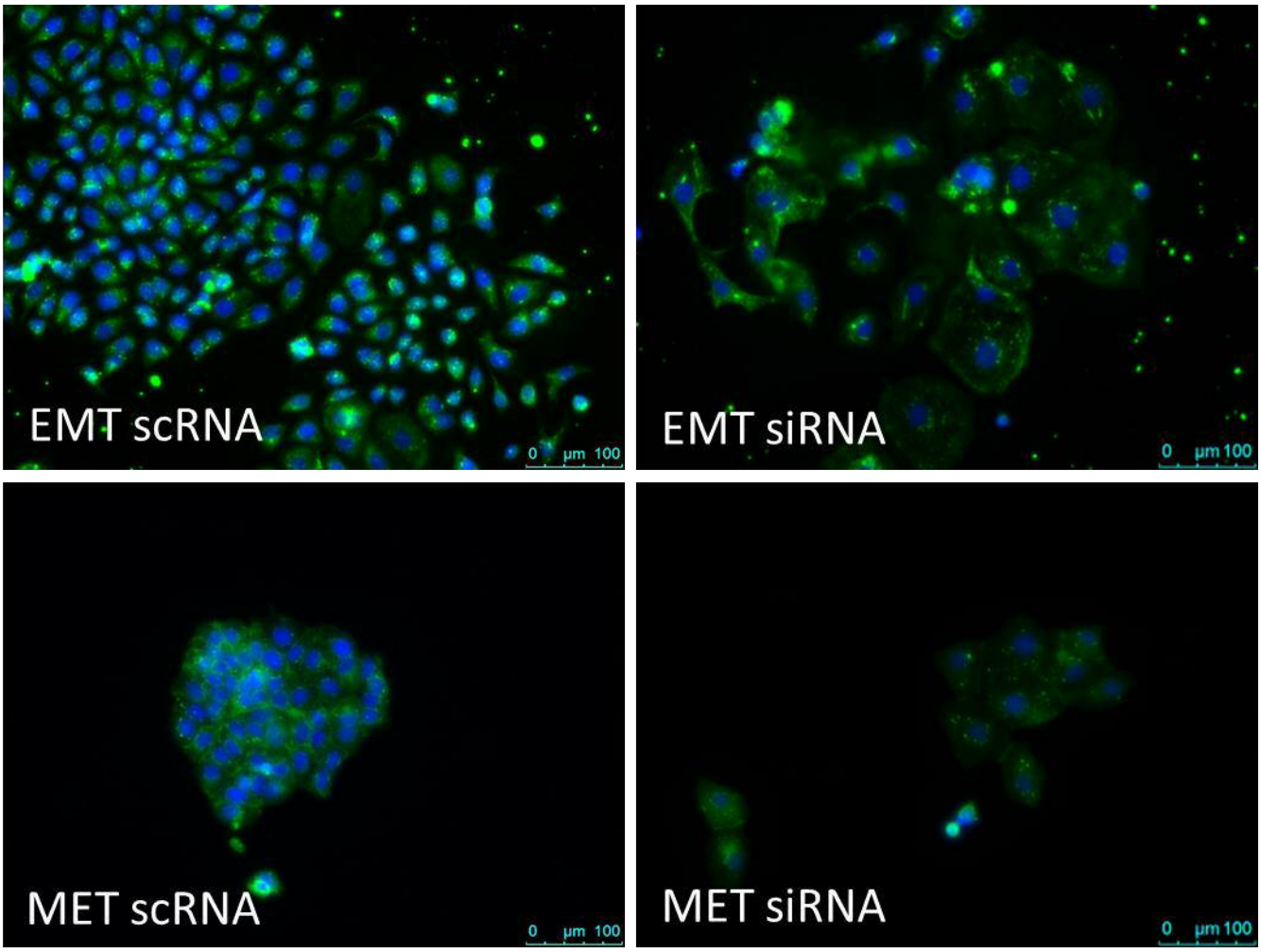


**Figure 4.15-Immunofluorescence staining of E-cadherin in EMT and MET MCF-7 cells –** Representative images of immunofluorescence performed on EMT MCF-7 and MET MCF-7 cells treated with either Bcl-3 siRNA or scRNA control. Cells were grown on coverslips and fixed at assay endpoints with 4% PFA before being stained for E-cadherin (Green) and DAPI (Blue). Images are representative of 2 independent experiments. Scale bar=100 µm.

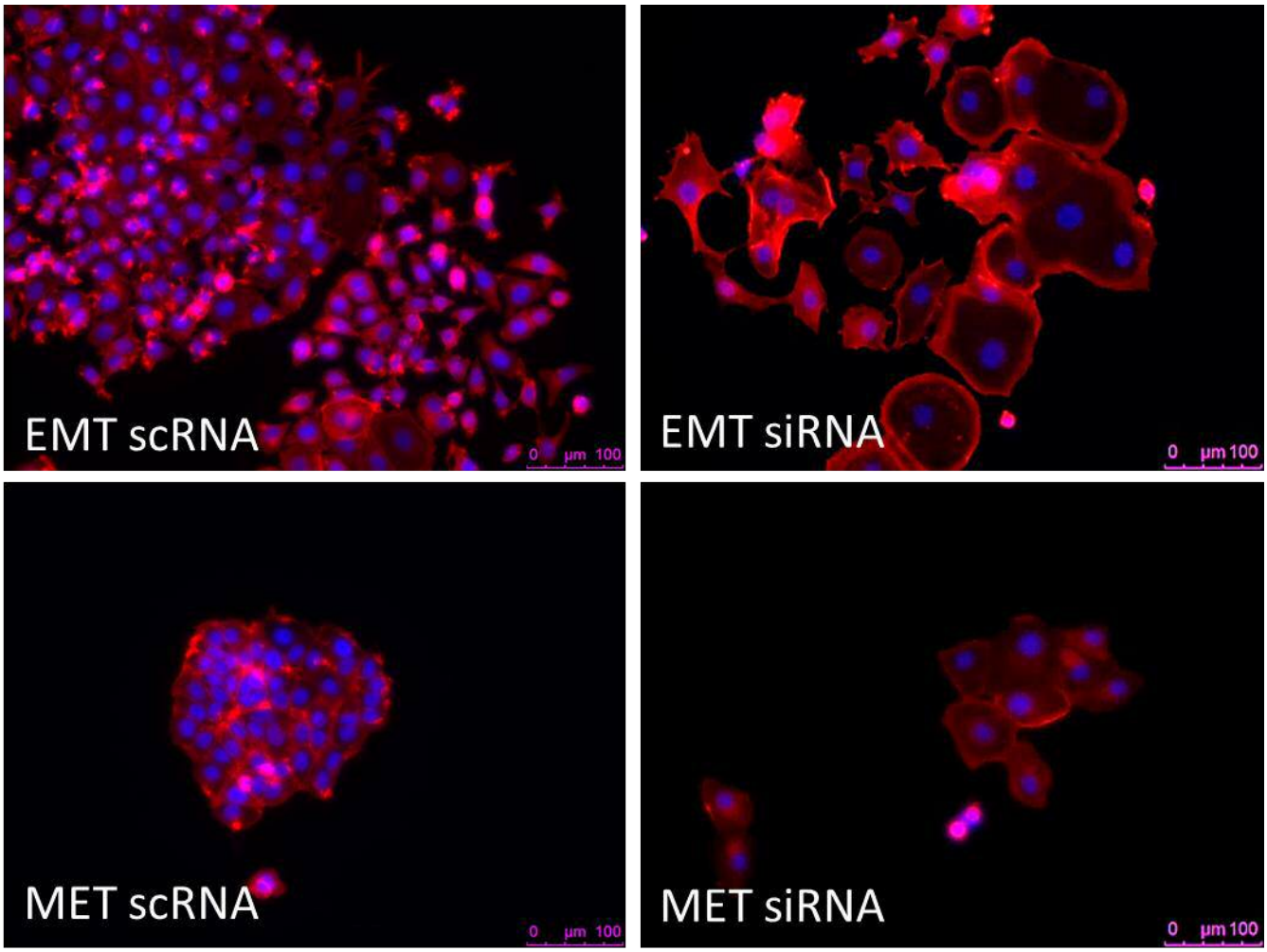


**Figure 4.16-Immunofluorescence staining of F-actin in EMT and MET MCF-7 cells –** Representative images of immunofluorescence performed on EMT MCF-7 and MET MCF-7 cells treated with either Bcl-3 siRNA or scRNA control. Cells were grown on coverslips and fixed at assay endpoints with 4% PFA before being stained for F-actin (Red) and DAPI (Blue). Images are representative of 2 independent experiments. Scale bar=100 µm.

### 4.4.7 Colony forming ability of MCF-7 cells was reduced after Bcl-3 inhibition

Following EMT, newly migratory cells have the ability to spread throughout the body, however before colonizing at distal sites and forming micro metastases the invading cells will revert back to their original epithelial-like state through MET [90]. This provides cells with the properties required to begin colonizing and is an important process in order for metastasis to occur. Therefore, we tested whether inhibition of Bcl-3 in MCF-7 cells that had undergone EMT could impair colony-formation. Cells were treated with either Bcl-3 siRNA or scRNA control and stimulated into EMT for 5 days before being re-seeded into colony forming assays at low confluency to test their ability to re-populate. MET MCF-7 cells were also seeded into colony conditions after 24h Bcl-3 siRNA treatment and 5 days of reversion as well as parental MCF- cells that were seeded after 6 days of Bcl-3 inhibition. Following Bcl-3 inhibition there was a significant reduction in the colony forming ability of both MCF-7 and MET MCF-7 cells with EMT MCF-7 cells showing a similar trend (Figure 4.18). MDA-MB-436 cells were also tested for their ability to form colonies after Bcl-3 inhibition; however these failed to create quantifiable colonies.

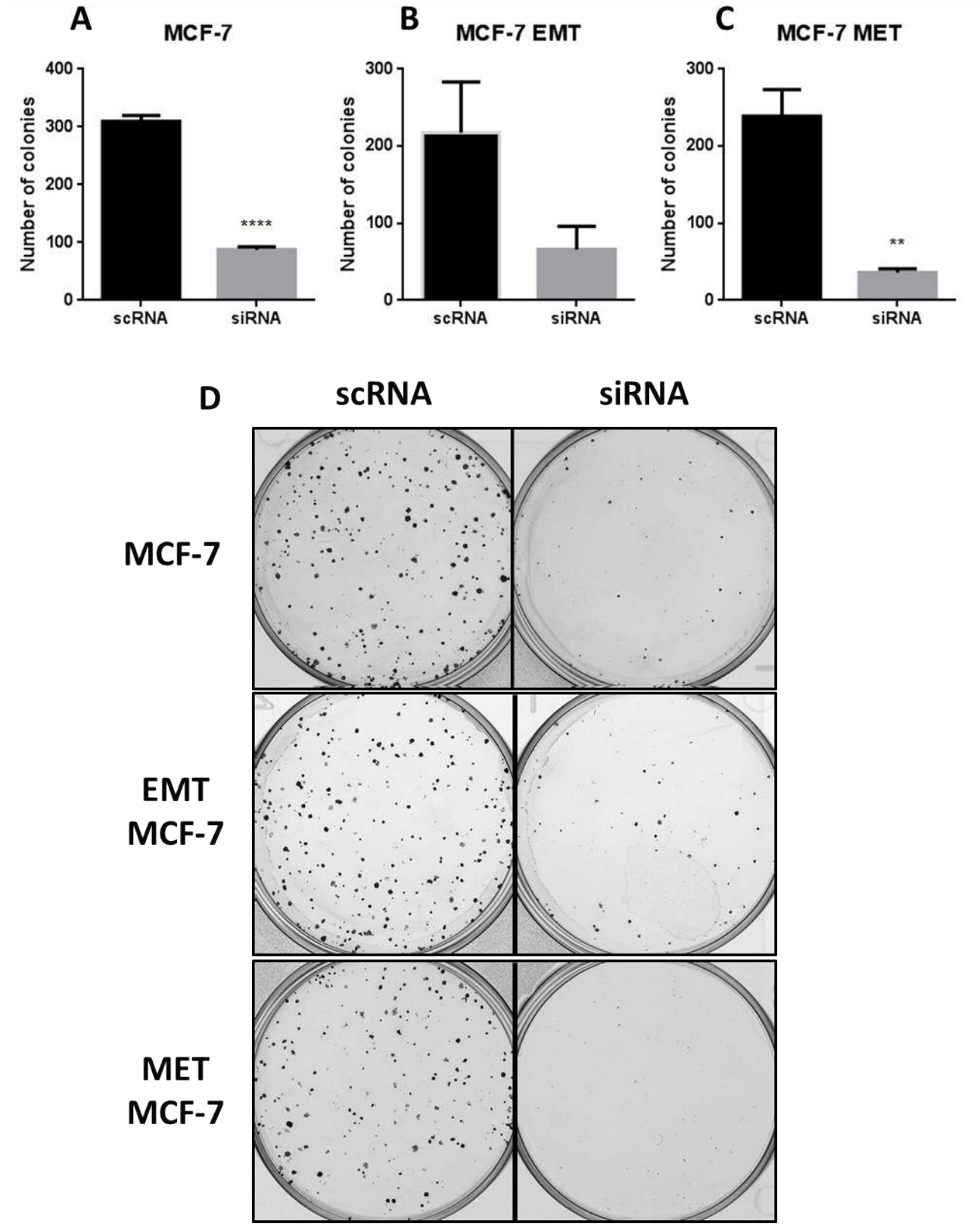


**Figure 4.17- Bcl-3 inhibition inhibited the colony forming ability of MCF-7, EMT MCF-7 and MET MCF-7 cells-** MCF-7 **(A)** EMT MCF-7 **(B)** and MET MCF-7 **(C)** cells treated with Bcl-3 siRNA or scRNA control were seeded into colony forming assays at low confluency and left for 8 days before being fixed and stained with crystal violet to visualise colony formation. Colonies were counted automatically using the Oxford Optronix gel counter. Error bars represent ± SEM of 3 independent experiments. (EMT MCF-7 colony N=2) (T-test, **=p<0.01, ****=P<0.0001 as compared to scRNA). **(D)** Representative images of the colony formation in each cell type with and without Bcl-3 inhibition.

## 4.5 Discussion

The process of EMT is a crucial step in metastasis that provides primary tumour cells with the properties required to invade their surrounding microenvironment and spread to distal sites, where reversion back through MET facilitates these cells to begin forming micro-metastases. Despite the importance of both processes the role of Bcl-3 in mediating this is relatively unknown, especially in breast cancer where only a limited amount of research has been performed. Therefore, the aim of this chapter was to explore the potential role Bcl-3 may play in regulating EMT and MET to promote metastasis.

In this chapter we have extensively characterised a new system for the study of both EMT and MET in the epithelial MCF-7 cell line. Using this model system a clear change in cell morphology and migratory phenotype was observed (Figure 4.3&4.4) suggesting a switch from an epithelial to a mesenchymal-like state in the bulk cell population. This was confirmed through protein and gene expression analysis which further supported an EMT switch that could be reversed through MET (Figure 4.5&4.6). We have also shown that NF-kB activity is upregulated during EMT in this model as well as the expression of Bcl-3 (Figure 4.6), an observation that has previously been seen in an EpH4 model of EMT but not explored further [241].

Given our findings that suggested Bcl-3 may be an important regulator of EMT, we proceeded to test the effects of Bcl-3 inhibition in our system, with initial tests showing a dramatic change in cell morphology after Bcl-3 inhibition in each of our MCF-7, EMT MCF-7 and MET MCF-7 cell types (Figure 4.8). Suppression of Bcl-3 in each cell type resulted in a clear enlargement of cell size, a hallmark of cells that are undergoing senescence. This surprising effect had not been observed previously, as in earlier experiments Bcl-3 inhibition was only performed for up to 48h, however as we wanted to inhibit Bcl-3 throughout a full EMT induction process this was extended to 6 days, with siRNA maintaining Bcl-3 expression below 70% after this longer treatment time. The differential effects of prolonged inhibition were supported by viability assays which also showed

significant reductions in cell viability after 6 days of Bcl-3 inhibition but no change after 48h (Figure 4.8). For this reason the effects of Bcl-3 inhibition on EMT migration were tested after 48h so that cell viability did not affect the output of this assay, with Bcl-3 RNAi significantly reducing the migratory potential of EMT MCF-7 cells (Figure 4.9), further supporting our previous results on migration. These differential effects of short and prolonged inhibition of Bcl-3 offer an interesting insight into how Bcl-3 may be more important for tumour cell homeostasis than first thought and will be explored more extensively in chapter 5.

Irrespective of how long Bcl-3 was inhibited in MCF-7 cells, no change was observed in NF-kB activation (Figure 4.10) despite its known role in the induction and regulation of EMT [151], and its activation in our model of EMT (Figure 4.6). When NF-kB activity was tested after Bcl-3 inhibition, no significant changes were observed, suggesting previous effects on morphology and viability were not due to changes in NF-kB activation. In contrast in MDA-MB-436 cells that we had already shown to possess higher basal NF-kB activity, a clear reduction was observed after 2 and 6 days of Bcl-3 inhibition. This follows previous data suggesting that ER-positive cells are less sensitive to changes in NF-kB activity after Bcl-3 inhibition, potentially due to their relatively low constitutive activation of NF-kB compared to ER-negative cells [144, 215].

In this chapter we have extensively analysed changes in gene expression after Bcl-3 inhibition in MCF-7, EMT MCF-7 and MET MCF-7 cells as well as the mesenchymal MDA-MB-436 cell line (Figure 4.11&4.12). In parental MCF-7 and MDA-MB-436 cells only small changes in gene expression were observed after 2 days of Bcl-3 RNAi compared to after prolonged 6 day inhibition where more dramatic changes were observed. This further demonstrates the potential importance of Bcl-3 in the long-term maintenance of tumour cells, and might also reflect long term changes in gene transcription associated with phenotypic switching. Despite clear differences in both genotype and phenotype of MCF-7 and MDA-MB-436 cells, some similar changes in gene expression after Bcl-3 inhibition were seen, with increases in Slug, FOXC2, mir-222 and Runx family members 1&2

observed. Interestingly, all of these genes have been linked with EMT-induction and are usually associated with poor prognosis in breast cancer [247-251]. Furthermore, Slug and mir-221 have been independently shown to be capable of regulating each other to induce migration, EMT and metastasis [250, 251]. This contradicts our previous data, which has shown Bcl-3 suppression to inhibit cell migration and metastasis, and has shown no indication of promoting an EMT-like phenotype. Given the significant loss in viability of these cells as well as the clear morphological disruption, it is plausible that the increase in these genes may be acting as some form of failed escape mechanism to combat the disruption in tumour cell homeostasis caused by Bcl-3 suppression. Aberrant Slug expression for example has been shown to promote resistance to programmed cell death, whereas high levels of Runx2 have been associated with cell survival in invasive breast cancers [252, 253]. An interesting explanation could be through the oncogene addiction phenomenon in which cells become 'addicted' to certain oncogenes that play no role in normal cells [254]. It has been suggested that Bcl-3 may exert its oncogenic effects in a similar manner to this and that if suppressed may have significant effects on tumour cell growth [3]. This is highlighted in colorectal cells where Bcl-3 is involved in a regulatory loop to suppress basal apoptosis with its depletion inducing an apoptotic effect that is not observed in non-cancerous cells, suggesting a Bcl-3 dependency in these tumour cells [209]. Whether Bcl-3 may play a similar role in breast cancer is currently unknown, however future experiments inhibiting Bcl-3 in normal mammary cells could elucidate a similar phenomenon.

When the same gene panel was assessed in EMT MCF-7 and MET MCF-7 cells after Bcl-3 inhibition some similar trends were observed, with increases in mir-221, Slug and Runx expression. In addition, the key EMT regulators N-cadherin, Twist and Vimentin were downregulated suggesting Bcl-3 inhibition may limit EMT transcription. When the expression data of MCF-7, EMT MCF-7 and MET MCF-7 cells was analysed together a similar pattern emerged in a number of EMT regulators. In MCF-7 and MET MCF-7 cells when gene expression appeared to be at basal levels Bcl-3 inhibition had little to no effect, however when these cells were stimulated into EMT these genes were

upregulated in control cells but maintained at basal levels after Bcl-3 inhibition. This suggests that Bcl-3 may be involved in regulating the transcription of some key EMT-initiating genes and its inhibition may stop them from becoming upregulated when they are stimulated into EMT. Bcl-3 has previously been shown to activate N-cadherin transcription in melanoma cells, however to our knowledge no links have been made previously between Bcl-3 and Twist or Vimentin [255]. Despite these interesting results this effect was not universal with other genes showing differential responses indicating the role of Bcl-3 in EMT is more complicated and requires further investigation. Future experiments using chromatin immunoprecipitation could confirm whether Bcl-3 is able to directly regulate these targets as well as further repeats in different cell lines to confirm these results.

Interestingly, recent work has shown an important role for Bcl-3 in regulating TGF-β signalling through stabilizing SMAD3 [188], both of which are known to be important for the initiation of EMT [242, 256], thus further supporting our data here that Bcl-3 may act as a key regulator of EMT. In this study it is also suggested that Bcl-3 inhibition and the disruption of TGF-β signalling in the mesenchymal MDA-MB-231 cell line may result in MET [188]. In this chapter we have performed comparable experiments in the similar MDA-MB-436 cell line, however no morphological reversion into an MET phenotype was observed. Furthermore, Bcl-3 inhibition resulted in the upregulation of a number of EMT-promoting genes, including Vimentin, whereas E-cadherin was significantly downregulated. This suggests that not only did these cells fail to revert through MET but actually enhanced their EMT phenotype, which is independent of the effect of Bcl-3 on cell migration. If true this would suggest a differential role for Bcl-3 in fully differentiated mesenchymal and epithelial cells that would require further investigation using cell lines of various phenotypes. Interestingly, in the previous chapter it was suggested that MDA-MB-231 cells are less differentiated than MDA-MB-436 cells and may be capable of changing their phenotype based on their environment. This plasticity could help explain why they may be capable of reverting back through MET compared to the more differentiated MDA-MB-436 cells. Further experiments treating

MDA-MB-231 cells with EMT stimulation would test this plasticity and determine whether they can be pushed even further towards a fully differentiated EMT-like phenotype and whether Bcl-3 inhibition can affect this.

Although E-cadherin expression did not change in either EMT or MET MCF-7 cells after Bcl-3 inhibition, our initial pilot study using Eph4 cells appeared to show a disruption in the localization of E-cadherin after treatment with small molecule Bcl-3 inhibitors. This did not appear to be repeated when tested in MCF-7 cells after RNAi of Bcl-3 suggesting that the effect observed was either cell-specific or compound-specific, which could be determined by testing Bcl-3 siRNA on Eph4 cells. Although compound inhibition of Bcl-3 was used sparingly in this chapter, gene expression analysis showed very little change in EMT and MET MCF-7 cells following CB-1 treatment, with no correlations with Bcl-3 siRNA inhibition. Although the half-life of CB-1 in cell culture is unknown, the prolonged nature of these assays with compound only being replenished in the media twice over 6 days was probably insufficient to initiate a response from Bcl-3 inhibition. Further investigation with higher concentrations of CB-1 and with more frequent replenishments may be sufficient to induce a similar response to siRNA inhibition of Bcl-3 which is much more stable and prolonged.

The ability to colonize distal sites requires tumour cells to adhere and survive in foreign environments as well as the ability to proliferate quickly, a process that is best suited to a more epithelial-like cell type. This process was mimicked *in vitro* using the colony forming assay with Bcl-3 inhibition reducing the ability of single cells to form colonies in MCF-7, EMT MCF-7 and MET MCF-7 cells. This correlates with bulk cell viability data that was performed previously and further signifies the effect of Bcl-3 inhibition on MCF-7 cell growth and proliferation. These tests also suggest that the effects of Bcl-3 inhibition are most likely permanent, as the transient nature of siRNA inhibition should have worn off by the experimental end point of these assays. Although Bcl-3 levels were not tested at the end point it is likely that Bcl-3 inhibition would have diminished during the colony-forming assay which was run over a total of 14 days after initial Bcl-3 siRNA treatment. As significant

effects of Bcl-3 inhibition on colony formation were observed in parental MCF-7 cells as well as those that had undergone EMT stimulation, it further suggests that this effect is not an EMT mediated response and further supports the importance of Bcl-3 for tumour cell growth.

In conclusion, in this chapter we have shown that Bcl-3 plays an important role in maintaining MCF-7 cell homeostasis, with prolonged inhibition resulting in marked effects on cell viability and morphology, which may initiate the upregulation of a number of pro-survival genes in order to counter this disruption. This observation may be through an oncogene addiction, with loss of Bcl-3 resulting in a significant loss of viability, potentially through the induction of senescence, a hypothesis that will be investigated further in the next chapter. We have also shown that Bcl-3 is upregulated during EMT in MCF-7 cells, an observation that has not been reported previously, and may play an important role in regulating a distinct set of EMT-associated genes during both EMT and MET. Based on our results and recent studies we hypothesise that Bcl-3 is upregulated during EMT to mediate the transcription of certain EMT-inducing genes. This may be via a TGF-β-mediated pathway through stabilizing SMAD3, however further work is required to confirm this.

# Chapter 5:
# The effect of prolonged Bcl-3 inhibition in breast cancer cell lines

# 5 The effect of prolonged Bcl-3 inhibition in breast cancer cell lines

## 5.1 Introduction

The prolonged inhibition (more than 2 days) of Bcl-3 was shown to induce a significant loss of viability as well as a profound morphological change in MCF-7 cells in the previous chapter, a phenotype that had not been observed previously after shorter periods of inhibition. This effect on viability was also observed in the MDA-MB-436 cell line without any obvious changes in cell morphology. Bcl-3 has previously been shown to suppress apoptosis in response to DNA damage in breast cancer cells and is responsible for suppressing apoptosis in a variety of tumour cells [208, 209]. It has also been shown to play a role in mediating proliferation in breast cancer by regulating the transition of G1 to S phase during the cell cycle by upregulating cyclin D1 [213]. The large, flattened morphology of MCF-7 cells after Bcl-3 inhibition suggested that these cells had been induced into a senescence-like phenotype; however there is no evidence in the literature linking Bcl-3 and senescence in cancer.

Senescence is often associated with a limiting of the cycling capacity of ageing cells due to telomere erosion, a process more commonly known as replicative senescence [35]. Senescence has however also been implicated in tumour suppression, providing an early defence mechanism against cancer formation. This type of senescence is known as oncogene-induced senescence (OIS) [36]. Both replicative and OIS induce a unique set of cellular traits which result in a permanent state of cell cycle arrest, making the induction of senescence an attractive therapeutic strategy for the treatment of uncontrolled proliferating tumour cells. Many hallmarks of senescence can also be induced through the exposure of tumour cells to non-lethal environmental stresses, furthering its potential as a novel therapeutic approach [257]. Stress-induced senescence, also termed therapeutic-induced senescence (TIS) offers a unique form of therapy that although does not result in total eradication of a cancer, can induce tumour cytostasis [257]. This can then be carefully

maintained to improve patient prognosis without the many side effects associated with more commonly used cytotoxic drugs [257].

The NF-kB signalling pathway has been implicated in the induction and maintenance of TIS through the regulation of the senescence-associated secretory phenotype (SASP) [258]. In a mouse lymphoma model, suppression of NF-kB through p65 was able to bypass TIS, promote drug resistance and reduce survival [259]. Alternatively, suppression of the non-canonical NF-kB pathway through siRNA inhibition of p52 has been shown to induce senescence through down-regulation of EZH2 in a melanoma model [260]. Furthermore, in a human fibroblast model, suppression of Bcl-3 induced a similar senescence phenotype through a reduction in EZH2 [261]. These data suggest differential roles of the canonical and non-canonical NF-kB pathways in the regulation of senescence, and a potential role for Bcl-3 in this process.

The aims of this chapter were to confirm whether the loss in cell viability observed after prolonged Bcl-3 suppression was due to an induction of senescence in MCF-7 cells. Furthermore, to test the effect of prolonged Bcl-3 inhibition on the phenotype of different cell lines to determine whether this is a universal effect or specific to certain breast tumour subtypes.

## 5.2 Testing the effect of prolonged Bcl-3 suppression in MCF-7 cells

The clear change in cell morphology observed after the prolonged inhibition of Bcl-3 in MCF-7 cells (chapter 4) mimicked one of the hallmarks of a senescent cell, with a large flattened 'fried egg' appearance. This change in morphology is one of a number of changes that can be associated with senescent cells; therefore to test the hypothesis that prolonged Bcl-3 inhibition could drive MCF-7 cells into senescence some other hallmarks of senescence were investigated.

### 5.2.1 Bcl-3 inhibition increased senescence-associated beta-galactosidase expression

One of the hallmarks of cellular senescence is the expression of senescence-associated beta-galactosidase (SA-β-gal), which is considered as an important biomarker of senescence. To confirm that the morphological change observed was indeed a senescence phenotype, MCF-7 cells were stained for SA-β-gal after 2 or 6 days of treatment with Bcl-3 siRNA or scRNA control. Images were taken from 5 randomly-selected fields of view with positively stained cells shown as a percentage of the total cell number.

After 2 days of siRNA treatment, no significant change was observed with both scRNA and siRNA treated cells showing SA-β-gal positive staining in less than 5% of the total cell population (Figure 5.1). MCF-7 cells with Bcl-3 inhibited for 6 days however showed a significant increase in the percentage of SA-β-gal positive cells compared to scRNA controls (Figure 5.2), confirming that the large, flattened, morphological change previously described was due to an induction of senescence. These results confirm that short-term (2 day) inhibition of Bcl-3 is insufficient to initiate a senescence response, which requires a more sustained inhibition over a longer time-frame.

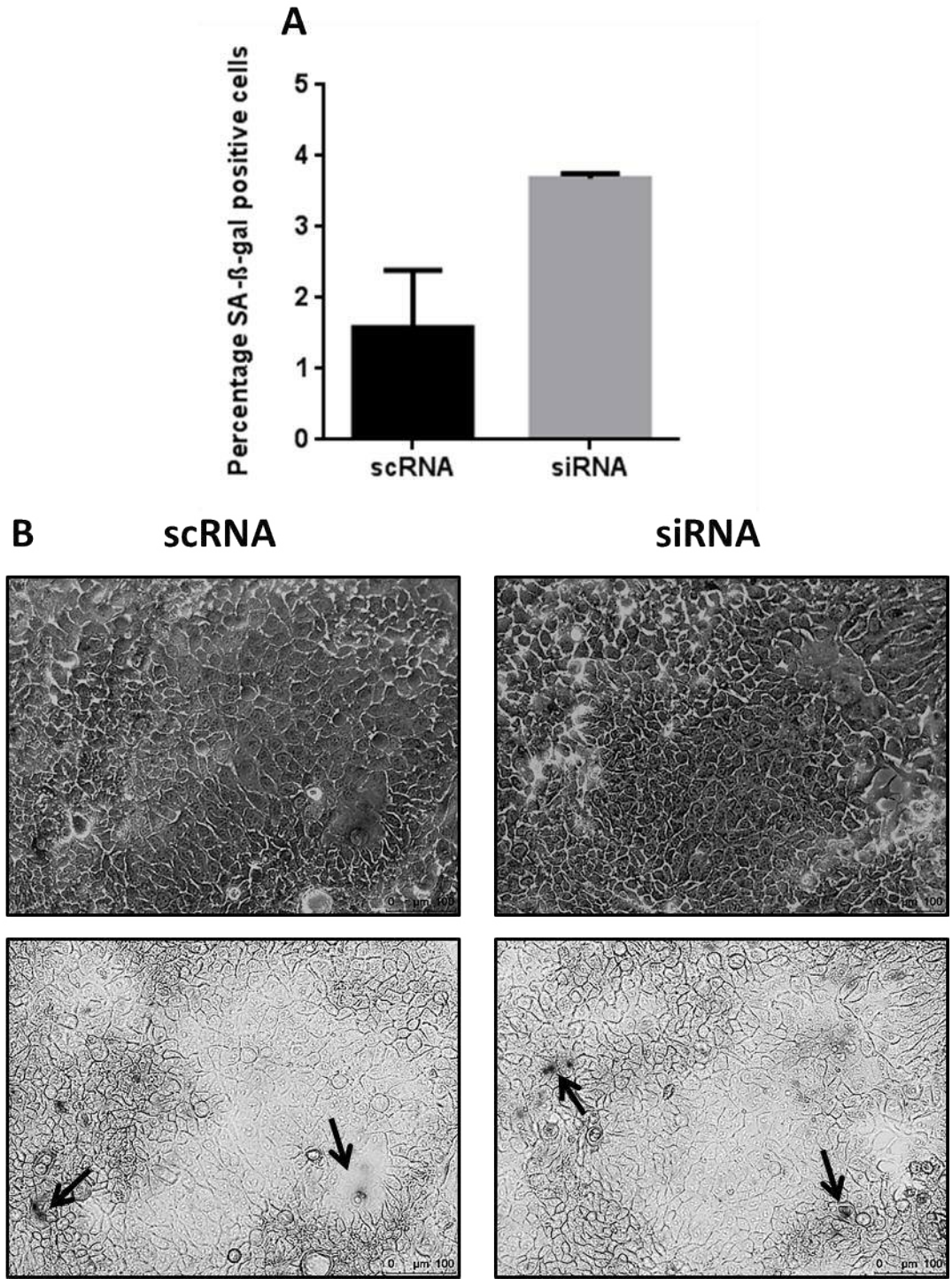


**Figure 5.1-2 day Bcl-3 inhibition resulted in a small increase in SA-β-gal positive cells-** MCF-7 cells were treated with either Bcl-3 siRNA or scRNA control for 2 days before cells were fixed and stained for SA-β-gal. **(A)** Pictures were taken from 5 randomly selected fields of view and counted for positively stained cells, these were then scored against the total cell population and represented as a percentage of total cells. Error bars represent ± SEM of 2 independent experiments. T-test, *=p<0.05 compared to scRNA. **(B)** Representative images of siRNA or scRNA treated cells taken with phase contrast or brightfield filters to highlight the positively stained cells. Scale bar= 100µm

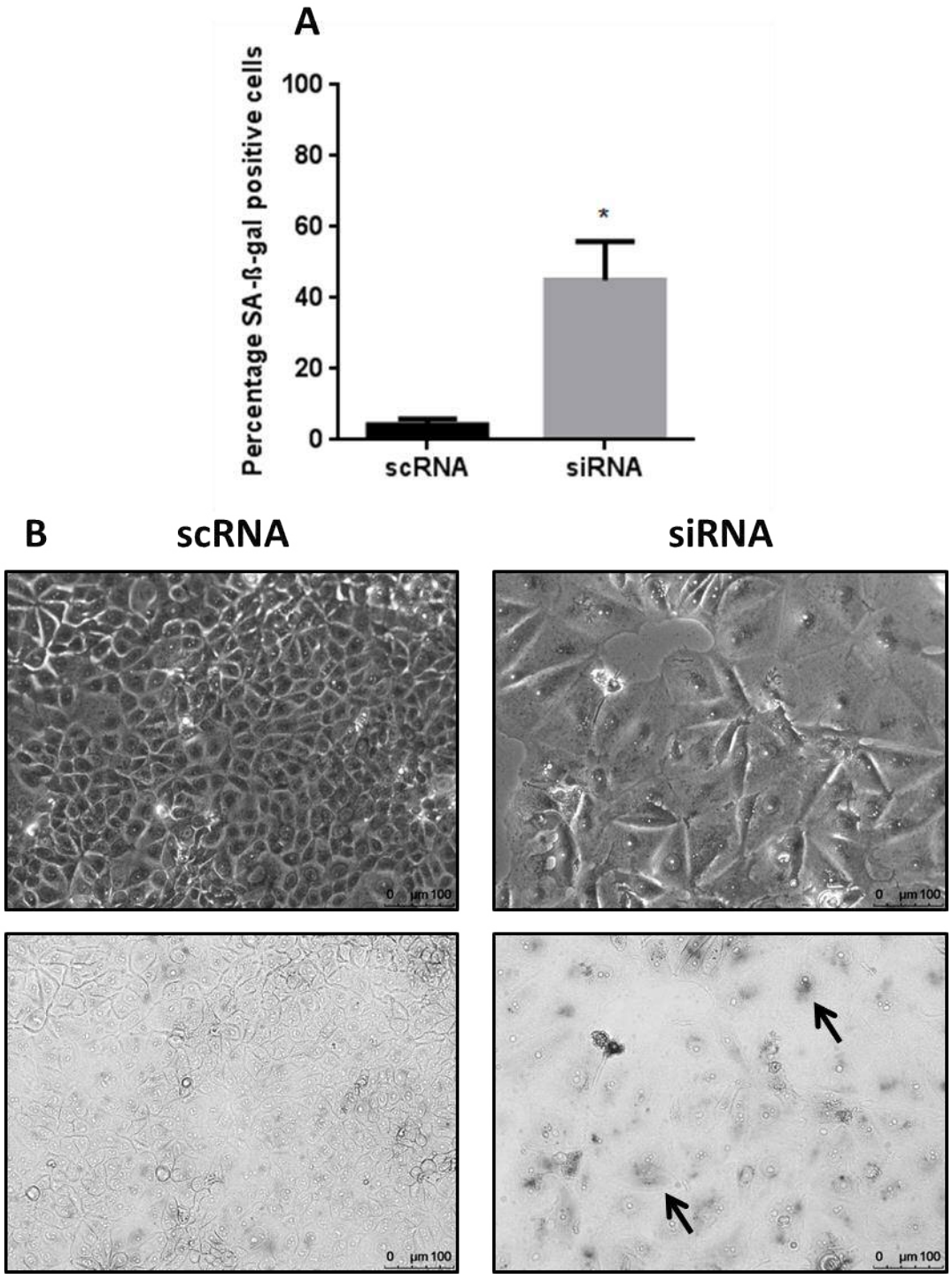


**Figure 5.2- 6 day Bcl-3 inhibition significantly increased the percentage SA-β-gal positive cells-** MCF-7 cells were treated with either Bcl-3 siRNA or scRNA control for 6 days before cells were fixed and stained for SA-β-gal. **(A)** Pictures were taken from 5 randomly selected fields of view and counted for positively stained cells, these were then scored against the total cell population and represented as a percentage of total cells. Error bars represent ± SEM of 3 independent experiments. T-test, *=p<0.05 compared to scRNA. **(B)** Representative images of siRNA or scRNA treated cells taken with phase contrast or brightfield filters to highlight the positively stained cells. Scale bar= 100µm.

### 5.2.2 Bcl-3 inhibition increased p15 and p21 gene expression

To further confirm the senescence phenotype observed after Bcl-3 inhibition, the expression of senescence-associated genes CDKN1A (p21), CDKN2A (p16) and CDKN2B (p15) were tested using qRT-PCR. After 2 days of Bcl-3 suppression the expression of p21 was significantly upregulated, with no significant change observed in p15 expression, indicating that p21 may be more important for initiating the senescence response (Figure 5.3). After 6 days of RNAi both p21 and p15 were significantly upregulated compared to controls, however no amplification was observed in p16 expression.

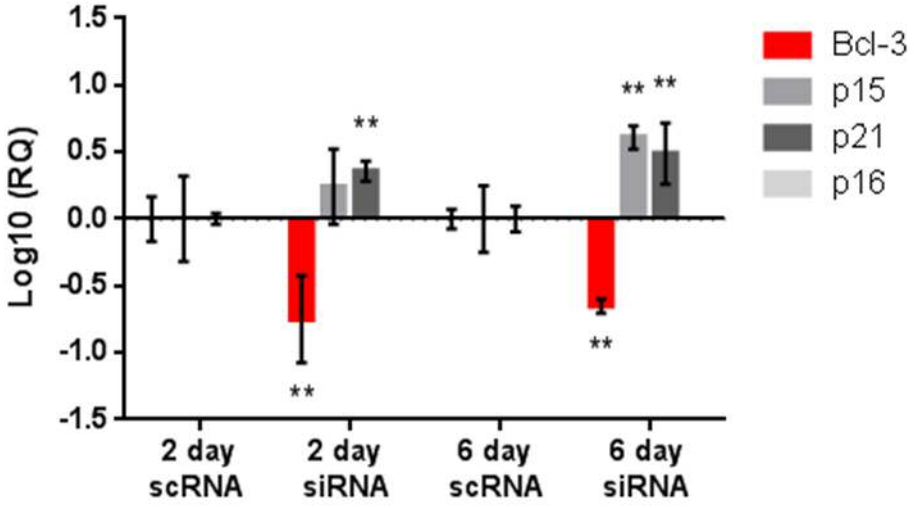


**Figure 5.3- Bcl-3 inhibition induced p21 and p15 expression-** MCF-7 cells were treated with either Bcl-3 siRNA or scRNA control for 2 or 6 days before cells were harvested for RNA. qRT-PCR was performed to compare the expression of p15, p21 and p16. Error bars represent 95% confidence intervals of 3 independent experiments. Significance was determined using the 95% confidence interval overlap rule described in [1].

### 5.2.3 p21 localised to senescent-like MCF-7 cells

To determine whether the increase in p21 expression translated to the protein level, immunofluorescence staining was performed on cells treated for 6 days with either Bcl-3 siRNA or scRNA control. Phalloidin was used to mark F-actin and determine cell morphology with p21 staining correlating with cells that had a senescence-like morphology (Figure 5.4). Immunofluorescence was also performed for p15 however cellular staining was difficult to distinguish and requires further optimization.

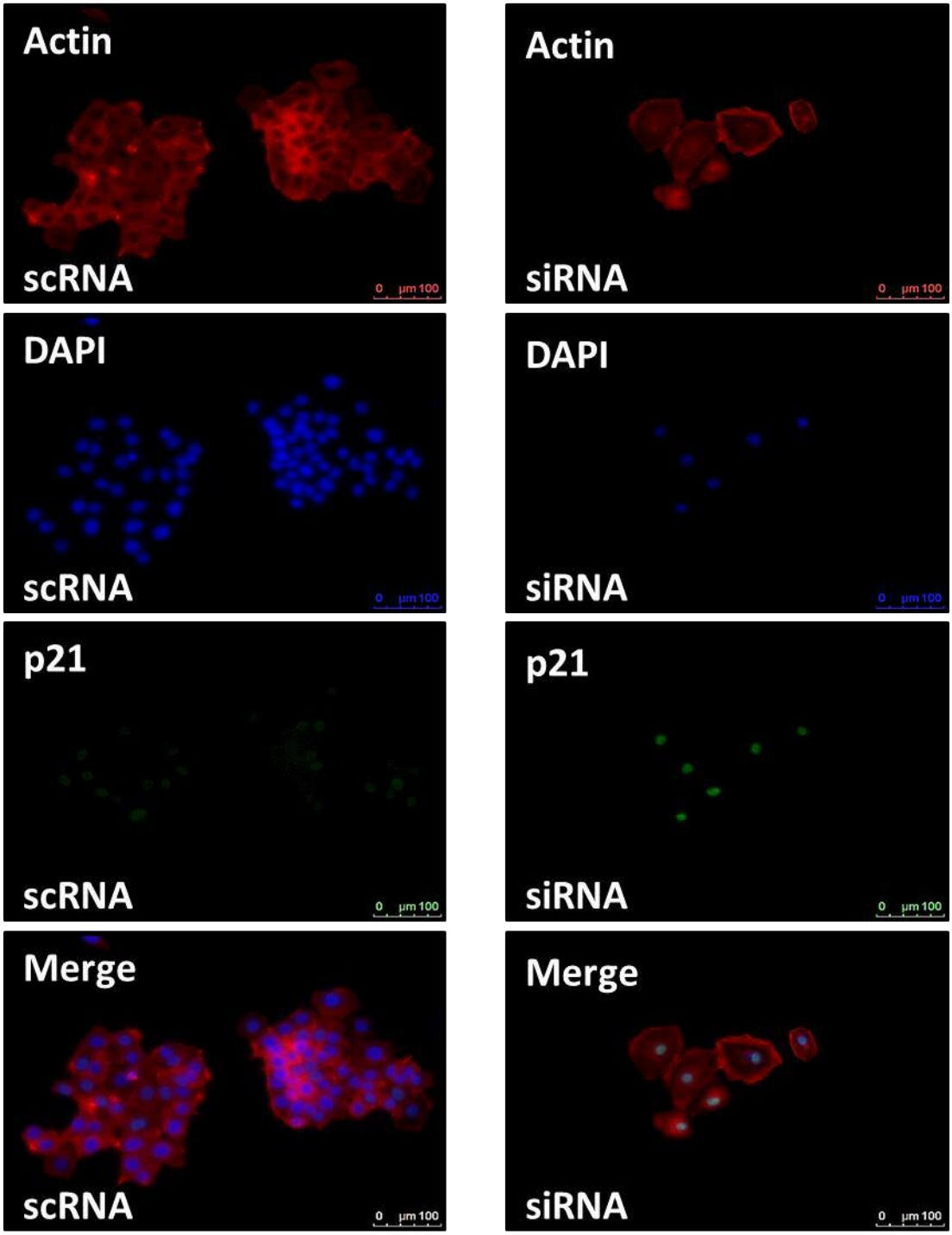


**Figure 5.4-p21 expression correlated with senescence-like phenotype in MCF-7 cells-** Representative images of immunofluorescence performed on MCF-7 cells treated for 6 days with either Bcl-3 siRNA or scRNA control. Cells were grown on coverslips and fixed at assay endpoints with 4% PFA before being stained for p21 (green) or phalloidin (F-actin) (red) and the nuclear marker DAPI (Blue). Images are representative of 2 independent experiments. Scale bar=100 µm

### 5.2.4 Bcl-3 inhibition induced a senescence-associated secretory phenotype (SASP)

The senescence-associated secretory phenotype (SASP) is another hallmark of senescence often attributed to the induction and maintenance of the senescence phenotype, and has also been linked to the NF-kB signalling pathway. Therefore, to assess whether Bcl-3-associated senescence was being mediated through SASP, both IL-6 and IL-8, two key modulators of SASP, along with C/EBP-β, which is a known regulator of both, were tested using qRT-PCR (Figure 5.5). The chemokine CXCL10, which has been previously identified by this lab as a target of Bcl-3 (unpublished) was also tested. After 2 days of Bcl-3 inhibition, IL-6 and C/EBP-β expression were significantly increased, with both IL-8 and CXCL10 showing no significant changes. When Bcl-3 was inhibited for 6 days, IL-6, IL-8 and CXCL10 were all significantly upregulated, however no change was observed in C/EBP-β expression.

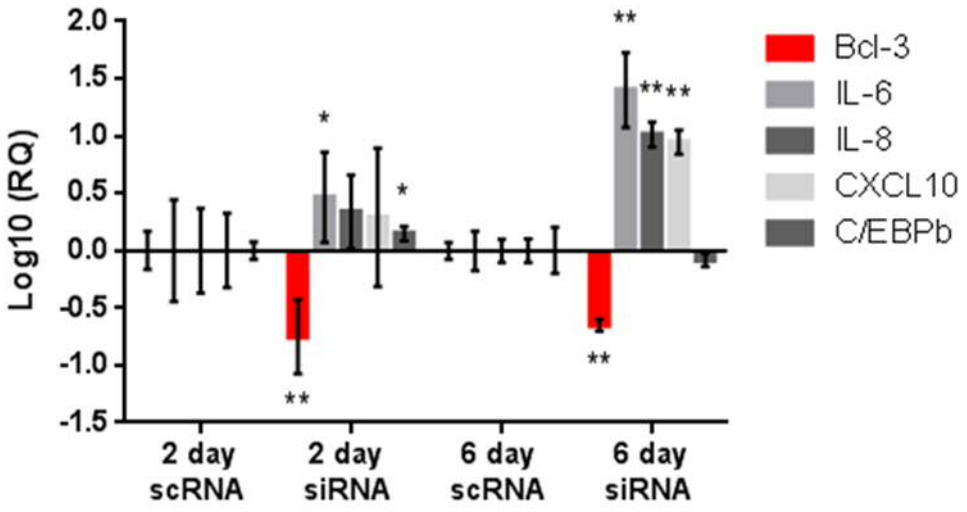


**Figure 5.5- Bcl-3 inhibition induced SASP expression-** MCF-7 cells were treated with either Bcl-3 siRNA or scRNA control for 2 or 6 days before cells were harvested for RNA. qRT-PCR was performed to compare the expression of IL-6, IL-8, CXCL10 and C/EBPβ. Error bars represent 95% confidence intervals of 3 independent experiments. Significance was determined using the 95% confidence interval overlap rule described in [1].

### 5.2.5 6 day Bcl-3 inhibition increased the population of G1 cells

The reduction in cell viability observed previously suggested either cytotoxic activity of prolonged Bcl-3 or an arrest in dividing cells. As senescence is associated with a permanent cell cycle arrest the cell cycle profile of MCF-7 cells after 2 days and 6 days of Bcl-3 inhibition using siRNA was investigated. To determine the percentage of cells in each stage of the cell cycle treated cells were stained with DAPI and assayed by flow cytometry to analyse differences in DNA content.

When Bcl-3 was inhibited for 2 days no difference was observed at any stage of the cell cycle (Figure 5.6), again highlighting the requirement of prolonged inhibition to induce a senescence response. After 6 days of Bcl-3 inhibition a small but significant increase in the G1 population was observed in siRNA treated cells compared to controls (Figure 5.7), with no significant changes observed in S or G2/M populations. Despite this very small effect on the cell cycle profile observed after 6 days of Bcl-3 inhibition, this was less profound than expected and was not consistent with the previously described senescence response. More detailed analysis using Pyronin Y combined with DAPI may be used in future work to distinguish G0 from G1 cell populations and show a more profound effect on cell cycle following Bcl-3 inhibition which could not be observed with DAPI staining alone.

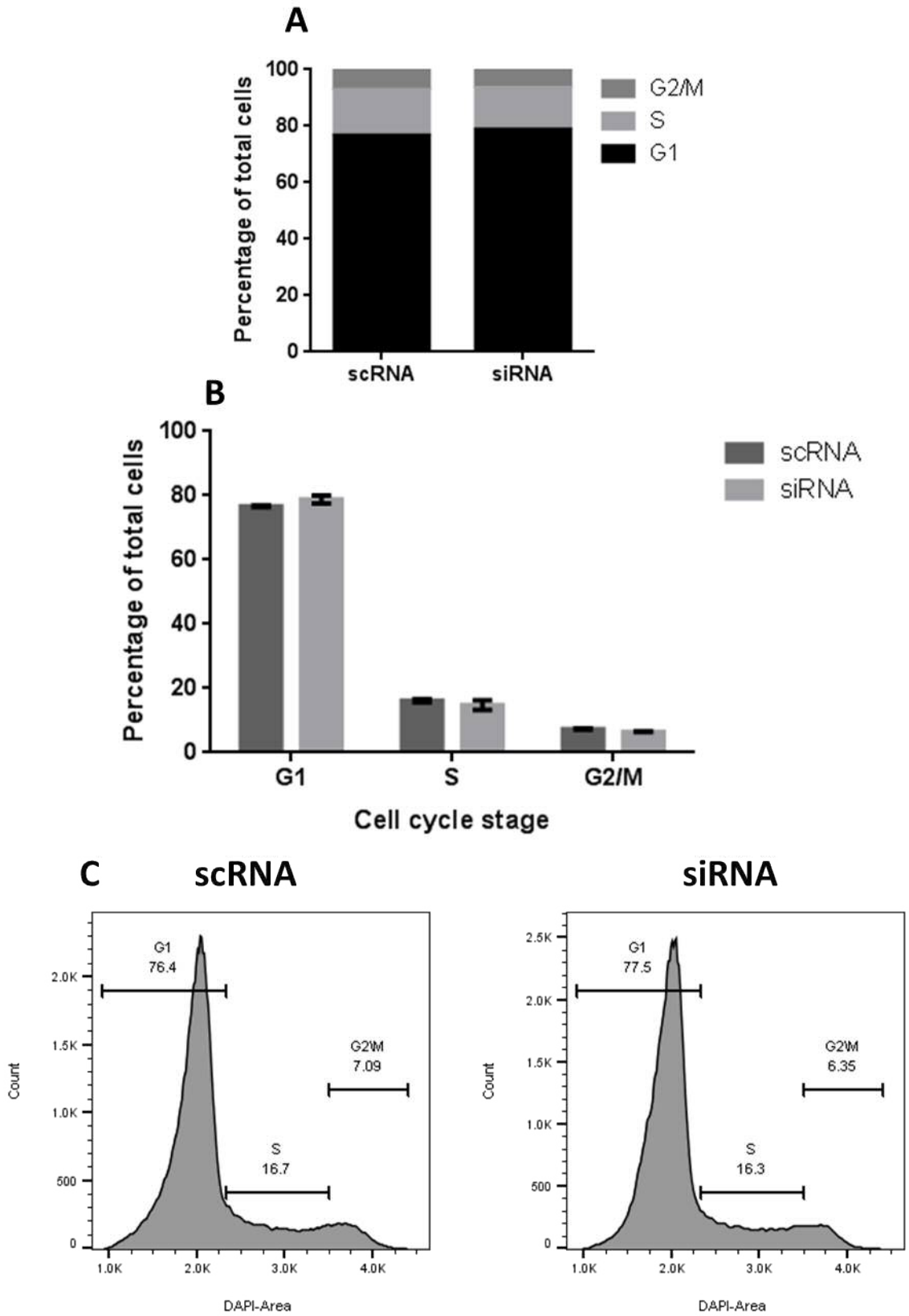


**Figure 5.6- 2 day Bcl-3 inhibition in MCF-7 cells had no effect on cell cycle-** MCF-7 cells were treated with either Bcl-3 siRNA or scRNA control for 2 days before cells were stained with DAPI solution. Initially cells were gated based on FSC-area and SSC-Area before single cells were selected based on FSC-Area and FSC-Height by flow cytometry, these were then analysed for DAPI expression with each population separated and analysed using FlowJo. **(A&B)** Cells were gated based on DAPI expression and shown as a percentage of the total cell population. Error bars represent ± SEM of 2 independent experiments. T-test, *=p<0.05 compared to scRNA. **(C)** Representative images of flow cytometry histogram plots analysed in FlowJo.

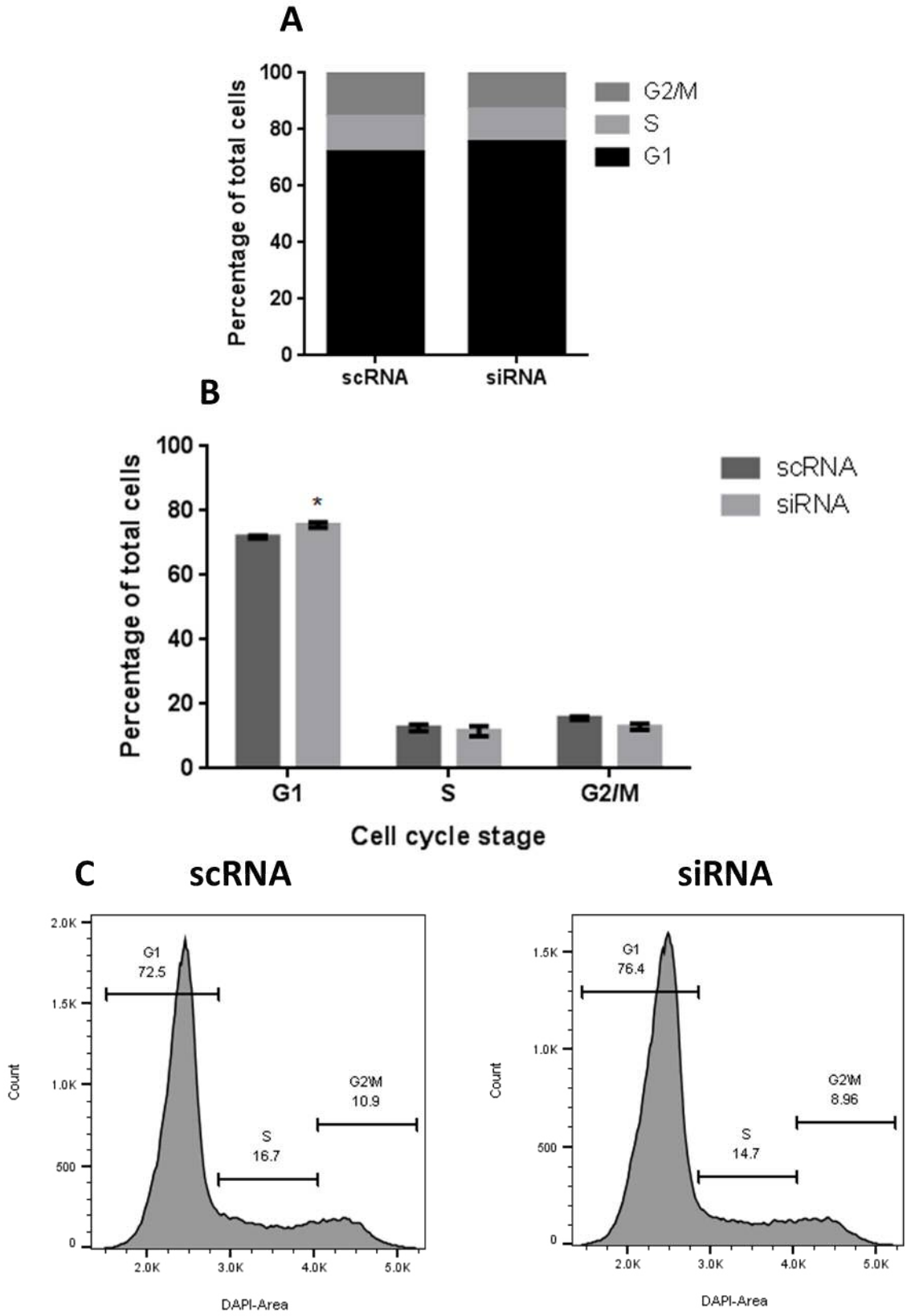


**Figure 5.7- 6 day Bcl-3 inhibition resulted in a small G1 cell cycle arrest-** MCF-7 cells were treated with either Bcl-3 siRNA or scRNA control for 6 days before cells were stained with DAPI solution. Initially cells were gated based on FSC-area and SSC-Area before single cells were selected based on FSC-Area and FSC-Height by flow cytometry, these were then analysed for DAPI expression with each population separated and analysed using FlowJo. **(A&B)** Cells were gated based on DAPI expression and shown as a percentage of the total cell population. Error bars represent ± SEM of 3 independent experiments. T-test, *=p<0.05 compared to scRNA. **(C)** Representative images of flow cytometry histogram plots analysed in FlowJo.

### 5.2.6 Bcl-3 inhibition reduced colony forming ability in MCF-7 cells

In the previous chapter it was shown that prolonged Bcl-3 inhibition could significantly reduce the colony forming ability of MCF-7 cells suggesting a permanent state of cell cycle arrest. To confirm this, colony forming assays were performed and analysed in greater detail to identify whether Bcl-3 inhibition reduced the size and/or altered the type of colonies formed as well as the overall number of colonies. Cells were treated with Bcl-3 siRNA for 2 or 6 days before being reseeded at low density to determine whether the cells could recover and repopulate. After 8 days cells were fixed and stained with crystal violet, before the number of colonies were counted. Colonies were then further characterised by cell number and type based on morphology.

After both 2 and 6 days of Bcl-3 inhibition the number of colonies observed was significantly reduced (Figure 5.8A). When MCF-7 cells were treated with siRNA or scRNA post-seeding, the number of colonies also appeared to be reduced, however this experiment was only performed once (Figure 5.8B). When individual colonies were analysed and scored, after both 2 and 6 days Bcl-3 siRNA-treated cells formed significantly smaller colonies based on the average number of cells that made up each colony (Figure 5.9 A&B). Furthermore, Bcl-3 inhibition at either time point resulted in a significant increase in senescent-like colonies and a reduction in normal-like colonies, although this was not significant after 6 day RNAi (Figure 5.9 C&D). When these senescent-like colonies were analysed further, Bcl-3 inhibition again reduced the average number of cells that made up each colony (Figure 5.9 E&F). Finally the number of individual senescent cells was increased by Bcl-3 inhibition; however this was only a significant change in 6 day Bcl-3-inhibited cells.

Together these results suggest Bcl-3 inhibition can reduce overall number of colonies as well as the ability of these cells to grow and proliferate, highlighted by the overall reduction in colony size. Furthermore, Bcl-3 inhibition resulted in a reduction of normal-like colonies and an increase in senescent-like colonies, which were also smaller than their scRNA treated counterparts.

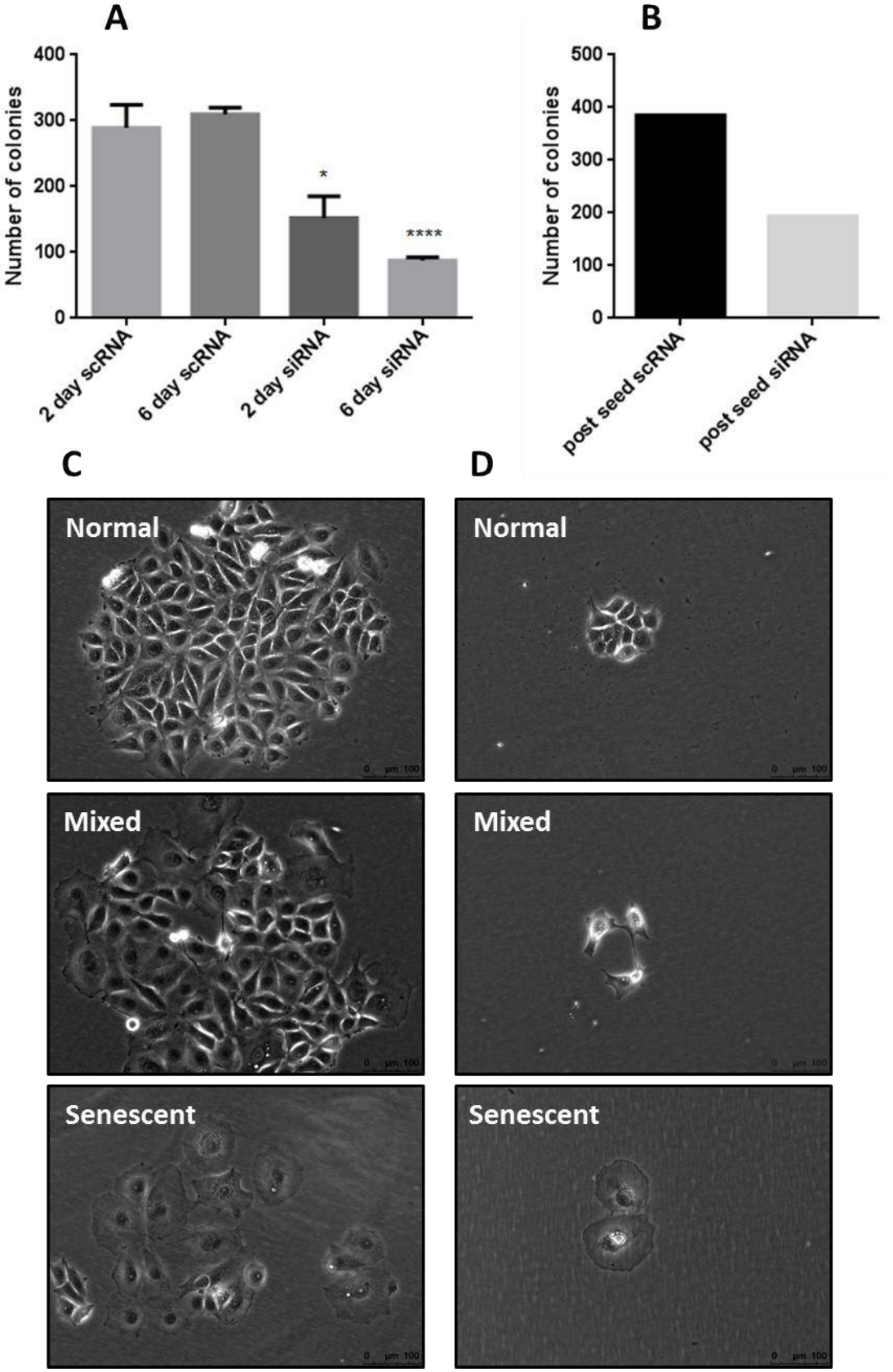


**Figure 5.8-Bcl-3 inhibition reduced the number of colonies formed in MCF-7 cells- (A)** MCF-7 cells were treated with Bcl-3 siRNA or scRNA control before being equally seeded into colony forming assays at low confluency. **(B)** MCF-7 cells were seeded into colony forming assays and left to adhere for 24h before being treated with either siRNA or scRNA. After 8 days of growth colonies were fixed and stained with crystal violet to visualise colony formation before being counted automatically using the Oxford Optronix gel counter. Error bars represent ± SEM of 3 independent experiments. (T-test,*=p<0.05, ****=P<0.0001 as compared to scRNA). **(C&D)** Representative images of the different colony types formed. Colonies were scored as normal, mixed or senescent-like as well as high **(C)** or low **(D)** based on the number of cells that made up the colony. Scale bar=100 µm.

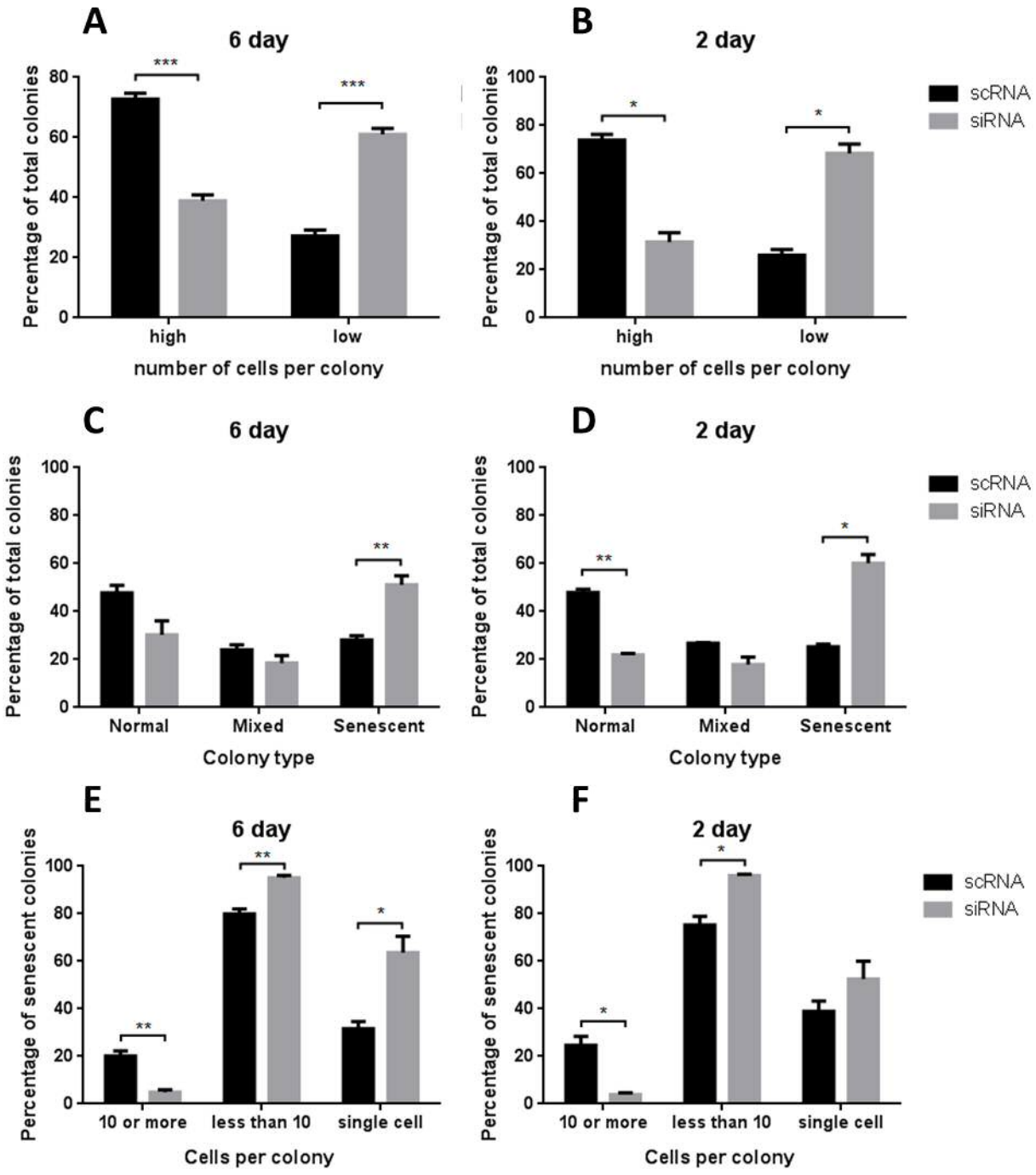


**Figure 5.9- Bcl-3 inhibition reduced the size and altered the type of colonies formed by MCF-7 cells-** MCF-7 cells were treated with Bcl-3 siRNA or scRNA control for 6 **(A,C,E)** or 2 **(B,D,E)** days before being equally seeded into colony forming assays at low confluency. After 8 days of growth colonies were fixed and stained with crystal violet to visualise colony formation before being counted and scored manually using a phase-contrast inverted microscope. **(A&B)** Colonies were scored based on the number of cells making up each individual colony with high representing 10 or more and low representing less than 10 cells. **(C&D)** Colonies were scored based on the type of cells making up each colony which was determined by cell morphology. **(E&F)** Senescent-like colonies were further scored based on the number of cells making up each colony. Error bars represent ± SEM of 3 independent experiments (2 day siRNA experiments N=2) (T-test,*=p<0.05, **=p<0.01, ***=P<0.005 as compared to scRNA).

### 5.2.7 Prolonged Bcl-3 inhibition did not induce apoptosis in MCF-7 cells

The previous results have shown how prolonged inhibition of Bcl-3 can induce senescence in MCF-7 cells, suggesting that this may be the primary cause of the reduced viability observed in chapter 4. Bcl-3 however is a known regulator of apoptosis in tumour cells and is upregulated during DNA damage responses in MCF-7 cells to inhibit cell death through this process. Therefore flow cytometry was used to test whether prolonged Bcl-3 inhibition in MCF-7 cells would also induce an apoptotic response. After 2 and 6 days of Bcl-3 siRNA treatment, attached and floating cells were harvested and stained for the apoptosis marker Annexin V and the DNA marker DAPI before being analysed.

After 2 days of Bcl-3 inhibition no significant changes were observed in the percentages of early or late apoptotic cells (Figure 5.10). The same results were observed following 6 days of Bcl-3 siRNA treatment, with no significant changes in any of the different cell populations (Figure 5.11). These results suggest that the loss of viability seen after prolonged Bcl-3 inhibition is due to senescence and not apoptosis. Furthermore, no change was observed in the percentage of live and dead cells, further indicating the effects of Bcl-3 suppression were not to induce cell death but senescence.

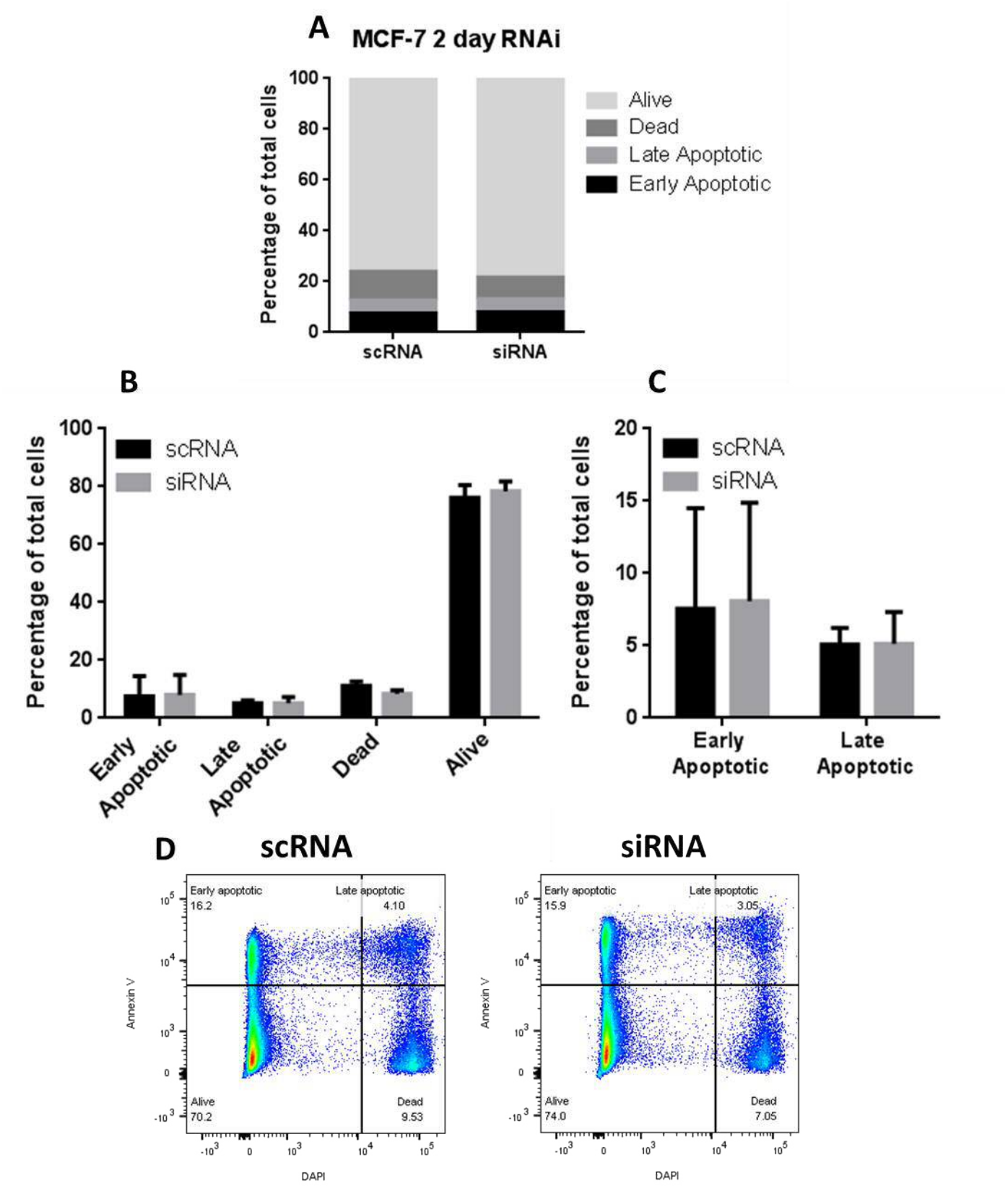


**Figure 5.10- Effect of 2 day Bcl-3 RNAi on Annexin V expression -** MCF-7 cells were treated with either Bcl-3 siRNA or scRNA control for 2 days before floating and attached cells were harvested and stained with apoptosis marker Annexin V and DNA marker DAPI. Initially cells were gated based on FSC-area and SSC-Area before single cells were selected based on FSC-Area and FSC-Height by flow cytometry, these were then analysed for Annexin V and DAPI expression with each population separated and analysed using FlowJo. **(A&B)** Cells were grouped based on expression and shown as a percentage of the total cell population. **(C)** Early and late apoptotic cells were separated by differences in DAPI staining. **(D)** Representative images of flow cytometry plots analysed in FlowJo. Error bars represent ± SEM of 2 independent experiments. T-test, *=p<0.05 compared to scRNA.

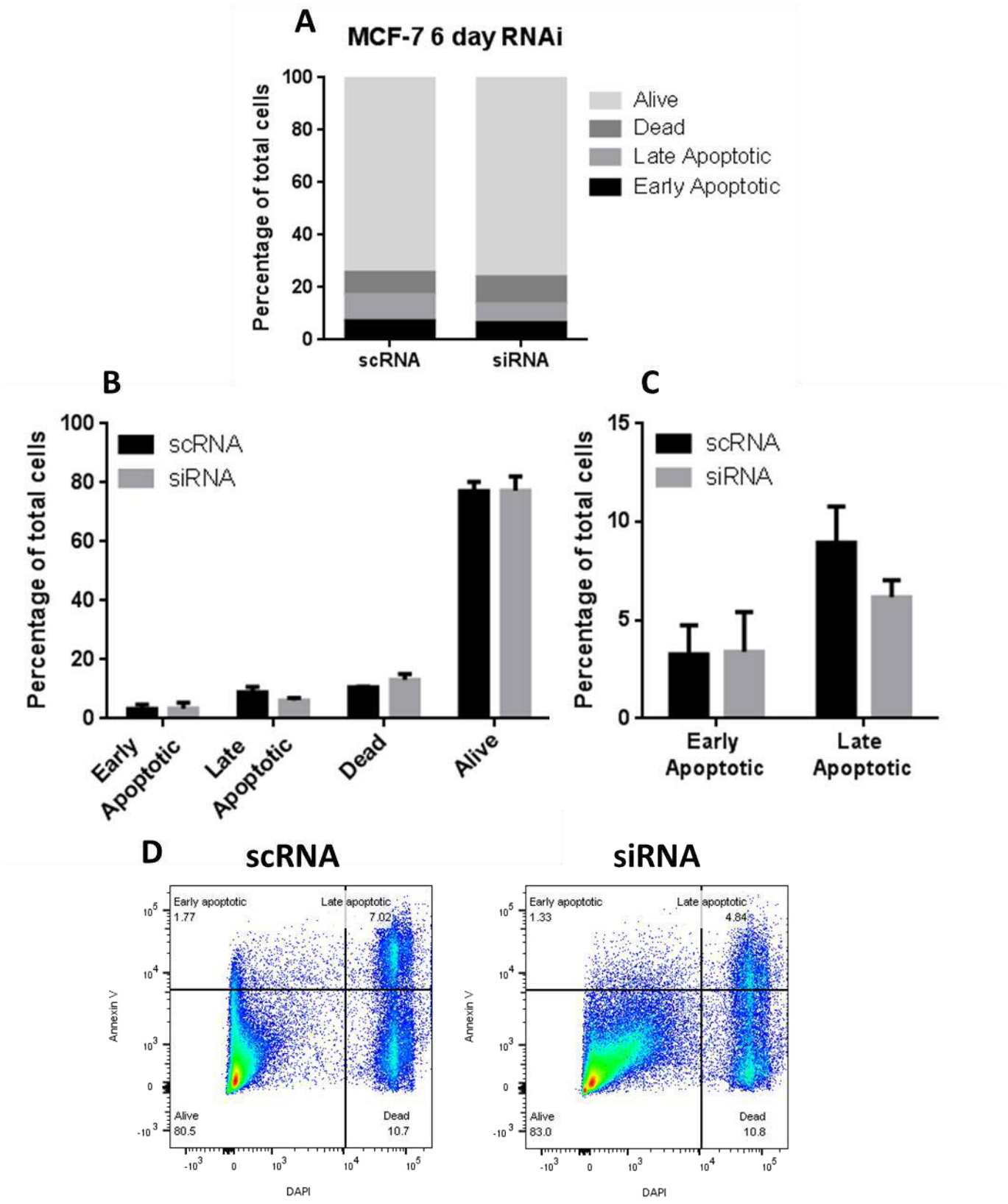


**Figure 5.11-Effect of 6 day Bcl-3 RNAi on Annexin V expression -** MCF-7 cells were treated with either Bcl-3 siRNA or scRNA control for 6 days before floating and attached cells were harvested and stained with apoptosis marker Annexin V and DNA marker DAPI. Initially cells were gated based on FSC-area and SSC-Area before single cells were selected based on FSC-Area and FSC-Height by flow cytometry, these were then analysed for Annexin V and DAPI expression with each population separated and analysed using FlowJo. **(A&B)** Cells were grouped based on expression and shown as a percentage of the total cell population. **(C)** Early and late apoptotic cells were separated by differences in DAPI staining. **(D)** Representative images of flow cytometry plots analysed in FlowJo. Error bars represent ± SEM of 2 independent experiments. T-test, *=p<0.05 compared to scRNA.

## 5.3 Effect of prolonged drug treatment on cell senescence

The prolonged inhibition of Bcl-3 has been shown to induce a senescence phenotype showing clear increases in SA-β-gal, which correlates with an increase in p21 and p15 expression as well as an upregulation of cytokines commonly associated with SASP. To test whether Bcl-3 inhibition using small-molecule inhibitors could mimic these effects, lead compound CB-1 as well as a newly synthesised analogue (CB-97), which based on chemical formulation was hypothesised to have better efficacy, were tested on MCF-7 cells. As previous data had suggested that 2 doses of CB-1 were insufficient to induce a significant Bcl-3 mediated response, each compound was administered daily for 6 days to see a maximal effect of these drugs.

### 5.3.1 Prolonged CB-1 and CB-97 inhibition had no effect on cell viability

Although previous data had suggested CB-1 treatment does not affect cell viability even at high concentrations, its effects on cell viability had not been tested after being administered daily for 6 days. Furthermore, new compound CB-97 had not yet been tested *in vitro* in any cell line. To test this, cell titre blue was used to measure the viability of MCF-7 cells after 6 days of daily treatment at either 10 µM or 100 µM. Media was changed every 24h with a fresh dose of compound, or equivalent DMSO concentration in control wells.

Daily treatment of CB-1 had no effect on cell viability at either 10 or 100 µM compared to DMSO controls. When CB-97 was administered at 100 µM it appeared to come out of solution and began crystallising on the culture plates which resulted in a loss of viability and was therefore not retested at this concentration. At 10 µM, CB-97 still appeared to come out of solution slightly but had no significant effect on cell viability. To overcome the issues with solubility, CB-97 was used at a lower concentration in all subsequent assays.

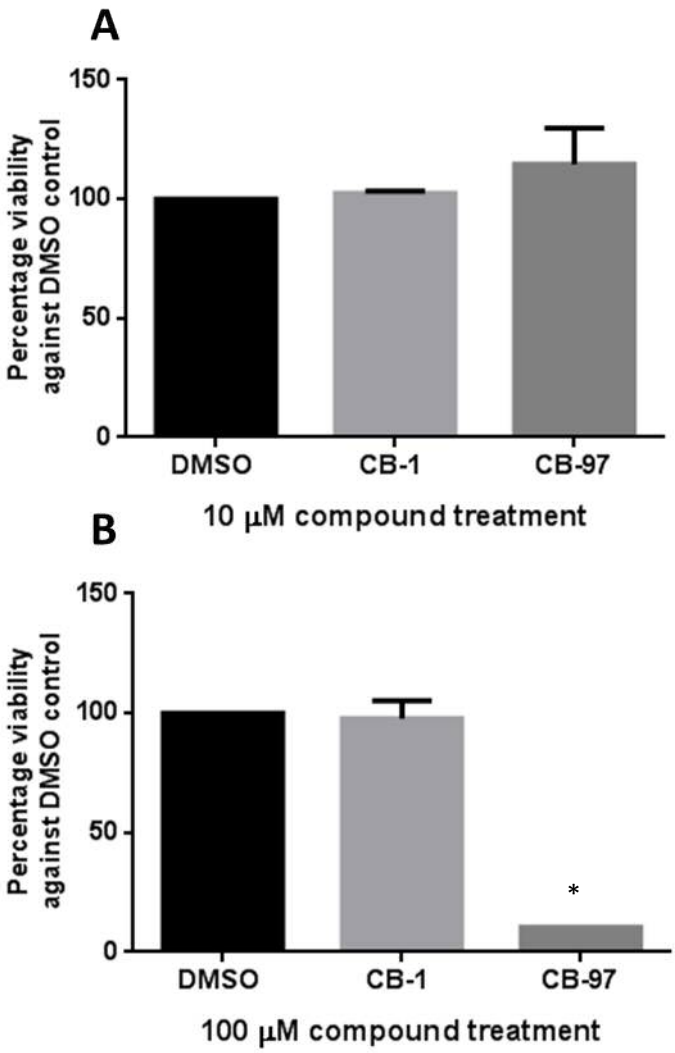


**Figure 5.12- Daily CB-1 treatment for 6 days had no effect on viability in MCF-7 cells-** MCF-7 cells were treated daily for 6 days with 10 µM **(A)** or 100 µM **(B)** of CB-1, CB-97 or equivalent DMSO concentration. Cell viability was determined using cell titre blue at the end point of each experiment. Error bars represent ± SEM of 3 independent experiments.
*= CB-97 came out of solution at 100 µM.

### 5.3.2 Prolonged inhibition of Bcl-3 by CB-1 increased SA-β-gal-positive senescent cells

The prolonged inhibition of Bcl-3 using siRNA was shown to induce a distinct change in cell morphology as well as an increase in the percentage of SA-β-gal-positive cells. To determine whether Bcl-3 inhibition using small-molecule inhibitors CB-1 and CB-97 could induce a similar change, MCF-7 cells were given daily doses of CB-1 and CB-97 at 100 µM and 2.5 µM respectively. After 6 days of treatment cells were fixed and stained for SA-β-gal.

After 6 days of 100 µM treatment some small patches of senescent-like cells appeared which stained positive for SA-β-gal. CB-97 was administered at 2.5 µM to avoid any compound from coming out of solution, however even at a much lower concentration than CB-1 a large number of senescent-like patches of cells that stained positive for SA-β-gal appeared. As these patches in both CB-1 and CB-97 treated cells were scattered across the plate and not representative of the total population they could not be quantified. Despite this, no senescent patches were observed in DMSO-treated controls suggesting that both compounds had the potential to induce a weak senescence response.

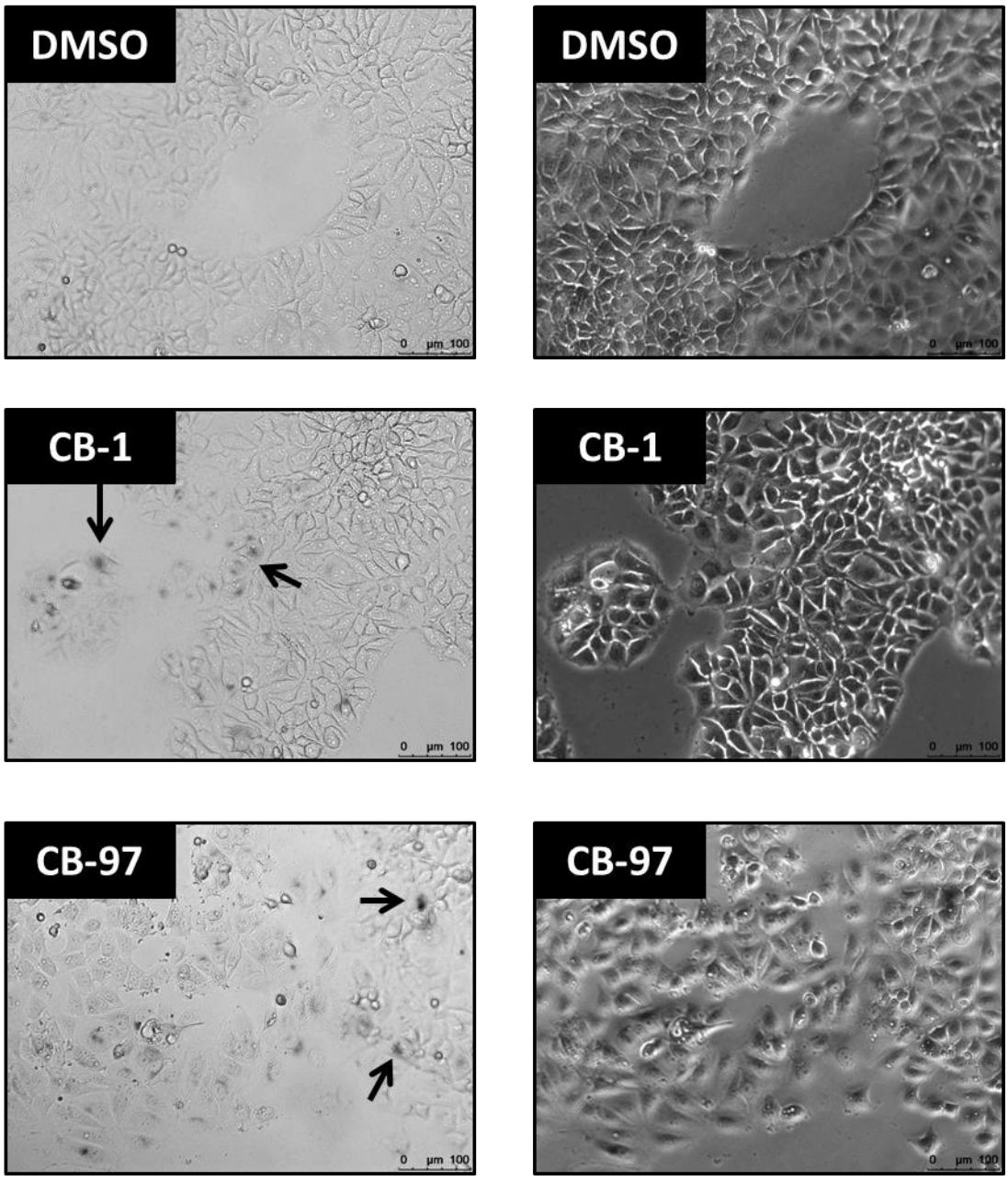


**Figure 5.13- Daily CB-1 and CB-97 treatment resulted in patches of SA-β-gal positive cells-** Representative images of MCF-7 cells treated with either 100 µM of CB-1, 2.5 µM of CB-97 or equivalent DMSO concentration. Compounds were replenished daily for 6 days before cells were fixed and stained for SA-β-gal. Scale bar= 100µm.

### 5.3.3 CB-1 and CB-97 significantly increased p21 and p15 expression in MCF-7 cells

The induction of senescence by Bcl-3 siRNA was correlated with an increase in both p21 and p15 expression both of which are known regulators of senescence. Therefore, RNA was harvested from MCF-7 cells treated daily with Bcl-3-inhibiting compounds to determine whether CB-1 or CB-97 could also increase p21 and/or a p15 expression.

After 6 days of daily CB-1 treatment at 100 µM, a significant increase in both p21 and p15 expression was observed compared to DMSO-treated controls (Figure 5.14A). This was replicated when 2.5 µM of CB-97 was given daily, with both p21 and p15 being upregulated significantly compared to controls (Figure 5.14B). The upregulation of both p21 and p15 observed was much higher in CB-97-treated cells compared to CB-1 treated cells, which correlates with the increase in SA-β-gal positive cell patches previously observed.

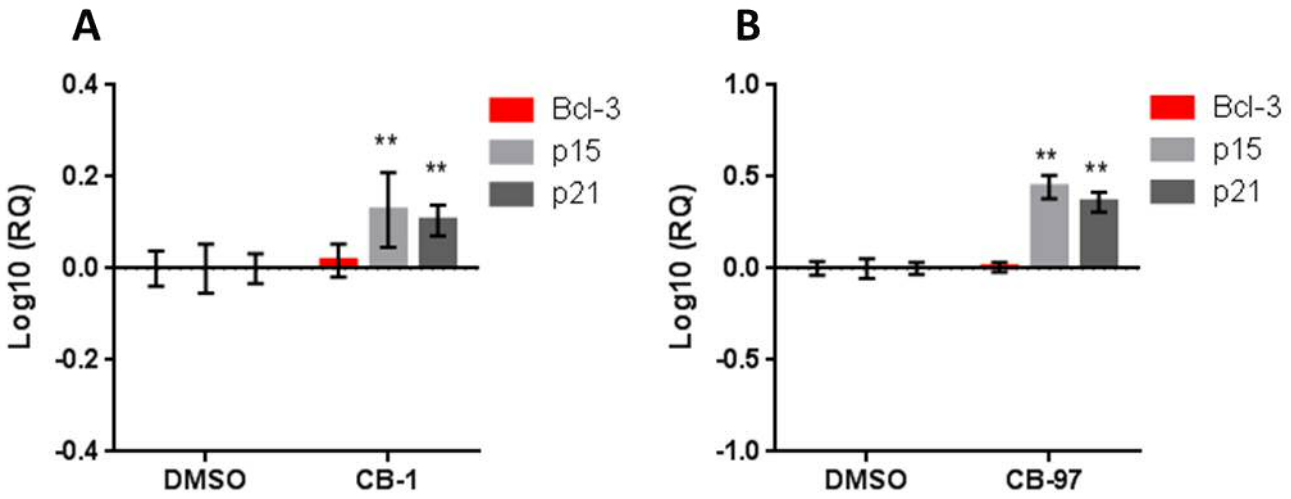


**Figure 5.14- CB-1 and CB-97 inhibition induced p21 and p15 expression**- MCF-7 cells were treated with either 100 µM of CB-1 **(A)**, 2.5 µM of CB-97 **(B)** or equivalent DMSO concentration daily for 6 days before cells were harvested for RNA. qRT-PCR was performed to compare the expression of p15 and p21 and normalized to DMSO controls. Error bars represent 95% confidence intervals of 3 independent experiments. Significance was determined using the 95% confidence interval overlap rule described in [1].

### 5.3.4 CB-97 induced SASP expression in MCF-7 cells but CB-1 did not

Senescence is often associated with an increase in secreted cytokines such as IL-6 and IL-8, a phenomenon known as SASP, which was previously shown to be induced by Bcl-3 inhibition using siRNA. To test whether the compounds CB-1 and CB-97 could also induce a SASP phenotype, the expression of IL-6, IL-8, CXCL10 and C/EBPβ was tested after 6 days of daily CB-1 or CB-97 treatment.

After 6 days of daily CB-1 treatment at 100 µM, a significant increase in IL-6 expression was observed but all other targets appeared to decrease slightly (Figure 5.15A). In contrast, 6 days of CB-97 treatment at 2.5 µM resulted in a significant increase in IL-6, IL-8, and CXCL10 expression, with no change observed in C/EBPβ expression (Figure 5.15B). These results suggest that daily CB-97 treatment is able to induce a full SASP signature, however daily CB-1 even at 100 µM cannot.

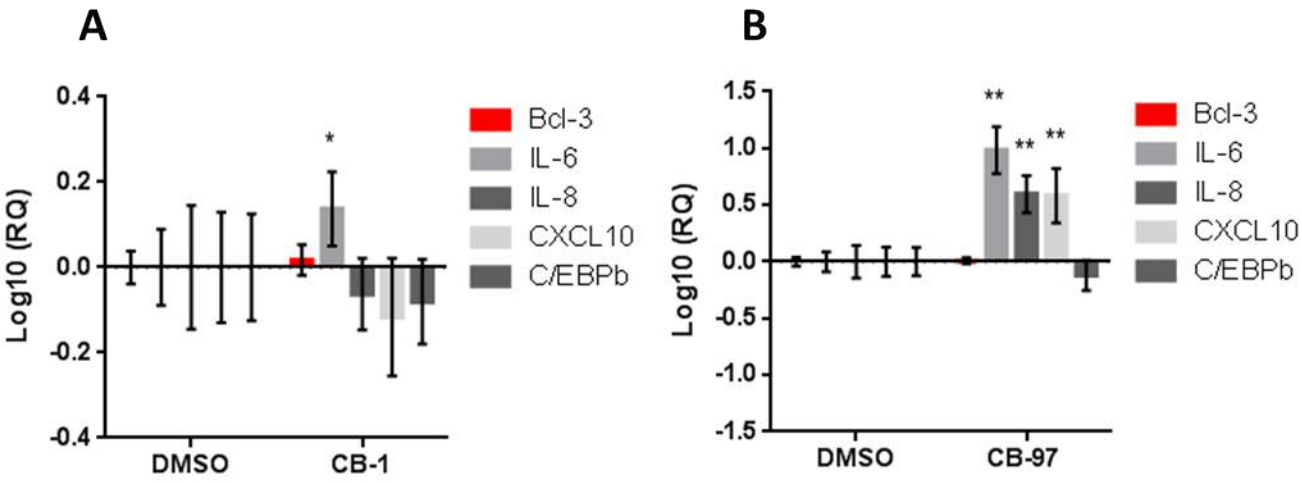


**Figure 5.15- CB-97 inhibition induced a SASP expression signature-** MCF-7 cells were treated with either 100 µM of CB-1 **(A)**, 2.5 µM of CB-97 **(B)** or equivalent DMSO concentration daily for 6 days before cells were harvested for RNA. qRT-PCR was performed to compare the expression of IL-6, IL-8, CXCL10 and C/EBPβ before being normalized to DMSO controls. Error bars represent 95% confidence intervals of 3 independent experiments. Significance was determined using the 95% confidence interval overlap rule described in [1].

## 5.4 Effect of prolonged Bcl-3 inhibition in MDA-MB-436 cells

Prolonged inhibition of Bcl-3 in MCF-7 cells was shown to induce senescence, resulting in a number of morphological and phenotypic changes including a number of the hallmarks that define senescence. To determine whether these effects could also be recapitulated within a different cell type, the triple negative MDA-MB-436 cell line, which had previously been shown to have significantly reduced cell viability after prolonged Bcl-3 suppression (chapter 4) was tested.

### 5.4.1 Bcl-3 inhibition did not induce SA-β-gal expression in MDA-MB-436 cells

The prolonged inhibition of Bcl-3 using siRNA in MCF-7 cells was previously shown to induce an increase in SA-β-gal-positive cells, a hallmark of senescence. To determine whether this senescence phenotype could also be induced in a different cell type, MDA-MB-436 cells were treated with Bcl-3 siRNA or scRNA control for 6 days before being stained for SA-β-gal. No clear change in morphology was observed as well as no increase in the number of SA-β-gal positively stained cells, indicating senescence had not been induced (Figure 5.16).

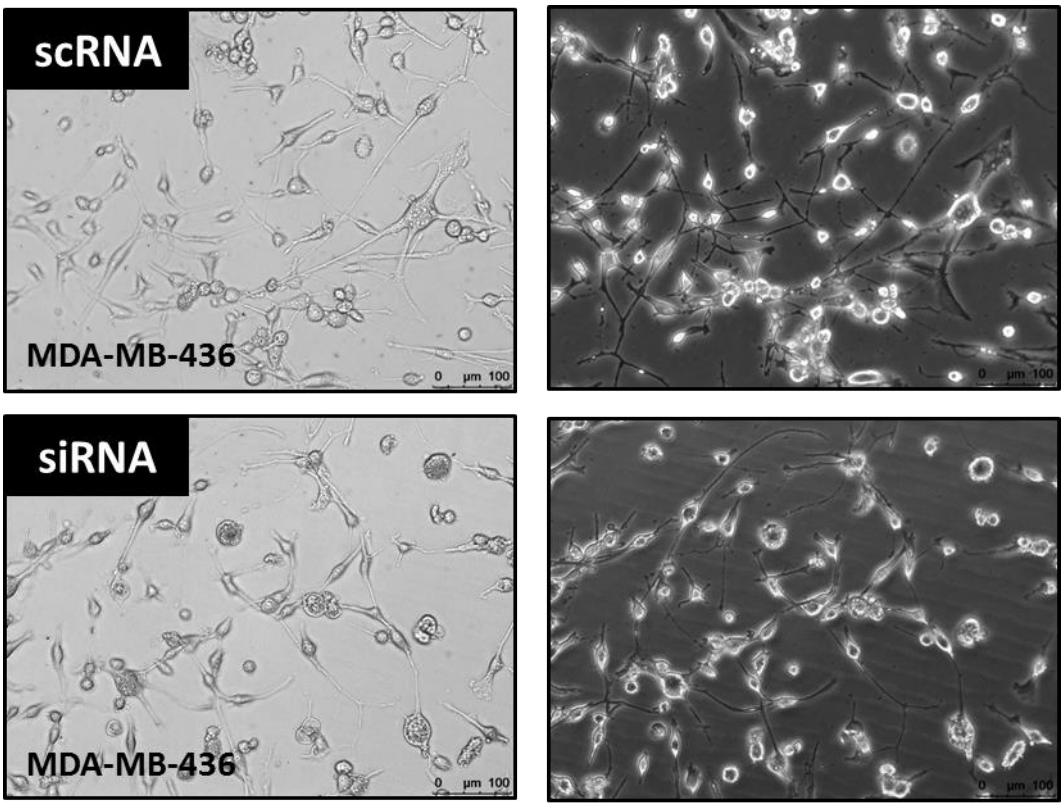


**Figure 5.16- 6 day Bcl-3 inhibition had no effect on cell morphology or SA-β-gal staining in MDA-MB-436 cells-** Representative images of MDA-MB-436 cells after 6 days of treatment with either Bcl-3 siRNA or scRNA control. Cells were fixed and stained for SA-β-gal after 6 days with images of siRNA or scRNA treated cells taken with phase contrast or brightfield filters to highlight the positively stained cells. Scale bar= 100µm.

### 5.4.2 Bcl-3 inhibition did not induce changes to cell cycle progression in MDA-MB-436 cells

It was previously shown that prolonged Bcl-3 inhibition in MCF-7 cells resulted in a small change to the G1 cell cycle population, an indication that Bcl-3 inhibition may be inducing a cell cycle arrest. To determine whether Bcl-3 may also regulate cell cycle progression in other cell types, MDA-MB-436 cells were treated with Bcl-3 siRNA for 6 days before analysis of DAPI staining by flow cytometry was used to determine the percentage of cells in each stage of the cell cycle.

MDA-MB-436 cells showed no increase in the G1 population after Bcl-3 inhibition, showing no significant differences compared to scRNA controls (Figures 5.17). Furthermore, no changes were observed after Bcl-3 inhibition in the percentage of cells in S or G2/M cell cycle stages.

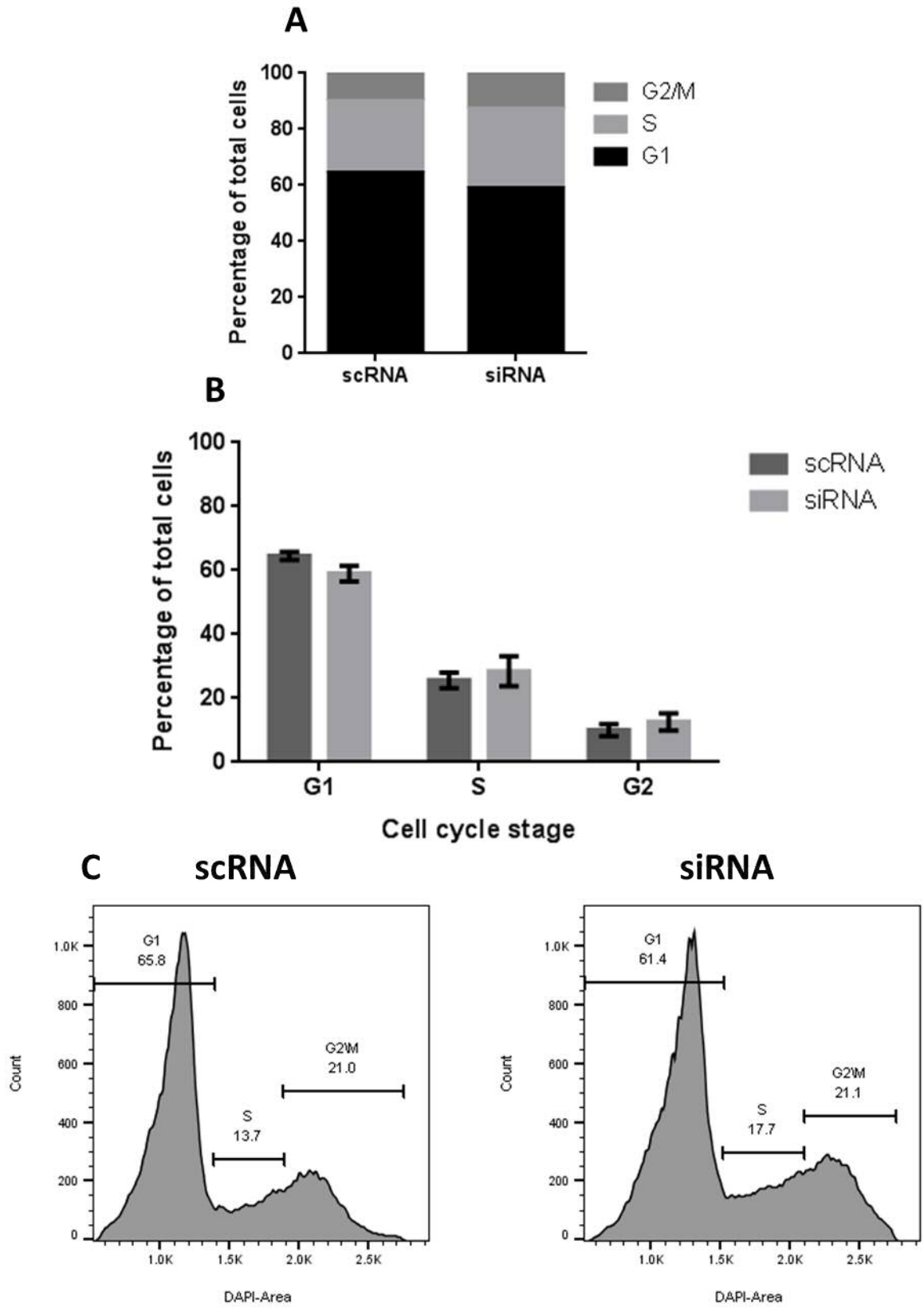


**Figure 5.17- 6 day Bcl-3 inhibition did not alter the cell cycle of MDA-MB-436 cells-** MDA-MB-436 cells were treated with either Bcl-3 siRNA or scRNA control for 6 days before cells were stained with DAPI solution. Initially cells were gated based on FSC-area and SSC-Area before single cells were selected based on FSC-Area and FSC-Height by flow cytometry, these were then analysed for DAPI expression with each population separated and analysed using FlowJo. **(A&B)** Cells were gated based on DAPI expression and shown as a percentage of the total cell population. Error bars represent ± SEM of 3 independent experiments. T-test, *=p<0.05 compared to scRNA. **(C)** Representative images of flow cytometry histogram plots analysed in FlowJo.

### 5.4.3 Bcl-3 inhibition upregulated p15 expression but not p21 in MDA-MB-436 cells

The inhibition of Bcl-3 in MCF-7 cells resulted in an increase in the expression of the senescence-associated markers p15 and p21, however no p16 expression was observed. To determine whether these genes were also regulated in MDA-MB-436 cells after prolonged Bcl-3 inhibition, qRT-PCR was performed on RNA harvested after 6 days of siRNA mediated Bcl-3 inhibition.

Bcl-3 suppression in MDA-MB-436 cells after 6 days of siRNA treatment showed an 80% reduction in Bcl-3 expression compared than scRNA controls. This resulted in a significant increase in p15 expression, however no change was observed in p21 or p16 expression (Figure 5.18A). These results suggest that Bcl-3 may modulate p15 in both cell lines independently of senescence.

### 5.4.4 Bcl-3 inhibition did not induce SASP in MDA-MB-436 cells

Despite no clear induction of senescence in MDA-MB-436 cells, the increase of senescence marker p15 suggested a potential transcriptional upregulation of senescence-mediating genes. To confirm whether this resulted in a similar SASP phenotype that was observed in MCF-7 cells after prolonged Bcl-3 inhibition, qRT-PCR was performed on the previously-selected gene panel of IL-6, IL-8, CXCL10, and C/EBPβ after 6 days RNAi inhibition of Bcl-3.

Following Bcl-3 inhibition in MDA-MB-436 cells no change except for a small but significant reduction in IL-8 expression was observed suggesting that Bcl-3 inhibition does not induce SASP in MDA-MB-436 cells (Figure 5.18B).

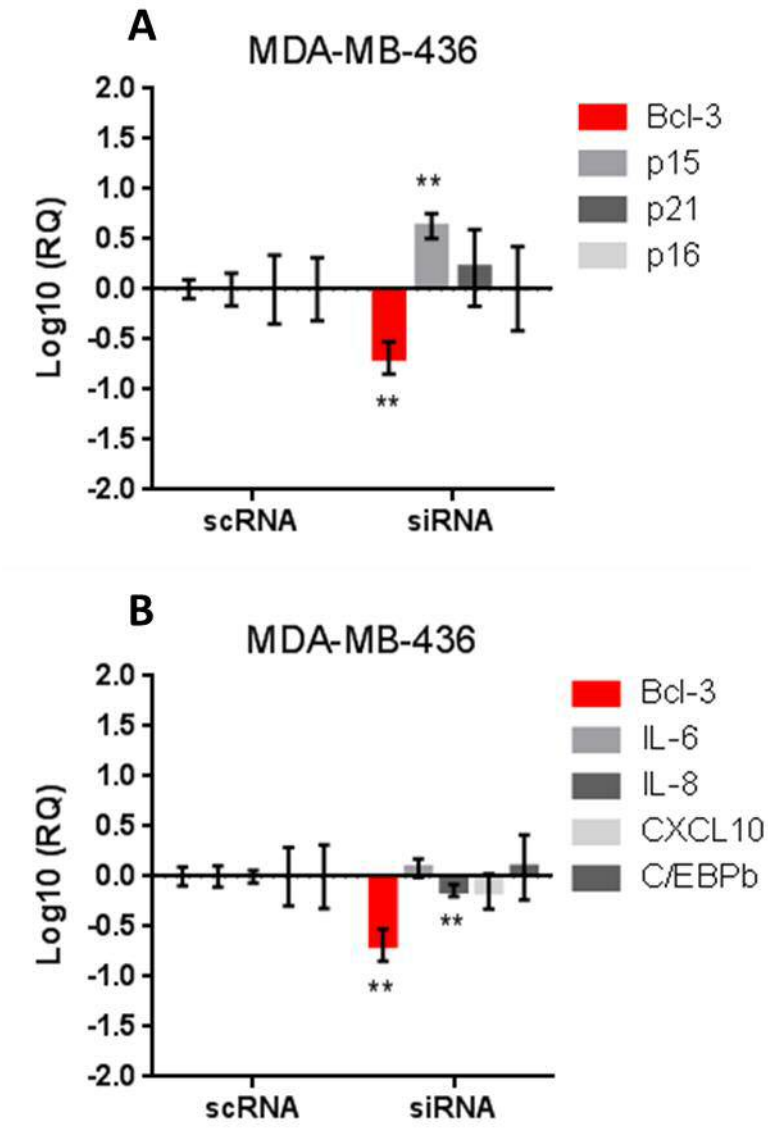


**Figure 5.18- Effect of 6 day Bcl-3 inhibition on senescence-related gene expression in MDA-MB-436 cells-** MDA-MB-436 cells were treated with either Bcl-3 siRNA or scRNA control for 6 days before cells were harvested for RNA. qRT-PCR was performed to compare the expression of **(A)** p15, p21 and p16 and **(B)** SASP cytokines which were normalized to scRNA controls. Error bars represent 95% confidence intervals of 3 independent experiments. Significance was determined using the 95% confidence interval overlap rule described in [1].

### 5.4.5 Prolonged Bcl-3 inhibition induced apoptosis in MDA-MB-436 cells

Despite the clear reduction in cell viability in MDA-MB-436 cells after prolonged Bcl-3 inhibition (chapter 4), no clear induction of senescence was observed. Bcl-3 is a known regulator of apoptosis; therefore flow cytometry was used to determine whether this reduction in cell viability was due to an increase in apoptosis. After 6 days of Bcl-3 inhibition using siRNA MDA-MB-436 cells were harvested and analysed by flow cytometry for the apoptosis marker Annexin V and the DNA marker DAPI.

MDA-MB-436 cells treated with Bcl-3 siRNA showed a significant increase in the late apoptotic cell population, with a similar non-significant increase observed in the early apoptosis population (Figure 5.19). This correlated with a slight non-significant reduction in the number of live cells. These results suggest that Bcl-3 may mediate apoptosis in MDA-MB-436 cells and not senescence.

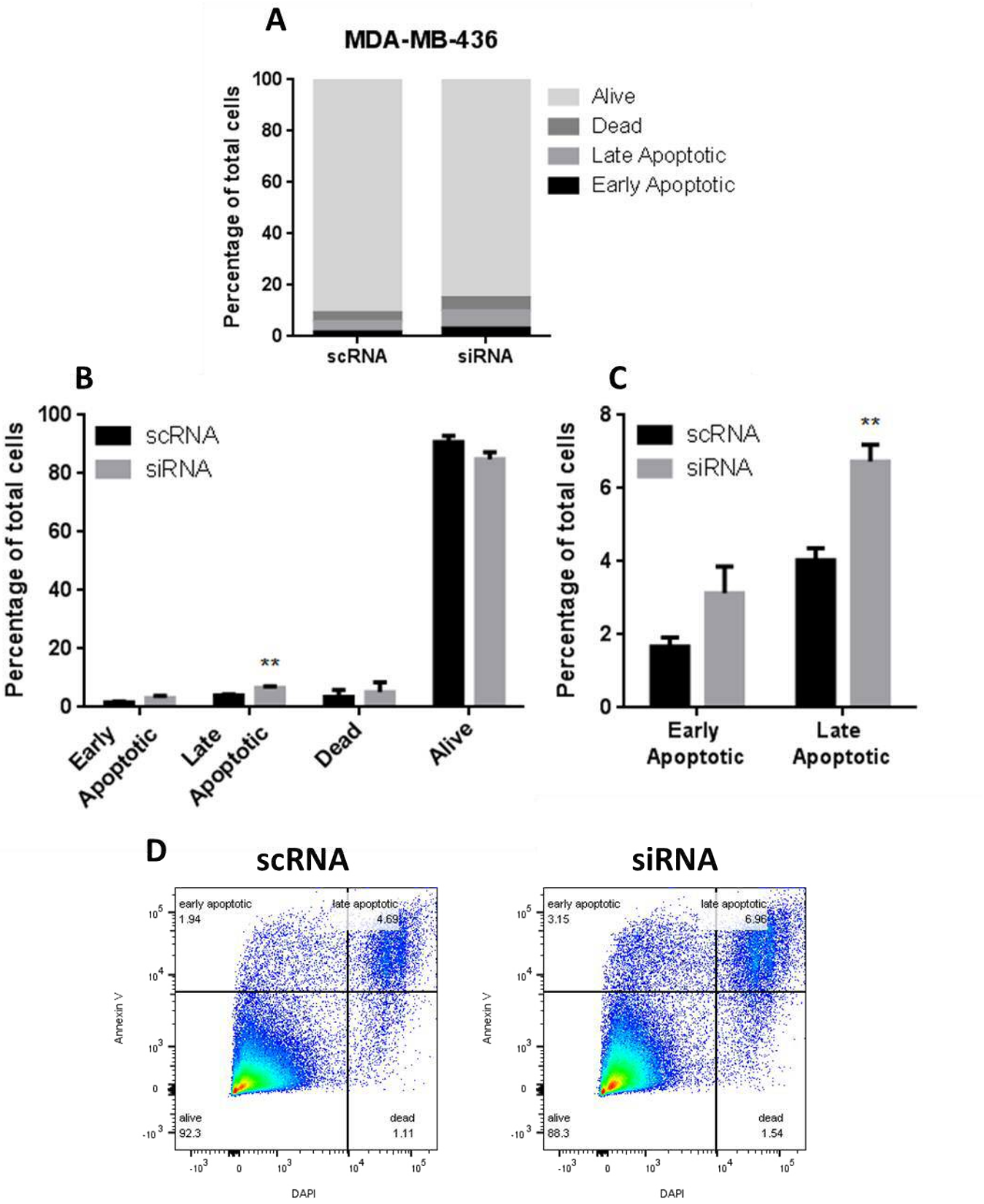


**Figure 5.19- 6 day Bcl-3 inhibition in MDA-MB-436 cells induced apoptosis-** MDA-MB-436 cells were treated with either Bcl-3 siRNA or scRNA control for 6 days before floating and attached cells were harvested and stained with apoptosis marker Annexin V and DNA marker DAPI. Initially cells were gated based on FSC-area and SSC-Area before single cells were selected based on FSC-Area and FSC-Height by flow cytometry, these were then analysed for Annexin V and DAPI expression with each population separated and analysed using FlowJo. **(A&B)** Cells were grouped based on expression and shown as a percentage of the total cell population. **(C)** Early and late apoptotic cells were separated by differences in DAPI staining. **(D)** Representative images of flow cytometry plots analysed in FlowJo. Error bars represent ± SEM of 3 independent experiments. T-test, *=p<0.05 compared to scRNA.

## 5.5 Identifying the mechanisms behind the differential effects of prolonged Bcl-3 inhibition

The previous results showed a differential effect of prolonged Bcl-3 inhibition on two different breast cancer cell lines, with 6 days of Bcl-3 siRNA treatment inducing senescence in MCF-7 cells and apoptosis in MDA-MB-436 cells respectively. One difference between these cell types which may account for the differential effects seen is the p53 status of these cell lines. MCF-7 cells are known to express wild type p53, however MDA-MB-436 cells have a mutated form of p53 [262]. Bcl-3 has previously been shown to be capable of regulating p53 in MCF-7 cells during a DNA damage response, and in primary fibroblasts Bcl-3 suppression resulted in a p53-dependent senescence response. Therefore, we hypothesised that Bcl-3-mediated senescence was mediated by p53 in MCF-7 cells, and that in the absence of p53, MDA-MB-436 cells were induced to die through apoptosis. To test this we performed a number of experiments to look at p53 signalling; to investigate the effect of interrupting p53 and p15 mediated senescence, as well as interrupting SASP through C/EBPβ and JAK inhibition to determine its role in Bcl-3-mediated senescence. A number of apoptosis markers were also analysed in MCF-7 and MDA-MB-436 cells to help further identify differences between the wildtype p53 and mutant cell lines.

### 5.5.1 Bcl-3 inhibition reduced both p53 and EZH2 expression but not MDM2 in MCF-7 cells

The role of p53 as a tumour suppressor is well known and many studies have shown a functional role for wildtype p53 in the regulation of senescence induction in breast cancer [263, 264]. This regulation is often mediated through a downregulation of the p53 regulator MDM2, which facilitates an increase in p53 DNA binding. Interestingly, another known regulator of senescence, EZH2, has been shown to be regulated through p53 in an NF-kB-dependent pathway that can be modulated through Bcl-3. Therefore, the effects of Bcl-3 inhibition on p53, MDM2 and EZH2 expression were tested in MCF-7 cells as well as MDA-MB-436 cells.

Inhibition of Bcl-3 in MCF-7 cells resulted in a significant reduction in both p53 and EZH2 expression, however no difference was observed in MDM2 expression (Figure 5.20A). In MDA-MB-436 cells no significant differences were observed in either p53 or EZH2 expression after Bcl-3 inhibition compared to control cells (Figure 5.20B).

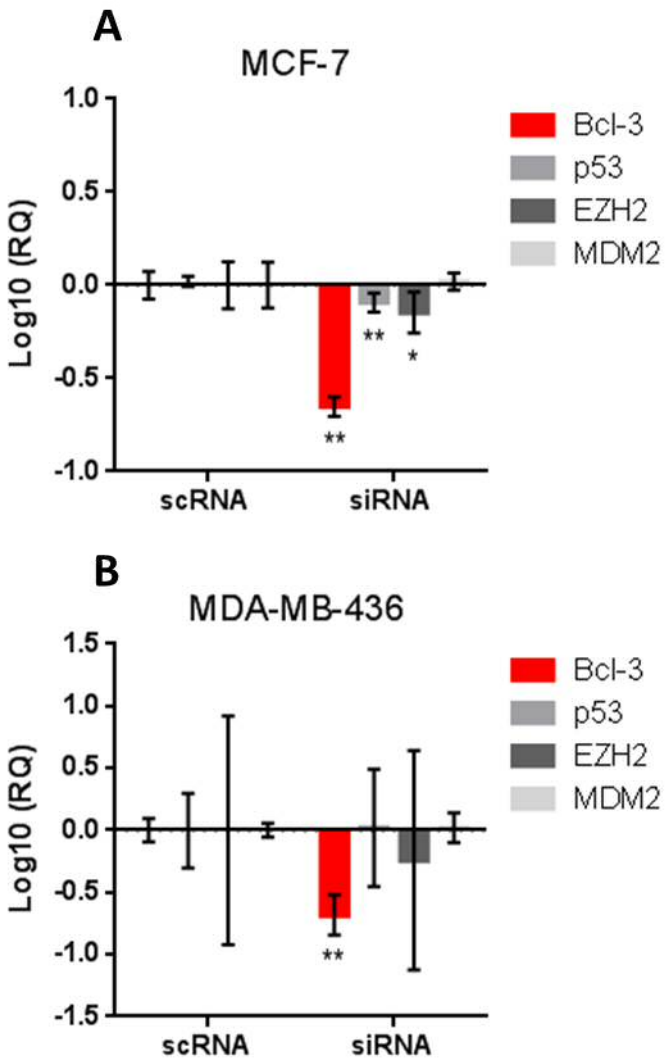


**Figure 5.20- Prolonged Bcl-3 inhibition reduced p53 and EZH2 expression in MCF-7 cells-** MCF-7 **(A)** and MDA-MB-436 **(B)** cells were treated with either Bcl-3 siRNA or scRNA control for 6 days before cells were harvested for RNA. qRT-PCR was performed to compare the expression of p53, MDM2 and EZH2 and normalized to scRNA controls. Error bars represent 95% confidence intervals of 3 independent experiments. Significance was determined using the 95% confidence interval overlap rule described in [1].

### 5.5.2 Prolonged Bcl-3 inhibition induced p53 stabilization in MCF-7 cells

The activation of p53 is often mediated post-transcriptionally, with changes to gene transcription playing a minor role in this process [265]. Therefore the effect of Bcl-3 inhibition on p53 at a protein level was analysed by western blot. After 2 and 6 days of Bcl-3 siRNA or scRNA treatment, MCF-7 cells were harvested and protein extracted. Western blots were then run by William Yang in order to visualize the levels of total p53 protein expression.

After 2 days of Bcl-3 inhibition the levels of p53 appeared to decrease slightly when the protein loading was taken into consideration and represented by densitometry (Figure 5.21B). When Bcl-3 was inhibited for 6 days the expression of p53 protein appeared to increase compared to scRNA, which was again highlighted by densitometry (Figure 5.21A&C). These data suggests a differential p53 response after short and long term Bcl-3 inhibition, however further repeats are required to confirm this.

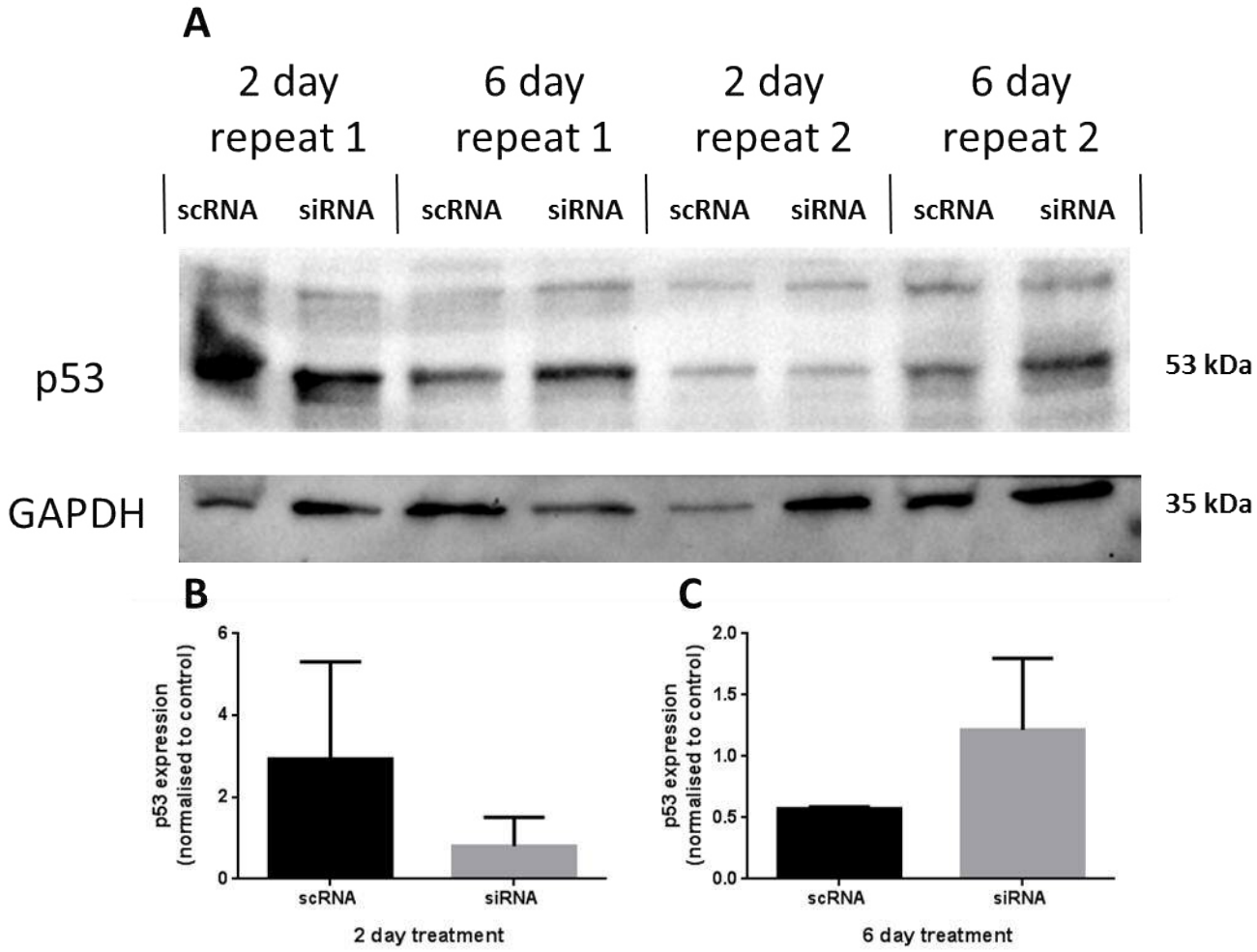


**Figure 5.21- Prolonged suppression of Bcl-3 increased p53 protein expression- (A)** Protein extracted from MCF-7 cells treated with either Bcl-3 siRNA or scRNA control for either 2 or 6 days was analysed using western blot for total p53 protein expression. Equal loading was determined by visualisation of GAPDH and was performed by William Yang. **(B&C)** Densitometry was performed in ImageJ using GAPDH as a loading control to normalize for p53 expression.

### 5.5.3 Analysing the effect of p53 suppression on Bcl-3-mediated senescence

The previous result suggested that the prolonged inhibition of Bcl-3 may stabilise p53 expression in MCF-7 cells, which we hypothesised to be regulating the senescence phenotype that accompanies this. Therefore, to test whether p53 was mediating the senescence induced by Bcl-3 inhibition in MCF-7 cells, double-knockdown experiments were performed using p53 siRNA. Bcl-3 was inhibited for 24h after which p53 was inhibited, with both suppressed using siRNA. Cells were left for a further 5 days before RNA was harvested from cells to be analysed by qRT-PCR for senescence-associated genes and SASP expression.

#### 5.5.3.1 Suppression of p53 inhibited p21 and p15 expression induced by Bcl-3 inhibition

RNA harvested from double-knockdown cells was analysed using qRT-PCR for the expression of senescence-associated p21 and p15 (Figure 5.22A). When Bcl-3 siRNA was transfected for 24h followed by scRNA transfection, Bcl-3 expression was significantly downregulated by 50%, however compared to previous knockdowns using a single transfection this was less than expected. Despite this reduced transfection efficiency, both p21 and p15 were significantly upregulated compared to double scRNA transfected controls, suggesting this was still sufficient to induce a senescence-like phenotype. When p53 was suppressed 24h after either scRNA or Bcl-3 siRNA treatment, p53 expression was reduced by more than 90%. This suppression of p53 resulted in a significant reduction in p21 and p15 expression in both scRNA controls and Bcl-3-inhibited cells, suggesting that the Bcl-3-induced increase in p21 and p15 expression was dependent on p53.

#### 5.5.3.2 Suppression of p53 did not inhibit Bcl-3 mediated SASP expression

To determine whether p53 suppression could also inhibit the expression of SASP, which was previously shown to become upregulated after prolonged Bcl-3 inhibition, RNA from double-transfected cells was analysed by qRT-PCR (Figure 5.22B). In Bcl-3-inhibited cells, IL-6, IL-8 and CXCL10 were significantly upregulated compared to double scRNA treated controls, suggesting an induction of SASP. When cells were treated with scRNA + p53 siRNA the upregulation of all 3 cytokines was reduced but was still upregulated compared to scRNA-treated controls. The expression of C/EBPβ was significantly upregulated in both p53-inhibited and double-knockdown cells. In Bcl-3 and p53-inhibited cells the expression of IL-6, IL-8 and CXCL10 was also significantly upregulated compared to controls and appeared to be more highly expressed in all three compared to Bcl-3 + scRNA cells. These results suggest that the upregulation of SASP-associated cytokines in MCF-7 cells is not p53-dependent, as they can still be upregulated in the absence of p53 expression.

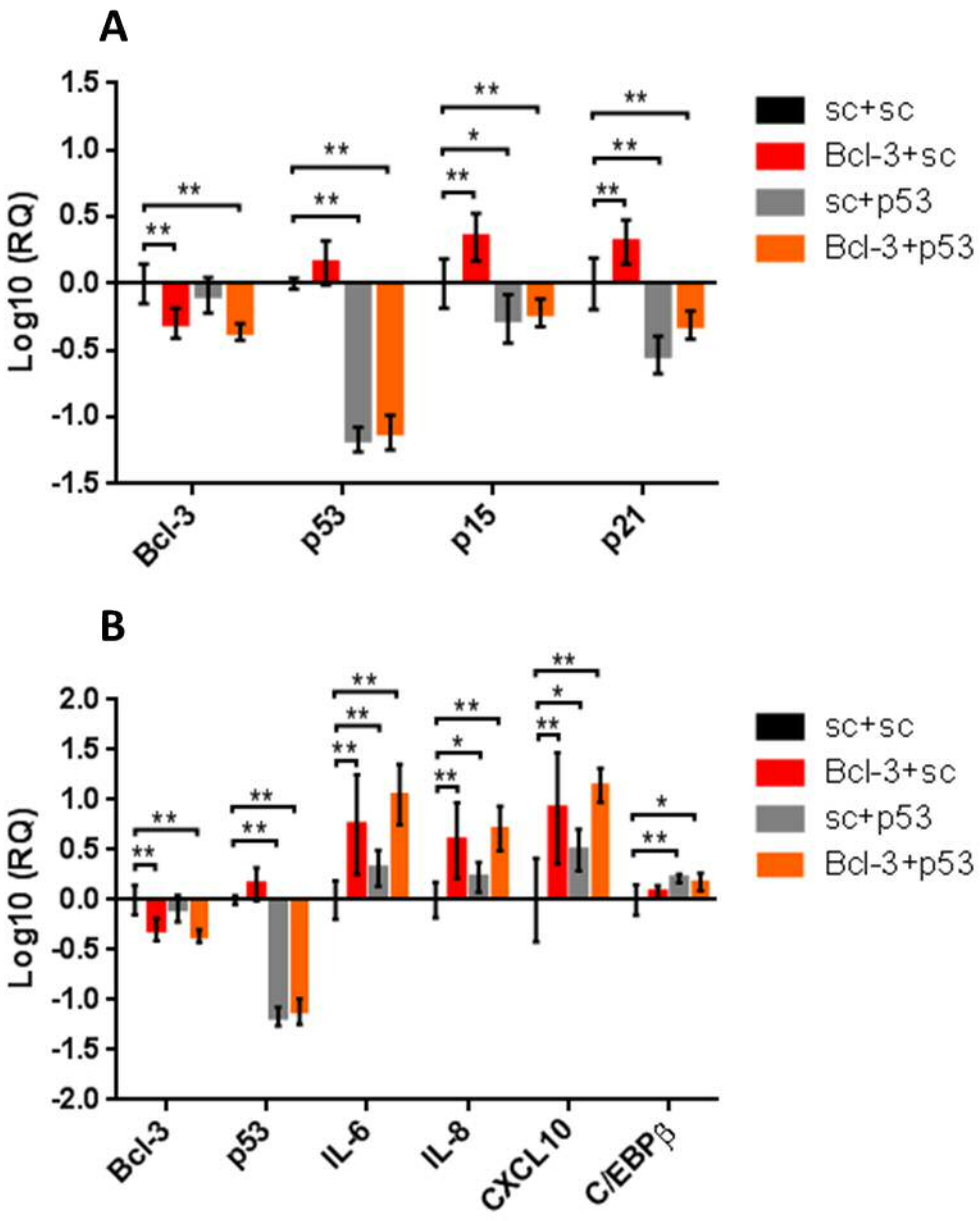


**Figure 5.22- p53 suppression inhibited Bcl-3 mediated expression of p21 and p15 but had no effect on SASP expression-** MCF-7 cells were treated with either Bcl-3 siRNA or scRNA for 24h before changing growth medium and treating with p53 siRNA or scRNA for a further 5 before cells were harvested for RNA. **(A)** qRT-PCR was performed to compare the expression of p15 and p21 after combined Bcl-3 and p53 suppression. **(B)** The same RNA was then analysed by qRT-PCR for changes in SASP cytokine expression. Error bars represent 95% confidence intervals of 3 independent experiments. Significance was determined using the 95% confidence interval overlap rule described in [1].

### 5.5.4 Analysing the effect of p15 inhibition on Bcl-3-mediated senescence

The results described previously suggested that prolonged inhibition of Bcl-3 may induce p53-dependent senescence in MCF-7 cells through upregulation of p15 and p21 expression. p21 is a well-established downstream effector of p53, however the role of p15 in this pathway is less well known. Therefore, in a similar manner to the previously described double siRNA-treated experiments, p15 was inhibited to determine whether its suppression was sufficient to rescue the Bcl-3-mediated phenotype. MCF-7 cells were treated with either scRNA or Bcl-3 siRNA for 24h before p15 siRNA was added to cells and left for a further 5 days, along with previously described scRNA + scRNA and Bcl-3 + scRNA controls.

#### 5.5.4.1 Suppression of p15 did not inhibit senescence-associated gene expression induced by prolonged Bcl-3 inhibition

qRT-PCR was performed on RNA harvested from p15-suppressed MCF-7 cells with and without Bcl-3 inhibition, to determine whether the senescence phenotype observed was due to a p15-mediated change in the expression of p21 or p53 (Figure 5.23A). Suppression of p15 alone resulted in a significant loss in p15 expression and a small but significant reduction in p53 expression, however no change in p21 expression was observed compared to double scRNA treated controls. When p15 was suppressed after 24h of Bcl-3 siRNA treatment, both Bcl-3 and p15 expression was significantly downregulated, which resulted in a significant reduction in p53 expression, however p21 was still significantly upregulated compared to scRNA controls. This suggests that the senescence phenotype observed through prolonged Bcl-3 inhibition is not dependent on p15 and can still be mediated through p21.

#### 5.5.4.2 p15 does not regulate SASP in MCF-7 cells

MCF-7 cells treated with siRNA targeting Bcl-3 and/or p15 were then tested for changes in the expression of SASP mediators IL-6, IL-8 and CXCL10 as well as C/EBPβ to determine whether p15-deficient senescence could still mediate SASP (Figure 5.23B). Suppression of p15 alone resulted in no change to the genes tested, with IL-6 appearing to be downregulated slightly, although this was not significant, indicating the SASP phenotype had not been induced. When Bcl-3 and p15 were both suppressed, SASP was restored, with IL-6, IL-8 and CXCL10 all significantly upregulated compared to scRNA controls. This further shows that Bcl-3-mediated senescence is not dependent on p15 and also that SASP formation is not driven through p15.

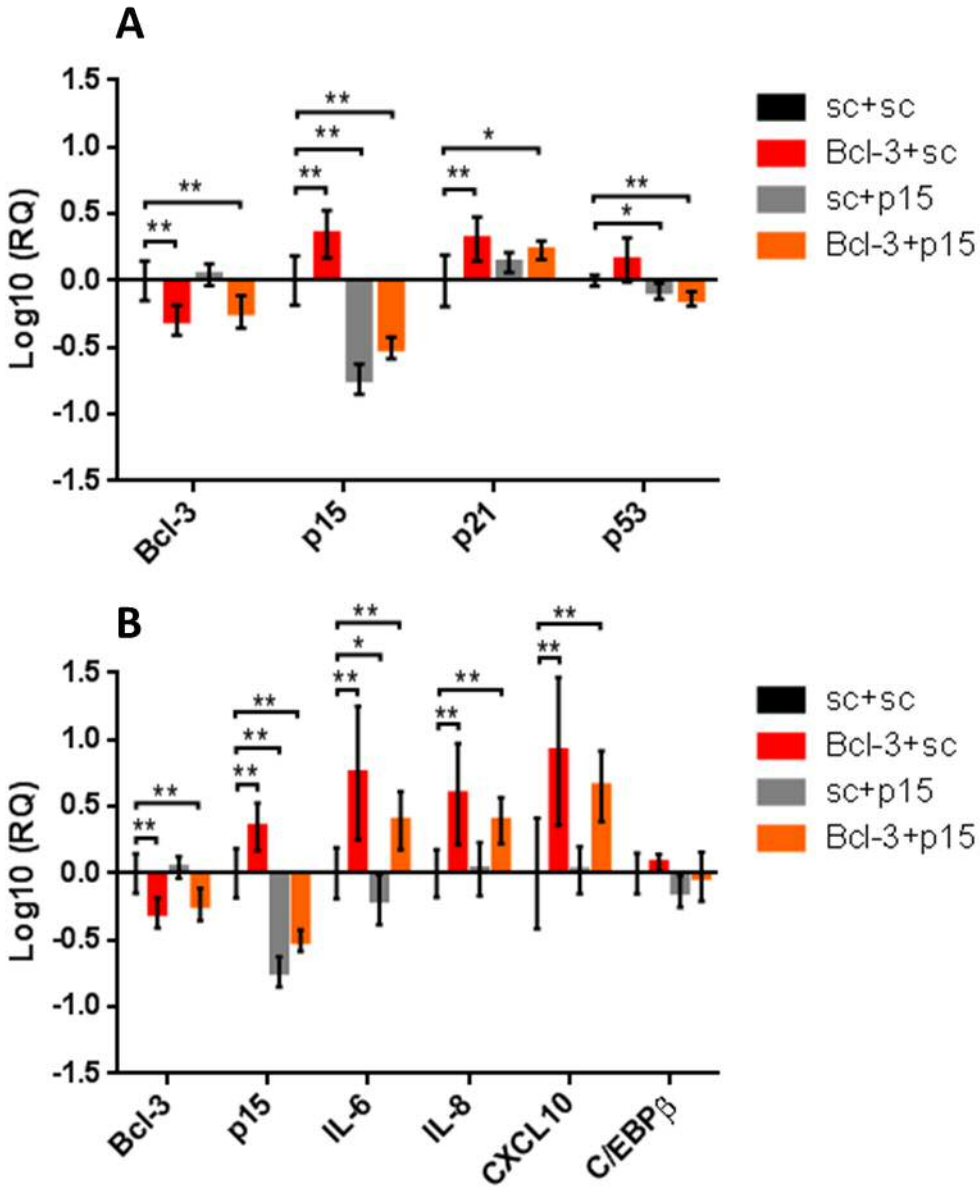


**Figure 5.23- p15 suppression does not inhibits Bcl-3 mediated expression of p21 or SASP** - MCF-7 cells were treated with either Bcl-3 siRNA or scRNA for 24h before changing growth medium and treating with p15 siRNA or scRNA for a further 5 days before cells were harvested for RNA. **(A)** qRT-PCR was performed to compare the expression of p21 and p53 after combined Bcl-3 and p15 suppression. **(B)** The same RNA was then analysed by qRT-PCR for changes in SASP cytokine expression. Error bars represent 95% confidence intervals of 3 independent experiments. Significance was determined using the 95% confidence interval overlap rule described in [1].

### 5.5.5 Analysing the effects of SASP inhibition on Bcl-3-mediated senescence

Previous results have shown how senescence induced through Bcl-3 suppression is driven through a p53-dependent pathway, but that this pathway does not regulate the expression of SASP, a hallmark of senescence that has been associated with both its induction and maintenance. Therefore, to determine the role of SASP induced by prolonged Bcl-3 inhibition, two known regulators of SASP were suppressed in order to see whether induction of senescence could be reversed. C/EBPβ, a known regulator of IL-6 and IL-8 during senescence, was inhibited in a similar manner to the previously described experiments using siRNA. The JAK/STAT signalling pathway was also inhibited using the JAK inhibitor Ruxolitinib, which has also been shown to alleviate senescence through SASP [266].

#### 5.5.5.1 C/EBPβ suppression inhibited the upregulation of SASP mediators during Bcl-3-mediated senescence

To determine whether suppression of C/EBPβ was sufficient to inhibit IL-6, IL-8 and CXCL10, qRT-PCR was performed on RNA harvested from MCF-7 cells treated with C/EBPβ siRNA with and without Bcl-3 suppression. Inhibition of C/EBPβ alone resulted in a significant reduction in IL-6, IL-8 and CXCL10 expression compared to scRNA controls (Figure 5.24A). Suppression of C/EBPβ after 24h of Bcl-3 siRNA treatment resulted in an increase in SASP expression compared to C/EBPβ inhibition alone, however this was not enough to fully rescue the full SASP phenotype acquired through prolonged Bcl-3 inhibition, suggesting that this had been repressed. These results suggest that despite no change in C/EBPβ expression when Bcl-3 is suppressed, it can play an important role in mediating the upregulation of these factors.

#### 5.5.5.2 Suppression of C/EBPβ inhibited the upregulation of p21 and p15 potentially through regulating p53 expression

The previously described downregulation of SASP cytokines through C/EBPβ suppression suggested that C/EBPβ inhibition could alleviate the SASP phenotype conferred through Bcl-3 inhibition. To determine whether this also resulted in an inhibition of the SASP phenotype RNA harvested from these cells was tested for changes in p15, p21 and p53 expression as these are believed to be the primary mediators of this phenotype (Figure 5.24B). Suppression of C/EBPβ alone resulted in a small insignificant reduction in p15 and p21 but a significant reduction in p53 expression compared to scRNA controls. When Bcl-3 was suppressed as well as C/EBPβ, a similar trend was observed with no change in p15 or p21 expression but a significant reduction in p53 expression. This suggests that senescence observed through Bcl-3 suppression is reliant on SASP to at least partially mediate this response; however this requires further investigation given C/EBPβ may play a role in the regulation of p53 independent of Bcl-3.

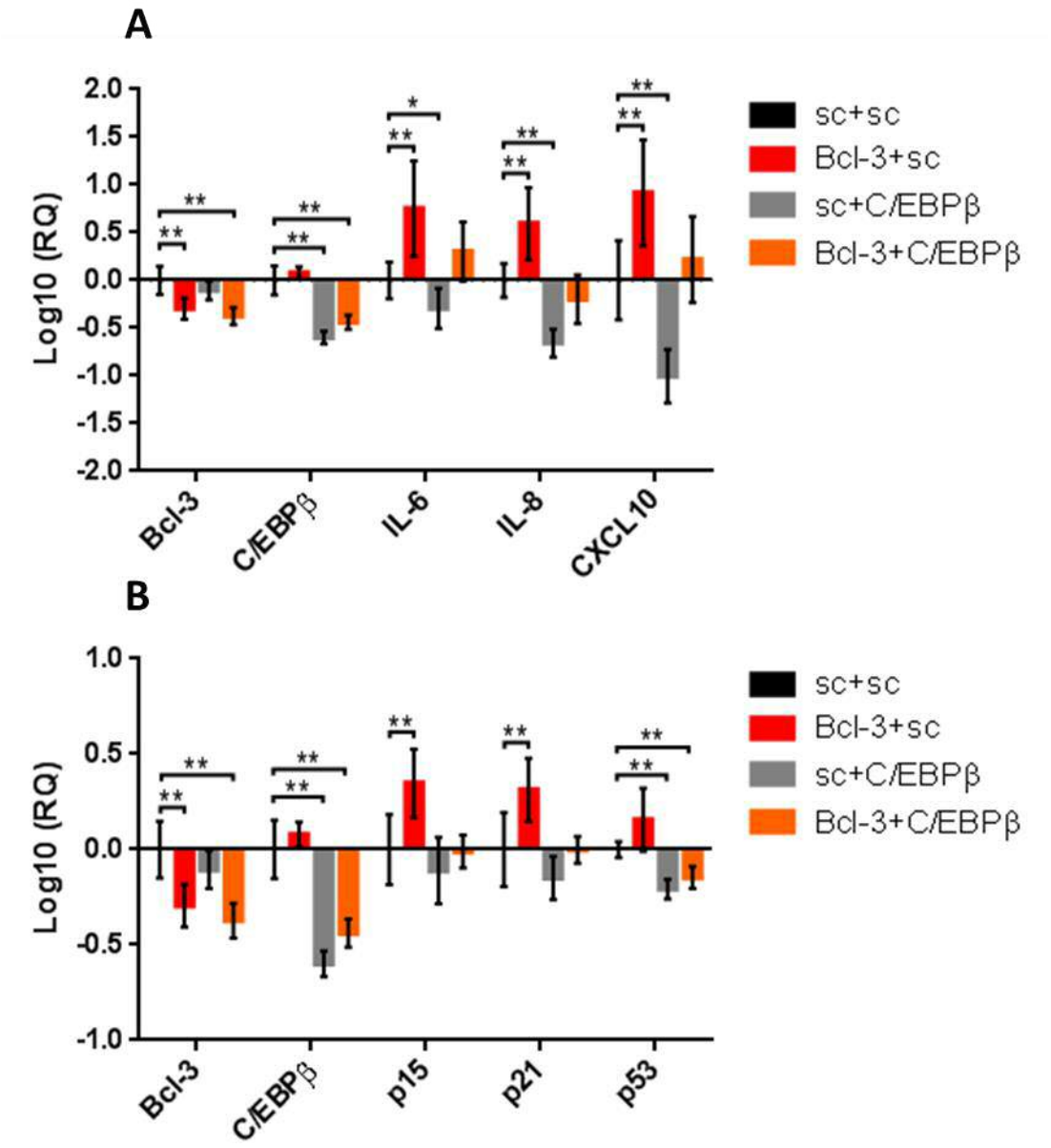


**Figure 5.24- Suppression of C/EBPβ inhibited SASP as well as p15, p21 and p53 expression** - MCF-7 cells were treated with either Bcl-3 siRNA or scRNA for 24h before changing growth medium and treating with C/EBPβ siRNA or scRNA for a further 5 days before cells were harvested for RNA. **(A)** qRT-PCR was performed to compare the expression of SASP mediators IL-6, IL-8 and CXCL10 after combined Bcl-3 and C/EBPβ suppression. **(B)** The same RNA was then analysed by qRT-PCR for changes in p15, p21 and p53 expression. Error bars represent 95% confidence intervals of 3 independent experiments. Significance was determined using the 95% confidence interval overlap rule described in [1].

#### 5.5.5.3 Analysing the effects of JAK inhibition on Bcl-3 suppression-mediated senescence

The previous results suggested that inhibition of SASP through suppression of C/EBPβ could inhibit the senescence phenotype observed through prolonged Bcl-3 suppression. To further confirm the role of SASP in Bcl-3-mediated senescence the JAK inhibitor Ruxolitinib was used to inhibit the JAK/STAT pathway which has been previously shown to alleviate SASP [267].

#### 5.5.5.4 JAK inhibition reduced but did not completely abrogate Bcl-3 mediated SASP

To determine the effects of JAK inhibition on the SASP-mediating cytokines IL-6, IL-8 and CXCL10, RNA was harvested from the cells treated with or without Ruxolitinib and analysed by qRT-PCR for changes in gene expression (Figure 5.25A). Unlike C/EBPβ suppression, the addition of Ruxolitinib alone did not downregulate the expression of C/EBPβ, IL-6 or IL-8. The expression of CXCL10 however was slightly downregulated. The addition of JAK inhibitor to Bcl-3-suppressed cells did significantly reduce the expression of SASP compared to Bcl-3-suppressed cells without JAK inhibition. Despite this reduction, the SASP phenotype was not rescued as IL-6, IL-8 and CXCL0 were all still significantly upregulated compared to scRNA treated cells, suggesting that JAK inhibition could reduce but not alleviate SASP, however the level of JAK inhibition was not quantified and may be optimized further to improve this response.

#### 5.5.5.5 JAK inhibition did not suppress the increase in p15 or p21 expression associated with prolonged Bcl-3 inhibition

Although SASP was not completely inhibited by Ruxolitinib treatment in Bcl-3-suppressed cells, Ruxolitinib did significantly reduce the expression of IL-6, IL-8 and CXCL10. Therefore, qRT-PCR was performed to determine whether this resulted in any change in the expression of the senescence mediators' p15 and p21 (Figure 5.25B). The addition of JAK inhibition to Bcl-3 siRNA-treated cells had no effect on the expression of p21; however it did significantly reduce the expression of p15.

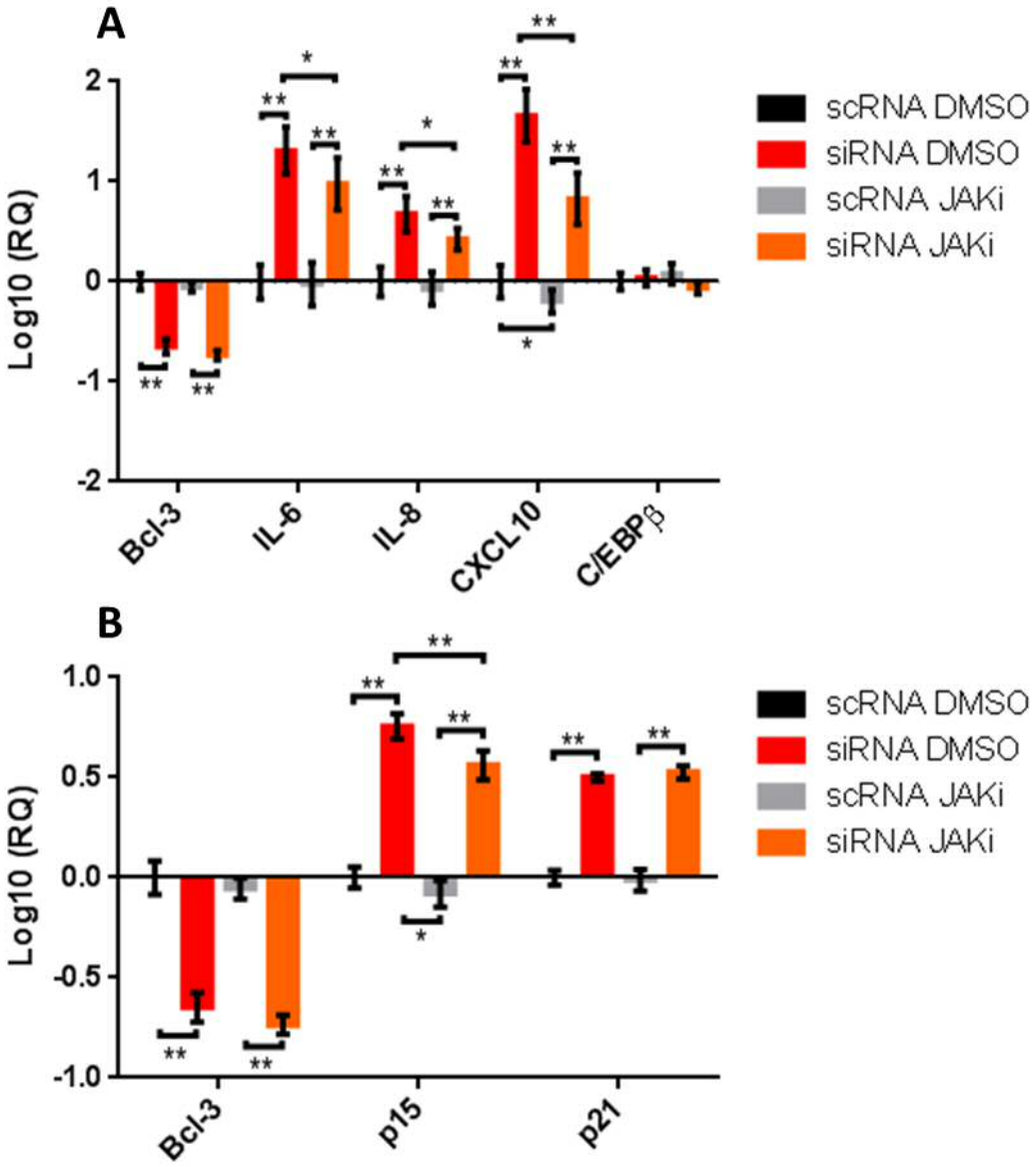


**Figure 5.25- JAK inhibition reduced SASP but did not inhibit p21 expression -** MCF-7 cells were treated with Bcl-3 siRNA or scRNA plus the addition of JAK inhibitor Ruxolitinib at 1 µM or equivalent DMSO concentration for 6 days before cells were harvested for RNA. **(A)** qRT-PCR was performed to compare the expression of SASP mediators IL-6, IL-8, CXCL10 and C/EBPβ after combined Bcl-3 and JAK suppression. **(B)** The same RNA was then analysed by qRT-PCR for changes in p15 and p21 expression. Error bars represent 95% confidence intervals of 3 independent experiments. Significance was determined using the 95% confidence interval overlap rule described in [1].

### 5.5.6 Analysing the role of p50 and p52 in senescence

The primary function of Bcl-3 is to regulate transcription through interactions with both p50 and p52 homodimers and can therefore regulate both canonical and non-canonical NF-kB signalling pathways. Previous data showing small molecule inhibition of Bcl-3 specifically designed to disrupt Bcl-3 binding to both p50 and p52 was shown to induce a similar senescence phenotype to that seen with Bcl-3 siRNA inhibition. This suggested that Bcl-3-mediated senescence may be due to a loss of either p50 or p52 homodimers. Therefore, to determine the role of both p50 and p52 in Bcl-3-mediated senescence both genes were individually suppressed using siRNA to determine whether either or both could induce a similar senescence phenotype.

#### 5.5.6.1 Suppression of p52 induced a senescence phenotype but suppression of p50 did not

To determine the effects of p50 and p52 suppression on the regulation of senescence mediators' p15, p21 and EZH2 expression RNA harvested from MCF-7 cells treated for 6 days with p50 or p52 siRNA was analysed. Inhibition of p50 resulted in a significant reduction in Bcl-3 expression as well as both p15 and p21 expression, however had no effect on the expression of EZH2 (Figure 5.26A). On the other hand suppression of p52 resulted in a significant increase in both p15 and p21 as well as reduction in EZH2, with no change observed in the expression of Bcl-3. This data suggests that the senescence phenotype described here is regulated through loss of Bcl-3:p52 mediated signalling and not Bcl-3:p50.

#### 5.5.6.2 Suppression of p50 induced a SASP phenotype but suppression of p52 did not

The previously described RNA was then analysed for changes in SASP expression to determine whether this phenotype was specifically regulated through either p50 or p52. Inhibition of p50 resulted in a significant upregulation of the SASP phenotype, however p52 suppression resulted in no change in the expression of any SASP cytokines (Figure 5.26B). This suggests that loss of p50 mediates SASP while p52 mediates senescence, showing differential roles for Bcl-3 in regulating both canonical and non-canonical NF-kB signalling.

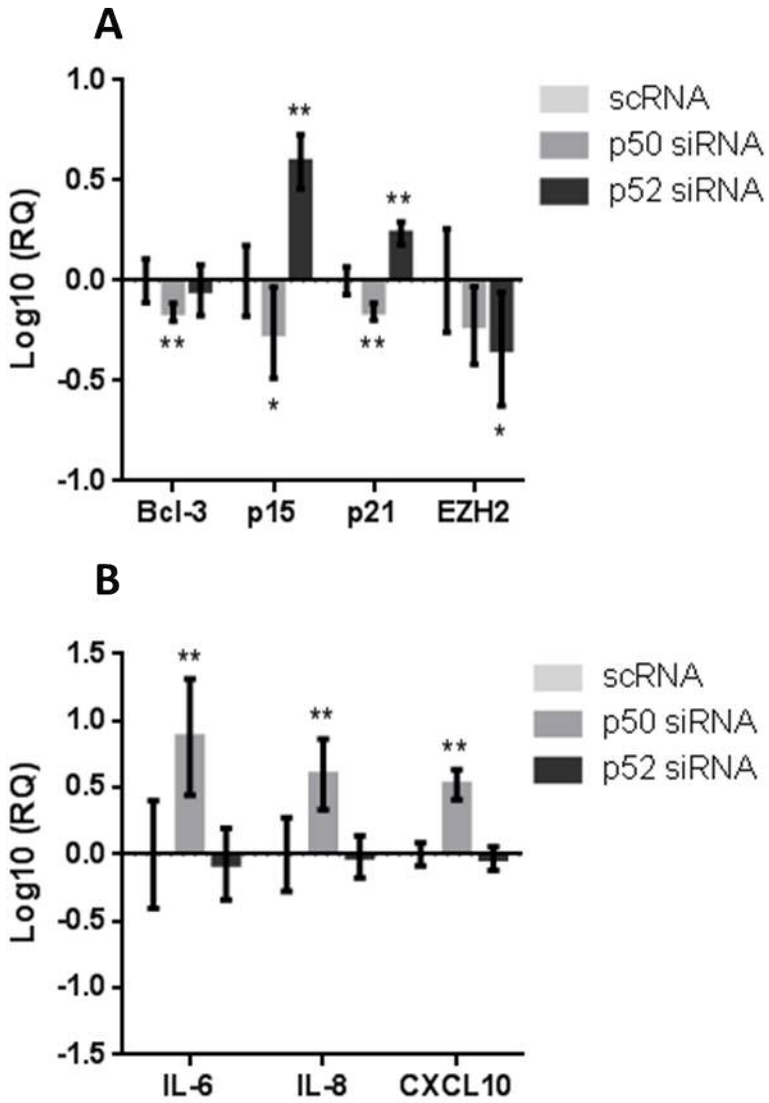


**Figure 5.26- p52 and p50 independently regulated senescence markers and SASP expression respectively in MCF-7 cells-** MCF-7 cells were treated with either p52 or p50 siRNA or scRNA for 6 days before cells were harvested for RNA. qRT-PCR was performed to compare the expression of **(A)** senescence-associated gene expression and **(B)** SASP cytokine expression which were normalized to scRNA controls. Error bars represent 95% confidence intervals of 3 independent experiments. Significance was determined using the 95% confidence interval overlap rule described in [1].

### 5.5.7 Bcl-3 inhibition induced the expression of apoptosis regulators Bcl-XL and PUMA in MDA-MB-436 cells

The previously characterised senescence phenotype observed in MCF-7 cells after prolonged Bcl-3 inhibition was not observed in the p53 mutant MDA-MB-436 cell line, however an induction of apoptosis was observed. Therefore, to try and identify how this apoptosis phenotype was being regulated the expression of 3 key apoptosis regulatory genes Bcl-2, Bcl-XL and PUMA was analysed after 6 days of Bcl-3 siRNA inhibition.

Suppression of Bcl-3 in MDA-MB-436 cells resulted in a significant increase in Bcl-XL and PUMA expression however no change was observed in the expression of Bcl-2 (Figure 5.27A). Bcl-3-inhibited MCF-7 cells were also tested, with no change observed in Bcl-XL or PUMA expression; however a significant reduction in Bcl-2 expression was seen (Figure 5.27B).

These results suggest a potential for Bcl-3 to regulate apoptosis in MDA-MB-436 cells through increasing PUMA expression which is a transcriptionally controlled BH3 only protein known to induce apoptosis. The reduction in the expression of apoptosis inhibitor Bcl-2 in MCF-7 cells suggest a potential role for Bcl-2 in regulating senescence in these cells, however requires further exploration.

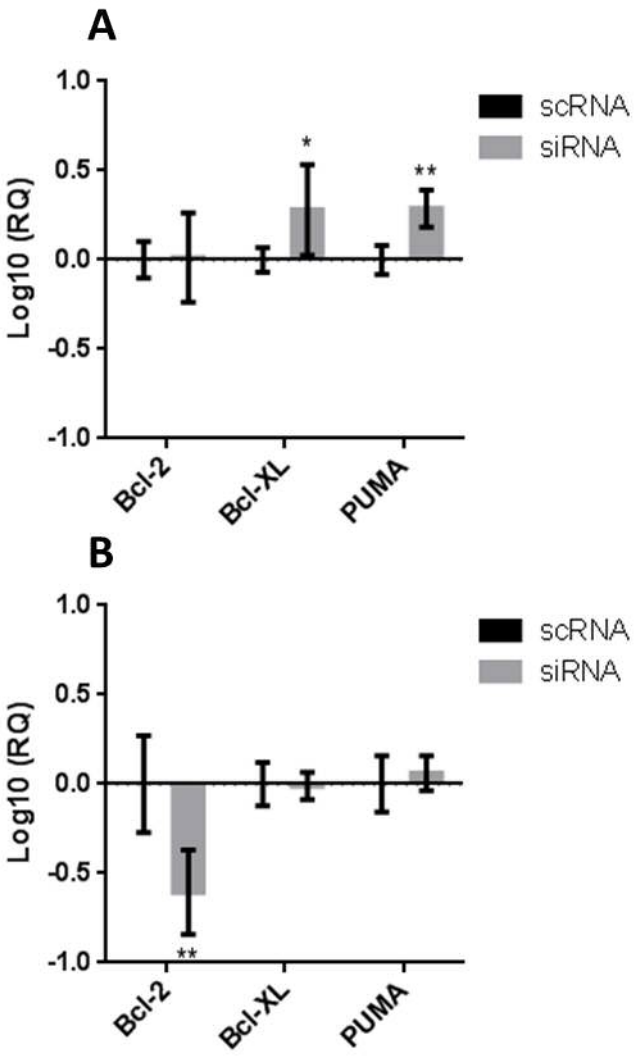


**Figure 5.27- Bcl-3 inhibition may differentially regulate apoptosis mediators Bcl-2, Bcl-XL and PUMA depending on cell type – (A)** MDA-MB-436 and **(B)** MCF-7 cells were treated with either Bcl-3 siRNA or scRNA for 6 days before cells were harvested for RNA. qRT-PCR was performed to compare the expression of apoptosis mediators Bcl-2, Bcl-XL and PUMA. Error bars represent 95% confidence intervals of 3 independent experiments. Significance was determined using the 95% confidence interval overlap rule described in [1].

## 5.6 Discussion

In the previous chapter a clear change in morphology and viability was observed in MCF-7 cells after prolonged Bcl-3 inhibition suggesting a disruption to cell homeostasis and an induction of a senescent-like state. Despite a number of studies investigating the role of Bcl-3 in regulating apoptosis during breast cancer, little is known about its role in mediating senescence. Therefore, the aims of this chapter were to confirm this senescence phenotype and try to understand the underlying causes of it.

Initial tests focussed on confirming this phenotype in MCF-7 cells by analysing some of the hallmarks of senescence which were all observed after prolonged Bcl-3 suppression. This included an increase in SA-β-gal expression (Figure 5.1) and an increase in the G1 cell population (Figure 5.6); however this change in cell cycle population was far less than expected and requires more detailed analysis to determine changes in the G0 arrested cell population that could not be observed in our assays. This could be performed by flow cytometry using Hoechst and Pyronin Y staining to distinguish G0 and G1 cell populations. Despite a lack of cell cycle arrest the significant upregulation of p21 and p15 as well as the clear presentation of SASP meant we could confidently state that prolonged Bcl-3 inhibition induced senescence in these cells (Figure 5.3 & 5.5).

A number of senescence hallmarks were also observed after daily compound inhibition which suggested this phenotype could be replicated through Bcl-3 inhibitor treatments. This also suggested an on target effect of these compounds by phenocopying the siRNA inhibition, although only to a limited extent, and suggested Bcl-3 mediated senescence could be due to a disruption of p50 or p52 dimers (Figure 5.14 & 5.15). Indeed this was confirmed through individual siRNA inhibition of p50 and p52 which showed differential effects by inducing SASP and senescence marker upregulation respectively (Figure 5.26). As CB-97 was capable of upregulating both these phenotypes it suggested an on target effect capable of blocking both p50 and p52 binding to Bcl-3. Optimization of this newly synthesised compound, which showed much greater efficacy at a lower

concentration than CB-1, may further improve these effects; however this is reliant on making it more soluble at higher doses.

After 2 days of Bcl-3 inhibition with siRNA, despite no clear induction of a senescence-like phenotype some interesting changes in gene expression were observed which may provide an insight into how senescence is being initiated. Firstly, despite a lack of morphological change or SA-β-gal expression, a significant upregulation of p21 was observed with no change in p15 expression (Figure 5.3). This suggests that the induction of senescence is mediated through p21, with p15 upregulation occurring at a later stage possibly to help maintain or to amplify the response. This was highlighted by the fact that inhibition of p21 through the suppression of p53 rescued the normal MCF-7 phenotype when Bcl-3 was also suppressed, with inhibition of p15 alone not appearing to rescue this, however SA-β-gal staining as well as the direct inhibition of p21 is required to confirm this.

Another interesting observation from 2 day Bcl-3 siRNA-treated MCF-7 cells was the upregulation of C/EBPβ and IL-6, which also appeared to be an early response to Bcl-3 inhibition (Figure 5.5). After 6 days of Bcl-3 inhibition the expression of C/EBPβ returned to a basal level suggesting that it may be upregulated early in the induction of senescence but was not required for the maintenance of the SASP-like phenotype which was amplified by day 6. However, a role for C/EBPβ in the maintenance of senescence should not be ruled out, as the regulation of C/EBPβ often occurs post-transcriptionally, therefore the importance of this transcription factor may be underestimated by our gene expression data [268]. This is supported by our data whereby inhibition of C/EBPβ and Bcl-3 resulted in an inhibition of SASP upregulation and senescence marker expression (Figure 5.24). Although further analysis such as SA-β-gal activity is required to confirm the rescue of senescence this data does suggest an important role for SASP during senescence induction and maintenance. Interestingly, C/EBPβ has been shown to regulate IL-6 and IL-8 synergistically with both p50 and p65 homodimers, suggesting a potential link between the regulation of Bcl-3-mediated

p50 and C/EBPβ which is supported by our findings here [269]. Together our data suggested that C/EBPβ may play an early role in the upregulation of SASP which may work synergistically with p50 to help regulate cytokine expression to help maintain senescence.

Further examination of SASPs role in Bcl-3-mediated senescence was performed by using the JAK inhibitor Ruxolitinib as another method of cytokine inhibition. Although the level of JAK inhibition was not quantified, treatment with Ruxolitinib alone at 1 μM in Bcl-3-inhibited cells was able to significantly reduce SASP expression, although this did not completely abrogate SASP as was seen with C/EBPβ suppression (Figure 5.25). Despite this, no change was observed in p21 expression suggesting that SASP did not directly mediate this and that C/EBPβ may have had a direct effect on p21 expression which was independent of its role in SASP. This is supported by our data which suggests senescence can be initiated without the induction of SASP through p52 suppression alone. Taken together with our data using C/EBPβ and p50/p52 inhibition, it appears that the upregulation of SASP is not required to initiate senescence; however it may play an important role in maintaining this phenotype.

Although the importance of SASP for initiating senescence is still fairly ambiguous from the data collected it is clear that senescence through prolonged Bcl-3 inhibition is reliant on cells maintaining a wildtype p53 status. This was first indicated by the lack of senescence induction observed in the p53 mutant MDA-MB-436 cell line. Despite a diverse array of signalling molecules thought to participate in senescence initiation, the activation of either p53-p21 or p16-pRB pathways are thought to be key to this process. We have confirmed that the senescence phenotype described here is relayed through p53-p21 signalling and is not dependent on p16 which is homozygously deleted in MCF-7 cells, an observation that was confirmed by our qRT-PCR results (Figure 5.3) [270]. The importance of p53 in Bcl-3-mediated senescence was confirmed by protein analysis showing p53 to be activated after 6 days of Bcl-3 inhibition despite no change in gene expression (Figure 5.21). Interestingly, the upregulation of senescence markers p15 and p21 was

rescued through double inhibition of Bcl-3 and p53 confirming that this was a p53-dependent event (Figure 5.22). Despite this the upregulation of SASP was not rescued suggesting that this process may be independent of p53, again supporting the idea that this phenotype is not required for the initiation of senescence.

Our data here suggested that Bcl-3 inhibition may stabilize p53 at the protein level, an observation previously identified in MCF-7 cells after DNA damage [208]. Interestingly, in this model p53 was mediated through Bcl-3-driven regulation of MDM2, an observation that was not replicated in our model [208]. It should be noted however that MDM2 protein expression was suppressed after 24h of Bcl-3 siRNA inhibition, whereas we have only observed the gene expression of MDM2 after 6 days of Bcl-3 suppression. Therefore, further experiments determining MDM2 expression at an earlier time point, as well as at a protein level, should be performed before concluding that it is not changing in our system. However, given that p53 protein expression appeared to be downregulated after 2 days of Bcl-3 inhibition it does further suggest that MDM2 is not mediating this senescence. One possibility is that Bcl-3 may be regulating p53 independently of MDM2, through SMAD3, which was recently shown to be stabilized by Bcl-3, and is known to directly bind to p53 [188, 271].

Interestingly, the stabilization of p53 also correlated with a downregulation of EZH2, a histone H3 K27 methylase that forms a functional component of the PRC2 complex involved in epigenetic gene regulation and is strongly correlated with invasive breast cancer and metastasis (Figure 5.20) [272]. Our results here correlate with previous data in primary human fibroblasts showing EZH2 to be repressed by p53 in a p21-dependent manner, a process that can be reversed through inhibition of Bcl-3 and p52 to induce a senescence-like phenotype [261, 273]. Although to our knowledge a similar pathway has not been observed in breast cancer until now, EZH2 knockdown in human melanoma cells results in a p21-driven senescence [274]. Furthermore, recent work has shown p52 to be a key regulator of EZH2 expression, with its suppression resulting in a decrease in EZH2 and an induction of senescence [260]. Here we have confirmed this finding with

p52 suppression resulting in a significant reduction in EZH2, suggesting that senescence driven through Bcl-3 suppression is due to alterations to the non-canonical NF-kB pathway via p52, which initiates senescence through downregulating EZH2 (Figure 5.26). Our data also suggests that loss of Bcl-3:p50 interactions may also contribute to the maintenance of senescence through changes to the canonical NF-kB pathway which results in the appearance of SASP (Figure 5.26).

Interestingly, a significant reduction in Bcl-2 expression was also observed in MCF-7 cells following Bcl-3 inhibition (Figure 5.27). Bcl-2 can be regulated through Bcl-3 transactivated p50 and p52 homodimers, however, as Bcl-2 reduction was not observed in MDA-MB-436 cells it suggests that this was not a direct effect of Bcl-3 inhibition [186]. Senescence in human fibroblasts is associated with increased Bcl-2 expression, however in endothelial cells expression of Bcl-2 is downregulated during senescence suggesting that its role may be cell and context specific [275, 276]. Further experiments are required to determine the role of Bcl-2 downregulation in a Bcl-3 inhibition context, however it does not appear to be related to apoptosis within MCF-7 cells.

On the other hand in the triple-negative MDA-MB-436 line, which has a truncating mutation of p53, a significant reduction in viability of MDA-MB-436 cells was observed after prolonged Bcl-3 inhibition, which was attributed to an increase in apoptosis and not senescence (Figure 5.19). This correlated with an increase in PUMA expression, a potent inducer of apoptosis that is capable of acting independently of p53, however the increase in antiapoptotic Bcl-XL does contradict this finding (Figure 5.27) [277]. Since apoptosis can be regulated through various pathways it is clear that further work is required to unravel the mechanisms in which Bcl-3 may be initiating apoptosis, however this could be a an interesting therapeutic option for p53 mutant breast tumours. Together these results implicate Bcl-3 in maintaining tumour cell homeostasis, with prolonged suppression of Bcl-3 resulting in either cell senescence or apoptosis depending on the p53 status of the cells, as highlighted in Figure 5.28.

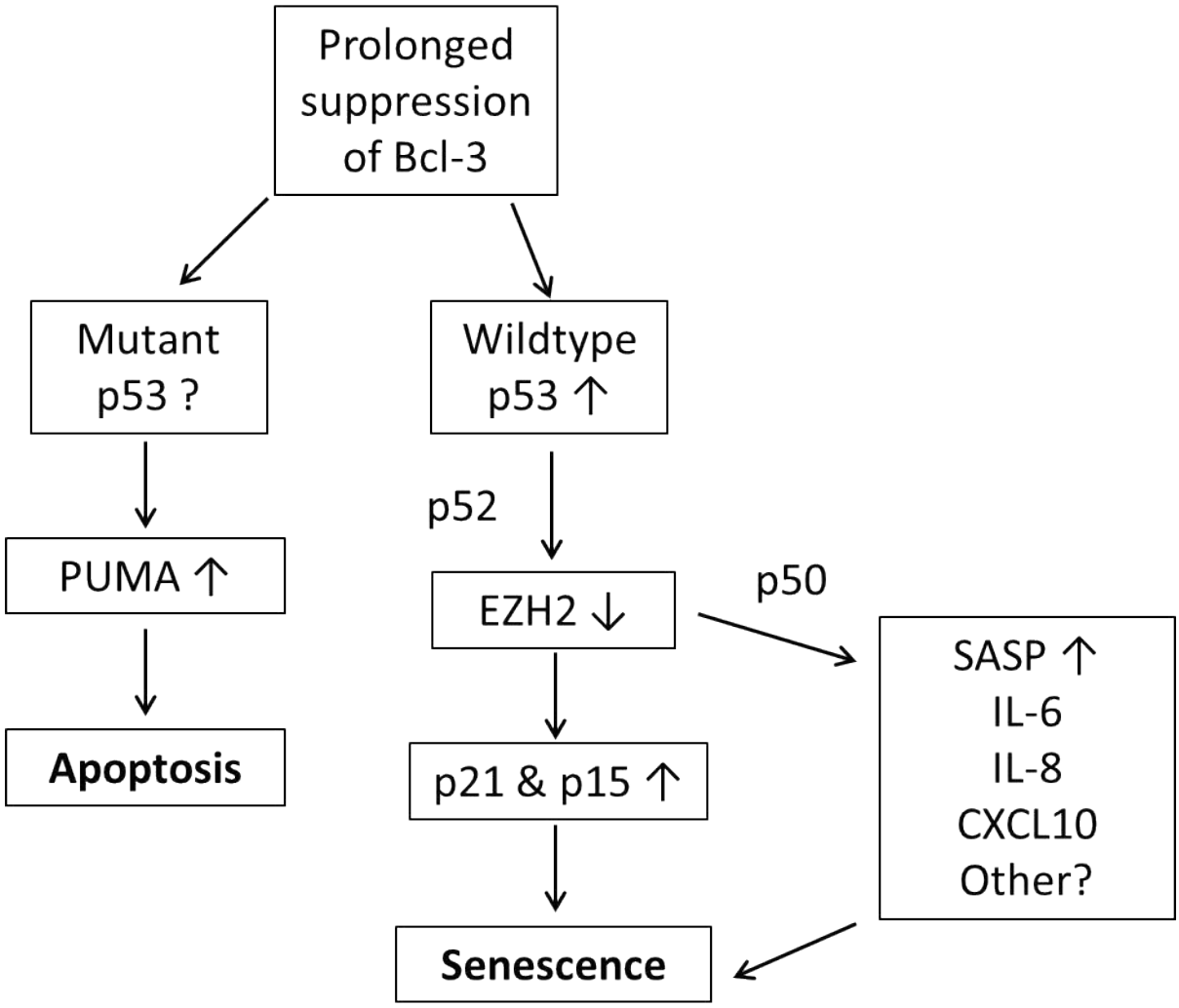


**Figure 5.28- Model of Bcl-3 mediated senescence and apoptosis-** Current model of the effects from prolonged suppression of Bcl-3 in breast cancer cell lines. In p53 wildtype cells loss of Bcl-3 activity induces a p53-driven senescence phenotype which is potentiated through the upregulation of p21, p15 and SASP. In p53 mutant cells prolonged loss of Bcl-3 activity induces and apoptotic response through the upregulation of PUMA.

To confirm the apoptotic role of mutant-p53 in breast cancer cell lines the HER2$^{+ve}$ HCC1954 cell line which carries mutated-p53 was also analysed after prolonged Bcl-3 inhibition, however neither apoptosis nor senescence was observed after Bcl-3 inhibition, with no loss to cell viability (Appendix A). Despite this, some changes in gene expression were observed such as an increase in p16 and IL-6, as well as a decrease in Bcl-XL, suggesting that Bcl-3 inhibition was altering the cell phenotype; however this effect could not initiate apoptosis (Appendix A). One potential reason for this lack of apoptotic response could be the significantly higher endogenous Bcl-3 levels in these cells compared to both MDA-MB-436 and MCF-7 cells (William Yang, unpublished). Coupled with the fact that Bcl-3 siRNA treatment only resulted in a 50% reduction in Bcl-3 expression, it is likely that the remaining Bcl-3 was sufficient to maintain homeostasis in these cells. An improved knockdown efficiency may produce a more substantial response in these cells, however further characterisation of mutant and wild-type p53 breast cancer cell lines will be required to more robustly test the hypothesis that Bcl3 mediates its effects in a p53-dependent manner. Interestingly more recent results do further suggest the importance of p53 with the p53 wild-type ZR75-1 cells line showing a similar senescence response to MCF-7 cells and the p53 mutant T47D and BT474 cell lines responding similarly to MDA-MB-436 cells following Bcl-3 inhibition. These promising results to further suggest the importance of p53 status in determining the induction of senescence or apoptosis following prolonged Bcl-3 inhibition.

The differential responses to Bcl-3 inhibition could potentially make it an interesting therapeutic option, with the use of senescence initiation subject to conflicting reports regarding its benefits and issues in a clinical setting. On one hand the induction of senescence has been suggested as a method for limiting tumour growth, therefore prolonging survival without the need for more toxic drugs, and has also been associated with initiating an immune cell mediated tumour clearance [257, 278]. On the other hand SASP cytokines such as IL-6 have been associated with tumour progression; whereas p53 induced senescence has also been associated with a poor response to chemotherapy and therefore may hinder secondary therapeutic options [263, 279]. Despite this the

apoptotic response of p53 mutant MDA-MB-436 cells may indicate that p53 could be used as a biomarker for deciding the suitability of Bcl-3 inhibition as a treatment from patient to patient. Furthermore, in higher risk patients expressing wild-type p53, Bcl-3 inhibition could be utilized as a last resort to slow tumour progression without the detrimental side effects of conventional chemotherapy.

In conclusion these results show the importance of Bcl-3 in mediating the survival of breast cancer cells, with its loss significantly effecting cell viability through either senescence or apoptosis. The fate of the cells appears to be dependent on their p53 status, with prolonged Bcl-3 suppression resulting in a stabilization of wildtype p53 and an EZH2/p21-driven senescence. Interestingly, small-molecule Bcl-3 inhibitors can at least in part mimic the loss of Bcl-3 in MCF-7 cells by blocking Bcl-3 binding to p50:p50 and p52:p52 homodimers which appear to independently regulate SASP and senescence initiation respectively. In the absence of wildtype p53, Bcl-3 suppression can initiate cell death through apoptosis, potentially through the pro-apoptotic gene PUMA, however this needs to be explored further. This could potentially be used as a therapeutic candidate for inducing cell cytostasis or death in p53 wildtype and mutant tumours respectively; however this has not been explored here and requires extensive pre-clinical evaluation. Finally, the effect of Bcl-3 on normal mammary cells has not been evaluated here and must be taken into consideration in future studies, as should the potential for prolonged Bcl-3 inhibition to be an effective therapeutic for other cancer types.

# Chapter 6:
# General discussion

# 6. General discussion

Breast cancer is one of the most common forms of cancer in women, and despite recent improvements in detection and treatments to primary tumours it remains incurable at its final metastatic stage. Tumour metastasis is a complex process that involves EMT, migration, intravasation, extravasation and colonization; however despite attempts to interrupt metastasis at these various stages, effective therapeutics remain elusive.

One anti-metastasis target that has been subject to much attention is the NF-kB signalling pathway which has long been associated with a role in tumour initiation and progression. Focus has largely been geared towards the discovery of novel ways to inhibit NF-kB pathways, however so far this search has remained unsuccessful, largely due to lack of specificity, which has now redirected focus towards finding ways to modulate rather than completely abrogate NF-kB signalling. Recent findings have highlighted the atypical NF-kB inhibitor Bcl-3 as one such target which has been found overexpressed in a number of cancer types, including breast cancer, where it has been associated with poor prognosis and reduced survival rates [188].

Bcl-3 is a known regulator of apoptosis and proliferation in cancer and has been implicated in the regulation of key oncogenes and tumour suppressors in breast cancer such as cyclinD1 and p53, making it an interesting therapeutic target [208, 213]. More recently Bcl-3 has been shown to play a role in the regulation of metastasis, with independent studies showing that suppression of Bcl-3 drastically reduces metastatic tumour burden *in vivo,* without effecting primary tumour growth [188, 214, 280]. This effect has largely been attributed to a general inhibition of cell motility, with recent work suggesting a potential role for Bcl-3 in mediating TGF-β signalling, however other than this little is known about the mechanisms behind Bcl-3-mediated metastasis [188].

Recent work within the lab has shown the diminished metastatic phenotype observed through Bcl-3 suppression can be mimicked by small-molecule inhibitors of Bcl-3, which target a novel binding pocket within the Bcl-3 protein to disrupt the binding of p50 and p52 dimers to Bcl-3

(Soukupova, unpublished). Early analogues of these molecules have shown promising results *in vivo,* however in order to progress these towards a more clinical setting it is important to fully understand the mechanisms behind how they are acting to inhibit metastasis.

Therefore, the aims of this project were to: (1) evaluate the migratory phenotype that Bcl-3 is regulating to promote metastasis; (2) establish a cell based model of EMT so that the role of Bcl-3 during both EMT and MET could be evaluated; and (3) characterise a new class of novel Bcl-3 inhibitor analogues and compare how their function may differ from siRNA inhibition of Bcl-3 in the regulation of metastasis.

We began by evaluating the role of Bcl-3 in regulating breast cancer migration in chapter 3, which has so far been solely attributed to the role of Bcl-3 in promoting metastasis. Previous work has shown how suppression of Bcl-3 is capable of inhibiting migration using Boyden chamber assays, in which cells utilise an amoeboid-like migratory phenotype to squeeze and propel through a porous membrane [188, 215]. Here we have confirmed the ability of Bcl-3 to regulate this form of motility as well as two other migratory phenotypes, single cell mesenchymal-like and collective migration, using various human breast cancer cell lines. Furthermore, we have shown that at least in MDA-MB-436 cells, this reduced migratory phenotype is independent of cell attachment to the ECM and is associated with a reduction in the GTPase activity of Rac1 and Cdc42.

This reduction in Rac1 and Cdc42 suggest Bcl-3 may be regulating actin cytoskeletal organization within migrating cells, a process required for the various migratory phenotypes. Although not explored further here, loss of Rac1 and Cdc42 activity may have wider implications in both Bcl-3-mediated EMT and senescence, (shown in chapters 4 and 5), with both processes associated with distinct cytoskeletal reorganisation. Unsurprisingly, both Rac1 and Cdc42 have been implicated in mediating cell-polarisation and initiating EMT-associated migration [281]. Furthermore, loss of Rac1 in primary mouse embryonic fibroblasts has been shown to induce premature senescence in a p53-dependent manner, where as in breast cancer Rac1 activity has also been found

to be decreased in senescing cells [282, 283]. Although Rac1 and Cdc42 activity has not been examined in our models of EMT or senescence it is possible that loss of their activity may be contributing to these phenotypes.

Along with the role of Bcl-3 in regulating migration, recent work showing the importance of Bcl-3 in TGF-β signalling through the stabilization of SMAD3 has suggested a role for Bcl-3 in EMT [188]. As TGF-β is one of the most studied initiators of EMT we hypothesised that Bcl-3 may play a role in promoting EMT through the regulation of TGF-β/SMAD3-mediated transcription. Interestingly, we have shown that the stimulation of MCF-7 cells into EMT, using a media supplement that includes recombinant TGF-β protein, resulted in an upregulation of a number of EMT-associated gene targets, including Bcl-3. This appears to be the first time that Bcl-3 has been directly implicated in EMT and suggests Bcl-3 may play a crucial role in the early initiation of metastasis. Furthermore, when Bcl-3 was inhibited in this model of EMT, the upregulation of specific EMT-mediating genes such as Vimentin, Twist, and N-cadherin was also inhibited, with their expression remaining at basal levels. Interestingly, downregulation of SMAD3 through the natural occurring agent beta-elemene has shown a similar transcriptional inhibition in MCF-7 cells following TGF-β stimulation, suggesting that Bcl-3 may be mediating EMT through its interaction with SMAD3 [284].

Despite the interesting changes observed in EMT transcription following Bcl-3 suppression in our model, it is possible that these changes may be a response to senescence induction, which we have confirmed is occurring in these cells in chapter 5. However, given that Bcl-3 appears to be inhibiting the upregulation of certain genes in response to EMT stimulation and not in normal unstimulated cells, it does suggest that this is a specific response to EMT and not senescence. Similar experiments in an epithelial, p53-mutant line, which does not senesce, would support this. On the other hand, a number of transcriptional changes were observed independently of EMT induction suggesting that these may have been in response to senescence. Furthermore, many of these

transcriptional changes were observed after 6 days of Bcl-3 inhibition in unstimulated MCF-7 cells compared to after 2 days, further suggesting these changes were due to the prolonged inhibition of Bcl-3 and therefore may contribute to Bcl-3-mediated senescence. Interestingly, Runx1 which was upregulated in both MCF-7 and MDA-MB-436 cells after 2 and 6 days of Bcl-3 inhibition has been shown to stimulate p53 protein levels in response to DNA damage, suggesting that its upregulation could be associated with this senescence phenotype [285]. Similarly Slug and mir-221, which are capable of regulating each other, were also upregulated independently of EMT stimulation which again appears to be a result of prolonged Bcl-3 inhibition. Both have been linked with senescence, with mir-221 known to directly target MDM2 and activate a p53 response in hepatocellular carcinoma, whereas Slug has been found to be upregulated in senescent chondrocytes [286, 287]. Whether these may play a similar role in breast cancer has not been explored but would be interesting to investigate in future work.

Although here we have implicated Bcl-3 in EMT via the regulation of TFG-β signalling, the interlink between Bcl-3 and TGF-β may be more important than to just regulate EMT given its role as a tumour suppressor in epithelial, endothelial, and hematopoietic cell types [288]. This link is supported by the fact that TGF-β signalling, through SMAD proteins, has been shown to regulate both p21 and p15, two key cell cycle inhibitors that we have found to be upregulated during our senescence phenotype [289]. Interestingly, both SMAD2 and SMAD3 have been shown to directly bind to p53, further suggesting that the senescence phenotype observed through loss of Bcl-3 may be mediated through the destabilisation of SMAD3 [271]. Furthermore, in lung cancer cells mutant p53 has been shown to preferentially bind SMAD3 to promote migration and tumourigenesis, while depletion of SMAD3 can increase Slug expression [290]. Although not tested here, future work should explore the role of SMAD3 destabilisation through loss of Bcl-3 in regulating both the senescence and apoptotic effects that have been observed.

Senescence was confirmed in chapter 5 with prolonged inhibition of Bcl-3 resulting in an increase in SA-β-gal, the upregulation of p15 and p21 and the appearance of SASP, a phenotype only observed in wildtype p53-expressing MCF-7 cells. This suggested that senescence was being driven through a p53-dependent pathway, a hypothesis that we have confirmed with suppression of p53 and Bcl-3 simultaneously which rescued the normal MCF-7 phenotype. Interestingly, an increase in SA-β-gal expression has also been observed in human fibroblasts after 7 days of Bcl-3 inhibition, which can be rescued through the combined inhibition of p53, further supporting the data we have shown here [261]. Given previous data in the literature, we hypothesised that Bcl-3 loss may correlate with a downregulation of MDM2; however no change in gene expression was observed. Despite this, further tests analysing MDM2 protein expression will need to be performed in future work to confirm this. Interestingly, EZH2 expression, which is associated with aggressive breast cancer and is a known regulatory target of p53, was found to be downregulated in our senescent MCF-7 cells [272, 273]. In human fibroblasts a regulatory pathway linking the non-canonical NF-kB pathway with the downregulation of EZH2 through both p53 and pRb has been shown [261]. Furthermore, p52 has also been shown to directly mediate EZH2 expression to suppress senescence, therefore we hypothesised that loss of Bcl-3 may inhibit EZH2-mediated regulation of p21 through a loss of p52 dimer activity [261]. Here we have confirmed this through knockdown of p52 in MCF-7 cells which resulted in a loss of EZH2 expression and an upregulation of p21 expression.

The hypothesis that senescence observed through Bcl-3 inhibition is mediated through NF-kB signalling is supported through our data here using small molecule Bcl-3 inhibitors, which have been designed to disrupt Bcl-3 binding to p50 and p52. Both lead compound CB-1 and new analogue CB-97 showed similar, although muted, senescence phenotypes when treated daily in MCF-7 cells, confirming that loss of Bcl-3 binding to p52 and/or p50 can drive senescence and not Bcl-3 directly. Knockdown experiments for both p50 and p52 further suggest that although senescence may be mediated through non-canonical p52 signalling, the appearance of SASP is mediated through a canonical p50-dependent pathway indicating differential roles for both NF-kB signalling pathways.

Interestingly, despite CB-1 showing a similar response to siRNA in regulating migration, a similar response to EMT-induction was not observed, suggesting that Bcl-3 regulation during EMT may be independent of p50 or p52, potentially through destabilisation of SMAD3. Suppression of p50 and p52 would confirm this, as could daily treatment of the more potent CB-97 in this system, which might elicit a similar response to siRNA.

The better responding analogue CB-97 was shown to be more potent at a lower molarity than previous lead compound CB-1, and could potentially be improved further by solving the solubility issues of this compound. Despite this, CB-1 has shown promising results here at inhibiting cell migration and metastasis in our CAM assays, with more recent *in vivo* work in the lab using different tumour models in mice further supporting its future therapeutic use. Recent results from a metastasis model in which tumour cells were injected directly into the mouse vasculature, to mimic the spreading of cells, has shown CB-1 treatment to inhibit pulmonary metastasis in a number of breast and colorectal cell lines (Clarkson, unpublished). Furthermore, CB-1 has also been shown to inhibit tumour growth in subcutaneous models, which has not been observed previously and was not seen in our CAM model of tumour growth here (Clarkson, unpublished). Interestingly, a recent patient-derived tumour xenograft (PDX) in a subcutaneous mouse model has shown a strong cytostatic response to CB-1, further supporting the use of Bcl-3 inhibitors in a clinical setting (Clarkson, unpublished). Importantly CB-1 has been shown to be effective when administered both through IP injections and oral gavage, with no toxicity observed at high doses in either mice or dogs making it a promising therapeutic option in the future (Clarkson, unpublished). Given the most likely use of these compounds will be in combination with more established chemotherapeutics and not as a monotherapy, future work combining Bcl-3 inhibition with standardised treatment regimens will be important in the clinical progression of these compounds.

One issue however, which needs to be carefully addressed if using senescence induction as a therapeutic option is the appearance of SASP which includes the upregulation of IL-6, a cytokine that

has been shown to promote tumourigenic effects [279]. From data in the literature it does however appear that the tumourigenic effect of IL-6 may be context dependent, however testing the effects of conditioned media from our senescent cells on normal mammary cells could be used as a test to determine its effects in our model. Alternatively, further compound modifications which enable the specific disruption of Bcl-3 to p52 homodimers and not p50 homodimer interactions may specifically induce senescence without the appearance of SASP.

Although further investigation is required we suggest here that SASP is not required for senescence induction and is more likely a secondary output of the phenotype that helps to maintain senescence. Both Bcl-3 and NF-kB signalling are established regulators of cytokine responses and inflammation, and it appears that Bcl-3 inhibition may upregulate these cytokines independently of p53, as they appeared to be significantly upregulated even when p53 was inhibited. An interesting Bcl-3 target that may be regulating this is STAT3, which is required for inducing senescence in human fibroblasts through IL-6 and is known to be downregulated by Bcl-3 in cervical cancer [291, 292]. In a tumour setting IL-6/STAT3 signalling is often deregulated resulting in increased proliferation and cell cycle progression, as well as inhibiting apoptosis [293, 294]. Furthermore, inhibition of STAT3 in a murine breast cancer model was shown to induce premature senescence which resulted in a significant upregulation of cytokines including IL-6 [295]. New data not shown here has suggested STAT3 expression is downregulated following prolonged Bcl-3 inhibition in MCF-7 cells; therefore it is possible that the increase in SASP as a result of Bcl-3 inhibition is at least partially due to a reduction in p50-mediated STAT3 expression. This however is not enough to cause senescence with loss of p52 signalling and functional p53 also required to mediate the senescence response. Interestingly, STAT3 is capable of regulating p53 expression with the blocking of STAT3 shown to activate p53 expression in human cancer cells [296]. Further work exploring the role of STAT3 in our model is required; however it does open an interesting avenue to explore.

Together our data here, along with more recent data confirming these effects in multiple cell lines, suggest an interesting role for Bcl-3 in regulating breast cancer with differential responses observed depending on the p53 status of the tumour cells. Given that p53 is one of the most mutated genes in cancer, if the apoptotic effect observed in the p53 mutant MDA-MB-436 cells can be confirmed in other p53 mutant cell lines it is possible that Bcl-3 inhibition could be applied to a number of other cancer types where Bcl-3 has been shown to be upregulated.

In conclusion, the results presented in this study have highlighted Bcl-3 as an interesting therapeutic target due to its varied roles in both tumour growth and metastasis (figure 6.1). Firstly, we have confirmed the role of Bcl-3 in regulating cell motility and have further shown that suppression of Bcl-3 inhibits multiple migratory phenotypes, which it appears to be regulating through inhibiting Rac1 and Cdc42 GTPase activity. Furthermore, we have shown for the first time that Bcl-3 is upregulated during EMT in breast cancer, which is likely to help regulate the expression of certain pro-EMT gene targets. We have also highlighted Bcl-3 as a key regulatory gene in breast cancer cells, with prolonged suppression resulting in either senescence or apoptosis which appears to be determined by the p53 status within the cell. Finally, we have shown that small molecule inhibitors of Bcl-3 are capable of mimicking, at least partially, Bcl-3 suppression and may be a viable therapeutic option for treating breast cancer and potentially other cancer types.

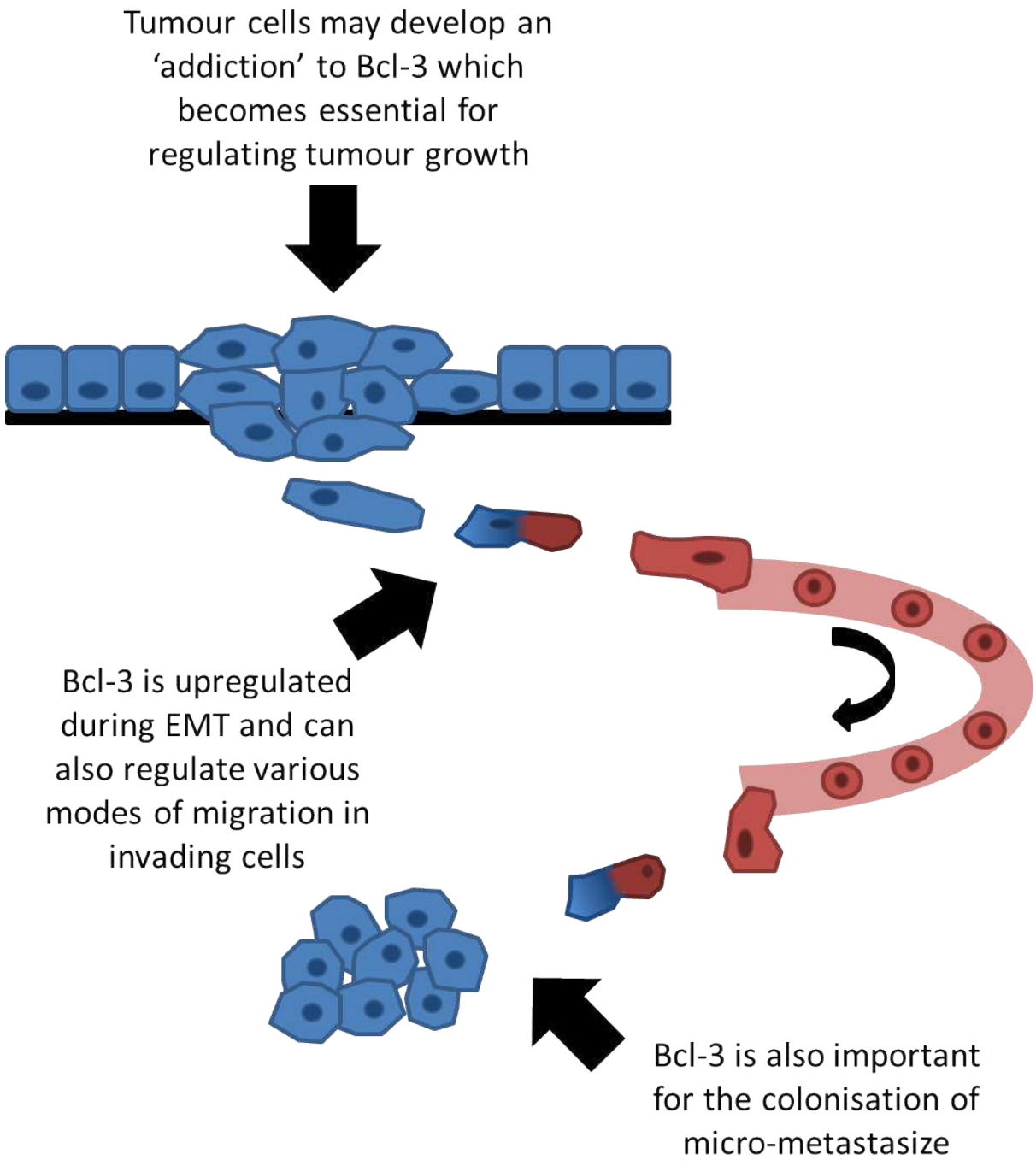


**Figure 6.1- A model for the role of Bcl-3 in breast cancer-** Based on the data presented here we suggest a new model where by Bcl-3 appears to regulate some of the key processes of breast cancer progression. Growing tumour cells appear to become 'addicted' to Bcl-3 with its prolonged removal resulting in loss of cell viability through either senescence or apoptosis. Bcl-3 also appears to be upregulated during EMT and may be involved in regulating gene transcription during this process. Following EMT invading cells migrate away from the primary tumour, with Bcl-3 also appearing to regulate the various modes of cell migration used to metastasis. Finally, given Bcl-3s role in EMT it is likely to play some role during MET and colony formation with recent data, not presented here, showing small molecule inhibition of Bcl-3 to significantly reduce this colony forming ability *in vivo*.

# Chapter 7:
# Appendices

# 7 Appendix A

The effect of prolonged Bcl-3 inhibition was tested in HER2-positive HCC1954 cells which express a mutant form of p53 to determine whether they would enter senescence or induce apoptosis. Firstly, the effect of 6 day Bcl-3 siRNA treatment was analysed for SA-β-gal expression and cell titre blue activity, with Bcl-3 inhibition having no effect on cell viability and showing no increase in SA-β-gal expression (Figure 7.1A&B). The effect of prolonged Bcl-3 inhibition on the cell cycle progression of these cells was then analysed using the DNA marker DAPI, however no changes were observed between Bcl-3 siRNA or scRNA treated cells (Figure 7.2). To further rule out senescence in HCC1954 cells, RNA was harvested after 6 days of Bcl-3 inhibition and analysed for the expression of senescence markers and the induction of SASP cytokines (Figure 7.3A&B). After 6 days of Bcl-3 siRNA treatment the level of Bcl-3 suppression was around 50% compared to scRNA controls which resulted in a significant reduction in p21 expression and an upregulation of p16, with the only change in SASP expression being a significant upregulation in IL-6. To determine whether HCC1954 cells were being pushed towards an apoptotic response similar to what was observed in the p53-mutant MDA-MB-436 cell line, annexin V expression was analysed by flow cytometry, however no significant changes were observed (Figure 7.4). Finally the expression of previously identified senescence and apoptosis-associated genes was analysed by qRT-PCR to confirm neither of these processes were being mediated through Bcl-3 suppression in HCC1954 cells. In Bcl-3 siRNA treated cells a significant reduction in MDM2 and Bcl-XL was observed, however no other changes were seen.

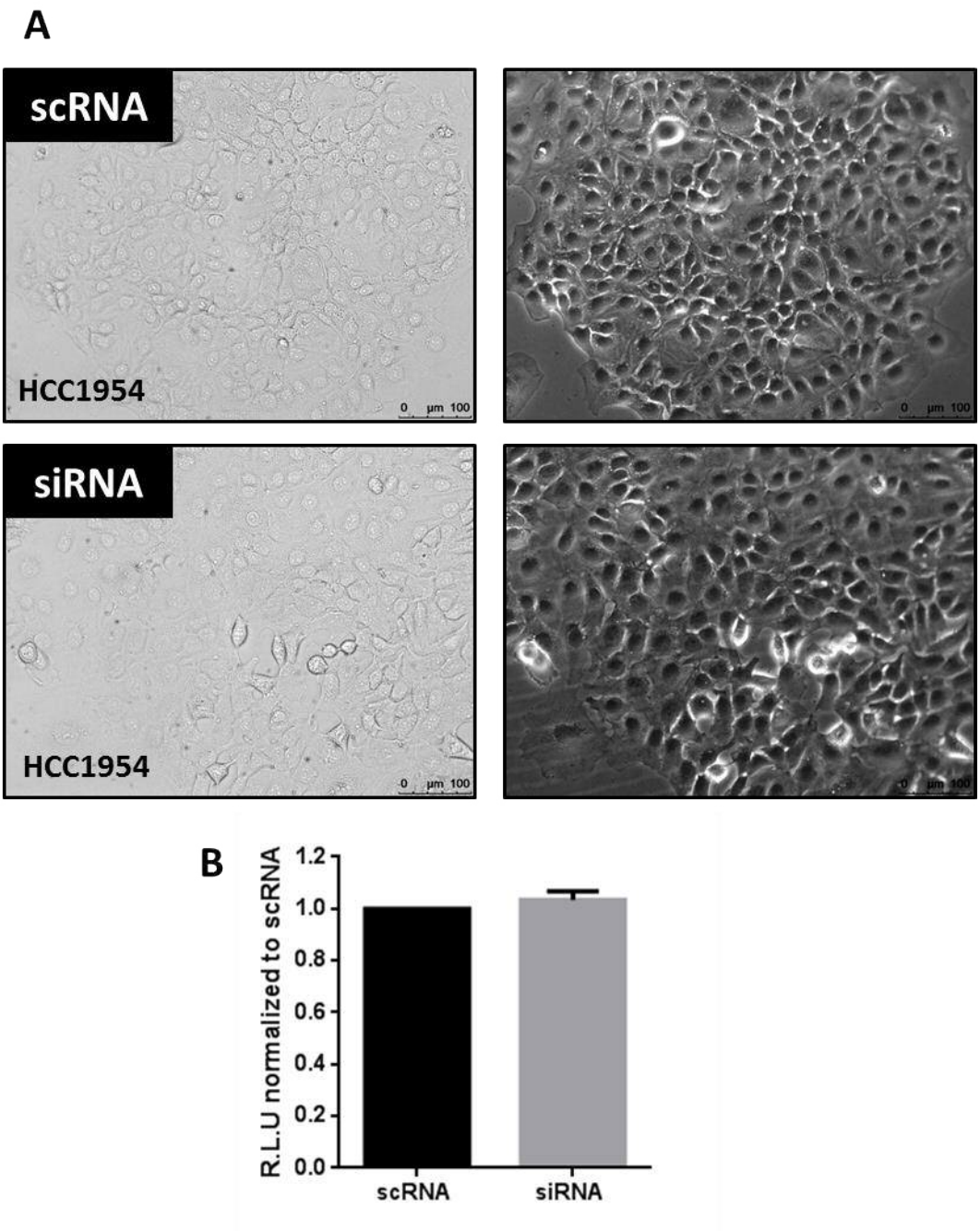


**Figure 7.1- 6 day Bcl-3 inhibition had no effect on HCC1954 cell viability or SA-β-gal staining**- **(A)** Representative images of HCC1954 cells after 6 days of treatment with either Bcl-3 siRNA or scRNA control. Cells were fixed and stained for SA-β-gal after 6 days with images of siRNA or scRNA treated cells taken with phase contrast or brightfield filters to highlight the positively stained cells. Scale bar= 100µm. **(B)** Cell titre blue was also performed on these cells to determine cell viability.

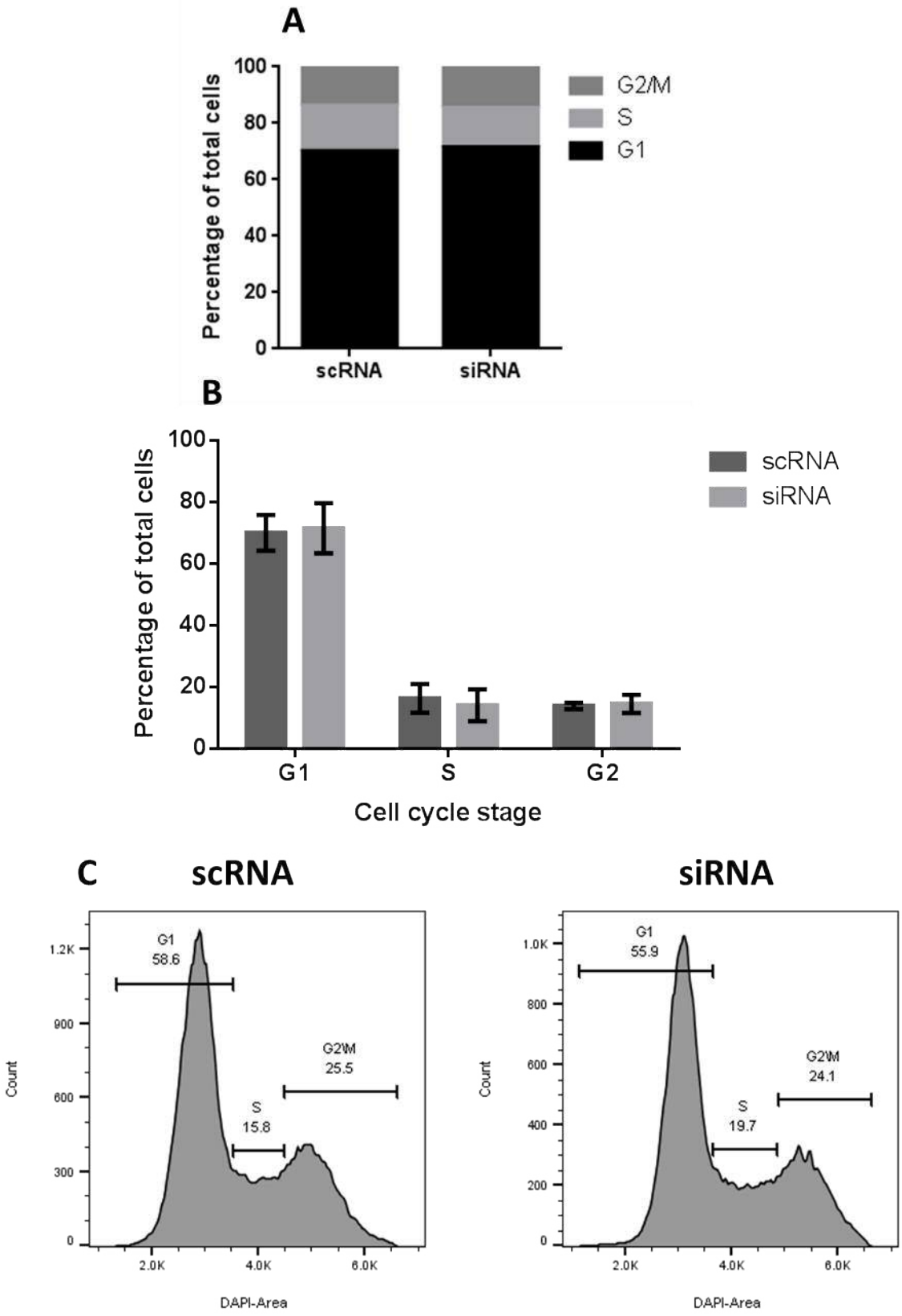


**Figure 7.2- 6 day Bcl-3 inhibition did not alter the cell cycle of HCC1954 cells-** HCC1954 cells were treated with either Bcl-3 siRNA or scRNA control for 6 days before cells were stained with DAPI solution. Initially cells were gated based on FSC-area and SSC-Area before single cells were selected based on FSC-Area and FSC-Height by flow cytometry, these were then analysed for DAPI expression with each population separated and analysed using FlowJo. **(A&B)** Cells were gated based on DAPI expression and shown as a percentage of the total cell population. Error bars represent ± SEM of 3 independent experiments. T-test, *=p<0.05 compared to scRNA. **(C)** Representative images of flow cytometry histogram plots analysed in FlowJo.

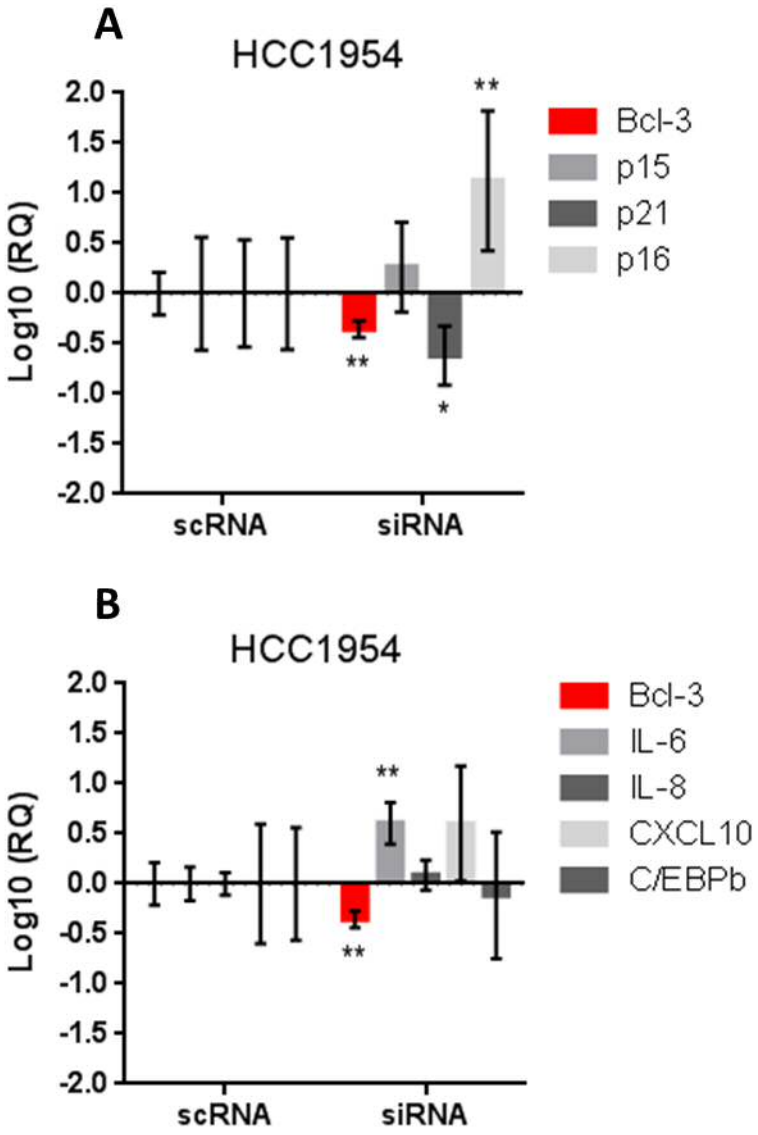


**Figure 7.3- Effect of 6 day Bcl-3 inhibition on senescence-related gene expression in HCC1954 cells-** HCC1954 cells were treated with either Bcl-3 siRNA or scRNA control for 6 days before cells were harvested for RNA. qRT-PCR was performed to compare the expression of **(A)** p15, p21 and p16 and **(B)** SASP cytokines which were normalized to scRNA controls. Error bars represent 95% confidence intervals of 3 independent experiments. Significance was determined using the 95% confidence interval overlap rule described in [1].

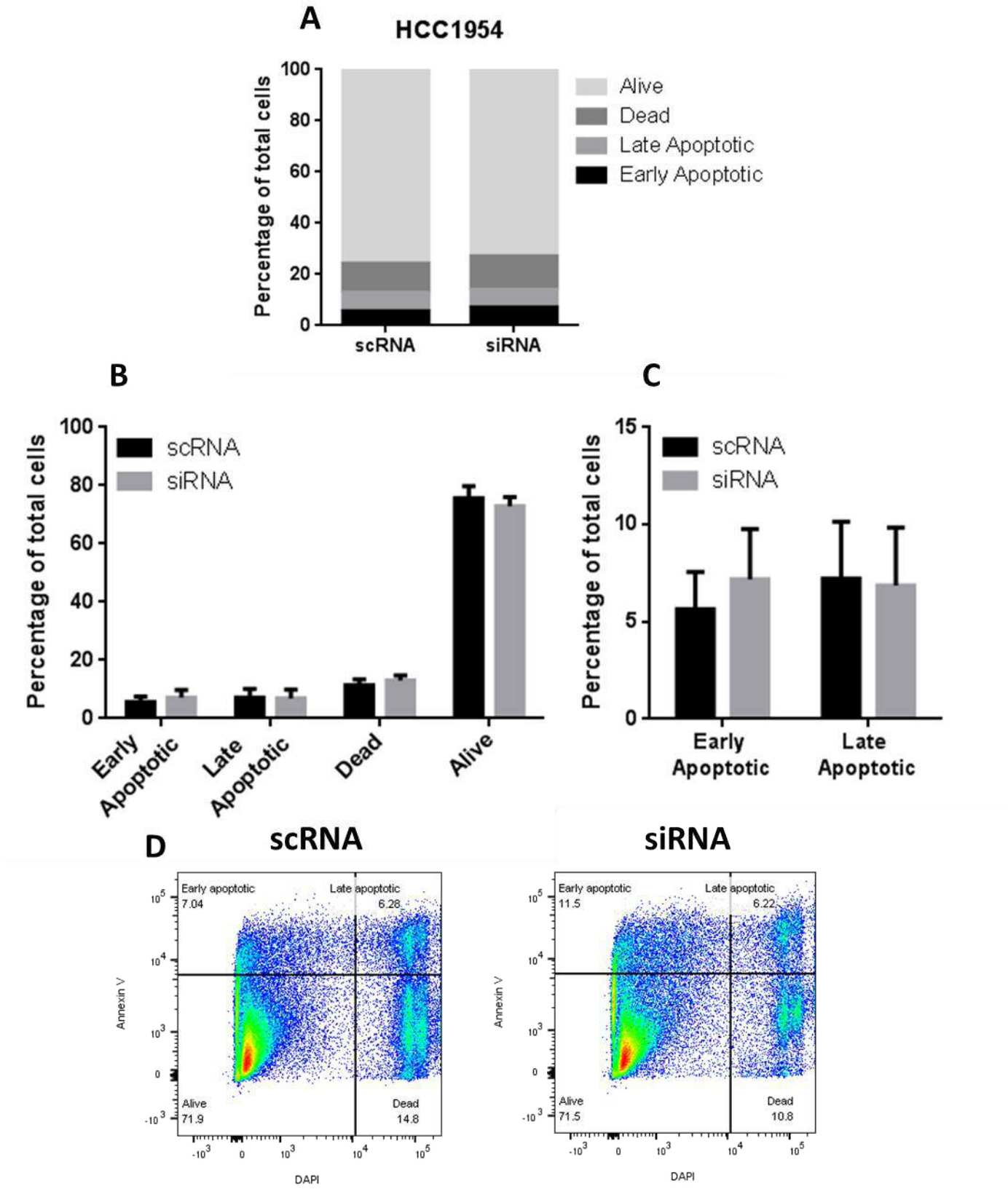


**Figure 7.4- 6 day Bcl-3 inhibition in HCC1954 cells did not affect Annexin V expression** - HCC1954 cells were treated with either Bcl-3 siRNA or scRNA control for 6 days before floating and attached cells were harvested and stained with apoptosis marker Annexin V and DNA marker DAPI. Initially cells were gated based on FSC-area and SSC-Area before single cells were selected based on FSC-Area and FSC-Height by flow cytometry, these were then analysed for Annexin V and DAPI expression with each population separated and analysed using FlowJo. **(A&B)** Cells were grouped based on expression and shown as a percentage of the total cell population. **(C)** Early and late apoptotic cells were separated by differences in DAPI staining. **(D)** Representative images of flow cytometry plots analysed in FlowJo. Error bars represent ± SEM of 3 independent experiments. T-test, *=$p<0.05$ compared to scRNA.

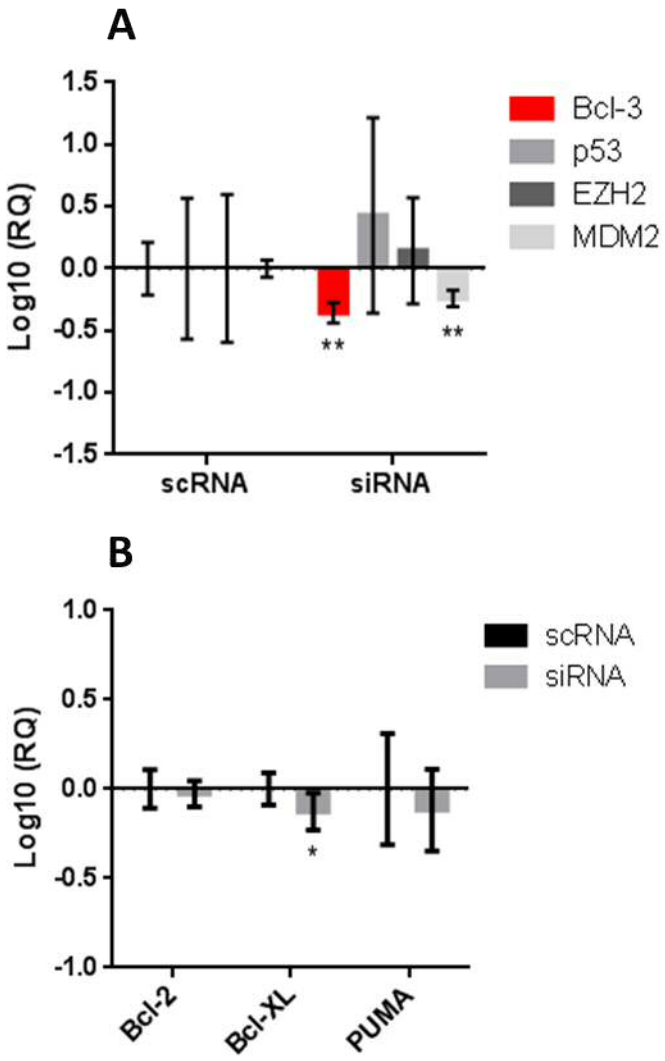


**Figure 7.5- The effect of prolonged Bcl-3 suppression in HCC1954 cells on senescence and apoptosis regulatory genes-** HCC1954 cells were treated with either Bcl-3 siRNA or scRNA control for 6 days before cells were harvested for RNA. qRT-PCR was performed to compare the expression of **(A)** senescence-related genes p53, EZH2 and MDM2 and **(B)** apoptosis-related genes Bcl-2, Bcl-XL and PUMA which were normalized to scRNA controls. Error bars represent 95% confidence intervals of 3 independent experiments. Significance was determined using the 95% confidence interval overlap rule described in [1].

# Chapter 8:
# Supplementary videos

# 8 Supplementary Videos

**Video 1-** Representative video of mesenchymal-like single cell migration in MDA-MB-436 cells after Bcl-3 siRNA treatment

**Video 2-** Representative video of mesenchymal-like single cell migration in MDA-MB-436 cells after non-targeting scRNA treatment

**Video 3-** Representative video of mesenchymal-like single cell migration in MDA-MB-231 cells after Bcl-3 siRNA treatment

**Video 4-** Representative video of mesenchymal-like single cell migration in MDA-MB-231 cells after Bcl-3 siRNA treatment

**Video 5-** Representative video of MCF-7 cell migration after 5 days of treatment with StemXVivo EMT-inducing supplement

**Video 6-** Representative video of MCF-7 cell migration under normal growth conditions

All supplementary videos can be accessed at:

https://www.dropbox.com/sh/iv7y3s09w35v84h/AAArMWXI5x5whe_i6gzNPBqQa?dl=0

# Chapter 9:
# Bibliography

# 9 Bibliography


1. Cumming, G., F. Fidler, and D.L. Vaux, *Error bars in experimental biology.* The Journal of Cell Biology, 2007. **177**(1): p. 7.
2. Gasco, M., S. Shami, and T. Crook, *The p53 pathway in breast cancer.* Breast Cancer Research, 2002. **4**(2): p. 70.
3. Maldonado, V. and J. Melendez-Zajgla, *Role of Bcl-3 in solid tumors.* Molecular Cancer, 2011. **10**: p. 152-152.
4. Massagué, J. and A.C. Obenauf, *Metastatic Colonization.* Nature, 2016. **529**(7586): p. 298-306.
5. Gerondakis, S., et al., *NF-[kappa]B control of T cell development.* Nat Immunol, 2014. **15**(1): p. 15-25.
6. Guo, F., et al., *Post-transcriptional regulatory network of epithelial-to-mesenchymal and mesenchymal-to-epithelial transitions.* Journal of Hematology & Oncology, 2014. **7**: p. 19-19.
7. UK, C.R. *Breast cancer statistics*. 2011; Available from: http://www.cancerresearchuk.org/health-professional/cancer-statistics/statistics-by-cancer-type/breast-cancer#heading-Zero
8. UK, C.R. *Breast cancer mortality statistics*. 2011.
9. Gudjonsson, T., et al., *Normal and tumor-derived myoepithelial cells differ in their ability to interact with luminal breast epithelial cells for polarity and basement membrane deposition.* J Cell Sci, 2002. **115**(Pt 1): p. 39-50.
10. Xiao, G., et al., *Suppression of breast cancer growth and metastasis by a serpin myoepithelium-derived serine proteinase inhibitor expressed in the mammary myoepithelial cells.* Proc Natl Acad Sci U S A, 1999. **96**(7): p. 3700-5.
11. Sternlicht, M.D., et al., *The human myoepithelial cell is a natural tumor suppressor.* Clin Cancer Res, 1997. **3**(11): p. 1949-58.
12. Haslam, S.Z., *Acquisition of estrogen-dependent progesterone receptors by normal mouse mammary gland. Ontogeny of mammary progesterone receptors.* J Steroid Biochem, 1988. **31**(1): p. 9-13.
13. Shehata, M., et al., *Phenotypic and functional characterisation of the luminal cell hierarchy of the mammary gland.* Breast Cancer Res, 2012. **14**(5): p. R134.
14. Shackleton, M., et al., *Generation of a functional mammary gland from a single stem cell.* Nature, 2006. **439**(7072): p. 84-88.
15. Van Keymeulen, A., et al., *Distinct stem cells contribute to mammary gland development and maintenance.* Nature, 2011. **479**(7372): p. 189-93.
16. Society, T.A.C., *About Breast cancer.* 2016.
17. Curtis, C., et al., *The genomic and transcriptomic architecture of 2,000 breast tumours reveals novel subgroups.* Nature, 2012. **486**(7403): p. 346-352.
18. Fan, C., et al., *Concordance among gene-expression-based predictors for breast cancer.* N Engl J Med, 2006. **355**(6): p. 560-9.
19. Sung, H., et al., *Heterogeneity of luminal breast cancer characterised by immunohistochemical expression of basal markers.* Br J Cancer, 2016. **114**(3): p. 298-304.
20. Blows, F.M., et al., *Subtyping of breast cancer by immunohistochemistry to investigate a relationship between subtype and short and long term survival: a collaborative analysis of data for 10,159 cases from 12 studies.* PLoS Med, 2010. **7**(5): p. e1000279.
21. Inic, Z., et al., *Difference between Luminal A and Luminal B Subtypes According to Ki-67, Tumor Size, and Progesterone Receptor Negativity Providing Prognostic Information.* Clinical Medicine Insights. Oncology, 2014. **8**: p. 107-111.
22. Brenton, J.D., et al., *Molecular classification and molecular forecasting of breast cancer: ready for clinical application?* J Clin Oncol, 2005. **23**(29): p. 7350-60.

23. Sorlie, T., et al., *Gene expression patterns of breast carcinomas distinguish tumor subclasses with clinical implications.* Proc Natl Acad Sci U S A, 2001. **98**(19): p. 10869-74.
24. Tran, B. and P.L. Bedard, *Luminal-B breast cancer and novel therapeutic targets.* Breast Cancer Res, 2011. **13**(6): p. 221.
25. Berry, D.A., et al., *Effect of screening and adjuvant therapy on mortality from breast cancer.* N Engl J Med, 2005. **353**(17): p. 1784-92.
26. Slamon, D.J., et al., *Human breast cancer: correlation of relapse and survival with amplification of the HER-2/neu oncogene.* Science, 1987. **235**(4785): p. 177-82.
27. Haffty, B.G., et al., *Locoregional relapse and distant metastasis in conservatively managed triple negative early-stage breast cancer.* J Clin Oncol, 2006. **24**(36): p. 5652-7.
28. Dent, R., et al., *Triple-negative breast cancer: clinical features and patterns of recurrence.* Clin Cancer Res, 2007. **13**(15 Pt 1): p. 4429-34.
29. Perou, C.M., et al., *Molecular portraits of human breast tumours.* Nature, 2000. **406**(6797): p. 747-52.
30. Lehmann, B.D., et al., *Identification of human triple-negative breast cancer subtypes and preclinical models for selection of targeted therapies.* J Clin Invest, 2011. **121**(7): p. 2750-67.
31. Dai, X., et al., *Breast cancer intrinsic subtype classification, clinical use and future trends.* American Journal of Cancer Research, 2015. **5**(10): p. 2929-2943.
32. Elloumi, F., et al., *Systematic bias in genomic classification due to contaminating non-neoplastic tissue in breast tumor samples.* BMC Med Genomics, 2011. **4**: p. 54.
33. Hayflick, L. and P.S. Moorhead, *The serial cultivation of human diploid cell strains.* Exp Cell Res, 1961. **25**: p. 585-621.
34. Schellenberg, A., et al., *Replicative senescence of mesenchymal stem cells causes DNA-methylation changes which correlate with repressive histone marks.* Aging (Albany NY), 2011. **3**(9): p. 873-88.
35. Harley, C.B., A.B. Futcher, and C.W. Greider, *Telomeres shorten during ageing of human fibroblasts.* Nature, 1990. **345**(6274): p. 458-60.
36. Chandeck, C. and W.J. Mooi, *Oncogene-induced cellular senescence.* Adv Anat Pathol, 2010. **17**(1): p. 42-8.
37. Hamajima, N., et al., *Alcohol, tobacco and breast cancer--collaborative reanalysis of individual data from 53 epidemiological studies, including 58,515 women with breast cancer and 95,067 women without the disease.* Br J Cancer, 2002. **87**(11): p. 1234-45.
38. Datta, K. and J. Biswas, *Influence of dietary habits, physical activity and affluence factors on breast cancer in East India: a case-control study.* Asian Pac J Cancer Prev, 2009. **10**(2): p. 219-22.
39. Calle, E.E., et al., *Overweight, obesity, and mortality from cancer in a prospectively studied cohort of U.S. adults.* N Engl J Med, 2003. **348**(17): p. 1625-38.
40. Britt, K., A. Ashworth, and M. Smalley, *Pregnancy and the risk of breast cancer.* Endocr Relat Cancer, 2007. **14**(4): p. 907-33.
41. Claus, E.B., N. Risch, and W.D. Thompson, *Genetic analysis of breast cancer in the cancer and steroid hormone study.* Am J Hum Genet, 1991. **48**(2): p. 232-42.
42. Osborne, C., P. Wilson, and D. Tripathy, *Oncogenes and tumor suppressor genes in breast cancer: potential diagnostic and therapeutic applications.* Oncologist, 2004. **9**(4): p. 361-77.
43. Howlader, N., et al., *US incidence of breast cancer subtypes defined by joint hormone receptor and HER2 status.* J Natl Cancer Inst, 2014. **106**(5).
44. Yarden, Y. and M.X. Sliwkowski, *Untangling the ErbB signalling network.* Nat Rev Mol Cell Biol, 2001. **2**(2): p. 127-37.
45. Zhou, X., et al., *Activation of the Akt/mammalian target of rapamycin/4E-BP1 pathway by ErbB2 overexpression predicts tumor progression in breast cancers.* Clin Cancer Res, 2004. **10**(20): p. 6779-88.

46. Zhu, X. and S. Verma, *Targeted therapy in her2-positive metastatic breast cancer: a review of the literature.* Curr Oncol, 2015. **22**(Suppl 1): p. S19-28.
47. Garnock-Jones, K.P., G.M. Keating, and L.J. Scott, *Trastuzumab: A review of its use as adjuvant treatment in human epidermal growth factor receptor 2 (HER2)-positive early breast cancer.* Drugs, 2010. **70**(2): p. 215-39.
48. Izumi, Y., et al., *Tumour biology: herceptin acts as an anti-angiogenic cocktail.* Nature, 2002. **416**(6878): p. 279-80.
49. Mohsin, S.K., et al., *Neoadjuvant trastuzumab induces apoptosis in primary breast cancers.* J Clin Oncol, 2005. **23**(11): p. 2460-8.
50. Lane, H.A., et al., *Modulation of p27/Cdk2 complex formation through 4D5-mediated inhibition of HER2 receptor signaling.* Ann Oncol, 2001. **12 Suppl 1**: p. S21-2.
51. Nass, S.J. and R.B. Dickson, *Defining a role for c-Myc in breast tumorigenesis.* Breast Cancer Res Treat, 1997. **44**(1): p. 1-22.
52. Blackwood, E.M. and R.N. Eisenman, *Max: a helix-loop-helix zipper protein that forms a sequence-specific DNA-binding complex with Myc.* Science, 1991. **251**(4998): p. 1211-7.
53. Mukherjee, S. and S.E. Conrad, *c-Myc suppresses p21WAF1/CIP1 expression during estrogen signaling and antiestrogen resistance in human breast cancer cells.* J Biol Chem, 2005. **280**(18): p. 17617-25.
54. Prall, O.W., E.M. Rogan, and R.L. Sutherland, *Estrogen regulation of cell cycle progression in breast cancer cells.* J Steroid Biochem Mol Biol, 1998. **65**(1-6): p. 169-74.
55. Al-Kuraya, K., et al., *Prognostic relevance of gene amplifications and coamplifications in breast cancer.* Cancer Res, 2004. **64**(23): p. 8534-40.
56. Vita, M. and M. Henriksson, *The Myc oncoprotein as a therapeutic target for human cancer.* Semin Cancer Biol, 2006. **16**(4): p. 318-30.
57. Wang, Y.-h., et al., *Knockdown of c-Myc expression by RNAi inhibits MCF-7 breast tumor cells growth in vitro and in vivo.* Breast Cancer Research, 2005. **7**(2): p. R220-R228.
58. Carroll, J.S., et al., *Mechanisms of growth arrest by c-myc antisense oligonucleotides in MCF-7 breast cancer cells: implications for the antiproliferative effects of antiestrogens.* Cancer Res, 2002. **62**(11): p. 3126-31.
59. Keyomarsi, K., et al., *Cyclin E and survival in patients with breast cancer.* N Engl J Med, 2002. **347**(20): p. 1566-75.
60. Sutherland, R.L. and E.A. Musgrove, *Cyclins and breast cancer.* J Mammary Gland Biol Neoplasia, 2004. **9**(1): p. 95-104.
61. Loden, M., et al., *The cyclin D1 high and cyclin E high subgroups of breast cancer: separate pathways in tumorogenesis based on pattern of genetic aberrations and inactivation of the pRb node.* Oncogene, 2002. **21**(30): p. 4680-90.
62. Tan, A.R. and S.M. Swain, *Review of flavopiridol, a cyclin-dependent kinase inhibitor, as breast cancer therapy.* Semin Oncol, 2002. **29**(3 Suppl 11): p. 77-85.
63. El-Rayes, B.F., et al., *A phase I study of flavopiridol and docetaxel.* Invest New Drugs, 2006. **24**(4): p. 305-10.
64. Hollstein, M., et al., *p53 mutations in human cancers.* Science, 1991. **253**(5015): p. 49-53.
65. Malkin, D., et al., *Germ line p53 mutations in a familial syndrome of breast cancer, sarcomas, and other neoplasms.* Science, 1990. **250**(4985): p. 1233-8.
66. Rivlin, N., G. Koifman, and V. Rotter, *p53 orchestrates between normal differentiation and cancer.* Semin Cancer Biol, 2015. **32**: p. 10-7.
67. Parrales, A. and T. Iwakuma, *Targeting Oncogenic Mutant p53 for Cancer Therapy.* Frontiers in Oncology, 2015. **5**: p. 288.
68. Friedler, A., et al., *A peptide that binds and stabilizes p53 core domain: chaperone strategy for rescue of oncogenic mutants.* Proc Natl Acad Sci U S A, 2002. **99**(2): p. 937-42.
69. Selivanova, G., et al., *Restoration of the growth suppression function of mutant p53 by a synthetic peptide derived from the p53 C-terminal domain.* Nat Med, 1997. **3**(6): p. 632-8.

70. Alexandrova, E.M., et al., *Improving survival by exploiting tumour dependence on stabilized mutant p53 for treatment.* Nature, 2015. **523**(7560): p. 352-6.
71. Li, D., et al., *Functional inactivation of endogenous MDM2 and CHIP by HSP90 causes aberrant stabilization of mutant p53 in human cancer cells.* Mol Cancer Res, 2011. **9**(5): p. 577-88.
72. Schubert, E.L., et al., *BRCA2 in American families with four or more cases of breast or ovarian cancer: recurrent and novel mutations, variable expression, penetrance, and the possibility of families whose cancer is not attributable to BRCA1 or BRCA2.* Am J Hum Genet, 1997. **60**(5): p. 1031-40.
73. Easton, D.F., D. Ford, and D.T. Bishop, *Breast and ovarian cancer incidence in BRCA1-mutation carriers. Breast Cancer Linkage Consortium.* Am J Hum Genet, 1995. **56**(1): p. 265-71.
74. Antoniou, A., et al., *Average risks of breast and ovarian cancer associated with BRCA1 or BRCA2 mutations detected in case Series unselected for family history: a combined analysis of 22 studies.* Am J Hum Genet, 2003. **72**(5): p. 1117-30.
75. Agalliu, I., et al., *Associations of High-Grade Prostate Cancer with BRCA1 and BRCA2 Founder Mutations.* Clinical cancer research : an official journal of the American Association for Cancer Research, 2009. **15**(3): p. 1112-1120.
76. Shattuck-Eidens, D., et al., *A collaborative survey of 80 mutations in the BRCA1 breast and ovarian cancer susceptibility gene. Implications for presymptomatic testing and screening.* Jama, 1995. **273**(7): p. 535-41.
77. Walsh, T., et al., *Spectrum of mutations in BRCA1, BRCA2, CHEK2, and TP53 in families at high risk of breast cancer.* Jama, 2006. **295**(12): p. 1379-88.
78. Fackenthal, J.D. and O.I. Olopade, *Breast cancer risk associated with BRCA1 and BRCA2 in diverse populations.* Nat Rev Cancer, 2007. **7**(12): p. 937-948.
79. Roy, R., J. Chun, and S.N. Powell, *BRCA1 and BRCA2: different roles in a common pathway of genome protection.* Nat Rev Cancer, 2012. **12**(1): p. 68-78.
80. Wong, A.K., et al., *RAD51 interacts with the evolutionarily conserved BRC motifs in the human breast cancer susceptibility gene brca2.* J Biol Chem, 1997. **272**(51): p. 31941-4.
81. King, M.C., J.H. Marks, and J.B. Mandell, *Breast and ovarian cancer risks due to inherited mutations in BRCA1 and BRCA2.* Science, 2003. **302**(5645): p. 643-6.
82. McDonald, J.A., A. Goyal, and M.B. Terry, *Alcohol Intake and Breast Cancer Risk: Weighing the Overall Evidence.* Current breast cancer reports, 2013. **5**(3): p. 10.1007/s12609-013-0114-z.
83. Meijers-Heijboer, H., et al., *Breast cancer after prophylactic bilateral mastectomy in women with a BRCA1 or BRCA2 mutation.* N Engl J Med, 2001. **345**(3): p. 159-64.
84. Cairns, J., *Mutation selection and the natural history of cancer.* Nature, 1975. **255**(5505): p. 197-200.
85. Klein, C.A., *Parallel progression of primary tumours and metastases.* Nat Rev Cancer, 2009. **9**(4): p. 302-312.
86. Chambers, A.F., A.C. Groom, and I.C. MacDonald, *Dissemination and growth of cancer cells in metastatic sites.* Nat Rev Cancer, 2002. **2**(8): p. 563-72.
87. O'Shaughnessy, J., *Extending Survival with Chemotherapy in Metastatic Breast Cancer.* The Oncologist, 2005. **10**(suppl 3): p. 20-29.
88. Thiery, J.P., et al., *Epithelial-mesenchymal transitions in development and disease.* Cell, 2009. **139**(5): p. 871-90.
89. Kalluri, R. and R.A. Weinberg, *The basics of epithelial-mesenchymal transition.* The Journal of Clinical Investigation, 2009. **119**(6): p. 1420-1428.
90. Nieto, M.A., et al., *EMT: 2016.* Cell, 2016. **166**(1): p. 21-45.
91. Grigore, A.D., et al., *Tumor Budding: The Name is EMT. Partial EMT.* Journal of Clinical Medicine, 2016. **5**(5): p. 51.

92. Wang, Y. and B.P. Zhou, *Epithelial-mesenchymal transition in breast cancer progression and metastasis.* Chin J Cancer, 2011. **30**(9): p. 603-11.
93. Hollier, B.G., K. Evans, and S.A. Mani, *The epithelial-to-mesenchymal transition and cancer stem cells: a coalition against cancer therapies.* J Mammary Gland Biol Neoplasia, 2009. **14**(1): p. 29-43.
94. Mani, S.A., et al., *The epithelial-mesenchymal transition generates cells with properties of stem cells.* Cell, 2008. **133**(4): p. 704-15.
95. Sahai, E. and C.J. Marshall, *Differing modes of tumour cell invasion have distinct requirements for Rho/ROCK signalling and extracellular proteolysis.* Nat Cell Biol, 2003. **5**(8): p. 711-9.
96. Parri, M. and P. Chiarugi, *Rac and Rho GTPases in cancer cell motility control.* Cell Commun Signal, 2010. **8**: p. 23.
97. Yoshioka, K., et al., *A role for LIM kinase in cancer invasion.* Proc Natl Acad Sci U S A, 2003. **100**(12): p. 7247-52.
98. Wang, W., et al., *Identification and testing of a gene expression signature of invasive carcinoma cells within primary mammary tumors.* Cancer Res, 2004. **64**(23): p. 8585-94.
99. Hui, R., et al., *EMS1 amplification can occur independently of CCND1 or INT-2 amplification at 11q13 and may identify different phenotypes in primary breast cancer.* Oncogene, 1997. **15**(13): p. 1617-23.
100. Schnelzer, A., et al., *Rac1 in human breast cancer: overexpression, mutation analysis, and characterization of a new isoform, Rac1b.* Oncogene, 2000. **19**(26): p. 3013-20.
101. Youngs, S.J., et al., *Chemokines induce migrational responses in human breast carcinoma cell lines.* Int J Cancer, 1997. **71**(2): p. 257-66.
102. Condeelis, J. and J.W. Pollard, *Macrophages: obligate partners for tumor cell migration, invasion, and metastasis.* Cell, 2006. **124**(2): p. 263-6.
103. Reymond, N., B.B. d'Agua, and A.J. Ridley, *Crossing the endothelial barrier during metastasis.* Nat Rev Cancer, 2013. **13**(12): p. 858-70.
104. Fidler, I.J., *Metastasis: guantitative analysis of distribution and fate of tumor embolilabeled with 125 I-5-iodo-2'-deoxyuridine.* J Natl Cancer Inst, 1970. **45**(4): p. 773-82.
105. Luzzi, K.J., et al., *Multistep nature of metastatic inefficiency: dormancy of solitary cells after successful extravasation and limited survival of early micrometastases.* Am J Pathol, 1998. **153**(3): p. 865-73.
106. Wong, S.Y. and R.O. Hynes, *Lymphatic or hematogenous dissemination: how does a metastatic tumor cell decide?* Cell Cycle, 2006. **5**(8): p. 812-7.
107. Weis, S.M. and D.A. Cheresh, *αv Integrins in Angiogenesis and Cancer.* Cold Spring Harbor Perspectives in Medicine:, 2011. **1**(1): p. a006478.
108. Hoeben, A., et al., *Vascular endothelial growth factor and angiogenesis.* Pharmacol Rev, 2004. **56**(4): p. 549-80.
109. Drabsch, Y. and P. ten Dijke, *TGF-beta signaling in breast cancer cell invasion and bone metastasis.* J Mammary Gland Biol Neoplasia, 2011. **16**(2): p. 97-108.
110. Lee, B.C., et al., *Involvement of the chemokine receptor CXCR4 and its ligand stromal cell-derived factor 1alpha in breast cancer cell migration through human brain microvascular endothelial cells.* Mol Cancer Res, 2004. **2**(6): p. 327-38.
111. Uchide, K., et al., *Cancer cells cause vascular endothelial cell (vEC) retraction via 12(S)HETE secretion; the possible role of cancer cell derived microparticle.* Ann Surg Oncol, 2007. **14**(2): p. 862-8.
112. Krebs, M.G., et al., *Circulating tumour cells: their utility in cancer management and predicting outcomes.* Therapeutic Advances in Medical Oncology, 2010. **2**(6): p. 351-365.
113. Stoletov, K., et al., *Visualizing extravasation dynamics of metastatic tumor cells.* J Cell Sci, 2010. **123**(Pt 13): p. 2332-41.

114. Strell, C. and F. Entschladen, *Extravasation of leukocytes in comparison to tumor cells.* Cell Commun Signal, 2008. **6**: p. 10.
115. Hiratsuka, S., et al., *Endothelial focal adhesion kinase mediates cancer cell homing to discrete regions of the lungs via E-selectin up-regulation.* Proc Natl Acad Sci U S A, 2011. **108**(9): p. 3725-30.
116. Ben-Baruch, A., *Organ selectivity in metastasis: regulation by chemokines and their receptors.* Clin Exp Metastasis, 2008. **25**(4): p. 345-56.
117. Miles, F.L., et al., *Stepping out of the flow: capillary extravasation in cancer metastasis.* Clin Exp Metastasis, 2008. **25**(4): p. 305-24.
118. Kobayashi, H., K.C. Boelte, and P.C. Lin, *Endothelial cell adhesion molecules and cancer progression.* Curr Med Chem, 2007. **14**(4): p. 377-86.
119. Petruzzelli, L., M. Takami, and H.D. Humes, *Structure and function of cell adhesion molecules.* Am J Med, 1999. **106**(4): p. 467-76.
120. Carman, C.V. and T.A. Springer, *Trans-cellular migration: cell-cell contacts get intimate.* Curr Opin Cell Biol, 2008. **20**(5): p. 533-40.
121. Vestweber, D., *Relevance of endothelial junctions in leukocyte extravasation and vascular permeability.* Ann N Y Acad Sci, 2012. **1257**: p. 184-92.
122. Paget, S., *The distribution of secondary growths in cancer of the breast. 1889.* Cancer Metastasis Rev, 1989. **8**(2): p. 98-101.
123. Shibue, T. and R.A. Weinberg, *Metastatic colonization: settlement, adaptation and propagation of tumor cells in a foreign tissue environment.* Semin Cancer Biol, 2011. **21**(2): p. 99-106.
124. Zhang, Xiang H.F., et al., *Selection of Bone Metastasis Seeds by Mesenchymal Signals in the Primary Tumor Stroma.* Cell. **154**(5): p. 1060-1073.
125. Malanchi, I., et al., *Interactions between cancer stem cells and their niche govern metastatic colonization.* Nature, 2011. **481**(7379): p. 85-9.
126. Kowalski, P.J., M.A. Rubin, and C.G. Kleer, *E-cadherin expression in primary carcinomas of the breast and its distant metastases.* Breast Cancer Res, 2003. **5**(6): p. R217-22.
127. Chao, Y.L., C.R. Shepard, and A. Wells, *Breast carcinoma cells re-express E-cadherin during mesenchymal to epithelial reverting transition.* Molecular Cancer, 2010. **9**: p. 179-179.
128. Gao, D., et al., *Myeloid progenitor cells in the premetastatic lung promote metastases by inducing mesenchymal to epithelial transition.* Cancer Res, 2012. **72**(6): p. 1384-94.
129. Tsai, J.H., et al., *Spatiotemporal regulation of epithelial-mesenchymal transition is essential for squamous cell carcinoma metastasis.* Cancer Cell, 2012. **22**(6): p. 725-36.
130. Ocana, O.H., et al., *Metastatic colonization requires the repression of the epithelial-mesenchymal transition inducer Prrx1.* Cancer Cell, 2012. **22**(6): p. 709-24.
131. Cardoso, F., et al., *ESO-ESMO 2nd international consensus guidelines for advanced breast cancer (ABC2).* Annals of Oncology, 2014.
132. Chambers, A.F., A.C. Groom, and I.C. MacDonald, *Metastasis: Dissemination and growth of cancer cells in metastatic sites.* Nat Rev Cancer, 2002. **2**(8): p. 563-572.
133. Pires, B.R.B., et al., *NF-kappaB Is Involved in the Regulation of EMT Genes in Breast Cancer Cells.* PLoS ONE, 2017. **12**(1): p. e0169622.
134. Helbig, G., et al., *NF-kappaB promotes breast cancer cell migration and metastasis by inducing the expression of the chemokine receptor CXCR4.* J Biol Chem, 2003. **278**(24): p. 21631-8.
135. Sen, R. and D. Baltimore, *Multiple nuclear factors interact with the immunoglobulin enhancer sequences.* Cell, 1986. **46**(5): p. 705-16.
136. Perkins, N.D., *Integrating cell-signalling pathways with NF-[kappa]B and IKK function.* Nat Rev Mol Cell Biol, 2007. **8**(1): p. 49-62.
137. Inoue, J.-i., et al., *NF-κB activation in development and progression of cancer.* Cancer Science, 2007. **98**(3): p. 268-274.

138. Gilmore, T.D., *Introduction to NF-kappaB: players, pathways, perspectives.* Oncogene, 2006. **25**(51): p. 6680-4.
139. Karin, M. and Y. Ben-Neriah, *Phosphorylation Meets Ubiquitination: The Control of NF-κB Activity.* Annual Review of Immunology, 2000. **18**(1): p. 621-663.
140. Karin, M., et al., *NF-kappaB in cancer: from innocent bystander to major culprit.* Nat Rev Cancer, 2002. **2**(4): p. 301-10.
141. Oeckinghaus, A., M.S. Hayden, and S. Ghosh, *Crosstalk in NF-[kappa]B signaling pathways.* Nat Immunol, 2011. **12**(8): p. 695-708.
142. Xiao, G., A. Fong, and S.C. Sun, *Induction of p100 processing by NF-kappaB-inducing kinase involves docking IkappaB kinase alpha (IKKalpha) to p100 and IKKalpha-mediated phosphorylation.* J Biol Chem, 2004. **279**(29): p. 30099-105.
143. Arenzana-Seisdedos, F., et al., *Nuclear localization of I kappa B alpha promotes active transport of NF-kappa B from the nucleus to the cytoplasm.* Journal of Cell Science, 1997. **110**(3): p. 369-378.
144. Biswas, D.K., et al., *NF-kappa B activation in human breast cancer specimens and its role in cell proliferation and apoptosis.* Proc Natl Acad Sci U S A, 2004. **101**(27): p. 10137-42.
145. Kuper, H., H.O. Adami, and D. Trichopoulos, *Infections as a major preventable cause of human cancer.* J Intern Med, 2000. **248**(3): p. 171-83.
146. Greten, F.R., et al., *IKKbeta links inflammation and tumorigenesis in a mouse model of colitis-associated cancer.* Cell, 2004. **118**(3): p. 285-296.
147. Pikarsky, E., et al., *NF-kappaB functions as a tumour promoter in inflammation-associated cancer.* Nature, 2004. **431**(7007): p. 461-466.
148. Huang, T.T., et al., *Sequential modification of NEMO/IKKgamma by SUMO-1 and ubiquitin mediates NF-kappaB activation by genotoxic stress.* Cell, 2003. **115**(5): p. 565-576.
149. Brantley, D.M., et al., *Nuclear factor-kappaB (NF-kappaB) regulates proliferation and branching in mouse mammary epithelium.* Mol Biol Cell, 2001. **12**(5): p. 1445-55.
150. Sovak, M.A., et al., *Aberrant nuclear factor-kappaB/Rel expression and the pathogenesis of breast cancer.* J Clin Invest, 1997. **100**(12): p. 2952-60.
151. Huber, M.A., et al., *NF-kappaB is essential for epithelial-mesenchymal transition and metastasis in a model of breast cancer progression.* J Clin Invest, 2004. **114**(4): p. 569-81.
152. Connelly, L., et al., *A transgenic model reveals important roles for the NF-kappa B alternative pathway (p100/p52) in mammary development and links to tumorigenesis.* J Biol Chem, 2007. **282**(13): p. 10028-35.
153. Yeo, S.K., et al., *Opposing roles of Nfkb2 gene products p100 and p52 in the regulation of breast cancer stem cells.* Breast Cancer Res Treat, 2017. **162**(3): p. 465-477.
154. Cusack, J.C., Jr., et al., *Enhanced chemosensitivity to CPT-11 with proteasome inhibitor PS-341: implications for systemic nuclear factor-kappaB inhibition.* Cancer research, 2001. **61**(9): p. 3535-3540.
155. Mabuchi, S., et al., *Inhibition of NFkappaB increases the efficacy of cisplatin in in vitro and in vivo ovarian cancer models.* The Journal of biological chemistry, 2004. **279**(22): p. 23477-23485.
156. Shah, S.A., et al., *26S proteasome inhibition induces apoptosis and limits growth of human pancreatic cancer.* Journal of cellular biochemistry, 2001. **82**(1): p. 110-122.
157. Gilmore, T.D. and M. Herscovitch, *Inhibitors of NF-kappaB signaling: 785 and counting.* Oncogene, 2006. **25**(51): p. 6887-6899.
158. Rauert-Wunderlich, H., et al., *The IKK Inhibitor Bay 11-7082 Induces Cell Death Independent from Inhibition of Activation of NFκB Transcription Factors.* PLoS ONE, 2013. **8**(3).
159. Kishore, N., et al., *A selective IKK-2 inhibitor blocks NF-kappa B-dependent gene expression in interleukin-1 beta-stimulated synovial fibroblasts.* J Biol Chem, 2003. **278**(35): p. 32861-71.

160. Jones, M.D., et al., *A proteasome inhibitor, bortezomib, inhibits breast cancer growth and reduces osteolysis by downregulating metastatic genes.* Clin Cancer Res, 2010. **16**(20): p. 4978-89.
161. Gupta, S.C., et al., *Inhibiting NF-κB Activation by Small Molecules As a Therapeutic Strategy.* Biochimica et biophysica acta, 2010. **1799**(10-12): p. 775-787.
162. Haffner, M.C., C. Berlato, and W. Doppler, *Exploiting our knowledge of NF-kappaB signaling for the treatment of mammary cancer.* Journal of mammary gland biology and neoplasia, 2006. **11**(1): p. 63-73.
163. Lin, Y.Z., et al., *Inhibition of nuclear translocation of transcription factor NF-kappa B by a synthetic peptide containing a cell membrane-permeable motif and nuclear localization sequence.* J Biol Chem, 1995. **270**(24): p. 14255-8.
164. Torgerson, T.R., et al., *Regulation of NF-kappa B, AP-1, NFAT, and STAT1 nuclear import in T lymphocytes by noninvasive delivery of peptide carrying the nuclear localization sequence of NF-kappa B p50.* J Immunol, 1998. **161**(11): p. 6084-92.
165. Zhang, L., et al., *The NFκB inhibitor, SN50, induces differentiation of glioma stem cells and suppresses their oncogenic phenotype.* Cancer Biology & Therapy, 2014. **15**(5): p. 602-611.
166. Kiernan, R., et al., *Post-activation turn-off of NF-kappa B-dependent transcription is regulated by acetylation of p65.* J Biol Chem, 2003. **278**(4): p. 2758-66.
167. Tomita, N., T. Ogihara, and R. Morishita, *Transcription factors as molecular targets: molecular mechanisms of decoy ODN and their design.* Curr Drug Targets, 2003. **4**(8): p. 603-8.
168. Fang, Y., et al., *Antitumor activity of NF-kB decoy oligodeoxynucleotides in a prostate cancer cell line.* Asian Pac J Cancer Prev, 2011. **12**(10): p. 2721-6.
169. Ryan, K.M., et al., *Role of NF-[kappa]B in p53-mediated programmed cell death.* Nature, 2000. **404**(6780): p. 892-897.
170. Revilla, Y., et al., *Inhibition of Nuclear Factor κB Activation by a Virus-encoded IκB-like Protein.* Journal of Biological Chemistry, 1998. **273**(9): p. 5405-5411.
171. Ma, Q., et al., *Inhibition of nuclear factor kappaB by phenolic antioxidants: interplay between antioxidant signaling and inflammatory cytokine expression.* Mol Pharmacol, 2003. **64**(2): p. 211-9.
172. Agrawal, A. and I.S. Fentiman, *NSAIDs and breast cancer: a possible prevention and treatment strategy.* Int J Clin Pract, 2008. **62**(3): p. 444-9.
173. Perkins, N.D., *The diverse and complex roles of NF-κB subunits in cancer.* Nature reviews. Cancer, 2012. **12**(2): p. 121-132.
174. Karin, M., *NF-kappaB as a critical link between inflammation and cancer.* Cold Spring Harb Perspect Biol, 2009. **1**(5): p. a000141.
175. McKeithan, T.W., et al., *BCL3 rearrangements and t(14;19) in chronic lymphocytic leukemia and other B-cell malignancies: A molecular and cytogenetic study.* Genes, Chromosomes and Cancer, 1997. **20**(1): p. 64-72.
176. Franzoso, G., et al., *The oncoprotein Bcl-3 can facilitate NF-kappa B-mediated transactivation by removing inhibiting p50 homodimers from select kappa B sites.* Embo j, 1993. **12**(10): p. 3893-901.
177. Bours, V., et al., *The oncoprotein Bcl-3 directly transactivates through kappa B motifs via association with DNA-binding p50B homodimers.* Cell, 1993. **72**(5): p. 729-39.
178. Zhang, Q., et al., *BCL3 encodes a nuclear protein which can alter the subcellular location of NF-kappa B proteins.* Mol Cell Biol, 1994. **14**(6): p. 3915-26.
179. Nolan, G.P., et al., *The bcl-3 proto-oncogene encodes a nuclear I kappa B-like molecule that preferentially interacts with NF-kappa B p50 and p52 in a phosphorylation-dependent manner.* Mol Cell Biol, 1993. **13**(6): p. 3557-66.
180. Wang, V.Y.-F., et al., *Bcl3 Phosphorylation by Akt, Erk2, and IKK Is Required for Its Transcriptional Activity.* Molecular Cell. **67**(3): p. 484-497.e5.

181. Chaudhary, S.C., et al., *Shh and p50/Bcl3 signaling crosstalk drives pathogenesis of BCCs in gorlin syndrome.* Oncotarget, 2015. **6**(34): p. 36789-36814.
182. Wessells, J., et al., *BCL-3 and NF-κB p50 Attenuate Lipopolysaccharide-induced Inflammatory Responses in Macrophages.* Journal of Biological Chemistry, 2004. **279**(48): p. 49995-50003.
183. Uffort, D.G., E.A. Grimm, and J.A. Ellerhorst, *NF-κB Mediates Mitogen-Activated Protein Kinase Pathway-Dependent iNOS Expression in Human Melanoma.* Journal of Investigative Dermatology, 2009. **129**(1): p. 148-154.
184. Wang, F., et al., *p52-Bcl3 complex promotes cyclin D1 expression in BEAS-2B cells in response to low concentration arsenite.* Toxicology, 2010. **273**(1-3): p. 12-8.
185. Pan, J. and R.P. McEver, *Regulation of the Human P-selectin Promoter by Bcl-3 and Specific Homodimeric Members of the NF-κB/Rel Family.* Journal of Biological Chemistry, 1995. **270**(39): p. 23077-23083.
186. Viatour, P., et al., *NF- kappa B2/p100 induces Bcl-2 expression.* Leukemia, 2003. **17**(7): p. 1349-56.
187. Na, S.Y., et al., *Bcl3, an IkappaB protein, stimulates activating protein-1 transactivation and cellular proliferation.* J Biol Chem, 1999. **274**(40): p. 28491-6.
188. Chen, X., et al., *Bcl-3 regulates TGF[beta] signaling by stabilizing Smad3 during breast cancer pulmonary metastasis.* Cell Death Dis, 2016. **7**: p. e2508.
189. Kuwata, H., et al., *IL-10-inducible Bcl-3 negatively regulates LPS-induced TNF-alpha production in macrophages.* Blood, 2003. **102**(12): p. 4123-9.
190. Elliott, S.F., et al., *Bcl-3 is an interleukin-1-responsive gene in chondrocytes and synovial fibroblasts that activates transcription of the matrix metalloproteinase 1 gene.* Arthritis Rheum, 2002. **46**(12): p. 3230-9.
191. Rebollo, A., et al., *Bcl-3 Expression Promotes Cell Survival following Interleukin-4 Deprivation and Is Controlled by AP1 and AP1-Like Transcription Factors.* Molecular and Cellular Biology, 2000. **20**(10): p. 3407-3416.
192. Heissmeyer, V., et al., *NF-kappaB p105 is a target of IkappaB kinases and controls signal induction of Bcl-3-p50 complexes.* The EMBO Journal, 1999. **18**(17): p. 4766-4778.
193. Brocke-Heidrich, K., et al., *BCL3 is induced by IL-6 via Stat3 binding to intronic enhancer HS4 and represses its own transcription.* Oncogene, 2006. **25**(55): p. 7297-304.
194. Rocha, S., et al., *p53 Represses Cyclin D1 Transcription through Down Regulation of Bcl-3 and Inducing Increased Association of the p52 NF-κB Subunit with Histone Deacetylase 1.* Molecular and Cellular Biology, 2003. **23**(13): p. 4713-4727.
195. Brasier, A.R., et al., *NF-kappa B-inducible BCL-3 expression is an autoregulatory loop controlling nuclear p50/NF-kappa B1 residence.* J Biol Chem, 2001. **276**(34): p. 32080-93.
196. Kraiss, L.W., et al., *Fluid flow activates a regulator of translation, p70/p85 S6 kinase, in human endothelial cells.* Am J Physiol Heart Circ Physiol, 2000. **278**(5): p. H1537-44.
197. Pabla, R., et al., *Integrin-dependent Control of Translation: Engagement of Integrin α<sub>IIb</sub>β<sub>3</sub> Regulates Synthesis of Proteins in Activated Human Platelets.* The Journal of Cell Biology, 1999. **144**(1): p. 175.
198. Keutgens, A., et al., *BCL-3 degradation involves its polyubiquitination through a FBW7-independent pathway and its binding to the proteasome subunit PSMB1.* J Biol Chem, 2010. **285**(33): p. 25831-40.
199. Viatour, P., et al., *GSK3-Mediated BCL-3 Phosphorylation Modulates Its Degradation and Its Oncogenicity.* Molecular Cell, 2004. **16**(1): p. 35-45.
200. Massoumi, R., et al., *Cyld Inhibits Tumor Cell Proliferation by Blocking Bcl-3-Dependent NF-κB Signaling.* Cell, 2006. **125**(4): p. 665-677.
201. Guan, Y., et al., *MiR-125b targets BCL3 and suppresses ovarian cancer proliferation.* Int J Cancer, 2011. **128**(10): p. 2274-83.
202. Puvvada, S.D., et al., *NF-kB and Bcl-3 activation are prognostic in metastatic colorectal cancer.* Oncology, 2010. **78**(3-4): p. 181-8.

203. Pallares, J., et al., *Abnormalities in the NF-kappaB family and related proteins in endometrial carcinoma.* J Pathol, 2004. **204**(5): p. 569-77.
204. Thornburg, N.J., R. Pathmanathan, and N. Raab-Traub, *Activation of nuclear factor-kappaB p50 homodimer/Bcl-3 complexes in nasopharyngeal carcinoma.* Cancer Res, 2003. **63**(23): p. 8293-301.
205. Cogswell, P.C., et al., *Selective activation of NF-kappa B subunits in human breast cancer: potential roles for NF-kappa B2/p52 and for Bcl-3.* Oncogene, 2000. **19**(9): p. 1123-31.
206. Ong, S.T., et al., *Lymphadenopathy, splenomegaly, and altered immunoglobulin production in BCL3 transgenic mice.* Oncogene, 1998. **16**(18): p. 2333-43.
207. Bauer, A., et al., *The NF-kappaB regulator Bcl-3 and the BH3-only proteins Bim and Puma control the death of activated T cells.* Proc Natl Acad Sci U S A, 2006. **103**(29): p. 10979-84.
208. Kashatus, D., P. Cogswell, and A.S. Baldwin, *Expression of the Bcl-3 proto-oncogene suppresses p53 activation.* Genes Dev, 2006. **20**(2): p. 225-35.
209. Ahmed, S.U. and J. Milner, *Basal Cancer Cell Survival Involves JNK2 Suppression of a Novel JNK1/c-Jun/Bcl-3 Apoptotic Network.* PLoS ONE, 2009. **4**(10): p. e7305.
210. Choi, H.J., et al., *Bcl3-dependent stabilization of CtBP1 is crucial for the inhibition of apoptosis and tumor progression in breast cancer.* Biochem Biophys Res Commun, 2010. **400**(3): p. 396-402.
211. Zhao, H., et al., *BCL3 exerts an oncogenic function by regulating STAT3 in human cervical cancer.* Onco Targets Ther, 2016. **9**: p. 6619-6629.
212. Zamora, R., et al., *Depletion of the oncoprotein Bcl-3 induces centrosome amplification and aneuploidy in cancer cells.* Molecular Cancer, 2010. **9**: p. 223-223.
213. Westerheide, S.D., et al., *The putative oncoprotein Bcl-3 induces cyclin D1 to stimulate G(1) transition.* Mol Cell Biol, 2001. **21**(24): p. 8428-36.
214. Wakefield, A., et al., *Bcl3 selectively promotes metastasis of ERBB2-driven mammary tumors.* Cancer Res, 2013. **73**(2): p. 745-55.
215. Soukupova, J., *Unpublished.* 2014.
216. van der Horst, E.H., et al., *TaqMan-based quantification of invasive cells in the chick embryo metastasis assay.* Biotechniques, 2004. **37**(6): p. 940-2, 944, 946.
217. Friedl, P., et al., *Classifying collective cancer cell invasion.* Nat Cell Biol, 2012. **14**(8): p. 777-83.
218. Pankova, K., et al., *The molecular mechanisms of transition between mesenchymal and amoeboid invasiveness in tumor cells.* Cell Mol Life Sci, 2010. **67**(1): p. 63-71.
219. Perona, R., et al., *Activation of the nuclear factor-kappaB by Rho, CDC42, and Rac-1 proteins.* Genes Dev, 1997. **11**(4): p. 463-75.
220. Kuroda, S., et al., *Regulation of cell-cell adhesion of MDCK cells by Cdc42 and Rac1 small GTPases.* Biochem Biophys Res Commun, 1997. **240**(2): p. 430-5.
221. Kuroda, S., et al., *Role of IQGAP1, a target of the small GTPases Cdc42 and Rac1, in regulation of E-cadherin- mediated cell-cell adhesion.* Science, 1998. **281**(5378): p. 832-5.
222. Godwin, P., et al., *Targeting Nuclear Factor-Kappa B to Overcome Resistance to Chemotherapy.* Frontiers in Oncology, 2013. **3**: p. 120.
223. Clarkson, R.W., *Unpublished.* 2016.
224. Ahlqvist, K., et al., *Expression of Id proteins is regulated by the Bcl-3 proto-oncogene in prostate cancer.* Oncogene, 2013. **32**(12): p. 1601-8.
225. Zhao, H., et al., *BCL3 exerts an oncogenic function by regulating STAT3 in human cervical cancer.* OncoTargets and therapy, 2016. **9**: p. 6619-6629.
226. Urban, B.C., et al., *BCL-3 expression promotes colorectal tumorigenesis through activation of AKT signalling.* Gut, 2016. **65**(7): p. 1151-64.
227. Thompson, E.W., et al., *Association of increased basement membrane invasiveness with absence of estrogen receptor and expression of vimentin in human breast cancer cell lines.* J Cell Physiol, 1992. **150**(3): p. 534-44.

228. Yang, X., et al., *KAI1, a putative marker for metastatic potential in human breast cancer.* Cancer Lett, 1997. **119**(2): p. 149-55.
229. Kozma, R., et al., *The GTPase-activating protein n-chimaerin cooperates with Rac1 and Cdc42Hs to induce the formation of lamellipodia and filopodia.* Mol Cell Biol, 1996. **16**(9): p. 5069-80.
230. Yamaguchi, H. and J. Condeelis, *Regulation of the actin cytoskeleton in cancer cell migration and invasion.* Biochim Biophys Acta, 2007. **1773**(5): p. 642-52.
231. Moissoglu, K., et al., *Rho GDP dissociation inhibitor 2 suppresses metastasis via unconventional regulation of RhoGTPases.* Cancer Res, 2009. **69**(7): p. 2838-44.
232. Agarwal, N.K., et al., *Rictor regulates cell migration by suppressing RhoGDI2.* Oncogene, 2013. **32**(20): p. 2521-6.
233. Katz, E., et al., *Targeting of Rac GTPases blocks the spread of intact human breast cancer.* Oncotarget, 2012. **3**(6): p. 608-19.
234. Braga, V.M., *Small GTPases and regulation of cadherin dependent cell-cell adhesion.* Mol Pathol, 1999. **52**(4): p. 197-202.
235. Parsons, J.T., A.R. Horwitz, and M.A. Schwartz, *Cell adhesion: integrating cytoskeletal dynamics and cellular tension.* Nat Rev Mol Cell Biol, 2010. **11**(9): p. 633-43.
236. Price, L.S., et al., *Activation of Rac and Cdc42 by Integrins Mediates Cell Spreading.* Molecular Biology of the Cell, 1998. **9**(7): p. 1863-1871.
237. Ai, J., et al., *Bcl-3 acts as a proto-oncogene in pancreatic cancer in humans and mice.* Z Gastroenterol, 2016. **54**(08): p. KV462.
238. Chua, H.L., et al., *NF-kappaB represses E-cadherin expression and enhances epithelial to mesenchymal transition of mammary epithelial cells: potential involvement of ZEB-1 and ZEB-2.* Oncogene, 2007. **26**(5): p. 711-24.
239. Criswell, T.L. and C.L. Arteaga, *Modulation of NFkappaB activity and E-cadherin by the type III transforming growth factor beta receptor regulates cell growth and motility.* J Biol Chem, 2007. **282**(44): p. 32491-500.
240. Miyazaki, I., et al., *A small-molecule inhibitor shows that pirin regulates migration of melanoma cells.* Nat Chem Biol, 2010. **6**(9): p. 667-73.
241. Jechlinger, M., et al., *Expression profiling of epithelial plasticity in tumor progression.* Oncogene, 2003. **22**(46): p. 7155-69.
242. Mahdi, S.H., et al., *The effect of TGF-beta-induced epithelial-mesenchymal transition on the expression of intracellular calcium-handling proteins in T47D and MCF-7 human breast cancer cells.* Arch Biochem Biophys, 2015. **583**: p. 18-26.
243. Wang, Y., et al., *Twist-mediated Epithelial-mesenchymal Transition Promotes Breast Tumor Cell Invasion via Inhibition of Hippo Pathway.* Scientific Reports, 2016. **6**: p. 24606.
244. Brown, K.A., et al., *Induction by transforming growth factor-beta1 of epithelial to mesenchymal transition is a rare event in vitro.* Breast Cancer Res, 2004. **6**(3): p. R215-31.
245. Tang, Y., et al., *Induction and analysis of epithelial to mesenchymal transition.* J Vis Exp, 2013(78).
246. Wang, V.Y.-F., et al., *The Transcriptional Specificity of NF-κB Dimers Is Coded within the κB DNA Response Elements.* Cell reports, 2012. **2**(4): p. 824-839.
247. Owens, T.W., et al., *Runx2 is a novel regulator of mammary epithelial cell fate in development and breast cancer.* Cancer research, 2014. **74**(18): p. 5277-5286.
248. van Bragt, M.P.A., et al., *RUNX1, a transcription factor mutated in breast cancer, controls the fate of ER-positive mammary luminal cells.* eLife, 2014. **3**: p. e03881.
249. Hollier, B.G., et al., *FOXC2 Expression Links Epithelial–Mesenchymal Transition and Stem Cell Properties in Breast Cancer.* Cancer Research, 2013. **73**(6): p. 1981.
250. Nassirpour, R., et al., *miR-221 Promotes Tumorigenesis in Human Triple Negative Breast Cancer Cells.* PLOS ONE, 2013. **8**(4): p. e62170.

251. Lambertini, E., et al., *Correlation between Slug transcription factor and miR-221 in MDA-MB-231 breast cancer cells.* BMC Cancer, 2012. **12**(1): p. 445.
252. Kajita, M., K.N. McClinic, and P.A. Wade, *Aberrant expression of the transcription factors snail and slug alters the response to genotoxic stress.* Mol Cell Biol, 2004. **24**(17): p. 7559-66.
253. Tandon, M., Z. Chen, and J. Pratap, *Runx2 activates PI3K/Akt signaling via mTORC2 regulation in invasive breast cancer cells.* Breast Cancer Res, 2014. **16**(1): p. R16.
254. Weinstein, I.B. and A. Joe, *Oncogene Addiction.* Cancer Research, 2008. **68**(9): p. 3077.
255. Massoumi, R., et al., *Down-regulation of CYLD expression by Snail promotes tumor progression in malignant melanoma.* J Exp Med, 2009. **206**(1): p. 221-32.
256. Yamazaki, K., et al., *Upregulated SMAD3 promotes epithelial-mesenchymal transition and predicts poor prognosis in pancreatic ductal adenocarcinoma.* Lab Invest, 2014. **94**(6): p. 683-91.
257. Ewald, J.A., et al., *Therapy-induced senescence in cancer.* J Natl Cancer Inst, 2010. **102**(20): p. 1536-46.
258. Jing, H. and S. Lee, *NF-κB in Cellular Senescence and Cancer Treatment.* Molecules and Cells, 2014. **37**(3): p. 189-195.
259. Chien, Y., et al., *Control of the senescence-associated secretory phenotype by NF-kappaB promotes senescence and enhances chemosensitivity.* Genes Dev, 2011. **25**(20): p. 2125-36.
260. De Donatis, G.M., et al., *NF-kB2 induces senescence bypass in melanoma via a direct transcriptional activation of EZH2.* Oncogene, 2016. **35**(21): p. 2735-45.
261. Iannetti, A., et al., *Regulation of p53 and Rb links the alternative NF-kappaB pathway to EZH2 expression and cell senescence.* PLoS Genet, 2014. **10**(9): p. e1004642.
262. Wasielewski, M., et al., *Thirteen new p53 gene mutants identified among 41 human breast cancer cell lines.* Breast Cancer Res Treat, 2006. **99**(1): p. 97-101.
263. Jackson, J.G., et al., *p53 mediated senescence impairs the apoptotic response to chemotherapy and clinical outcome in breast cancer.* Cancer Cell, 2012. **21**(6): p. 793-806.
264. Sugrue, M.M., et al., *Wild-type p53 triggers a rapid senescence program in human tumor cells lacking functional p53.* Proceedings of the National Academy of Sciences, 1997. **94**(18): p. 9648-9653.
265. Zhang, J. and X. Chen, *Posttranscriptional Regulation of p53 and Its Targets by RNA-Binding Proteins.* Current molecular medicine, 2008. **8**(8): p. 845-849.
266. Kojima, H., et al., *IL-6-STAT3 signaling and premature senescence.* JAK-STAT, 2013. **2**(4): p. e25763.
267. Xu, M., et al., *JAK inhibition alleviates the cellular senescence-associated secretory phenotype and frailty in old age.* Proc Natl Acad Sci U S A, 2015. **112**(46): p. E6301-10.
268. Zahnow, C.A., *CCAAT/enhancer-binding protein β: its role in breast cancer and associations with receptor tyrosine kinases.* Expert reviews in molecular medicine, 2009. **11**: p. e12-e12.
269. Matsusaka, T., et al., *Transcription factors NF-IL6 and NF-kappa B synergistically activate transcription of the inflammatory cytokines, interleukin 6 and interleukin 8.* Proc Natl Acad Sci U S A, 1993. **90**(21): p. 10193-7.
270. Xu, L., et al., *Mutational analysis of CDKN2 (MTS1/p16ink4) in human breast carcinomas.* Cancer Res, 1994. **54**(20): p. 5262-4.
271. Cordenonsi, M., et al., *Links between tumor suppressors: p53 is required for TGF-beta gene responses by cooperating with Smads.* Cell, 2003. **113**(3): p. 301-14.
272. Kleer, C.G., et al., *EZH2 is a marker of aggressive breast cancer and promotes neoplastic transformation of breast epithelial cells.* Proc Natl Acad Sci U S A, 2003. **100**(20): p. 11606-11.
273. Tang, X., et al., *Activated p53 suppresses the histone methyltransferase EZH2 gene.* Oncogene, 2004. **23**(34): p. 5759-69.
274. Fan, T., et al., *EZH2-dependent suppression of a cellular senescence phenotype in melanoma cells by inhibition of p21/CDKN1A expression.* Mol Cancer Res, 2011. **9**(4): p. 418-29.

275. Tombor, B., K. Rundell, and Z.N. Oltvai, *Bcl-2 promotes premature senescence induced by oncogenic Ras.* Biochem Biophys Res Commun, 2003. **303**(3): p. 800-7.
276. Uraoka, M., et al., *Loss of bcl-2 during the senescence exacerbates the impaired angiogenic functions in endothelial cells by deteriorating the mitochondrial redox state.* Hypertension, 2011. **58**(2): p. 254-63.
277. Yu, J. and L. Zhang, *PUMA, a potent killer with or without p53.* Oncogene, 2008. **27**(Suppl 1): p. S71-S83.
278. Xue, W., et al., *Senescence and tumour clearance is triggered by p53 restoration in murine liver carcinomas.* Nature, 2007. **445**(7128): p. 656-60.
279. Kumari, N., et al., *Role of interleukin-6 in cancer progression and therapeutic resistance.* Tumour Biol, 2016. **37**(9): p. 11553-11572.
280. Wakefield, A., et al., *Bcl3 selectively promotes metastasis of ERBB2-driven mammary tumors.* Cancer research, 2013. **73**(2): p. 745-755.
281. Lamouille, S., J. Xu, and R. Derynck, *Molecular mechanisms of epithelial-mesenchymal transition.* Nat Rev Mol Cell Biol, 2014. **15**(3): p. 178-96.
282. Debidda, M., D.A. Williams, and Y. Zheng, *Rac1 GTPase regulates cell genomic stability and senescence.* J Biol Chem, 2006. **281**(50): p. 38519-28.
283. Alexander, K., H.-S. Yang, and P.W. Hinds, *Cellular Senescence Requires CDK5 Repression of Rac1 Activity.* Molecular and Cellular Biology, 2004. **24**(7): p. 2808-2819.
284. Zhang, X., et al., *Beta-elemene blocks epithelial-mesenchymal transition in human breast cancer cell line MCF-7 through Smad3-mediated down-regulation of nuclear transcription factors.* PLoS One, 2013. **8**(3): p. e58719.
285. Wu, D., et al., *Runt-related transcription factor 1 (RUNX1) stimulates tumor suppressor p53 protein in response to DNA damage through complex formation and acetylation.* J Biol Chem, 2013. **288**(2): p. 1353-64.
286. Fornari, F., et al., *p53/mdm2 feedback loop sustains miR-221 expression and dictates the response to anticancer treatments in hepatocellular carcinoma.* Mol Cancer Res, 2014. **12**(2): p. 203-16.
287. Piva, R., et al., *Slug transcription factor and nuclear Lamin B1 are upregulated in osteoarthritic chondrocytes.* Osteoarthritis Cartilage, 2015. **23**(7): p. 1226-30.
288. Siegel, P.M. and J. Massague, *Cytostatic and apoptotic actions of TGF-beta in homeostasis and cancer.* Nat Rev Cancer, 2003. **3**(11): p. 807-21.
289. Ten Dijke, P., et al., *Regulation of cell proliferation by Smad proteins.* J Cell Physiol, 2002. **191**(1): p. 1-16.
290. Ji, L., et al., *Mutant p53 promotes tumor cell malignancy by both positive and negative regulation of the transforming growth factor beta (TGF-beta) pathway.* J Biol Chem, 2015. **290**(18): p. 11729-40.
291. Kojima, H., et al., *The STAT3-IGFBP5 axis is critical for IL-6/gp130-induced premature senescence in human fibroblasts.* Cell Cycle, 2012. **11**(4): p. 730-9.
292. Maldonado, V., et al., *Gene regulation by BCL3 in a cervical cancer cell line.* Folia Biol (Praha), 2010. **56**(4): p. 183-93.
293. Yun, U.J., et al., *DNA damage induces the IL-6/STAT3 signaling pathway, which has anti-senescence and growth-promoting functions in human tumors.* Cancer Lett, 2012. **323**(2): p. 155-60.
294. Gritsko, T., et al., *Persistent activation of stat3 signaling induces survivin gene expression and confers resistance to apoptosis in human breast cancer cells.* Clin Cancer Res, 2006. **12**(1): p. 11-9.
295. Tkach, M., et al., *Targeting Stat3 induces senescence in tumor cells and elicits prophylactic and therapeutic immune responses against breast cancer growth mediated by NK cells and CD4+ T cells.* J Immunol, 2012. **189**(3): p. 1162-72.

296. Niu, G., et al., *Role of Stat3 in Regulating p53 Expression and Function.* Molecular and Cellular Biology, 2005. **25**(17): p. 7432-7440.